UNIVERSIDADE FEDERAL DO RIO GRANDE DO SUL
PROGRAMA DE PÓS-GRADUAÇÃO EM CIÊNCIAS FARMACÊUTICAS
FACULDADE DE FARMÁCIA

SÍNTESE DE COMPOSTOS HETEROCÍCLICOS QUIRAIS E AQUIRAIS INIBIDORES DE CRUZAÍNA E RODESAÍNA: POTENCIAIS AGENTES PARA TRATAMENTO DE TRIPANOSSOMÍASES

DÉBORA ASSUMPÇÃO ROCHA

Porto Alegre, maio de 2022.

UNIVERSIDADE FEDERAL DO RIO GRANDE DO SUL
PROGRAMA DE PÓS-GRADUAÇÃO EM CIÊNCIAS FARMACÊUTICAS
FACULDADE DE FARMÁCIA

SÍNTESE DE COMPOSTOS HETEROCÍCLICOS QUIRAIS E AQUIRAIS INIBIDORES DE CRUZAÍNA E RODESAÍNA: POTENCIAIS AGENTES PARA TRATAMENTO DE TRIPANOSSOMÍASES

Tese apresentada por **Débora Assumpção Rocha** para obtenção do GRAU DE DOUTORA em Ciências Farmacêuticas

ORIENTADOR: PROF. DR. SAULO FERNANDES DE ANDRADE
COORIENTADORA: PROF. DRA. RAFAELA SALGADO FERREIRA

Porto Alegre, maio de 2022.

Tese apresentada ao Programa de Pós-Graduação em Ciências Farmacêuticas, em nível de Doutorado Acadêmico da Faculdade de Farmácia da Universidade Federal do Rio Grande do Sul e aprovada em 30 de maio de 2022, pela Banca Examinadora constituída por:

Profa. Dra. Livia Kmetzsch Rosa e Silva
Universidade Federal do Rio Grande do Sul

Profa. Dra. Simone Cristina Baggio Gnoatto
Universidade Federal do Rio Grande do Sul e

Prof. Dra. Stefânia Neiva Lavorato
Universidade Federal do Oeste da Bahia

Profa. Dra. Tiana Tasca
Universidade Federal do Rio Grande do Sul

Rocha, Débora Assumpção
Síntese De Compostos Heterocíclicos Quirais E Aquirais Inibidores De Cruzaína E Rodesaína: Potenciais Agentes Para Tratamento De Tripanossomíases / Débora Assumpção Rocha. -- 2022.
220 f.
Orientador: Saulo Fernandes De Andrade.

Coorientador: Rafaela Salgado Ferreira.

Tese (Doutorado) -- Universidade Federal do Rio Grande do Sul, Faculdade de Farmácia, Programa de Pós-Graduação em Ciências Farmacêuticas, Porto Alegre, BR-RS, 2022.

1. Doença de Chagas. 2. Doença do Sono Africana. 3. Cruzaína. 4. TbrCATL. 5. Síntese Assimétrica . I. De Andrade, Saulo Fernandes, orient. II. Ferreira, Rafaela Salgado, coorient. III. Título.

Este trabalho foi desenvolvido no Laboratório 705B – PHARSG – Laboratório de Síntese Farmacêutica do Departamento de Produção e Controle de Matéria-Prima da Faculdade de Farmácia da UFRGS e no Departamento de Bioquímica e Imunologia do Instituto de Ciências Biológicas, Universidade Federal de Minas Gerais, Belo Horizonte, MG, Brazil, com financiamento da CAPES, FAPERGS e CNPq - Universal 01/2016, 402318/2016-1.

A autora recebeu bolsa de estudos do CNPq - 141841/2018-4.

AGRADECIMENTOS

Agradeço a Deus por nunca me abandonar, mesmo em momentos em que eu me esquecia dele e me perdia em meio a este trabalho.

Aos meus pais Maria Regina e Regis, por sempre me apoiarem em todas as minhas decisões, pelos sábios conselhos e por serem meus amigos e mimadores nos momentos em que mais precisei. Ao meu irmão Daniel, por ter cuidado de mim desde quando criança, por ter sido protetor e me ensinado a me defender e me valorizar.

Ao meu marido e companheiro de vida Norton, por me dar todo apoio amoroso, científico e suporte tecnológico. Por me ensinar a não desistir de forma alguma do meu objetivo, procurar sempre a minha melhor versão, ser um incentivador do meu trabalho e pedir minha comida favorita quando eu estava na pior. Aos meus sogros Magaly e Vitor por todo apoio e compressão ao longo deste período e pelos domingos de churrasco e idas ao Beira-Rio. A minha cunhada Nicolle, por ser o meu primeiro modelo científico, que me ensinou muito dentro e fora do laboratório - quando fui sua IC e quando me apresentou para o seu irmão. Aos meus demais familiares por todo apoio durante os meus estudos, em especial aos meus padrinhos, Marlene e Renato e a minha prima querida Paula.

Aos colegas da Sociedade Espírita de Natanael pelas palavras de conforto nos momentos difíceis, pelo carinho e por todos os ensinamentos não somente da doutrina, mas de vida.

As colegas do Lab 105 por terem me recebido tão bem no laboratório, em especial, a Prof. Dra. Grace Gosmann, por todos os ensinamentos. A Prof. Dra. Rafaela Salgado Ferreira, pela ótima coorientação e parceria, mesmo que a distância. A Elany, por todo apoio neste trabalho e pelas dicas e colaborações.

Aos colegas do Laboratório de Síntese Farmacêutica por todo apoio técnico, culinário e na realização de sistemas tecnológicos de improviso sempre que necessário. Em especial as queridas Sauletes: Thais, por todo apoio e palavras amigas, Caroline por todo carinho, companheirismo e por me compreender também como colorada, a Isadora por ter sido minha IC por todo período do meu mestrado e parte deste doutorado, assim como uma amiga querida. A Angélica por ser uma companheira e irmã que a síntese me trouxe. Muito obrigada por todo apoio emocional na realização deste trabalho, e parceria nas idas ao Mc nos momentos tristes ou felizes. A Marcela por ser um exemplo de ser humano para todos nós, por todo apoio

AGRADECIMENTOS (Continuação)

e pelas palavras de carinho ao longo dessa trajetória, assim como por todo o auxílio científico. Ao meu orientador, Prof Saulo pela oportunidade de desenvolver esse trabalho, por todo apoio, amizade e ensinamentos. Sem contar a infinita paciência quanto as minhas dúvidas e por acreditar no meu potencial.

“We must have perseverance, and above all, confidence in ourselves. We must believe that we are gifted for something and that this thing must be attained.”

—Marie Curie

RESUMO

A Doença de Chagas e a Tripanossomíase Africana (HAT) são doenças negligenciadas, cujos agentes etiológicos são *Trypanosoma cruzi* e *Trypanosoma brucei*, respectivamente. Um dos alvos validados para o desenvolvimento de medicamentos para o tratamento dessas doenças são as proteases, como a cruzaína, principal cisteíno-protease do *T. cruzi* e a T*br*CATL para *T. brucei*. Após uma triagem, utilizando docking e High-throughput screening (HTS), o composto quiral *N*-(1-((2-(furan-2-il)-2-(piperidin-1-il)etil)amino)-3-metil-1-oxobutan-2-il)furan-2-carboxamida **2** foi identificado como um inibidor não covalente de cruzaína. Em outra triagem foi identificado o composto N^4-benzil-N^2-fenilquinazolina-2,4-diamina **PH100** como inibidor não covalente das enzimas cruzaína e T*br*CATL. Neste trabalho é descrita a síntese de quatro intermediários-chave para obtenção dos quatro estereoisômeros do composto **2**, assim como a síntese dos quatro possíveis estereoisômeros deste composto. A síntese de nove análogos de **PH100** também é descrita. Os building blocks foram sintetizados a partir do furfural ou ácido furóico, utilizando reagentes comerciais. Inicialmente, o furfural foi convertido em ácido furanilpropenóico através da reação de Doebner. Este ácido foi descarboxilado resultando em um vinilfurano, que foi submetido à dihidroxilação assimétrica de Sharpless, fornecendo um glicol *S* ou *R*. A proteção das hidroxilas foi seguida de uma SN2 com NaN_3 resultando no derivado azido álcool, estereoespecificamente, com inversão da configuração. Reduzimos o grupamento azido para obter um aminoálcool, que foi protegido com $(Boc)_2O$ e em seguida sua hidroxila foi ativada com TsCl. Em seguida, substituímos o grupamento OTs por um grupamento azido em reação com NaN_3. Posteriormente o grupo Boc foi removido e o anel piperidina foi formado. O grupamento azido foi reduzido, resultando no derivado de diamina **11***S* ou *R*, totalizando doze etapas para cada estereoisômero *S* ou *R*. Para obter os outros dois building blocks começamos com o ácido furóico **17** sendo acoplado ao *S*- ou *R*-2-amino-3-metilbutanoato de metila. Convertemos este éster a ácido carboxílico, e logo após ao éster ativado 2,5-dioxopyrrolidin-1-yl 2-(furan-2-carboxamido)-3-metilbutanoato (**20***R* ou *S*). Finalizamos a rota realizando o acoplamento dos building blocks **11***S* ou *R* e **20***R* ou *S*, em diferentes reações, resultando nos quatro estereoisômeros do composto **2**. Os compostos foram caracterizados por seus espectros no IV e RMN.

Palavras-chave: Doença de Chagas; HAT; cruzaína; T*br*CATL; síntese assimétrica.

ABSTRACT

Chagas disease and Human African trypanosomiasis (HAT) are neglected diseases, whose etiological agents are *Trypanosoma cruzi* and *Trypanosoma brucei*, respectively. One of the validated drug target class for the treatment of these diseases are proteases, such as cruzain, the main *T. cruzi* cysteine protease and T*br*CATL for *T. brucei*. After a screening, using docking and High-throughput screening (HTS), the chiral compound *N*-(1-((2-(furan-2-yl)-2-(piperidin-1-yl)ethyl)amino)-3-methyl-1-oxobutan-2-yl)furan-2-carboxamide **2** was identified as a non-covalent inhibitor of cruzain. In another computational trial, with commercially available compounds from database, N^4-benzyl-N^2-phenylquinazoline-2,4-diamine **PH100** was identified as non-covalent inhibitor for cruzain and T*br*CATL. In this work, we described the synthesis of four building blocks to obtain the four stereoisomers of **2**, as well as the synthesis of these four stereoisomers. The synthesis of nine **PH100** derivatives is described too. The building blocks were synthesized in several steps starting from furfural or 2-furoic acid and using commercially available reagents. First, furfural was converted to furanylpropenoic acid by Doebner reaction. This acid was decarboxylated providing vinylfuran, that was submitted to asymmetric Sharpless dihydroxylation providing *S* or *R* enantiomer glycol. Protection of hydroxyl groups followed by reaction with NaN_3 provided the azido alcohol derivative, stereospecifically with inversion of configuration. We proceeded reducing the azido group to obtain an amino alcohol. This amino was protected with $(Boc)_2O$ and then the hydroxyl was activated with TsCl. Next, we replaced the OTs with NaN_3 and then the Boc group was removed. At last, we made the formation of a piperidine ring and the azido group was reduced resulting in the diamine derivative **11***S* or *R* in 12 steps for each stereoisomer. To obtain the two another building blocks to synthesize **2** stereoisomers, we started with 2-furoic acid **17** being coupled to *S*- or *R*- methyl 2-amino-3-methylbutanoate. After, we convert the ester to carboxylic acid resulting in *S*- or *R*-2-(furan-2-carboxamido)-3-methylbutanoic acid **19**. At last, we coupled the building blocks **11***S* or *R* and **20***R* or *S* affording four stereoisomers of compound **2**. Compounds were characterized by its IR and NMR spectra.

Keywords: Chagas disease; HAT; cruzain; T*br*CATL; asymmetric synthesis.

Lista de Figuras

A lista de figuras desta seção, que na tese defendida ocupa o intervalo de páginas 15-23, foi parcialmente suprimida por tratar-se de informações para publicação em periódico científico. As figuras suprimidas constam da descrição de todos os métodos de síntese utilizados para obter os compostos descritos neste trabalho.

Lista de Abreviaturas

Asn182	Asparagine 182
BOC	Tert-Butyloxycarbonyl
$(BOC)_2O$	Di-Tert-Butyl Dicarbonate
BBB	Blood Brain Barrier
BHE	Barreira Hematoencefálica
BSA	Albumina do Soro Bovino
CC_{50}	50% cytotoxic concentration
$CDCl_3$	Deuterated Chloroform
CH_3COCl	Acetyl Chloride
CH_2Cl_2	Dichloromethane
CH_3Cl	Chloroform
CD_3OD	Deuterated Methanol
CO_2	Carbon Dioxide
COSY	Homonuclear Correlation Spectroscopy
Cs_2CO_3	Cesium Carbonate
Cu_2O	Óxido De Cobre II
$CuSO_4.5H_2O$	Copper Sulfate Pentahydrate
Cys25	Cysteine 25
d	Doublet
dd	Doublet of Doublets
DIAD	Diisopropyl Azodicarboxylate
DIPEA	*N,N*-Diisopropylethylamine
DMA	*N,N*-Dimethylaniline
DMAP	4-dimethylaminopyridine
DMF	*N,N*-dimethylformamide
DCM	Dichloromethane
DMSO	Dimethyl Sulfoxide
DMSO-*d*6	Deuterated DMSO
E64	L-trans-epoxissuccinil-leucilamido (4-guanidino) butano
EC_{50}	Half Maximal Effective Concentration
EDC	1-Ethyl-3-(3-dimethylaminopropyl)carbodiimide
ESI	Electrospray Ionization

Et_3N	triethylamine
EtOH	ethanol
HMBC	Heteronuclear Multiple Bond Correlation
HCl	Hydrochloric Acid
His162	Histidine 162
HPLC	High Performance Liquid Chromatography
HRMS	High-Resolution Mass Spectrometry
HSQC	Heteronuclear Single Quantum Correlation
HTS	High-Throughput Screening
HTVS	High Throughput Virtual Screening
Hz	Hertz
IC_{50}	Half Maximal Inhibitory Concentration
ICH_3	Iodomethane
IR	Infrared spectrometry
IV	Infravermelho
IS	Índice de Seletividade
J	Coupling Constant
K_2CO_3	Potassium Carbonate;
Ki	Constante de inibição
$K_3Fe(CN)_6$	Potassium hexacyanoferrate(III)
KOH	Potassium hydroxide
$K_2OsO_2(OH)_4$	Potassium osmate(VI) dihydrate
LiOH	Lithium Hydroxide
m	Multiplet
MeOH	Methanol
MHz	Megahertz
MW	Molecular Weight
$NaBH_4$	Sodium Borohydride
$NaHCO_3$	Sodium Bicarbonate
NaN_3	Sodium Azide
NaOH	Sodium Hydroxide
Na_2SO_4	Sodium Sulfate
NHS	N-hidroxissuccinimida
NMR	Nuclear Magnetic Resonance

PDB	Protein Data Bank
$Pd(OAc)_2$	Palladium(II) Acetate
PM	Peso Molecular
PPh_3	Triphenylphosphine
ppm	Parts Per Million
$POCl_3$	Phosphoryl Chloride
PTLC	Preparative Thin-Layer Chromatography
Py	Pyridine
q	Quartet
quint	Quintet
REA	Relação Estrutura Atividade
RMN	Ressonância Magnética Nuclear
rt	Room Temperature
s	Singlet
SAR	Structure−Activity Relationship
SFB	Serum Fetal Bovine
sl	Singlet Large
t	Triplet
ta	Temperatura Ambiente
td	Triplet of Doublets
T. brucei	*Trypanosoma brucei*
T. cruzi	*Trypanosoma cruzi*
THF	Tetrahydrofuran
TLC	Thin-Layer Chromatography
TMS	Tetramethylsilane
TsCl	*p*-Toluenesulfonyl chloride
UV	Ultraviolet
Z-FRAMC	Z-Phe-Arg-aminomethylcoumarin
δ	Chemical Shifts

Sumário

1 Introdução

As doenças tropicais negligenciadas são endêmicas afetando mais de um bilhão de pessoas em todo o mundo. As condições de pobreza, como falta de saneamento adequado e contato próximo com vetores infecciosos, estão diretamente relacionadas a essas infecções. Dentre este grupo encontram-se as tripanossomíases, Doença de Chagas e Doença do Sono Africana, ambas causadas por tripanossomatídeos. *Trypanosoma cruzi* é o agente causador da doença de Chagas, enquanto o *Trypanosoma brucei* causa a Doença do Sono Africana. Estas tripanossomíases se apresentam em fase aguda e crônica, na qual a fase crônica é mais sintomática e onde ocorrem os maiores agravos ao paciente. Nifurtimox (Lampit®) e benznidazol (Rochagan®) são os fármacos disponíveis para o tratamento da Doença de Chagas, ambos estando em uso há mais de 5 décadas, com mecanismos de ação baseados na ação de radicais livres inespecíficos para o parasito e com baixa eficácia na fase crônica e sintomática da enfermidade. Para Doença do Sono dispomos de 2 opções de tratamento para fase aguda: pentamidina (NebuPent®), suramina (Germanin®) e duas opções de tratamento para fase crônica: melarsoprol (Arsobal®) e eflornitina (Ornidyl®). Desde 2019 há uma nova opção de tratamento apenas para casos causados pelo *T. b. gambiense*, o fármaco fexinidazol.

Em comum estas parasitoses apresentam como suas principais cisteíno-proteases cruzaína e T*br*CATL (rodesaína), enzimas que apresentam alta homologia em suas estruturas primárias, assim como em seus sítios ativos. Ambas são alvos terapêuticos validados e realizam papéis fundamentais para a sobrevivência do parasito no hospedeiro. Diversos estudos utilizando as estruturas tridimensionais disponíveis destas enzimas foram desenvolvidos na busca por seus inibidores, tendo sido identificados muito compostos promissores. Em uma parceria, nosso grupo de pesquisa desenvolveu duas frentes de investigação com base em estudos computacionais utilizando estas enzimas como alvos terapêuticos. Nestes estudos trabalhamos com dois candidatos a inibidores enzimáticos, uma quinazolina que foi ativa para ambas as enzimas e um composto difuranil quiral que foi investigado somente para cruzaína. O composto quinazolínico foi priorizado em um estudo utilizando o *Malária Box* como fonte de compostos, por suas boas atividades frente cruzaína e T*br*CATL. Diante destes resultados investimos em estudos computacionais

na busca por duas séries de análogos deste composto. Como resultado do *High Throughput Virtual Screening* (HTVS) obtivemos uma vasta gama de compostos, os quais foram selecionados chegando a um grupo de compostos chaves que foram objeto de um estudo de Docking XP, pela qual uma análise minuciosa dos candidatos a análogos foi conduzida. Foi proposta uma série primária de 10 compostos, resultando em um composto com IC_{50} (*Half Maximal Inhibitory Concentration*) frente a cruzaína de 2,4 µM e um EC_{50} (*Half Maximal Effective Concentration*) de 0,5 µM para *T. cruzi*. Infelizmente, ao avaliar se o composto realizava somente inibição competitiva foi identificado alto potencial na formação de agregados moleculares, indicando inibição dual e/ou inespecífica. Este perfil de inibição foi observado para a maioria dos compostos da série, estando diretamente relacionado aos compostos com clogP próximo a 5 e contendo substituintes mais hidrofóbicos. Diante destes resultados foi proposta uma otimização baseada na estrutura destes compostos obtendo uma nova série de nove compostos, focando em substituintes mais polares, com a finalidade de evitar inibição inespecífica. Nesta série secundária nenhum composto demonstrou propriedades agregantes e as atividades enzimáticas e tripanocidas foram mantidas. Em outro estudo virtual um composto difuranil quiral foi identificado como potencial inibidor de cruzaína. Na série destes compostos quirais foi realizada a síntese de quatro estereoisômeros deste composto em 16 passos de síntese, sua caracterização e elucidação estrutural.

2 Revisão do Tema

2.1 Doenças Tropicais Negligenciadas

As doenças tropicais negligenciadas (DNTs) são endêmicas principalmente entre populações carentes, afetando mais de um bilhão de pessoas em todo o mundo[1]. As condições de pobreza, como falta de saneamento adequado e contato próximo com vetores infecciosos, estão diretamente relacionadas a essas infecções[2]. A doença de Chagas é uma DTN prevalente na América Latina, a qual afeta entre 6-7 milhões de pessoas no mundo[2,3](Figura 1). O agente etiológico desta doença é o protozoário *Trypanosoma cruzi*, que possui três estágios de vida: epimastigota, presente no vetor (triatomíneo); amastigota, forma intracelular e replicativa e tripomastigota, forma infectante e circulante no sangue[4]. Esta parasitose se divide em dois estágios: fase aguda e crônica. A fase aguda é tipicamente assintomática, apesar da alta carga parasitária no sangue do hospedeiro, persistindo por 4-8 semanas. Nesta fase os parasitos utilizam diversos mecanismos para evadir a resposta imune, a fim de estabelecer a infecção no organismo. Há relatos de que o *T. cruzi* é capaz de modular vias de sinalização em células de mamíferos[5]. O *T. cruzi* evade a resposta imune do hospedeiro através da variação antigênica e da ação de proteases, evitando a lise e opsonização mediadas pelo sistema complemento, obtendo condições ideais para estabelecer a infecção. Esta persistência a longo prazo nos tecidos acarreta na evolução para a fase crônica[6], que geralmente dura toda a vida do hospedeiro. Após driblar a resposta imune celular e humoral o parasito invade fagócitos onde persiste e se multiplica formando os chamados ninhos de amastigotas. Neste processo estímulos imunológicos são produzidos ocasionando dano tecidual e a resposta inflamatória através do mimetismo molecular, acarretando na produção de autoanticorpos[6]. Como consequências desta fase, temos o crescimento anormal de órgãos do sistema digestivo e/ou do coração, sendo a miocardite a principal causa de morte[7].

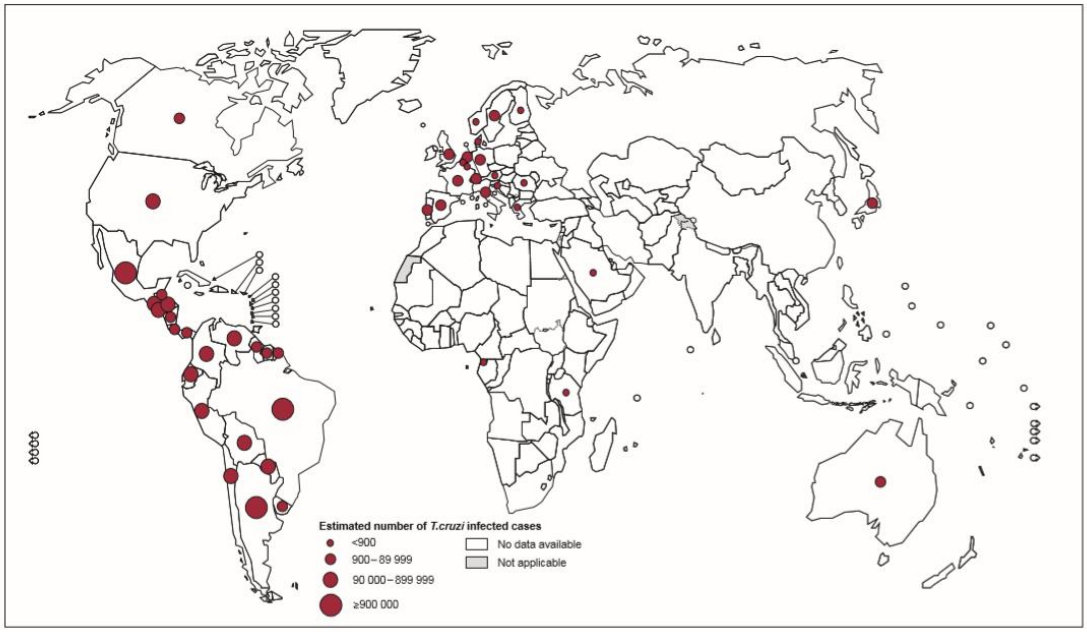

Figura 1 – Distribuição global de casos da Doença de Chagas em todo o mundo, com base em estimativas da Organização Mundial de Saúde em 2018. Fonte: Organização Mundial de Saúde.

Neste mesmo contexto de doenças tropicais negligenciadas temos a tripanossomíase humana africana (HAT), conhecida mais popularmente como doença do sono africana. Esta parasitose é causada por outro protozoário do gênero *Trypanosoma*, podendo ser causada por duas subespécies diferentes de *Trypanosoma brucei*: *T. brucei gambiense* e *T. brucei rhodesiense*. A transmissão acontece mediante picada da mosca tsé-tsé *(glossina spp*). Esse parasito possui quatro estágios de vida: tripomastigota metacíclico (forma infecciosa), tripomastigota (forma de multiplicação em fluidos como sangue e linfa no hospedeiro), epimastigota (vetor) e tripomastigota procíclico (formas de multiplicação presentes apenas no vetor)[1,8]. A parasitose tem duas fases: aguda ou hemolinfática, que pode persistir por meses e causar febre e linfoedemopatia; e a fase crônica ou neurológica, na qual o parasito atravessa a barreira hematoencefálica (BHE) causando alterações no sono, distúrbios psiquiátricos e sensoriais que podem levar à morte[9]. Mais de 98% dos casos de HAT são causados por *T. b. gambiense*, ocorrendo em 24 países da África Subsaariana, onde 57 milhões de pessoas vivem em áreas de risco de contaminação[10]. Em 2009, houve uma diminuição de novos casos de HAT, e pela primeira vez foram relatados menos de 10.000 casos em um ano[2].

Para a doença de Chagas, existem dois medicamentos disponíveis como tratamento: nifurtimox (Lampit®) e benznidazol (Rochagan®), no entanto, esses

medicamentos estão sendo usados para tratar essa doença há mais de 5 décadas e seus mecanismos de ação ainda não estão totalmente esclarecidos[11,12] (Figura 2).

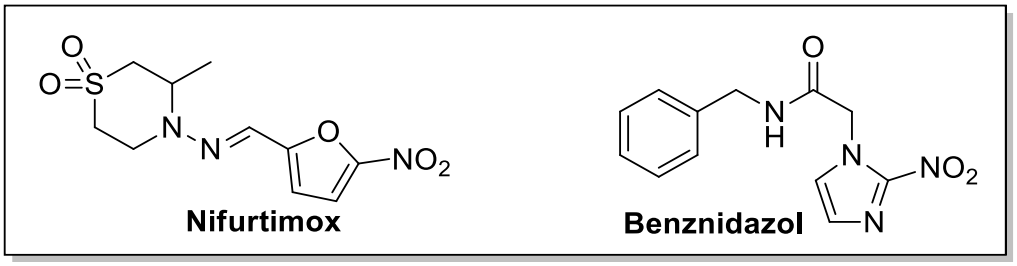

Figura 2 – Nifurtimox e benznidazol, fármacos disponíveis para o tratamento da Doença de Chagas.

Ambos são considerados pró-fármacos, sendo ativados pelas nitroredutases e atuando pela formação de radicais livres, resultantes da bioredução do grupo nitro. Esses efeitos tripanossomicidas foram atribuídos a essas espécies radicais, devido a mecanismos complexos que envolvem sua reação com lipídios, proteínas e DNA do *T. cruzi*[13,14]. Os radicais livres e os metabólitos eletrofílicos formados por esses fármacos não são específicos para o parasito, sendo também prejudiciais às células do hospedeiro. Essa baixa seletividade causa diversos efeitos adversos graves[15–17], que muitas vezes ocasionam em abandono do tratamento[18]. Além disso, estes fármacos apresentam baixa eficácia na fase crônica da doença[19], não sendo capazes de eliminar completamente o parasito e estão associados a múltiplos casos de resistência ao longo dos anos[20]. O diagnóstico geralmente é feito no estágio crônico, durante o qual os tratamentos disponíveis são menos eficazes.

Os medicamentos disponíveis para o tratamento da HAT são: pentamidina (NebuPent®), suramina (Germanin®), melarsoprol (Arsobal®) e eflornitina (Ornidyl®) (Figura 3). Pentamidina e suramina podem ser utilizadas apenas na fase aguda da doença, pois não atravessam a BHE para tratar os sintomas neurológicos comuns na fase crônica[21,22]. Acredita-se que diaminas como a pentamidina interferem nos mecanismos nucleares, inibindo a síntese de DNA e RNA interferindo nos processos de replicação e transcrição, enquanto a suramina apresentou inibiucao de enzimática justificando sua atividade tripanocida, sendo ativa frente enzimas como diidrofolato redutase, timidina quinase e enzimas glicolíticas[23,24]. O melarsoprol e a eflornitina são capazes de atravessar a BHE e podem ser utilizados na fase crônica, no entanto, esses medicamentos apresentam importantes limitações em termos de eficácia, desenvolvimento de resistência e toxicidade para o paciente[22,25,26]. Eflornitina age

através da inibição da síntese de poliaminas, agindo na ornitina descarboxilase, enquanto o merlasoprol não possui seu mecanismo de ação elucidado[23], sabe-se que há afinidade por grupos sulfidrila em proteínas, por apresentar arsênico trivalente em sua estrutura apresenta alta toxicidade[25], como encefalopatia[27]. Essas informações reforçam a ideia de que existe uma grande necessidade de desenvolvimento de novos fármacos capazes de tratar essas doenças, evitando efeitos adversos e aumentando a qualidade de vida do paciente e sua adesão ao tratamento[28]. Em 2018 foi aprovado pelo *European Medicines Agency* (EMA) o primeiro medicamento de uso oral para HAT, desenvolvido pelo *Drugs for Neglected Diseases initiative* (DNDi) em parceria com a Sanofi[29,30]. Foi necessária uma década de pesquisas até a aprovação no EMA e o desenvolvimento deste medicamento foi possível graças ao incentivo de diversas instituições públicas e privadas para o financiamento de pesquisas para DTNs, demonstrando que com incentivo é possível desenvolver novas terapias para estas enfermidades. O medicamento foi aprovado com o nome de Fexinidazol Winthrop® e é produzido pela Sanofi, sendo um derivado 5-nitroimidazol, que não possui um mecanismo de ação totalmente eluciadado, mas é sugerido que ocorre ativação via nitrorredutases[29,31]. Na figura 3 constam todas as estruturas dos fármacos disponíveis para o tratamento da HAT.

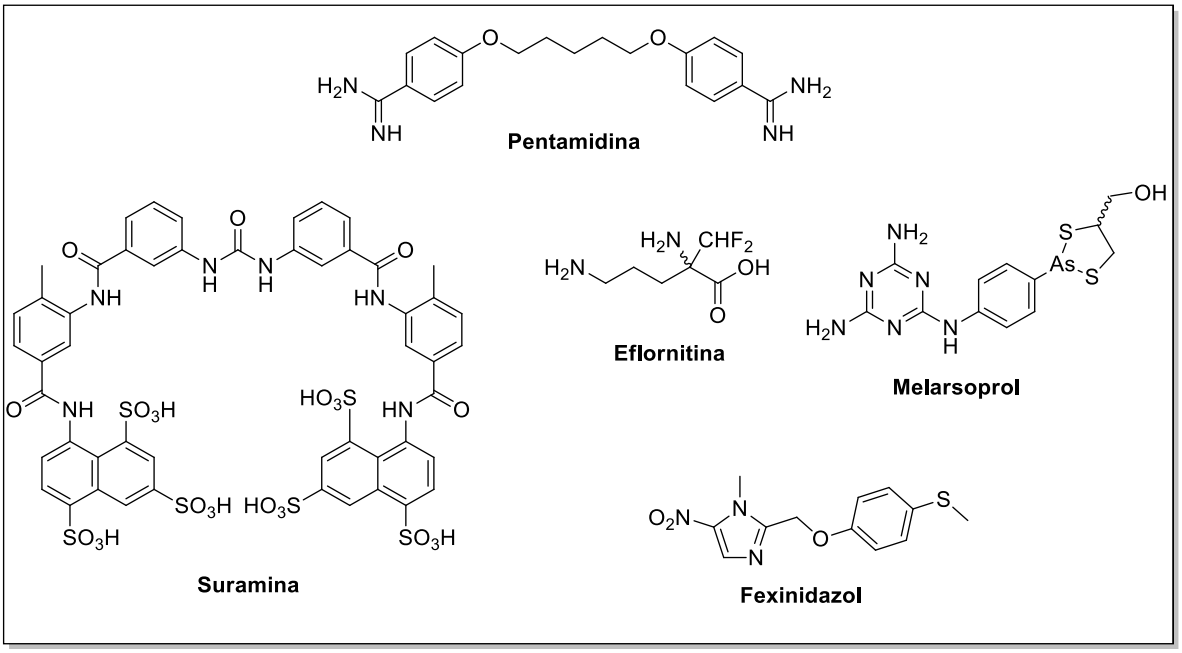

Figura 3 – Estrutura dos fármacos utilizados no tratamento da HAT: Pentamidina, suramina, melarsoprol, eflornitina e fexinidazol.

2.2 Cisteíno-Proteases e seus Inibidores

Uma estratégia potencial para o tratamento de doenças parasitárias é a síntese de compostos que inibem seletivamente enzimas cruciais para os parasitos[32]. Uma das classes de alvos validados para o desenvolvimento de medicamentos para o tratamento destas doenças são as proteases, devido à sua importância para a sobrevivência do parasito no hospedeiro[4]. Dentro desta classe de proteases, a inibição de cisteíno-proteases é uma estratégia promissora para o desenvolvimento de novos fármacos anti-trypanosoma. A enzima cruzaína é a principal cisteíno-protease do *T. cruzi*, presente em todas as suas formas de vida, importante na aquisição de nutrientes, invasão de macrófagos por tripomastigotas, evasão da resposta imune, proliferação, e sobrevivência no hospedeiro[18,33,34]. Cruzaína é considerada um alvo molecular validado para o desenvolvimento de seus inibidores como opções de tratamento para doença de Chagas por conta do efeito antiparasitário observado *in vitro* associado à inibição da enzima[5]. Esta validação ocorre somente de forma química, visto que não é possivel confirmar a essencialidade da enzima através do nocaute do gene por se tratar de múltiplas cópias[35]. Em 1995, McGrath e colaboradores publicaram a primeira estrutura 3D da cruzaína complexada com um inibidor irreversível de peptídeos (Z-Phe-Ala-fluorometiletilcetona **1**), através de cristalografia por difração de raios-X (Figura 4). Este estudo demonstrou que a cruzaína possui 215 aminoácidos em sua estrutura, organizados em dois domínios: um predominantemente formado por α-hélices e o outro por folhas β antiparalelas. Entre esses domínios, encontra-se seu sítio ativo, formado pelos resíduos cisteína 25, histidina 159 e asparagina 175.

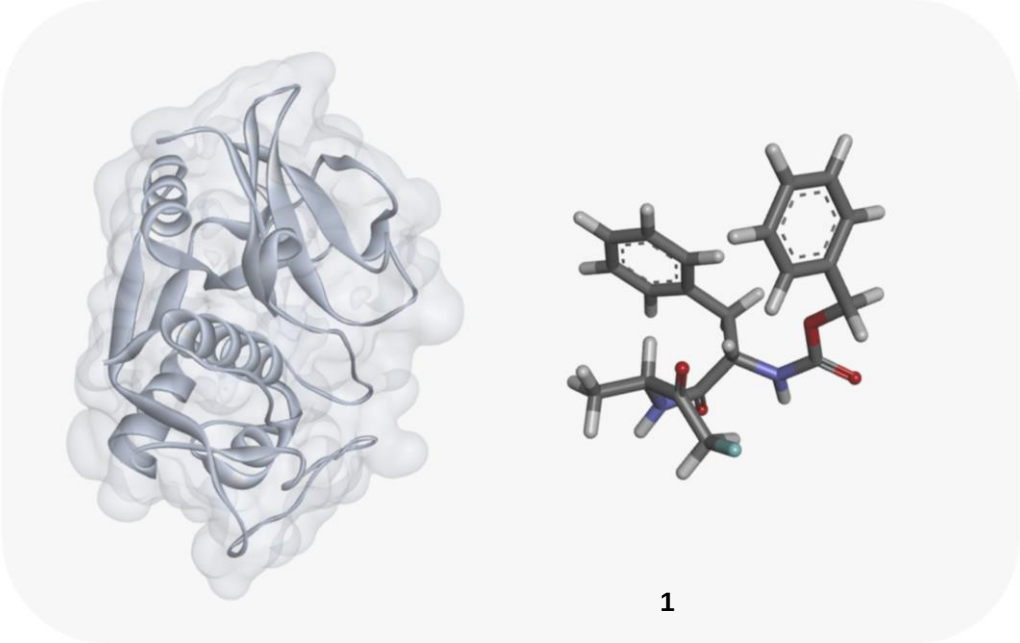

Figura 4 – Estrutura 3D da cruzaína e do inibidor irreversível de peptídeos Z-Phe-Ala-fluorometiletilcetona **1**. PDB ID: 1ME3. Figura preparada através do software BIOVIA Discovery Studio Visualizer 2020 (BIOVIA, 2019).

A principal cisteíno-protease do *T. brucei* é a T*br*CATL, popularmente conhecida como rodesaína, termo que atualmente está em desuso[36]. Esta enzima é essencial no processo de infecção, evasão da resposta imune do hospedeiro e essencial para o parasito ser capaz de atravessar a BHE e causar os sintomas neurológicos e mais graves durante a fase crônica[37,38]. Ambas as enzimas têm suas estruturas cristalográficas publicadas[32,39] e, comparando suas estruturas primárias, foi observada uma homologia de 70% dentre elas (Figura 5). A publicação dessas estruturas estimulou o desenvolvimento racional de várias classes de inibidores dessas enzimas e, devido a essa alta homologia, é provável que inibidores de uma das enzimas também inibam a outra[20].

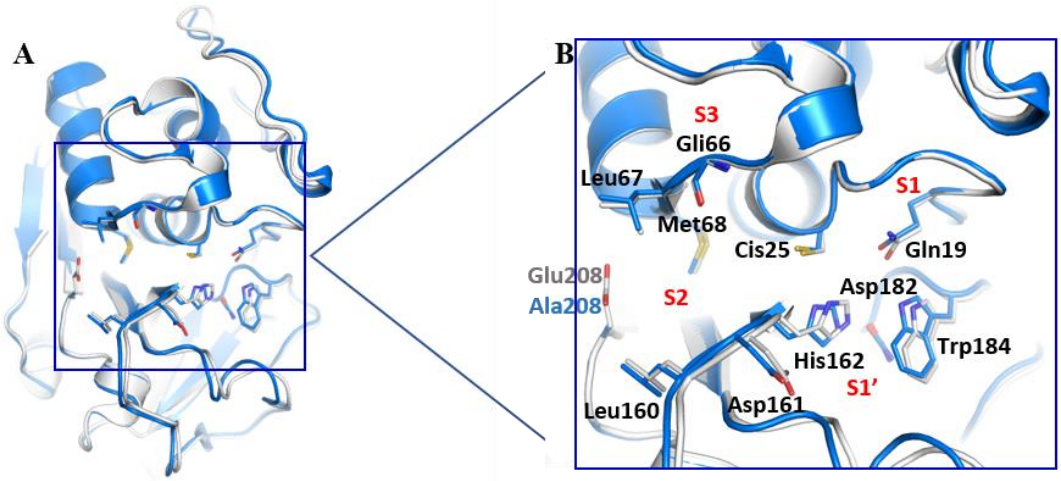

Figura 5 – Comparação das estruturas cristalográficas de cruzaína e T*br*CATL: A) Sobreposição de cruzaína e T*br*CATL; B) Sobreposição dos resíduos de aminoácidos de seus sítios ativos. Fonte: Figura preparada por Elany Barbosa Silva.

Na busca por candidatos a inibidores destas enzimas diversas classes de moléculas foram estudadas e avaliadas, dentre estes inibidores enzimáticos, as vinilsulfonas são a classe de maior destaque, sendo estudadas desde 1995[40]. Estes compostos são inibidores enzimáticos covalentes e irreversíveis, classificados como aceptores de Michael. Seu mecanismo de ação consiste na ligação covalente a enzima através de um ataque nucleofílico da cisteína 25 do sítio ativo da enzima ao centro eletrofílico destes inibidores[41]. Alguns compostos desta classe se destacaram como K02: com boas atividades contra epimastigotas de *T. cruzi*[42], camundongos infectados com o parasito[43] e sua estrutura foi obtida por cristalografia complexada a T*br*CATL[44]. Com base na estrutura do K02, o composto K777 foi desenvolvido e demonstrou melhora na atividade em relação a K02, apresentando atividade frente cruzaína e T*br*CATL[39], tripanossomicida para tripomastigotas *in vitro*[45]. Ensaios de metabolismo em microssomas hepáticos[46] e de perfis farmacocinéticos em camundongos[43,47] e cães[48] também foram realizados, confirmando o potencial da classe. Com base na estrutura destas vinilsulfonas mais promissoras, vários derivados foram desenvolvidos almejando obter melhores propriedades[49–55]. Entre os derivados mais promissores encontrados estão os derivados de nitroalquenos nos quais a porção vinilsulfona foi substituída por este grupo e também os derivados peptideomiméticos vinil heterocíclicos (PVHIs)[56,57]. Ambas as classes demonstraram boas atividades frente as enzimas, sendo inibidores reversíveis, apresentando-se como promissoras novas classes de inibidores enzimáticos a serem estudadas.

Dentre as outras classes estudadas, destacam-se: tiossemicarbazonas[58–60], compostos que possuem baixo peso molecular e custo de produção, alinhados com mecanismo de inibição covalente reversível[61]; tiazóis e tiazolidinas[17,62–64]; derivados contendo nitrilas[20,65–69]; bromoisoxazolinas[70–72] e outros[73–76] (Figura 6).

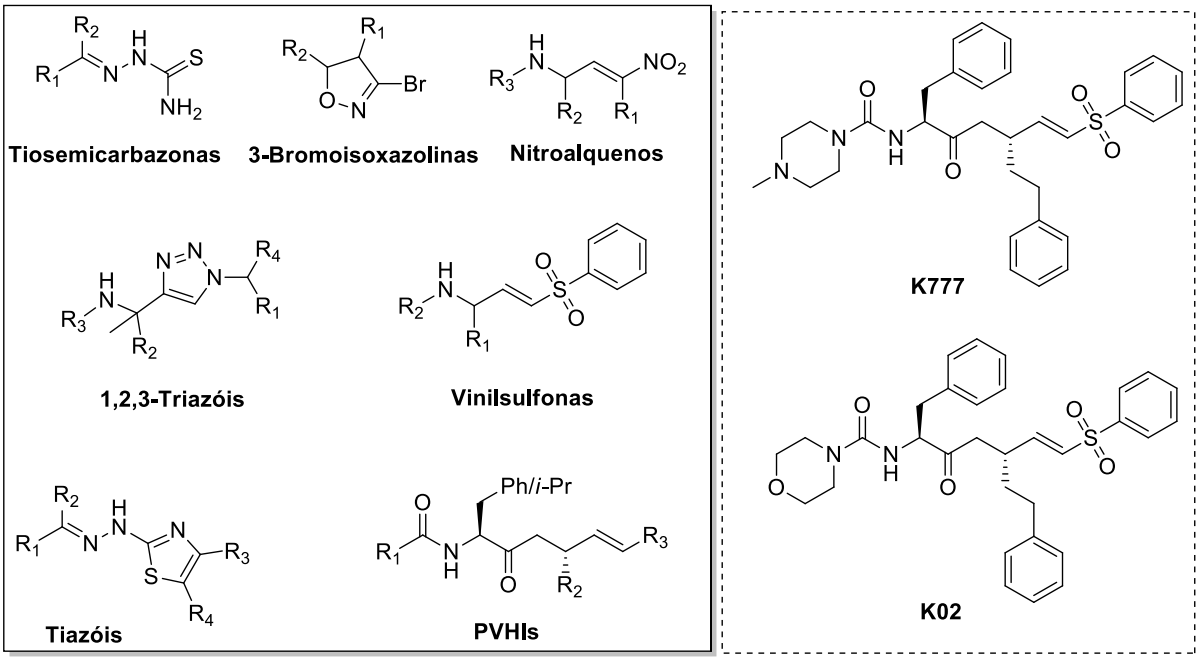

Figura 6 – Estrutura geral das principais classes de inibidores de cruzaína e rodesaína, destacando **K777** e **K02**.

Em geral é preferível identificar inibidores não covalentes para evitar possíveis causas de toxicidade, sendo a identificação de novos inibidores não covalentes de cruzaína e T*br*CATL de grande importância na busca de novos fármacos para tratar essas doenças.

2.3 Identificação de Potenciais Inibidores de Cruzaína e T*br*CATL em nosso Grupo de Pesquisa em parceria com a UFMG.

Em 2010, Ferreira e colaboradores[77] realizaram um estudo de triagem computacional utilizando *High Throughput Screening* (HTS), pelo qual foram analisados em torno de 200 mil compostos. Após a utilização de diversos filtros como retirada de compostos com peso molecular superior a 500 g/mol, inibidores inespecíficos e formadores de agregados, 5 classes de inibidores de cruzaína (Figura

7) foram selecionadas. Estes compostos demonstraram potenciais atividades frente a cruzaína não sendo ativos frente a enzima homóloga a cruzaína em humanos.

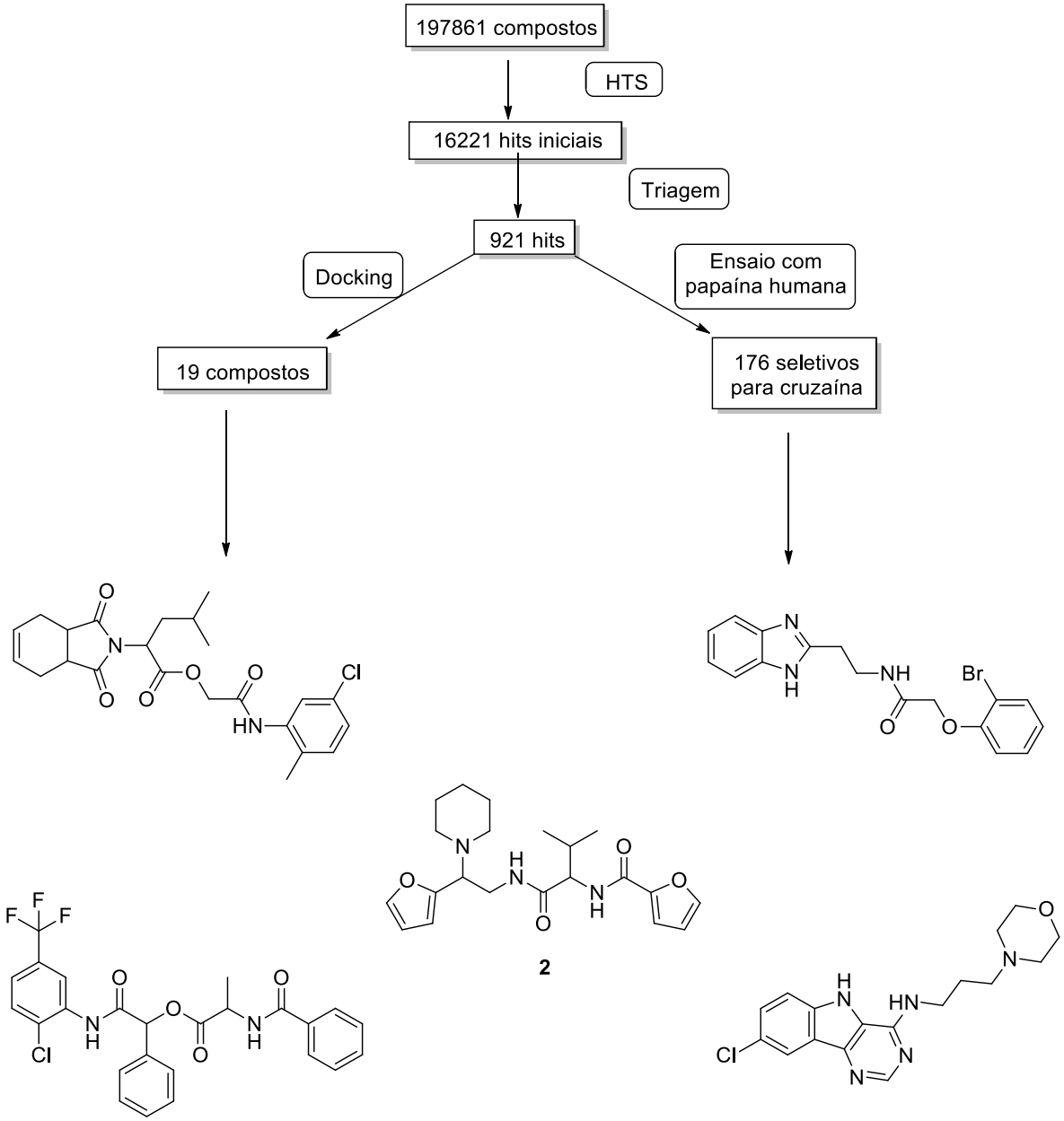

Figura 7 – Demonstração das sucessivas etapas de triagem feitas utilizando *Docking* e HTS de modo paralelo resultando em 5 classes de inibidores competitivos de cruzaína, incluindo o composto selecionado para nosso estudo (**2**).

Dentre estes compostos, temos o composto quiral N-(1-((2-(furan-2-il)-2-(piperidin-1-il)etil)amino)-3-metil-1-oxobutan-2-il)furan-2-carboxamida **2** que apresenta dois estereocentros em sua estrutura, podendo ser obtido como quatro estereoisômeros diferentes (Figura 8). Neste estudo o composto **2** foi adquirido da

base ZINC, possivelmente como uma mistura dos 4 estereoisômeros, já que não havia indicação contrária. Considerando que a atividade dos diferentes estereoisômeros é geralmente bastante variável, é provável que o estereoisômero mais potente dentre os quatro possíveis seja muito mais ativo do que a mistura que já mostrou uma atividade muito relevante neste estudo de 2010 (IC_{50} de 6 µM frente a enzima cruzaína).

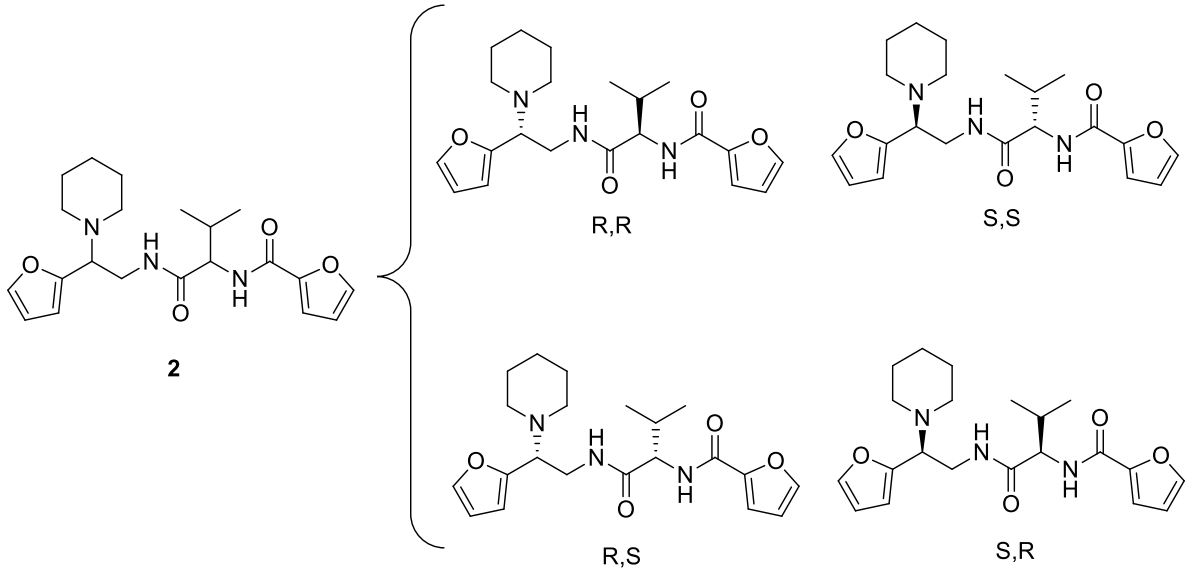

Figura 8 – Estruturas dos quatro estereoisômeros possíveis do composto **2**.

Em outro estudo com intuito de identificar possíveis inibidores não-covalentes para cruzaína e T*br*CATL foram avaliados cerca de 400 compostos advindos sem custos do Malária Box[78]. Neste estudo foram selecionados alguns inibidores competitivos potenciais de ambas as enzimas, dentre estes o composto quinazolínico N^4-benzil-N^2-fenilquinazolina-2,4-diamina, denominado no presente trabalho de **PH100** (Figura 9). O composto **PH100** pertence a uma classe química da qual fazem parte os fármacos antitumorais inibidores de tirosina-quinase, gefitinibe e erlotinibe. Temos relatos na literatura de uma série de atividades relacionadas a classe das quinazolinas, como atividades antitumorais[79,80], antiparasitárias[81–84,] antimicrobiana[85,86] e antivirais[87,88].

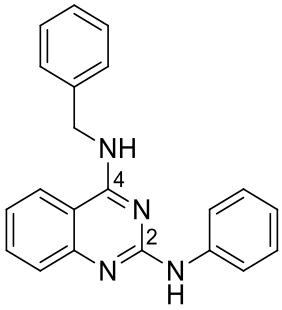

PH100

Figura 9 – Estrutura do composto **PH100**.

Devido ao potencial já demonstrado pela classe de quinazolinas, aliado aos resultados do composto **PH100** frente a cruzaína nestes estudos, foi realizada uma triagem virtual (*High Throughput Virtual Screening* - HTVS) para identificar análogos do **PH100** a serem sintetizados. Nesta triagem virtual foram utilizados três núcleos diferentes: quinazolina, purina e pirimidina sendo combinadas a 94 diferentes aminas, como resultado 280.166 compostos foram encontrados. No passo seguinte foi aplicado um filtro de peso molecular (PM) priorizando compostos com PM inferior a 350 g/mol, devido à possibilidade de apresentarem melhores propriedades farmacocinéticas. Após esse filtro foram obtidos 67.221 compostos, entre os quais 3.365 eram derivados quinazolínicos. Dentre este grupo de quinazolinas 5% dos compostos (47) mais bem pontuados foram submetidos a um estudo de docking XP, pelo qual uma análise minuciosa dos candidatos a análogos foi conduzida (Figura 10)[89].

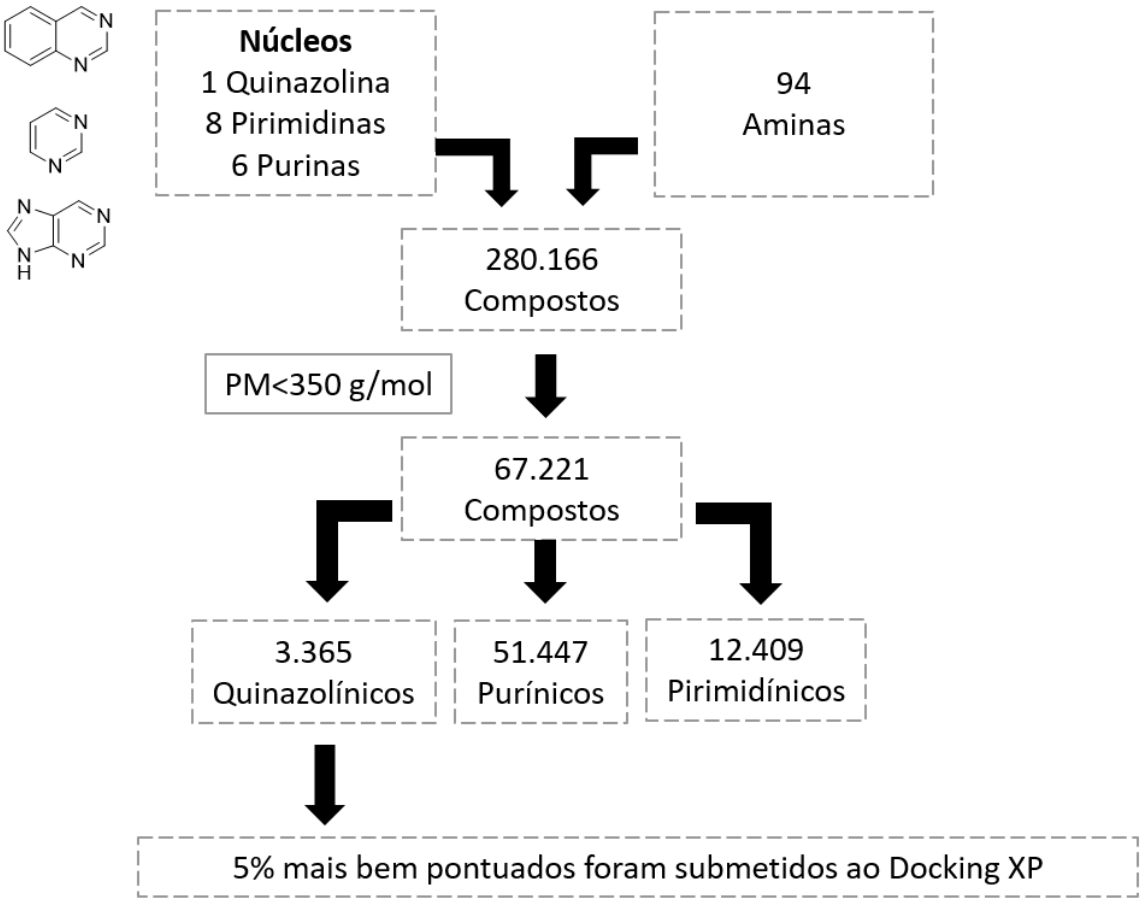

Figura 10 – Triagem Virtual e construção da biblioteca de potenciais inibidores de cruzaína e T*br*CATL.

Após análise minuciosa das poses destes compostos chave, bem como dos grupos substituintes mais frequentes nos derivados com poses consistentes com modos de interação já conhecidos para a enzima, foram priorizados 6 derivados quinazolínicos para síntese, além do composto **PH100**. Utilizando estratégias clássicas de modificação molecular outros 4 derivados foram desenhados, além dos derivados purínicos e pirimidínicos para comparação, totalizando 14 compostos para síntese. Nesta triagem foram priorizados compostos com o mesmo padrão de substituição de **PH100**, com aminas como substituintes nas posições 2 e 4 do anel quinazolínico, sendo esta série primária somente com variações na posição 2. Na série primária destes compostos **PH100** e **PH107** (derivado contendo uma *para*-cloroanilina na posição 2) demonstraram as melhores atividades frente a enzima e ao parasito, não apresentando toxicidade significativa. **PH100** apresentou um IC_{50} frente a cruzaína de 8 µM, inibição da enzima de 94% e um EC_{50} de 0,047 µM para *T. cruzi*. Além disso, o composto não demonstra importante citotoxicidade frente a mioblastos

C212 com Índice de Seletividade (IS) de 211. Enquanto **PH107** apresentou um IC_{50} frente a cruzaína de 2,4 µM, inibição da enzima de 78% e um EC_{50} de 0,5 µM para *T. cruzi*. Também sem apresentar citotoxicidade e com IS de 21. Ao sintetizar análogos estruturais destes compostos mais ativos da série primária promovendo a troca do núcleo quinazolínico por um núcleo purínico ou pirimidínico ocorreu perda da atividade dos compostos. Estes dados demonstram que o núcleo quinazolínico foi essencial para atividade destes compostos[89]. Com base nos dados obtidos foram propostas avaliações quanto a propriedades de inibição inespecífica desta série primária e após a análise destes resultados foi proposta uma nova série de compostos com uma otimização baseada na estrutura.

2.4 Objetivos

2.4.1 Objetivos Gerais

Sintetizar compostos planejados via modelagem molecular e avaliar suas atividades frente cruzaína e T*br*CATL, a fim de identificar novas entidades químicas com potencial para tratar Doença de Chagas e Doença do Sono Africana.

2.4.2 Objetivos Específicos

a) Sintetizar 9 análogos quinazolínicos com variação na posição 4 baseados em atividades previamente relatadas.

b) Avaliar a atividade inibitória dos compostos quinazolínicos frente as enzimas cruzaína e T*br*CATL.

c) Avaliar as atividades *in vitro* dos compostos quinazolínicos contra formas amastigotas de *T. cruzi e T. b. brucei*.

d) Avaliar a citotoxicidade dos compostos quinazolínicos frente a mioblastos C2C12.

e) Padronizar e sintetizar rota sintética para obtenção dos quatro *building blocks* necessários para sintetizar os estereoisômeros do composto **2.**

f) Sintetizar, purificar e caracterizar quimicamente os quatro estereoisômeros do composto **2**.

3 Capítulo 1 - Estereoisômeros

O texto completo desta seção, que na tese defendida ocupa o intervalo de páginas 49-88, foi suprimido por tratar-se de informações para publicação em periódico científico. Consta da descrição de todos os métodos de síntese utilizados para obter os compostos descritos neste trabalho.

4 Capítulo 2 - Quinazolinas

Structure-Based Optimization of Quinazolines as Cruzain and *Tbr*CATL Inhibitors

Elany Barbosa da Silva[a,b,#], Débora A. Rocha[c,d,#], Isadora S. Fortes[c,d], Wenqian Yang[b], Ludovica Monti[b], Jair L. Siqueira-Neto[b], Conor R. Caffrey[b], James McKerrow[b], Saulo F. Andrade[c,d,e*], and Rafaela S. Ferreira[a*].

a. Biochemistry and Immunology Department, Biological Sciences Institute - Federal University of Minas Gerais (UFMG), Belo Horizonte, MG, 31270-901, Brazil.
b. Center for Discovery and Innovation in Parasitic Diseases, Skaggs School of Pharmacy and Pharmaceutical Sciences, University of California San Diego, La Jolla, California, 92093-0657, United States of America.
c. Pharmaceutical Synthesis Group (PHARSG), Federal University of Rio Grande do Sul, Porto Alegre, RS, 90040-060, Brazil
d. Pharmaceutical Sciences Graduate Program, Federal University of Rio Grande do Sul, Porto Alegre, RS, 90040-060, Brazil.
e. Graduate Program in Agricultural and Environmental Microbiology, Federal University of Rio Grande do Sul, Porto Alegre, RS, 90040-060, Brazil.
#E.B.d.S. and D.A.R. contributed equally to this work.

Corresponding author e-mail addresses: saulo.fernandes@ufrgs.br (Saulo F. Andrade) and rafaelasf@icb.ufmg.br (R.S. Ferreira).

Artigo publicado no *Journal of Medicinal Chemistry* – disponível em: https://doi.org/10.1021/acs.jmedchem.1c01151

4.1 Abstract

Chagas disease and Human African trypanosomiasis are neglected diseases, and *Trypanosoma cruzi* and *Trypanosoma brucei* are its etiologic agents, respectively.

Proteases are a class of therapeutic targets validated for the treatment of these diseases, such as cruzain, the main cysteine protease (CP) of *T. cruzi* and *Tbr*CATL (a.k.a. rhodesain), the main CP of *T. brucei*. Recently, we have identified N^4-benzyl-N^2-phenylquinazoline-2,4-diamine named **PH100** as a potential reversible inhibitor of these enzymes. Next, we have prioritized its derivatives using High–Throughput Virtual Screening, docking XP or classical medicinal chemistry modifications. In this work, we synthesized 19 quinazolinic compounds and 4 compounds replacing the quinazoline core by a pyrimidine or purine core. All compounds were evaluated for their inhibitory activities against the enzymes, as well as for their trypanocidal activities *in vitro* against amastigotes for *T. cruzi*. All of synthesized compounds were active against the parasite and most of them have presented enzyme inhibition. In general, quinazoline derivatives were more potent than pyrimidine and purine derivatives being promising to be developed as novel antitrypanosomal agents.

Keywords: Chagas disease. Human African Trypanosomiasis. *Trypanosoma cruzi*. *Trypanosoma brucei*. Cruzain. *Tbr*CATL. Reversible inhibitors. Buchwald-Hartwig Reaction.

4.2 Introduction

Chagas Disease and Human African trypanosomiasis (HAT) are neglected tropical diseases. Chagas disease is widespread in Latin America, affecting 6-7 million people around the world[1,2] and it is caused by protozoa *Trypanosoma cruzi*. HAT occurs in 24 countries of sub-Saharan Africa where 57 million of people lives are in risk areas[3], it is caused by two different subspecies of *Trypanosoma brucei*: *gambiense* and *rhodesiense*[4]. Both diseases have two stages, acute and chronic phase. Nifurtimox (Lampit®) and benznidazole (Rochagan®) are the available drugs Chagas Disease's therapy5. However, both drugs have severe limitations in its use, as several resistance cases and side effects[6,7], which occasionally induces treatment discontinuation[8]. For HAT, pentamidine (NebuPent®) and suramine (Germanin®) are prescribed only in the acute phase[9], cause are not able to cross the blood-brain barrier (BBB)[10,11]. Melarsoprol (Arsobal®) and eflornithine (Ornidyl®) are prescribed to treat the neurological symptoms that are common in the chronic phase of HAT[10,11]. As well as Chagas disease treatments, these drugs are associated with severe side effects due to their nonspecific mechanism of action. Recently, WHO approved a new option to treat HAT infections caused by *gambiense* subspecies, fexinidazole (Fexinidazole Winthrop®)[12–14]. Unfortunately, infections caused by *rhodesiense* subspecies in chronic phase are only treatable with melarsoprol[9]. Due to these trypanosomiases' treatment issues, becoming the search for new effective treatments is crucial.

Cruzain and T*br*CATL (rhodesain – outdated term[15]) are the main cysteine protease of *T. cruzi* and *T. brucei*, respectively, and therapeutic targets for drug development. These enzymes are involved in processes like immune evasion, acquisition of nutrients, proliferation and differentiation steps for *T. cruzi*[8,16] and immune evasion and BBB crossing for *T. brucei*[17,18]. Due to these essential roles, many efforts were made to find potent inhibitors to these enzymes[16,19] and several chemical classes were studied and evaluated. Among them, vinylsulfones are the most prominent class, being studied since 1995[20]. These compounds are covalent and irreversible enzyme inhibitors, regarded as Michael acceptors[21]. Some compounds of this class stood out with good activities against cruzain, T*br*CATL and *T. cruzi*[20,22–25], cured mice[26] and dog[27] infected with *T. cruzi*. Other classes were studied with good outcomes: thiosemicarbazones[28–30], thiazoles and thiazolidines[31–34]; derivatives

containing nitriles[7,35–39]; bromoisoxazolines[40–42] and others[43–46]. Previously, our group have screened 400 compounds from Malaria Box, provided by *Medicines for Malaria Venture*, against cruzain and T*br*CATL in order to find new potential competitive inhibitors[47]. Compound *N*4-benzyl-*N*2-phenylquinazoline-2,4-diamine, denominated in the present work **PH100**, showed promising activities against cruzain and T*br*CATL. **PH100** belongs to a chemical class with many reports in the literature of activities as antitumor[48,49], antiparasitic[50–52], antimicrobial[53,54] and antiviral[55,56]. Grounded in all these data, a virtual screening was proposed aiming new series of antitrypanosomal compounds. In this work, we designed these series, synthesized and characterized these compounds, evaluated against both enzymes and parasites as well as performed toxicity tests.

4.3 Results and Discussion

Chemistry

In this work, we synthesized 18 quinazoline derivatives of compound **PH100**, to explore the impact of modifications at positions 2 and 4, and four compounds bearing a pyrimidine or purine core, to evaluate the role of the central ring. To prepare quinazoline compounds, anthranilic acid **1** was reacted with urea, providing 2,4-dioxaquinazoline **2**, which was submitted to a dichlorination at positions 2 and 4 of the ring with $POCl_3$ (phosphoryl chloride) and DMA (*N*, *N*-dimethylaniline) resulting in 2,4-dichloroquinazoline **3**. With **3** in hand, positions 2 and 4 were substituted with adequate amines. In position 4 a nucleophilic aromatic substitution (S_NAr) with appropriate amine was performed[50]. For position 2 the compounds were prepared by S_NAr or Buchwald-Hartwig reaction (Figure 11)[57].

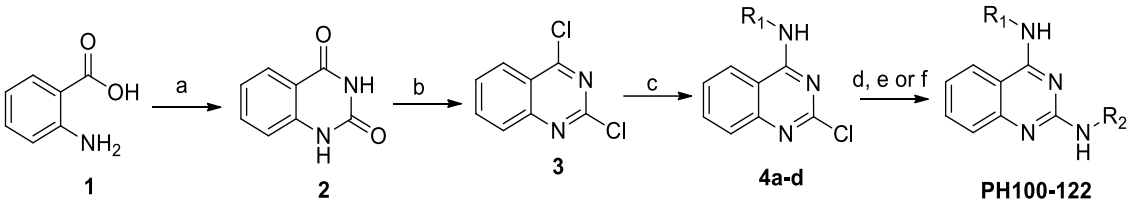

Figure 11 –Synthetic procedures to obtain 2.4-dichloroquinazoline **3**. *Reagents and conditions:* a) urea, 200 ºC, 73%; b) $POCl_3$, DMA, 100 ºC, 20%; c) appropriate amine, sodium acetate, THF:H_2O, 65 ºC, 62%; d) appropriate amine, EtOH, 120 ºC, 28- 88%; e) appropriate amine, $Pd(OAc)_2$, xantphos, Cs_2CO_3, DMF, 140 ºC, 10-52%; f) appropriate amine, EtOH, 120 ºC, 18 h, 38%.

To synthesize compounds **PH108**, **PH109**, **PH116**, **PH119** and **PH120** the amines coupled to position 2 were previously prepared in two steps. First, we couple an aniline or a morpholine to *p*-nitrobenzoic acid **5**[58] and after the nitro group was reduced to amino in presence of aqueous hydrazine giving **7a** or **7b**[59] (Figure 12).

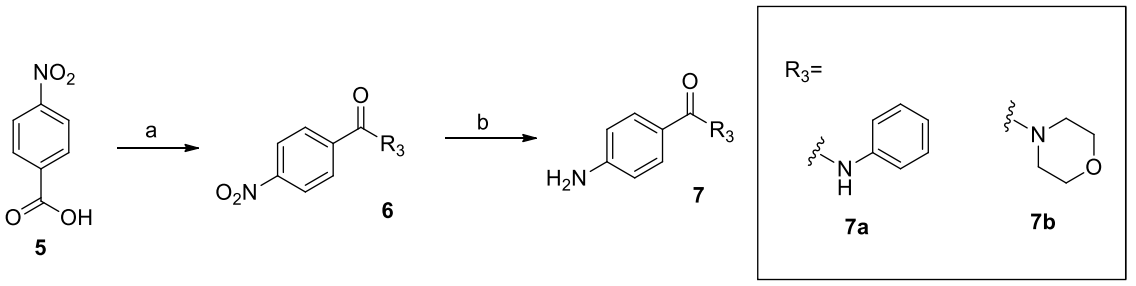

Figure 12 – Synthesis of 4-*amino-N-phenylbenzamid* **7a** and *(4-aminophenyl)(piperidin-1-yl)methanone* **7b** to obtain **PH108, PH109, PH116, PH119** and **PH120**. *Reagents and conditions:* a) aniline or morpholine, EDC, DMAP, CH_2Cl_2, rt, 3 h; b) aqueous hydrazine 16 %, palladium acetate (II), isopropyl alcohol, 82°C, 3 h.

The pyrimidine compounds (**PH110** and **PH112)** were obtained from the 2,4-dichloropyrimidine **9**, under similar conditions described for the quinazoline series above (Figure 13).

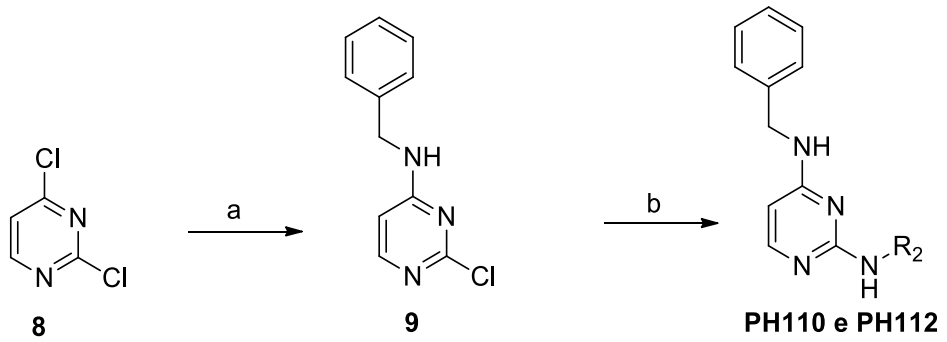

Figure 13 – Synthetic procedures for pyrimidinic compounds **PH110** and **PH112**. *Reagents and conditions:* a) appropriate amine, sodium acetate, THF:H_2O, 65 ºC, 25 %; b) appropriate amine, EtOH, 120 ºC, 28-35%.

Purine analogues were prepared starting from 2,6-dichloro-9H-purine **10**, which was methylated with iodomethane[58]. The resulting 2,6-dichloro-9-metyl-9H-purine **11** was treated in similar, previously described conditions with benzylamine providing intermediate **12**. Then, the substitution with appropriate amine at position 2 of the ring provided **PH111** and **PH113** in a Buchwald-Hartwig reaction[57] (Figure 14).

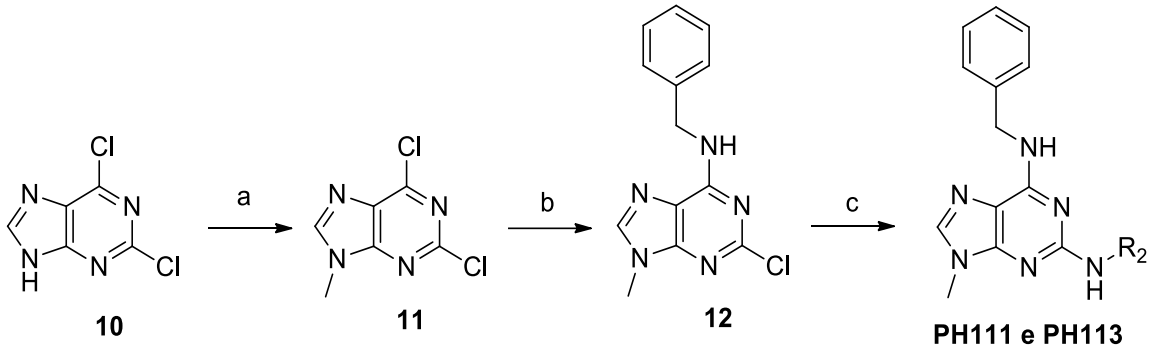

Figure 14 – Synthetic procedures to obtain purinic compounds **PH111** and **PH113**. *Reagents and conditions:* a) CH_3I, K_2CO_3, DMF, 0 ºC, 77%; b) appropriate amine, sodium acetate, THF:H_2O, 65 ºC, 36%; c) appropriate amine, $Pd(OAc)_2$, xantphos, Cs_2CO_3, DMF, 140 ºC, 39-42%.

Biological Evaluation

All compounds were evaluated against the enzymes and parasites as illustrated in table 1. In the first series 9 derivatives of **PH100** was designed by the modification of the substituent of phenyl ring at position 2 of quinazoline ring (**PH102**, **103**, **106** and **107**) or replacement of the phenyl ring with heterocyclic cores (**PH104** and **106**) or with alkyl substituents (**PH101**) or by the extension of the structure (**PH108** and **PH109**). All complete structures as well as enzyme activities are described in Table 1.

Table 1. IC_{50} for cruzain and *Tbr*CATL by **PH100** analogs.

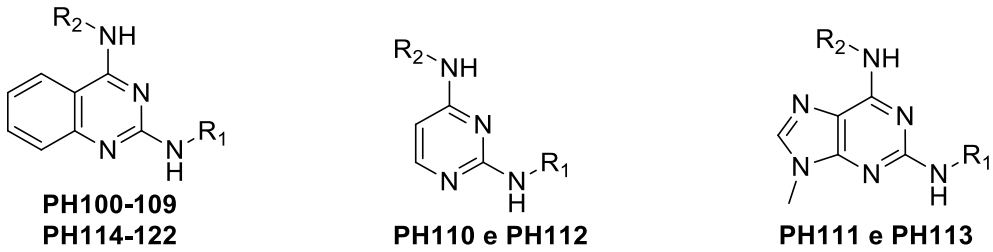

Compound	R_1	R_2	IC_{50} cruzain [b] (μM)	*T. cruzi* EC_{50} (μM)[a]	IC_{50} *Tbr*CATL [b] (μM)	*T. b. brucei* EC_{50} (μM)[c]

PH100	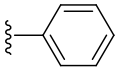	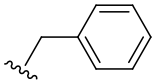	8 ± 1	0.047 ± 0.008	17.5 ± 0.5	17.5 ± 5.2
PH101	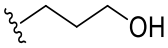	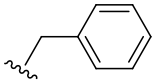	22 ± 1	0.5 ± 0.2	LA	>50
PH102	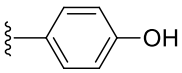	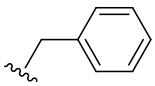	18 ± 3	5.9 ± 3.2	23 ± 2	>50
PH103	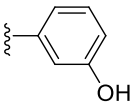	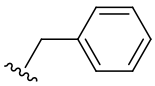	18 ± 3	0.93 ± 0.04	26 ± 2	13.8 ± 5.2
PH104	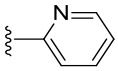	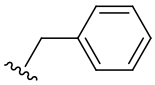	LA	2.7 ± 0.9	LA	>50
PH105		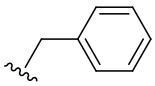	16 ± 2	5.6 ± 3.7	12.5 ± 0.5	>50
PH106	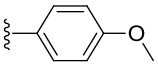	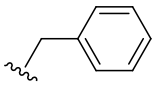	52 ± 4	0.5 ± 0.3	33 ± 2	15.1 ± 8.3
PH107[b]	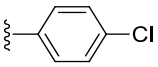	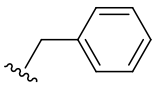	2.4 ± 0.2	0.5 ± 0.3	3 ± 3	9.3 ± 5.2
PH108[b]	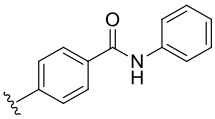	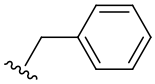	LA	1.8 ± 1.4	LA	>50
PH109	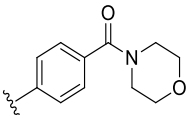	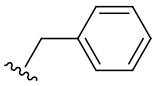	7 ± 1	0.8 ± 0.5	22 ± 3	>50
PH110	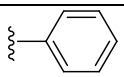	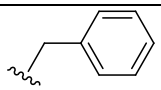	LA	7 ± 1	LA	>50
PH112[b]	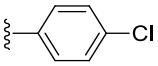	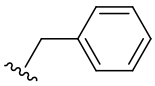	LA	7 ± 4	LA	25.0 ± 5.9
PH111	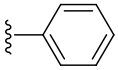	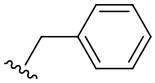	LA	2.2 ± 0.9	LA	23.8 ± 11.3
PH113	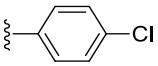	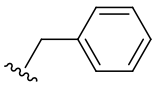	LA	12 ± 4	LA	18.4 ± 4.7
PH114	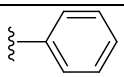	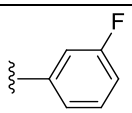	LA	0.07 ± 0.01	LA	9.0 ± 3.2
PH115	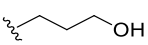	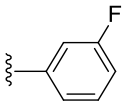	25 ± 5	0.09 ± 0.04	LA	17.8 ± 6.5

PH116	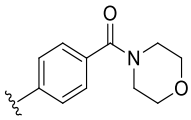	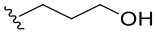	15 ± 4	22 ± 9	LA	>50
PH118	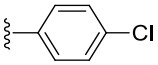	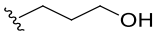	7.30 ± 0.02	0.25 ± 0.03	LA	9.0 ± 1.4
PH117 [b]	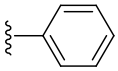	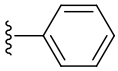	14 ± 2	0.9 ± 0.5	LA	16.5 ± 5.2
PH119	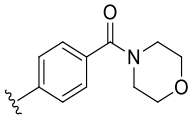	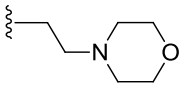	13.5 ± 0.5	15 ± 3	LA	>50
PH120	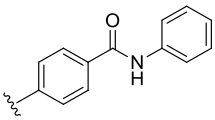	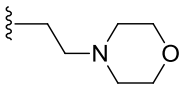	LA	0.8 ± 0.1	LA	2.7 ± 0.7
PH121	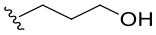	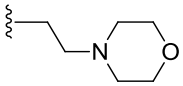	LA	35 ± 5	LA	>50
PH122	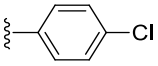	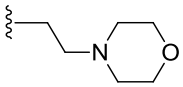	2.50 ± 0.01	0.370 ± 0.003	LA	23.6 ± 2.2
Benznidazole	-	-	-	5.4 ± 0.3		LA
Pentamidine	-	-	-	-		0.026 ± 0.004
E64 (1 μM)	-		0.030 ± 0.009	-	0.0037 ± 0.0006	-

[a] IC_{50} values represent averages and standard errors of the mean obtained from at least two independent experiments, which were determined using seven different concentrations of the compounds in triplicate. Most curves were obtained from assays without pre-incubation with the enzymes, except for **PH106** and **PH117**, which were pre-incubated with the enzymes for 10 minutes before addition of the substrate. [b] Compound evaluated at 20 μM due to limited solubility. LA -low activity.

The majority of compounds of the first series have inhibited at least 50% of enzymes activity at 100 μM. Only derivatives with a percentage of inhibition higher than 50% against the enzymes were considered for the IC_{50} determination and they presented IC_{50} ranges between 2.4-52 μM for cruzain and 3-33 μM for T*br*CATL. In general, this series was more active against cruzain than against T*br*CATL. Among the derivatives designed by the modification of ring substituent, we highlight derivative **PH107** which bears a hydrophobic and electron-withdrawing group (-Cl). It was active against cruzain and T*br*CATL with a IC_{50} value of 2.4 and 3 μM, respectively. On the other hand, the presence of polar substituents (**PH102**, **PH103** and **PH106**) or the replacement of phenyl by a polar ring (**PH104** and **PH105**) decreased the activity of the series while the extension of the structure (**PH109**) kept the activity. Based on

PH100 and **PH107** activities we synthesized some analogues replacing the core with a pyrimidine (**PH110** - **PH112**) or purine ring (**PH111** - **PH113**). Interestingly, these compounds showed poor activities for both enzymes, leading us to believe that the quinazoline ring is essential for enzyme inhibition.

In order to evaluate if the inhibitory activities could be related to aggregation properties some confirmatory assays against cruzain in presence of Triton-X100 and BSA[60] were performed. In these assays the activities against the enzyme were disturbed for some compounds including **PH100** and **PH107** indicating at least part of the activity could result from this unspecific mechanism.

Fortunately, compounds **PH101** and **PH109**, which are hydrophilic compounds in comparison with **PH100**, were not affected neither by BSA preincubation nor by Triton X100 concentrations. Based on all these biological activities we designed a new series of hydrophilic quinazoline derivatives bearing different substituents in position 4 of the quinazolinic ring and the most promising groups found at 2-position with the first series (**PH114** to **PH122**).

In general, these modifications resulted in poor activities against *Tbr*CATL and modest to good activities against cruzain. In this new series, **PH118** and **PH122** showed better activities for cruzain with IC_{50} values of 7.3 and 2.5 μM, respectively. Both compounds have polar substituents in position 4 and a *para*-chlorophenyl in position 2, confirming that this substituent is effective for cruzain. Furthermore, confirmatory assays using BSA and Triton X100 in different concentrations were also performed and none of the compounds were sensitive[60]. These data corroborate with the idea that polar groups at 4-position are more acceptable to achieve a competitive inhibition against cruzain. It is important to note that compounds **PH118** and **PH122** are analogs of **PH107** demonstrating that the benzylamine substituent could be involved in the aggregator behavior since both compounds had *para*-chlorophenyl and do not presented these characteristics. Also in Table 1, we present the results for anti-trypanosomal activities. All 23 compounds were active against *T. cruzi* with no important cytotoxicity against the myoblasts and 13 compounds were active against *T. b. brucei*. Even compounds that were inactive for the enzymes presented cytotoxicity against the parasites, indicating that other targets could also be involved. Twelve compounds presented an EC_{50} for *T. cruzi* <1 μM, while the lowest EC_{50} against *T. b. brucei* was 2.7 μM. Compounds **PH118** and **PH122** stood out as the best inhibitors for cruzain and achieved EC_{50} for *T. cruzi* values of 0.9 and 0.37 μM, respectively.

Comparing these compounds, **PH122** was almost 3-fold more potent against cruzain than **PH118** and **PH122** was more specific, being not able to inhibit T*br*CATL or *T. b. brucei* growth. Six compounds evaluated in this series showed EC_{50}, allied to SI, with better values than the drug recommended for the treatment of Chagas Disease, benznidazole. Compound **PH118** was 6-fold more potent than benznidazole (EC_{50} = 5.4 µM), while **PH122** was 15-fold more potent combined with an SI of 27. **PH100** had an EC_{50} for *T. cruzi* of 0.047 µM, but it was not a competitive inhibitor of cruzain. Thus, the search of the molecular target of its action will continue. On the other hand, **PH122** was able to inhibit cruzain with better IC_{50} values and maintaining the trypanocidal potential and Selectivity Index. For *T. b. brucei*, **PH120** was the best compound, presenting an EC_{50} of 2.7 µM, but not able to inhibit T*br*CATL. In general, the compounds were not as active for *T. brucei* as for *T. cruzi,* but four compounds presented IC_{50} values lower than 10 µM, being considered good prototypes for further development.

4.4 Conclusion

In this work, we synthesized 23 compounds, 19 compounds with the quinazoline core and 4 compounds replacing the quinazoline core by a pyrimidine or purine core. All compounds were evaluated for their inhibitory activities against the enzymes cruzain and T*br*CATL, as well as for their trypanocidal activities *in vitro* against the trypanosomes. All of synthesized compounds were active against the parasite and most of them have presented enzyme inhibition. In general, quinazoline derivatives were more potent than pyrimidine and purine derivatives being promising to be developed as novel antitrypanosomal agents.

4.5 Experimental Section

General

All reagents and solvents were purchased from commercial sources (Sigma-Aldrich, Synth, Fluka, Merck) and used without further purification. The NMR spectra

were obtained in a Bruker 400 MHz or Varian 400 MHz spectrometer (H^1 and C^{13}), tetramethylsilane (TMS) was the internal standard. The solvents used in the NMR spectrum were obtained from Sigma-Aldrich. High-resolution mass spectrometry (HRMS) was performed in a Bruker Impact II equipment using the electrospray ionization (ESI) technique.

Synthesis

*Synthesis of 2,4-dichloroquinazoline (**3**)* Anthranilic acid **1** (0.5 g, 3.65 mmol) and urea (0.77 g, 12.7 mmol) were triturated and added to a round-bottom flask. The mixture was heated at 200 °C under stirring. After 3 h, it was cooled, diluted with water and triturated. The resulting mixture was filtered to give 2,4-dioxaquinazoline **2** (434 mg, 73 % yield) which was used in the next step without further purification.
To a stirred solution of **2** (0.62 g, 3.81 mmol) in phosphorus oxychloride (5.26 g, 34 mmol) was added *N*,*N*-dimethylaniline (0.46 g, 3.81 mmol) under N_2 atmosphere at 100 °C. After 18 h, it was cooled, diluted with cold water (30 mL) and chloroform (15 mL) and the resulting suspension was filtered. The filtrate was extracted with chloroform (3x15 mL). The combined organic layers were dried over Na_2SO_4, filtered and concentrated under reduced pressure. The residue was purified by silica gel column chromatography (hexanes/ethyl acetate 8:2) to give **3** as a white solid, 206 mg (20 % yield). ^{1}H NMR (400 MHz, $CDCl_3$) δ (ppm): 8.27- 8.24 (m, 1H), 7.99- 8.00 (m, 2H) e 7.76 - 7.72 (m, 1H). ^{13}C NMR (100 MHz, $CDCl_3$) δ (ppm): 164.12, 155.25, 152.49, 136.27, 129.38, 128.14, 126.18, 122.48.

*General Procedure to obtain **4a**-**d**.* To a solution of 2.4-dichloroquinazoline **3** (0.5 g, 2.51 mmol) in THF/H_2O (3:1) (15 mL), sodium acetate (0.226 g, 2.76 mmol) and appropriate amine (2.76 mmol) were added. The mixture was stirred for 6 h at 65 °C. After, it was cooled and diluted with ethyl acetate (40 mL) and water (40 mL) and the organic layer was washed with water (2x40 mL), dried over Na_2SO_4, filtered and concentrated under reduced pressure. The residue was purified by silica gel column chromatography.

N-benzyl-2-chloroquinazolin-4-amine (**4a**). Obtained as 0.462 g of a white solid, 62% yield.^{1}H NMR (400 MHz, $(CD_3)_2CO$) δ (ppm): 8.41 (br, 1H), 8.24–8.21 (m, 1H), 7.83–

7.78 (m, 1H), 7.67–7.65 (m, 1H), 7.54–7.50 (m, 1H), 7.46–7.43 (m, 2H), 7.35–7.31 (m, 2H), 7.27-7.23 (m, 1H), 4.88 (d, 2H, *J* = 5.6 Hz); ^{13}C NMR (100 MHz, $(CD_3)_2CO$) *δ* (ppm): 162.3, 158.4, 152.0, 139.4, 134.3, 129.3, 128.7, 128.1, 128.0, 127.0, 123.2, 114.6, 45.4. In accordance with ref [50].

2-chloro-N-(3-fluorophenyl)quinazolin-4-amine (**4b**). Obtained as 0.15 g of a white solid, 36% yield. ^{1}H NMR (400 MHz, $CDCl_3$) δ (ppm): 7.90 (d, 2H), 7.81–7.73 (m, 3H), 7.55–7.51 (m, 1H), 7.41–7.39 (m, 1H), 7.35–7.29 (m, 1H), 6.89–6.84 (m, 1H). ^{13}C NMR (100 MHz, $CDCl_3$) *δ* (ppm): 164.3, 161.8, 158.5, 157.0, 151.3, 139.2, 139.1, 134.2, 130.3, 130.2, 128.2, 127.0, 120.8, 116.9, 116.8, 113.5, 111.9, 111.7, 109.2, 109.0.

3-((2-(chloroamino)quinazolin-4-yl)amino)propan-1-ol (**4c**). Obtained as 0.223 g of a white solid, 62% yield. ^{1}H NMR (400 MHz, DMSO-*d6*) δ (ppm): 8.69 (t, 1H, *J* = 5.4 Hz), 8.25 (dd, 1H, *J* = 1.0 Hz, *J* = 8.0 Hz), 7.79-7.75 (m, 1H), 7.61-7.59 (m, 1H), 7.53-7.49 (m, 1H), 4.56 (s, 1H), 3.58–3.50 (m, 4H), 1.81 (quint, 2H, *J* = 6.7 Hz). ^{13}C NMR (100 MHz, $CDCl_3$) *δ* (ppm): 161.1, 157.0, 150.2, 133.5, 126.6, 126.0, 123.1, 113.6, 58.5, 38.3, 31.5. In accordance with ref [61].

2-chloro-N-(2-morpholinoethyl)quinazolin-4-amine (**4d**). Obtained as 0.169 g of a white solid, 39% yield. ^{1}H NMR (400 MHz, $CDCl_3$) δ (ppm): 7.75–7.69 (m, 3H), 7.47-7.43 (m, 1H,), 6.97 (s, 1H), 3.77–3.71 (m, 6H), 2.73 (t, 2H, *J* = 5.8 Hz), 2.58 (d, 4H, *J* = 4.4 Hz). ^{13}C NMR (100 MHz, $CDCl_3$) *δ* (ppm): 160.9, 157.8, 150.8, 133.6, 127.8, 126.3, 121.1, 113.5, 67.0, 56.4, 53.3, 37.2. In accordance with ref [62].

General Procedure for the preparation of quinazolinic compounds (**PH100**-**103, PH106**-**107, PH114**-**PH115 PH118** and **PH121**) To a stirred solution of *N*-substituted-2-chloroquinazolin 4-amine (1 eq.) in ethanol at 0.4 M concentration, the appropriate amine was added (1.5 eq.) and heated to 120 °C. After 3 h, it was cooled, diluted with ethyl acetate and washed with a saturated aqueous $NaHCO_3$ and water. The organic layer was dried over Na_2SO_4, filtered and concentrated under reduced pressure. The residue was purified by silica gel column chromatography.

Compound **PH100**. Obtained as 0.196 g of a yellow solid, 81% yield. ^{1}H NMR (400 MHz, DMSO-*d6*) *δ* 9.02 (s, 1H, 8.68 (t, 1H, *J* = 5.4 Hz), 8.16 (d, 1H, *J* = 8.0 Hz),

7.84 – 7.82 (m, 2H), 7.60 (t, 1H, *J* = 8.0 Hz), 7.44- 7.40 (m, 3H), 7.33 (t, 2H, *J* = 7.4 Hz), 7.25- 7.18 (m, 4H), 6.86 (t, 1H, *J* = 7.2 Hz), 4.83 (d, 2H, *J* = 5,4 Hz). ^{13}C NMR (100 MHz, DMSO-*d6*) *δ* 160.10, 156.95, 151.35, 141.42, 139.68, 132.64, 128.29, 128.24, 127.10, 126.71, 125.33, 122.78, 121.48, 120.43, 118.57, 111.63, 43.54. HRMS: m/z calcd for $C_{21}H_{19}N_4$ [M + H]+ 327.1604; found 327.1604. In accordance with ref [50].

Compound **PH101**. Obtained as 0.024 g of a yellow oil, 84% yield. ^{1}H NMR (400 MHz, DMSO-*d6*) *δ* 7.85 (d, 1H, *J* = 8 Hz), 7.47-7.43 (m, 1H) 7.34-7.01 (m, 7H, CH), 4.75 (sl, 2H), 3.60- 3.59 (m, 2H), 3.48- 3.47 (m, 2H), 1.73- 1.72 (m, 2H). ^{13}C NMR (100 MHz, $CDCl_3$) *δ* 160.11, 150.89, 138.52, 133.13, 128.88, 127.97, 127.71, 125.07, 121.59, 120.99, 111.15, 58.04, 45.15, 37.18, 34.04. HRMS: m/z calcd for $C_{18}H_{21}N_4O$ [M + H]+ 309.1710; found 309.1706.

Compound **PH102**. Obtained as 0.0221 g of a brown solid, 68% yield. ^{1}H NMR (400 MHz, CD_3OD) *δ* 7.98 (dd,1H, *J* = 1.0 Hz, *J* = 8.2 Hz), 7.62- 7.59 (m, 1H), 7.41 (d, 1H, *J* = 8.2 Hz), 7.36- 7.19 (m, 8H), 6.71 (d, 2H, *J* = 8.8 Hz), 4.80 (sl, 2H). ^{13}C NMR (100 MHz, CD_3OD) *δ* 162.02, 158.75, 154.22, 151.17, 140.54, 134.12, 133.20, 129.40, 128.35, 127.92, 124.68, 124.08, 123.48, 123.06, 116.12, 112.71, 45.39. HRMS: m/z calcd for $C_{21}H_{19}$ N_4O [M + H]+ 343.1553; found 343.1549.

Compound **PH103**. Obtained as 0.0233 g of a brown solid, 74% yield. ^{1}H NMR (400 MHz, DMSO-*d6*) *δ* 9.17 (s, 1H), 8.86 (s, 1H), 8.61 (t, 1H, *J* = 5.6 Hz), 8.12 (d, 1H, *J*= 8.2 Hz), 7.60 (t, 1H, *J* = 8.2 Hz), 7.47 (d, 1H, *J* = 1.6 Hz), 7.41 (d, 3H), 7.33- 7.30 (m, 2H), 7.25- 7.16 (m, 3H), 6.99- 6.95 (m, 1H), 6.32- 6.29 (m, 1H), 4.82 (d, 2H, *J* = 5.6 Hz). ^{13}C NMR (100 MHz, DMSO-*d6*) *δ* 160.06, 157.42, 156.98, 151.37, 142.52, 139.80, 132.69, 128.86, 128.35, 127.39, 126.81, 125.41, 122.79, 121.55, 111.67, 109.86, 107.86, 105.92, 43.55. HRMS: m/z calcd for $C_{21}H_{19}$ N_4O [M + H]+ 343.1553; found 343.1554.

Compound **PH106**. Obtained as 0.0369 g of an ivory solid, 28% yield. ^{1}H NMR (400 MHz, DMSO-*d6*) *δ* 8.84 (s, 1H), 8.61 (t, 1H, *J* = 5.4 Hz), 8.12 (d, 1H, *J* = 8.2 Hz), 7.72- 7.70 (m, 2H), 7.57 (t, 1H, *J* = 8.2 Hz), 7.41-7.31 (m, 5H), 7.25-7.13 (m, 2H), 6.80 (d, 2H, *J* = 9.2 Hz), 4.80 (d, 2H, *J* = 5.4 Hz), 3.71 (s, 3H). ^{13}C NMR (100 MHz, CD_3OD) *δ* 162.11, 159.06, 156.63, 152.11, 140.66, 134.74, 133.97, 129.40, 128.26, 127.89,

125.34, 123.36, 122.92, 114.78, 112.84, 55.93, 45.33. HRMS: m/z calcd for $C_{22}H_{21}N_4O$ [M + H]+ 357.1710; found 357.1704. In accordance with ref [63].

Compound **PH107**. Obtained as 0.121 g of an ivory solid, 60% yield. ^{1}H NMR (400 MHz, DMSO-*d6*) δ 9.20 (s, 1H, 8.74 (t, 1H, *J* = 5.8 Hz), 8.16 (dd, 1H, *J* = 8.2 Hz, *J* = 1.0 Hz), 7.87- 7.85 (m, 2H), 7.63- 7.59 (m, 1H, CH), 7.44 (dd, 1H, *J* = 8.4 Hz, *J* = 0.8 Hz), 7.42- 7.39 (m, 2H), 7.35- 7.31 (m, 2H), 7.25- 7.19 (m, 4H), 4.82 (d, 2H, *J* = 5.8 Hz). ^{13}C NMR (100 MHz, DMSO-*d6*) δ 160.22, 156.77, 151.21, 140.49, 139.63, 132.82, 128.38, 128.10, 127.10, 126.81, 125.47, 123.89, 122.87, 121.86, 119.99, 111.77, 43.64. HRMS: m/z calcd for $C_{21}H_{18}ClN_4$ [M + H]+ 361.1215; found 361.1211. In accordance with ref [63].

Compound **PH114**. Obtained as 0.0265 g of a white solid, 88% yield. ^{1}H NMR (400 MHz, DMSO-*d6*) *δ* (ppm): 11.28 (s, 1H), 10.66 (s, 1H), 8.78 (dd, 1H, *J* = 8,4 Hz), 7.92- 7.88 (m, 1H), 7.69- 7.66 (m, 1H), 7.63 (dd, 1H, *J* = 8,4 Hz), 7.57- 7.51 (m, 2H), 7.49- 7.46 (m, 2H), 7.44- 7.40 (m, 1H), 7.36- 7.31 (m, 2H), 7.22- 7.18 (m, 1H), 7.13- 7.08 (m, 1H). ^{13}C NMR (100 MHz, *d6*- DMSO) *δ* (ppm): 162.91, 160.49, 159.43, 151.64, 139.48, 138.65, 138.54, 136.33, 135.72, 129.72, 129.86, 128.69, 125.10, 124.89, 122.47, 120.28, 117.43, 112.69, 111.74, 110.39. HRMS: m/z calcd for $C_{20}H_{16}FN_4$ [M + H]+ 331.1354; found 331.1353.

Compound **PH115**. Obtained as 0.010 g of a white solid, 35% yield. ^{1}H NMR (400 MHz, DMSO-*d6*) δ (ppm): 9.48 (s,1H), 8.29 (d, 1H, *J*=7.6 Hz), 8.08 (d, 1H, *J*= 12.4 Hz), 7.74 (dd, 1H, *J*=1.7 Hz, *J*= 8.2Hz), 7.59- 7.55 (m, 1H), 7.40- 7.31 (m, 1H), 7.14 (t, 1H, *J*=7.4 Hz), 6.93 (t, 1H, *J*= 5.6Hz), 6.87 (td, 1H, *J*= 2.4Hz), 3.50 (t, 2H, *J*= 6.4 Hz), 3.44- 3.39 (m, 2H), 1.73 (qui, 2H, *J*= 6.4 Hz). ^{13}C NMR (100 MHz, DMSO- *d6*) *δ* (ppm): 163.29, 160.90, 158.84, 158.84, 157.82, 141.78, 132.87, 129.82, 124.94, 123.03, 120.47, 116.85, 109.16, 108.09, 58.64, 37.89, 32.71. HRMS: m/z calcd for $C_{17}H_{18}FN_4O$ [M + H]+ 313.1459; found 313.1458.

Compound **PH118**. Obtained as 0.0217 g of a white solid, 63% yield. ^{1}H NMR (400 MHz, DMSO-*d6*) δ (ppm): 9.19 (s,1H), 8.12- 8.06 (m, 2H), 7.99 (d, 2H, *J*= 8.2 Hz), 7.58 (t, 1H, *J*= 7.6 Hz), 7.40 (d, 1H, *J*= 8 Hz), 7.28 (d, 2H, *J*= 8.2 Hz), 7.17 (t, 1H, *J*= 8 Hz), 4.55 (s, 1H), 3.63- 3.35 (m, 4H), 1.92- 1.86 (m, 2H). ^{13}C NMR (100 MHz, DMSO-

d6) *δ* (ppm): 160.17, 156.80, 150.94, 140.63, 132.53, 128.10, 125.33, 123.78, 122.77, 121.58, 119.93, 111.81, 58.79, 38.09, 31.94. HRMS: m/z calcd for $C_{17}H_{18}ClN_4O$ [M + H]+ 329.1164; found 329.1164.

Compound **PH121**. Obtained as 0.0091 g of a white solid, 32% yield. ^{1}H NMR (400 MHz, DMSO-*d6*) δ (ppm): 7.89 (d, 1H, *J*= 8 Hz), 7.41 (t, 1H, *J*= 7.5 Hz) 7.15 (t, 1H, *J*= 8 Hz), 6.96 (d, 1H, *J*= 7.5 Hz), 3.55- 3.50 (m, 8H), 3.40 (t, 2H, *J*= 6.3 Hz), 3.31 (q, 2H, *J*= 6.4 Hz), 2.44- 2.39 (m, 4H), 1.61 (qui, 2H, *J*= 6.3 Hz). ^{13}C NMR (100 MHz, $CDCl_3$) *δ* (ppm): 159.85, 159.35, 151.18, 132.31, 124.11, 122.79, 120.05, 111.16, 66.24, 58.56, 57.05, 53.45, 37.70, 37.49, 32.90. HRMS: m/z calcd for $C_{17}H_{26}N_5O_2$ [M + H]+ 332.2081; found 332.2078.

General Procedure to obtain 4-amino-N-phenylbenzamide (**7a**) and *(4-aminophenyl) (piperidin-1-yl)methanone* (**7b**) to synthesized **PH108** and **PH109**. To a stirred solution of 4-nitrobenzoic acid **5** (0.2 g, 1.2 mmol) in dichloromethane (4 mL), EDC (0.37 g, 1.92 mmol) and DMAP (0.015 g, 0.12 mmol) were added. After 5 min, the appropriate amine was added (1.92 mmol) at room temperature. After 3 h, it was diluted with ethyl acetate (30 mL) and washed with aqueous HCl 0.5M (15 mL), saturated aqueous $NaHCO_3$ (15 mL) and water (20 mL). The organic layer was dried with Na_2SO_4, filtered and concentrated under reduced pressure. The resulting product was used in the next step without further purification. Compound **6** (0.110 g, 0.454 mmol) was solubilized in isopropyl alcohol (5.5 mL), palladium acetate (II) (0.014 g, 0.056mmol) and aqueous hydrazine 16 % (0.32 mL) were added. The mixture was stirred for 3 h at 82°C. After, the mixture was filtrated hot, washed with heated isopropyl alcohol (25 mL) and concentrated under reduced pressure. The resulting 4-amino-N-phenylbenzamide **7a** or (4-aminophenyl) (piperidin-1-yl) methanone **7b** was used in the next step without further purification.

*General Procedure for the preparation of quinazolinic compounds (***PH104**-**105***,* **PH108**-**109**, **PH116, PH119**-**120** *and* **PH122***)* To a stirred solution of *N*-substituted-2-chloroquinazolin-4-amine **4** (1 eq.) in toluene or DMF at 0.06 M concentration, palladium acetate (II) (0.007 equiv), xantphos (0.007 equiv), appropriate amine (1.5 equiv) and cesium carbonate (2 equiv) were added and heated to 140°C under N_2 atmosphere. After 18 h, it was cooled, diluted with ethyl acetate and filtered, the

solution was concentrated under reduced pressure. The residue was purified by silica gel column chromatography.

Compound **PH104**. Obtained as 0.008 g of a brown solid, 26% yield. ^{1}H NMR (400 MHz, CD_3OD) *δ* 8.17 (d, 1H), 8.06 (d, 1H, *J* = 8.4 Hz), 7.87- 7.86 (m, 1H), 7.69- 7.59 (m, 2H), 7.53 (d, 1H, *J* = 8.4 Hz), 7.47- 7.29 (m, 4H), 7.26- 7.22 (m, 1H,), 6.96- 6.93 (m, 1Hl), 6.60- 6.56 (m, 1H), 4.58 (sl, 2H). ^{13}C NMR (100 MHz, CD_3OD) *δ* 162.40, 154.61, 148.28, 147.72,140.35, 139.34, 134.31, 129.53, 128.11, 128.04, 124.27, 123.51, 118.49, 114.71, 113.94, 113.30, 110.34, 45.65. HRMS: m/z calcd for $C_{20}H_{18}N_5$ [M + H]+ 328.1557; found 328.1557.

Compound **PH105**. Obtained as 0.0089 g of a yellow solid, 26% yield. ^{1}H NMR (400 MHz, DMSO-*d6*) *δ* 8.88 (t, 1H, *J* = 6 Hz), 8.18 (d, 1H, *J* = 8 Hz), 7.69- 7.65 (m, 1H), 7.51 (d, 1H, *J* = 8.4 Hz), 7.45- 7.43 (m, 2H), 7.36- 7.21 (m, 5H), 7.01 (d, 1H), 4.90 (d, 2H, *J* = 6 Hz). ^{13}C NMR (100 MHz, DMSO-*d6*) *δ* 160.51, 154.24, 150.26, 139.46, 137.58, 133.23, 128.39, 127.71, 126.97, 125.24, 123.08, 122.73, 111.98, 109.34, 43.99. HRMS: m/z calcd for $C_{18}H_{16}N_5S$ [M + H]+ 334.1121; found 334.1120.

Compound **PH108**. Obtained as 0.0723 g of a white solid, 52% yield. ^{1}H NMR (400 MHz, DMSO-*d6*) *δ* 10.03 (s,1H), 9.44 (s, 1H), 8.80 (t, 1H, *J* = 5.7 Hz), 8.20 (d, 1H, *J* = 7.7 Hz), 8.00 (d, 2H, *J* = 8.4 Hz), 7.89 (d, 2H, *J* = 8.4 Hz), 7.79 (dd, 2H, *J* = 8.4 Hz, *J* = 0.8 Hz), 7.65 (td, 1H, *J* = 1.1 Hz, *J* = 7.7 Hz), 7.50- 7.48 (m, 1H, 7.45- 7.43 (m, 2H), 7.37- 7.32 (m, 4H), 7.27- 7.23 (m, 2H), 7.10- 7.05 (m, 1H), 4.87 (d, 2H, *J* = 5.7Hz). ^{13}C NMR (100 MHz, DMSO-*d6*) *δ* 165.24, 160.27, 156.68, 151.09, 144.70, 139.57, 139.53, 132.86, 128.58, 128.38, 127.18, 126.84, 126.18, 125.57, 123.32, 122.87, 122.87, 122.11, 120.34, 117.44, 111.85, 43.67. HRMS: m/z calcd for $C_{28}H_{24}N_5O$ [M + H]+ 446.1975; found 446.1971.

Compound **PH109**. Obtained as 0.0175 g of a yellow solid, 22% yield. ^{1}H NMR (400 MHz, DMSO-*d6*) *δ* 9.29 (s, 1H), 8.74 (t, 1H, *J* = 5.8 Hz), 8.16 (d, 1H, *J* = 8.0 Hz), 7.87 (d, 2H, *J* = 8.8 Hz), 7.65- 7.60 (m, 1H), 7.46- 7.40 (m, 3H), 7.34 (t, 2H, *J* = 7.4 Hz), 7-28- 7.20 (m, 4H), 4.83 (d, 2H, *J* = 5.8 Hz), 3.60 (d, 4H, *J* = 4.4 Hz), 3.50 (sl, 4H). ^{13}C NMR (100 MHz, $CDCl_3$) *δ* 170.83, 160.31, 156.53, 151.38, 142.31, 138.30, 133.18,

129.00, 128.62, 127.87, 127.77, 126.63, 122.80, 120.89, 118.28, 111.73, 67.11, 45.48. HRMS: m/z calcd for $C_{26}H_{26}N_5O_2$ [M + H]+ 440.2081; found 440.2075.

Compound **PH116**. Obtained as 0.0346 g of a white solid, 41% yield. ^{1}H NMR (400 MHz, $CDCl_3$) δ (ppm): 7.77- 7.72 (m, 2H), 7.56- 7.48 (m, 3H), 7.38- 7.31 (m, 2H), 7.12- 7.08 (m, 2H), 3.75- 3.68 (m, 13H), 1.84 (s, 2H). ^{13}C NMR (100 MHz, $CDCl_3$) *δ* (ppm): 170.95, 160.58, 155.63, 149.19, 142.11, 133.27, 128.39, 127.84, 124.91, 122.94, 121.57, 118.74, 111.54, 67.02, 60.82, 39.78, 31.20. HRMS: m/z calcd for $C_{22}H_{26}N_5O_3$ [M + H]+ 408.2030; found 408.2030.

Compound **PH119**. Obtained as 0.017 g of a white solid, 22% yield. ^{1}H NMR (400 MHz, $CDCl_3$) δ (ppm): 7.81 (d, 2H, *J*= 7.6 Hz), 7.63- 7.57 (m, 3H), 7.39 (d, 2H, *J*= 8.4 Hz), 7.22 (t, 1H, *J*= 7.6 Hz), 6.73 (s, 1H), 4.53 (s, 1H), 3.77- 3.75 (m, 4H), 3.68- 3.63 (m, 10H), 2.71 (t, 2H, *J*= 6.0 Hz), 2.54 (d, 4H). ^{13}C NMR (100 MHz, $CDCl_3$) *δ* (ppm): 170.78, 160.32, 156.19, 150.04, 142.22, 133.25, 128.54, 127.88, 125.60, 122.89, 121.15, 118.51, 111.69, 67.11, 67.05, 56.49, 53.36, 37.34. HRMS: m/z calcd for $C_{25}H_{31}N_6O_3$ [M + H]+ 463.2452; found 463.2449.

Compound **PH120**. Obtained as 0.010 g of a white solid, 10% yield. ^{1}H NMR (400 MHz, $CDCl_3$) δ (ppm): 8.04 (d, 1H, *J*= 3.2 Hz), 7.84- 7.79 (m, 4H), 7.68- 7.56 (m, 6H), 7.33 (t, 2H, *J*= 7.3 Hz), 7.23- 7.19 (m, 1H), 7.11 (t, 1H, *J*= 7.3 Hz), 6.65 (s, 1H), 3.75 (d, 4H, *J*= 3.6 Hz), 3.67- 3.61 (m, 2H), 2.69 (t, 2H, *J*= 5.8 Hz), 2.52 (s, 4H). ^{13}C NMR (100 MHz, $CDCl_3$) *δ* (ppm): 165.67, 160.29, 156.42, 150.76, 144.05, 138.37, 133.10, 129.11, 128.21, 127.22, 126.25, 124.31, 122.89, 121.11, 120.33, 118.18, 111.92, 67.10, 56.50, 53.34, 37.31. HRMS: m/z calcd for $C_{27}H_{29}N_6O_2$ [M + H]+ 469.2347; found 469.2343.

Compound **PH122**. Obtained as 0.018 g of a white solid, 23% yield. ^{1}H NMR (400 MHz, DMSO-*d6*) δ (ppm): 7.70- 7.66 (m, 2H), 7.60 (d, 2H, *J*= 7.6 Hz) 7.55 (dd, 1H, *J*= 1.4 Hz, *J*= 8.8 Hz), 7.28- 7.27 (m, 1H), 7.25- 7.24 (m, 1H), 7.22 (dd, 1H, *J*= 1.4 Hz, *J*= 8.8 Hz), 6.88 (s, 1H), 3.77 (t, 4H, *J*= 4.4 Hz), 3.68 (s, 2H), 2.72 (t, 2H, *J*= 6 Hz), 2.55 (t, 4H, *J*= 4.4 Hz). ^{13}C NMR (100 MHz, $CDCl_3$) *δ* (ppm): 179.81, 160.33, 155.46, 138.46, 133.72, 128.80, 127.95, 123.98, 123.13, 121.30, 121.05, 111.12, 67.05, 56.36, 53.39, 37.52. HRMS: m/z calcd for $C_{20}H_{23}ClN_5O$ [M + H]+ 384.1586; found 384.1576.

General Procedure for the preparation of quinazolinic compound **PH117***.* To a stirred solution of 2,4-dichloroquinazoline **3** (0.1 g, 0.502 mmol) in ethanol (3 mL), sodium acetate (0.082 g, 1 mmol) and aniline (0.327 g, 3.52 mmol) were added and heated to 120 °C. After 18 h, it was cooled and diluted with ethyl acetate (20 mL) and with saturated aqueous $NaHCO_3$ (20 mL). The organic layer was washed with water (2x20 mL), dried over Na_2SO_4, filtered and concentrated under reduced pressure. The residue was purified by silica gel column chromatography (hexanes/ethyl acetate 8:2) to give **PH117** as a white solid, 0.0589 g (38 % yield). ^{1}H NMR (400 MHz, $CDCl_3$) δ (ppm): 7.67- 7.65 (m, 4H), 7.61- 7.57 (m, 2H), 7.39- 7.34 (m, 2H), 7.26 (t, 2H), 7.21- 7.16 (m, 2H), 7.14- 7.12 (m, 1H), 7.00- 6.96 (m, 1H). ^{13}C NMR (100 MHz, $CDCl_3$) *δ* (ppm): 158.68, 156.59, 152.06, 140.11, 138.36, 133.25, 129.05, 128.84, 126.78, 124.52, 122.71, 122.21, 122.17, 120.63, 119.62, 111.68. HRMS: m/z calcd for $C_{20}H_{17}N_4$ [M + H]+ 313.1448; found 313.1449. In accordance with ref [63].

Intermediate **9**. To a stirred solution of 2,4-dichloropyrimidine **8** (0.3 g, 2.01 mmol) in THF/H_2O (6.75/2.25 mL), sodium acetate (0.182 g, 2.22 mmol) and appropriate amine (0.238 g, 2.22 mmol) were added and heated to 65 °C. After 6 h, it was cooled and diluted with ethyl acetate (40 mL) and water (40 mL). The organic layer was washed with water (2x40 mL), dried over Na_2SO_4, filtered and concentrated under reduced pressure. The residue was purified by silica gel column chromatography (hexanes/EtOAc 8:2) to give **9** as a white solid, 0.110 g (25% yield). ^{1}H NMR (400 MHz, $CDCl_3$) *δ* 7.89 (sl, 1H), 7.26- 7.16 (m, 5H), 6.46 (d, 1H, *J* = 4.8 Hz), 6.19 (sl, 1H), 4.55 (d, 2H, *J* = 6.0 Hz). ^{13}C NMR (100 MHz, $CDCl_3$) δ 162.37, 159.19, 138.57, 128.75, 127.70, 127.51, 110.29, 45.61. In accordance with ref [64].

General Procedure for the preparation of pyrimidinic compounds **PH110** *and* **PH112**. To a stirred solution of **9** (0.05 g, 0.23 mmol) in ethanol (1 mL) the appropriate amine was added (0.34 mmol) and heated to 120 °C. After 3 h, it was cooled, diluted with ethyl acetate (20 mL) and washed with saturated aqueous $NaHCO_3$ (20 mL). The organic layer was washed with water (20 mL), dried over Na_2SO_4, filtered and concentrated under reduced pressure. The residue was purified by silica gel column chromatography.

Compound **PH110**. Obtained as 0.0218 g of a yellow solid, 35% yield. ^{1}H NMR (400 MHz, DMSO-*d6*) *δ* 7.92 (d, 1H, *J*= 5.8 Hz) 7.37- 7.24 (m, 9H), 7.12- 7.07 (m, 1H), 6.76 (s, 1H), 6.04 (d, 1H, *J*= 5.8 Hz), 5.51 (sl, 1H) e 4.62 (d, 2H, *J*= 5.6 Hz). ^{13}C NMR (100 MHz, DMSO-*d6*) *δ* 161.93, 160.57, 156,18, 140.97, 140.49, 128.50, 128.10, 126.88, 126.35, 121.40, 119.23, 96.80, 44.11. HRMS: m/z calcd for $C_{17}H_{17}N_4$ [M + H]+ 277.1448; found 277.1446.

Compound **PH112**. Obtained as 0.032 g of a white solid, 28% yield. ^{1}H NMR (400 MHz, DMSO-*d6*) *δ* (ppm): 9.14 (s, 1H), 7.84−7.70 (m, 4H), 7.34−7.33 (m, 4H), 7.26−7.18 (m, 3H), 6.04 (br s, 1H), 4.54 (br s, 2H). ^{13}C NMR (100 MHz, DMSO-*d6*) *δ* 161.87, 160.33, 156.49, 140.86, 139.54, 128.29, 128.16, 126.82, 126.40, 124.73, 120.54, 96.66, 44.14. HRMS: m/z calcd for $C_{17}H_{16}ClN_4$ [M + H]+ 311.1058; found 311.1056.

*Synthesis of 2,6-dichloro-9-methyl-9H-purine (***11***)* To a stirred solution of 2,6-dichloro-9H-purine **10** (0.3 g, 1.59 mmol) in DMF (2 mL), potassium carbonate (0.66 g, 4.77 mmol) and iodomethane (0.5 mL, 8.75 mmol) were added at for 1 h and 4h rt. After, it was diluted with ethyl acetate (30 mL) and water (30 mL). The aqueous layer was washed with ethyl acetate (30 mL), the organic layer was dried over Na_2SO_4, filtered and concentrated under reduced pressure. The residue was purified by silica gel column chromatography (hexanes/EtOAc 7:3) to give **11** as a white solid, 0.248 g, (77 % yield). ^{1}H NMR (400 MHz, $CDCl_3$) *δ* 8.09 (s, 1H), 3.91 (s, 3H). ^{13}C NMR (100 MHz, $CDCl_3$) *δ* 153.60, 153.19, 151.90, 146.43, 130.77 e 30.65. In accordance with ref [65].

Synthesis of Intermediate **12**. To a stirred solution of **11** (0.15 g, 0.739 mmol) in THF/H_2O (6 mL/2 mL), sodium acetate (0.067 g, 0,813 mmol) and appropriate amine (0.87 g, 0.813 mmol) were added and heated to 65 °C. After 18 h, it was cooled and diluted with ethyl acetate (40 mL) and water (40 mL). The organic layer was washed with water (2x40 mL), dried over Na_2SO_4, filtered and concentrated under reduced pressure. The residue was purified by silica gel column chromatography (hexanes/EtOAc 6:4) to give **12** as a white solid, 0.072 g (36 % yield). ^{1}H NMR (400 MHz, DMSO-*d6*) *δ* 8.76 (t, 1H, *J* = 5.6 Hz), 8.11 (s, 1H), 7.35- 7.28 (m, 4H), 7.24- 7.20 (m, 1H), 4.64 (d, 2H, *J*=5.6 Hz), 3.69 (s, 3H). ^{13}C NMR (100 MHz, DMSO-*d6*) *δ* 154.93,

153.05, 150.32, 142.06, 139.35, 128.33, 127.30, 126.87, 118.07, 43.18, 29.69. In accordance with ref [65].

General Procedure for the preparation of purinic compounds **PH111** *and* **PH113**. To a stirred solution of **12** in DMF (1 mL), palladium acetate (II) (0.003 g, 0.0128 mmol), xantphos (0.008 g, 0.0128 mmol), appropriate amine (0.274 mmol) and cesium carbonate (0.119 g, 0.365 mmol) were added and heated to 140°C under N_2 atmosphere. After 18 h, it was cooled, diluted with ethyl acetate (20 mL), filtered and concentrated under reduced pressure. The residue was purified by silica gel column chromatography.

Compound **PH111**. Obtained as 0.0237 g of a white solid, 39% yield. ^{1}H NMR (400 MHz, DMSO-*d6*) *δ* 8.95 (s, 1H), 8.12 (d, 1H, *J* = 6.4 Hz), 7.83 (s, 1H), 7.76- 7.75 (m, 2H), 7.38 (d, 2H, *J* = 7.4 Hz), 7.30 (t, 2H, *J* = 7.4 Hz), 7.22- 7.14 (m, 3H), 6.82 (t, 1H, *J* = 7.2 Hz), 4.72 (sl, 2H), 3.65 (s, 3H). ^{13}C NMR (100 MHz, DMSO-*d6*) *δ* 156.21, 154.44, 150.90, 141.72, 140.42, 139.03, 128.21, 127.04, 126.56, 120.03, 118.08, 114.17, 43.11, 29.18. HRMS: m/z calcd for $C_{19}H_{19}N_6$ [M + H]+ 331.1666; found 331.1661.

Compound **PH113**. Obtained as 0.028 g of a white solid, 42% yield.^{1}H NMR (400 MHz, DMSO-*d6*) *δ* 9.13 (s, 1H), 8.17 (sl, 1H), 7.85 (s, 1H), 7.76 (d, 2H, *J* = 7.2 Hz), 7.36 (d, 2H, *J* = 7.2 Hz), 7.30 (t, 2H, *J* = 7.2 Hz), 7.25- 7.15 (m, 3H), 4.71 (s, 2H), 3.65 (s, 3H). ^{13}C NMR (100 MHz, DMSO-*d6*) *δ* (ppm): 155.91, 154.49, 140.73, 140.31, 139.27, 128.25, 128.02, 127.30, 126.95, 126.60, 123.36, 119.44, 43.18, 29.26. HRMS: m/z calcd for $C_{19}H_{18}ClN_6$ [M + H]+ 365.1276; found 365.1274.

Cruzain and Rhodesain Inhibition Assays

Cruzain and rhodesain activity was measured by monitoring the cleavage of the fluorescent substrate Z-Phe-Arg-aminomethylcoumarin (Z-FR-AMC), in a Synergy 2 (Biotek) fluorimeter, of the Centre for Flow Cytometry Fluorimetry at the Department of Biochemistry and Immunology (UFMG). All assays were performed in 96-well plate format, in a final volume of 200 µL, in a buffer solution of 0.1 M sodium acetate pH 5.5 in the presence of 0.1 mM beta-mercaptoethanol, 0.01% Triton X-100, 0.5 nM cruzain

or rhodesain and 2.5 µM of the substrate, as described previously[47]. The assay was performed without and with pre-incubation of the compounds with the enzyme. The initial screen was performed with 100 µM of inhibitors. For each assay, two independent experiments were performed, each in triplicates and monitored for 5 minutes. Enzymatic activities were calculated based on comparison with a DMSO control, from initial rates of reaction. E64 was used as positive control at the concentration of 1 µM in the assay. Compounds were observed to be no time-dependent, then all subsequent assays were performed without pre-incubation. IC_{50} curves were determined in two independent experiments, each involving at least seven compound concentrations in triplicates. IC_{50} curves were determined with GraphPad Prism.

Assays using Triton-X 100 Assay and Preincubation with BSA.

Assays were performed as described in[60].

Intracellular Trypanosoma cruzi Assays and Cytotoxicity

These tests were carried out in partnership with Professor Jair Siqueira's group at the University of California, San Diego (UCSD). Mouse myoblast cell line C2C12 was cultivated in Dulbecco's Modified Eagle's Medium containing 4.5 g/l glucose (DMEM), supplemented with 5% fetal bovine serum (FBS), 1% of penicillin and streptomycin. *T. cruzi* CA-I/72 trypomastigotes were obtained from C2C12 infected-culture supernatants after 7 days of infection. Cultures were maintained at 37°C with 5% CO_2. To assess anti-parasitic activity of the compounds, 500 C2C12 cells were seeded in 384-well plate in 50 µL of DMEM media per well and 7500 parasites/well. Compounds were added at 10 mM in 50 nL per well using a Biomek FX (Beckman Coulter) for a final 10 µM concentration in 50 µl total volume. The plate was incubated for 72 h at 37°C with 5% CO_2. After the incubation, the plate was fixed with the addition of a 4% paraformaldehyde solution for 1 h, followed by two successive washing steps using phosphate buffered saline (PBS). Finally, a staining solution containing 0.2 µg/ml of 4',6-diamidino-2-phenylindole (DAPI) was added to each well of the plate and incubated for at least 2 hours. The analysis was performed using the ImageXpress device, and for differential cell and parasite counting, the MetaXpress software was

used. The size parameters used to segment host and parasite organelles were 125 μm^2 for host nucleus, and 1–2 μm^2 for parasite nucleus/kinetoplast. Numbers of host cells and intracellular amastigotes were determined based on host cell and parasite nucleus quantification, providing a measure of growth inhibition during the first 72 h of post-infection treatment compared to untreated controls. The anti-parasitic results were expressed in terms of relative activity normalized based on the average infection ratio (number of infected cells/total number of cells) of negative controls (1% DMSO, 0% activity) and positive controls (50 µM of benznidazole, EC_{100}, 100% activity). The host cell viability was assessed based on the total number of cells divided by the average number of cells from untreated controls (1% DMSO), when <0.5 considered a cytotoxic compound. The test was performed in duplicate[66].

Intracellular Trypanosoma b. brucei Assays

These tests were carried out in partnership with Professor Jair Siqueira's group at the University of California, San Diego (UCSD). Bloodstream forms of *T. b. brucei* Lister 427 were cultured in modified HMI-9 medium[67,68] in T25 vented flasks (Thermo Fisher Scientific; Cat Nº. FB012933) in a humidified atmosphere of 5% CO_2 at 37ºC. Parasites were conserved in log-phase growth and passaged every 48 h. The SYBR Green assay was used to determine the compounds' effects on *T. b. brucei* growth. Compounds were serially diluted over eight concentrations ranging from 50 µM to 390 nM. The positive drug control, pentamidine, was diluted from 4 µM to 0.88 nM. All compounds were added to the cultures as solutions in dimethyl sulfoxide (DMSO; Thermo Scientific™ 85190 (Cat Nº. PI85190). Data reported are from two biological experiments and a total of three or four technical replicates, except for **PH108** for which the data are from two technical replicates. Trypanosomes in log-phase growth were suspended as $2x10^5$ trypanosomes/mL in modified HMI-9 medium under continuous agitation, and dispensed (100 µL/well) into 96-well plates (Corning 3903) containing 1 µL of the test compound in 0.5% DMSO and 100 µL/well of fresh medium (20,000 cells/well). The plates were incubated for 72 h at 37 °C and 5% CO_2, followed by addition of 50 µL/well of lysis solution (30 mM Tris pH 7.5, 7.5 mM EDTA, 0.012% saponin (Sigma-Aldrich Cat. No. S9430), and 0.12% Triton X-100 (Thermo Fisher Scientific; CAS 9002-93-1)) containing 0.3 µL/mL SYBR Green I (10,000x in DMSO; Invitrogen, Carlsbad, CA). After incubation in the dark for at least 1 h at room

temperature, plates were read on the 2104 EnVision® multilabel plate reader (PerkinElmer, Waltham, MA) with excitation at 485 nm and emission at 535 nm. The activity of test compounds was normalized against DMSO controls from the same plate. Half-maximal effective concentration (EC_{50}) values were calculated using GraphPad Prism software, version 9.00 for MAC OS.

Acknowledgements

We thank Dr. Rafael Pinto Vieira for the contribution in the assembly of the virtual screening library employed in this study and Dr. Marcela Silva Lopes, Faculdade de Farmácia, UFRGS, Brazil, for HPLC analysis. This research was partially funded by the Brazilian agencies CAPES, CNPq, FAPEMIG, and FAPERGS, through grants: Ph.D. scholarship from CNPq grant 141841/2018-4 to DAR; CNPq Universal 01/2016, 402318/2016-1 to S.F.A.; and CAPES (Edital 51/2013 Biologia Computacional), FAPEMIG (Rede Mineira de Imunobiologicos grant # REDE-00140-16 and PPM-00342- 16), and CNPq (Bolsa de Produtividade em Pequisa, processo 306606/2017-8) to R.S.F. E.B.S. received a Ph.D. scholarship from CAPES. C.R.C., L.M., and W.Y. acknowledge the grant support from NIH-NIAID R21AI141210 and R21AI133394.

4.6 References

(1) https://www.who.int/. WHO.

(2) https://dndi.org/. https://dndi.org/.

(3) Organization, W. H. *Control and Surveillance of Human African Trypanosomiasis: Report of a WHO Expert Committee*; 2013.

(4) https://www.cdc.gov/parasites/chagas/gen_info/detailed.html. CDC.

(5) Dias, L. C.; Dessoy, M. A.; Silva, J. J. N.; Thiemann, O. H.; Oliva, G.; Andricopulo, A. D. Quimioterapia Da Doença de Chagas: Estado Da Arte e

Perspectivas No Desenvolvimento de Novos Fármacos. *Quim. Nova* **2009**, *32* (9), 2444–2457. https://doi.org/10.1590/S0100-40422009000900038.

(6) Bermudez, J.; Davies, C.; Simonazzi, A.; Pablo Real, J.; Palma, S. Current Drug Therapy and Pharmaceutical Challenges for Chagas Disease. *Acta Trop.* **2016**, *156*, 1–16. https://doi.org/10.1016/j.actatropica.2015.12.017.

(7) Mott, B. T.; Ferreira, R. S.; Simeonov, A.; Jadhav, A.; Ang, K. K.-H.; Leister, W.; Shen, M.; Silveira, J. T.; Doyle, P. S.; Arkin, M. R.; McKerrow, J. H.; Inglese, J.; Austin, C. P.; Thomas, C. J.; Shoichet, B. K.; Maloney, D. J. Identification and Optimization of Inhibitors of Trypanosomal Cysteine Proteases: Cruzain, Rhodesain, and TbCatB. *J. Med. Chem.* **2010**, *53* (1), 52–60. https://doi.org/10.1021/jm901069a.

(8) Sajid, M.; Robertson, S. A.; Brinen, L. S.; McKerrow, J. H. Cruzain; 2011; pp 100–115. https://doi.org/10.1007/978-1-4419-8414-2_7.

(9) Bottieau, E.; Clerinx, J. Human African Trypanosomiasis. *Infect. Dis. Clin. North Am.* **2019**, *33* (1), 61–77. https://doi.org/10.1016/j.idc.2018.10.003.

(10) Delespaux, V.; de Koning, H. P. Drugs and Drug Resistance in African Trypanosomiasis. *Drug Resist. Updat.* **2007**, *10* (1–2), 30–50. https://doi.org/10.1016/j.drup.2007.02.004.

(11) Hawking, F. Concentration of Bayer 205 (Germanin) in Human Blood and Cerebrospinal Fluid after Treatment. *Trans. R. Soc. Trop. Med. Hyg.* **1940**, *34* (1), 37–52. https://doi.org/10.1016/S0035-9203(40)90088-8.

(12) Mesu, V. K. B. K.; Kalonji, W. M.; Bardonneau, C.; Mordt, O. V.; Blesson, S.; Simon, F.; Delhomme, S.; Bernhard, S.; Kuziena, W.; Lubaki, J.-P. F.; Vuvu, S. L.; Ngima, P. N.; Mbembo, H. M.; Ilunga, M.; Bonama, A. K.; Heradi, J. A.; Solomo, J. L. L.; Mandula, G.; Badibabi, L. K.; Dama, F. R.; Lukula, P. K.; Tete, D. N.; Lumbala, C.; Scherrer, B.; Strub-Wourgaft, N.; Tarral, A. Oral Fexinidazole for Late-Stage African Trypanosoma Brucei Gambiense Trypanosomiasis: A Pivotal Multicentre,

Randomised, Non-Inferiority Trial. *Lancet* **2018**, *391* (10116), 144–154. https://doi.org/10.1016/S0140-6736(17)32758-7.

(13) Deeks, E. D. Fexinidazole: First Global Approval. *Drugs* **2019**, *79* (2), 215–220. https://doi.org/10.1007/s40265-019-1051-6.

(14) Lindner, A. K.; Lejon, V.; Chappuis, F.; Seixas, J.; Kazumba, L.; Barrett, M. P.; Mwamba, E.; Erphas, O.; Akl, E. A.; Villanueva, G.; Bergman, H.; Simarro, P.; Kadima Ebeja, A.; Priotto, G.; Franco, J. R. New WHO Guidelines for Treatment of Gambiense Human African Trypanosomiasis Including Fexinidazole: Substantial Changes for Clinical Practice. *Lancet Infect. Dis.* **2020**, *20* (2), e38–e46. https://doi.org/10.1016/S1473-3099(19)30612-7.

(15) Steverding, D.; Caffrey, C. R. Should the Enzyme Name 'Rhodesain' Be Discontinued? *Mol. Biochem. Parasitol.* **2021**, *245*, 111395. https://doi.org/10.1016/j.molbiopara.2021.111395.

(16) Ferreira, L. G.; Andricopulo, A. D. Targeting Cysteine Proteases in Trypanosomatid Disease Drug Discovery. *Pharmacol. Ther.* **2017**, *180*, 49–61. https://doi.org/10.1016/j.pharmthera.2017.06.004.

(17) Santos, C. C.; Coombs, G. H.; Lima, A. P. C. A.; Mottram, J. C. Role of the Trypanosoma Brucei Natural Cysteine Peptidase Inhibitor ICP in Differentiation and Virulence. *Mol. Microbiol.* **2007**, *66* (4), 991–1002. https://doi.org/10.1111/j.1365-2958.2007.05970.x.

(18) da Silva, E. B.; do Nascimento Pereira, G. A.; Ferreira, R. S. Trypanosomal Cysteine Peptidases: Target Validation and Drug Design Strategies. In *Comprehensive Analysis of Parasite Biology: From Metabolism to Drug Discovery*; Wiley-VCH Verlag GmbH & Co. KGaA: Weinheim, Germany, 2016; pp 121–145. https://doi.org/10.1002/9783527694082.ch5.

(19) Rocha, D. A.; Silva, E. B.; Fortes, I. S.; Lopes, M. S.; Ferreira, R. S.; Andrade, S. F. Synthesis and Structure-Activity Relationship Studies of Cruzain and Rhodesain

Inhibitors. *Eur. J. Med. Chem.* **2018**, *157*, 1426–1459. https://doi.org/10.1016/j.ejmech.2018.08.079.

(20) Palmer, J. T.; Rasnick, D.; Klaus, J. L.; Bromme, D. Vinyl Sulfones as Mechanism-Based Cysteine Protease Inhibitors. *J. Med. Chem.* **1995**, *38* (17), 3193–3196. https://doi.org/10.1021/jm00017a002.

(21) Santos, M.; Moreira, R. Michael Acceptors as Cysteine Protease Inhibitors. *Mini-Reviews Med. Chem.* **2007**, *7* (10), 1040–1050. https://doi.org/10.2174/138955707782110105.

(22) Engel, J. C.; Doyle, P. S.; Hsieh, I.; McKerrow, J. H. Cysteine Protease Inhibitors Cure an Experimental Trypanosoma Cruzi Infection. *J. Exp. Med.* **1998**, *188* (4), 725–734. https://doi.org/10.1084/jem.188.4.725.

(23) Chen, Y. T.; Brinen, L. S.; Kerr, I. D.; Hansell, E.; Doyle, P. S.; McKerrow, J. H.; Roush, W. R. In Vitro and In Vivo Studies of the Trypanocidal Properties of WRR-483 against Trypanosoma Cruzi. *PLoS Negl. Trop. Dis.* **2010**, *4* (9), e825. https://doi.org/10.1371/journal.pntd.0000825.

(24) Jones, B. D.; Tochowicz, A.; Tang, Y.; Cameron, M. D.; McCall, L.-I.; Hirata, K.; Siqueira-Neto, J. L.; Reed, S. L.; McKerrow, J. H.; Roush, W. R. Synthesis and Evaluation of Oxyguanidine Analogues of the Cysteine Protease Inhibitor WRR-483 against Cruzain. *ACS Med. Chem. Lett.* **2016**, *7* (1), 77–82. https://doi.org/10.1021/acsmedchemlett.5b00336.

(25) Kerr, I. D.; Lee, J. H.; Farady, C. J.; Marion, R.; Rickert, M.; Sajid, M.; Pandey, K. C.; Caffrey, C. R.; Legac, J.; Hansell, E.; McKerrow, J. H.; Craik, C. S.; Rosenthal, P. J.; Brinen, L. S. Vinyl Sulfones as Antiparasitic Agents and a Structural Basis for Drug Design. *J. Biol. Chem.* **2009**, *284* (38), 25697–25703. https://doi.org/10.1074/jbc.M109.014340.

(26) Doyle, P. S.; Zhou, Y. M.; Engel, J. C.; McKerrow, J. H. A Cysteine Protease Inhibitor Cures Chagas' Disease in an Immunodeficient-Mouse Model of Infection.

Antimicrob. Agents Chemother. **2007**, *51* (11), 3932–3939. https://doi.org/10.1128/AAC.00436-07.

(27) Barr, S. C.; Warner, K. L.; Kornreic, B. G.; Piscitelli, J.; Wolfe, A.; Benet, L.; McKerrow, J. H. A Cysteine Protease Inhibitor Protects Dogs from Cardiac Damage during Infection by Trypanosoma Cruzi. *Antimicrob. Agents Chemother.* **2005**, *49* (12), 5160–5161. https://doi.org/10.1128/AAC.49.12.5160-5161.2005.

(28) Caputto, M. E.; Fabian, L. E.; Benítez, D.; Merlino, A.; Ríos, N.; Cerecetto, H.; Moltrasio, G. Y.; Moglioni, A. G.; González, M.; Finkielsztein, L. M. Thiosemicarbazones Derived from 1-Indanones as New Anti-Trypanosoma Cruzi Agents. *Bioorg. Med. Chem.* **2011**, *19* (22), 6818–6826. https://doi.org/10.1016/j.bmc.2011.09.037.

(29) Fonseca, N. C.; da Cruz, L. F.; da Silva Villela, F.; do Nascimento Pereira, G. A.; de Siqueira-Neto, J. L.; Kellar, D.; Suzuki, B. M.; Ray, D.; de Souza, T. B.; Alves, R. J.; Júnior, P. A. S.; Romanha, A. J.; Murta, S. M. F.; McKerrow, J. H.; Caffrey, C. R.; de Oliveira, R. B.; Ferreira, R. S. Synthesis of a Sugar-Based Thiosemicarbazone Series and Structure-Activity Relationship versus the Parasite Cysteine Proteases Rhodesain, Cruzain, and Schistosoma Mansoni Cathepsin B1. *Antimicrob. Agents Chemother.* **2015**, *59* (5), 2666–2677. https://doi.org/10.1128/AAC.04601-14.

(30) Espíndola, J. W. P.; Cardoso, M. V. de O.; Filho, G. B. de O.; Oliveira e Silva, D. A.; Moreira, D. R. M.; Bastos, T. M.; Simone, C. A. de; Soares, M. B. P.; Villela, F. S.; Ferreira, R. S.; Castro, M. C. A. B. de; Pereira, V. R. A.; Murta, S. M. F.; Sales Junior, P. A.; Romanha, A. J.; Leite, A. C. L. Synthesis and Structure–Activity Relationship Study of a New Series of Antiparasitic Aryloxyl Thiosemicarbazones Inhibiting Trypanosoma Cruzi Cruzain. *Eur. J. Med. Chem.* **2015**, *101*, 818–835. https://doi.org/10.1016/j.ejmech.2015.06.048.

(31) da Silva, E. B.; Oliveira e Silva, D. A.; Oliveira, A. R.; da Silva Mendes, C. H.; dos Santos, T. A. R.; da Silva, A. C.; de Castro, M. C. A.; Ferreira, R. S.; Moreira, D. R. M.; Cardoso, M. V. de O.; de Simone, C. A.; Pereira, V. R. A.; Leite, A. C. L. Desing and Synthesis of Potent Anti - Trypanosoma Cruzi Agents New Thiazoles Derivatives

Which Induce Apoptotic Parasite Death. *Eur. J. Med. Chem.* **2017**, *130*, 39–50. https://doi.org/10.1016/j.ejmech.2017.02.026.

(32) de Moraes Gomes, P. A. T.; de Oliveira Barbosa, M.; Farias Santiago, E.; de Oliveira Cardoso, M. V.; Capistrano Costa, N. T.; Hernandes, M. Z.; Moreira, D. R. M.; da Silva, A. C.; dos Santos, T. A. R.; Pereira, V. R. A.; Brayner dos Santosd, F. A.; do Nascimento Pereira, G. A.; Ferreira, R. S.; Leite, A. C. L. New 1,3-Thiazole Derivatives and Their Biological and Ultrastructural Effects on Trypanosoma Cruzi. *Eur. J. Med. Chem.* **2016**, *121*, 387–398. https://doi.org/10.1016/j.ejmech.2016.05.050.

(33) de Oliveira Filho, G. B.; Cardoso, M. V. de O.; Espíndola, J. W. P.; Oliveira e Silva, D. A.; Ferreira, R. S.; Coelho, P. L.; Anjos, P. S. dos; Santos, E. de S.; Meira, C. S.; Moreira, D. R. M.; Soares, M. B. P.; Leite, A. C. L. Structural Design, Synthesis and Pharmacological Evaluation of Thiazoles against Trypanosoma Cruzi. *Eur. J. Med. Chem.* **2017**, *141*, 346–361. https://doi.org/10.1016/j.ejmech.2017.09.047.

(34) Silva-Júnior, E. F.; Silva, E. P. S.; França, P. H. B.; Silva, J. P. N.; Barreto, E. O.; Silva, E. B.; Ferreira, R. S.; Gatto, C. C.; Moreira, D. R. M.; Siqueira-Neto, J. L.; Mendonça-Júnior, F. J. B.; Lima, M. C. A.; Bortoluzzi, J. H.; Scotti, M. T.; Scotti, L.; Meneghetti, M. R.; Aquino, T. M.; Araújo-Júnior, J. X. Design, Synthesis, Molecular Docking and Biological Evaluation of Thiophen-2-Iminothiazolidine Derivatives for Use against Trypanosoma Cruzi. *Bioorg. Med. Chem.* **2016**, *24* (18), 4228–4240. https://doi.org/10.1016/j.bmc.2016.07.013.

(35) Avelar, L. A. A.; Camilo, C. D.; de Albuquerque, S.; Fernandes, W. B.; Gonçalez, C.; Kenny, P. W.; Leitão, A.; McKerrow, J. H.; Montanari, C. A.; Orozco, E. V. M.; Ribeiro, J. F. R.; Rocha, J. R.; Rosini, F.; Saidel, M. E. Molecular Design, Synthesis and Trypanocidal Activity of Dipeptidyl Nitriles as Cruzain Inhibitors. *PLoS Negl. Trop. Dis.* **2015**, *9* (7), e0003916. https://doi.org/10.1371/journal.pntd.0003916.

(36) Burtoloso, A. C. B.; de Albuquerque, S.; Furber, M.; Gomes, J. C.; Gonçalez, C.; Kenny, P. W.; Leitão, A.; Montanari, C. A.; Quilles, J. C.; Ribeiro, J. F. R.; Rocha, J. R. Anti-Trypanosomal Activity of Non-Peptidic Nitrile-Based Cysteine Protease

Inhibitors. *PLoS Negl. Trop. Dis.* **2017**, *11* (2), e0005343. https://doi.org/10.1371/journal.pntd.0005343.

(37) Giroud, M.; Kuhn, B.; Saint-Auret, S.; Kuratli, C.; Martin, R. E.; Schuler, F.; Diederich, F.; Kaiser, M.; Brun, R.; Schirmeister, T.; Haap, W. 2 H -1,2,3-Triazole-Based Dipeptidyl Nitriles: Potent, Selective, and Trypanocidal Rhodesain Inhibitors by Structure-Based Design. *J. Med. Chem.* **2018**, *61* (8), 3370–3388. https://doi.org/10.1021/acs.jmedchem.7b01870.

(38) Löser, R.; Schilling, K.; Dimmig, E.; Gütschow, M. Interaction of Papain-like Cysteine Proteases with Dipeptide-Derived Nitriles †. *J. Med. Chem.* **2005**, *48* (24), 7688–7707. https://doi.org/10.1021/jm050686b.

(39) Silva, J. R. A.; Cianni, L.; Araujo, D.; Batista, P. H. J.; de Vita, D.; Rosini, F.; Leitão, A.; Lameira, J.; Montanari, C. A. Assessment of the Cruzain Cysteine Protease Reversible and Irreversible Covalent Inhibition Mechanism. *J. Chem. Inf. Model.* **2020**, *60* (3), 1666–1677. https://doi.org/10.1021/acs.jcim.9b01138.

(40) Ettari, R.; Tamborini, L.; Angelo, I. C.; Grasso, S.; Schirmeister, T.; Lo Presti, L.; De Micheli, C.; Pinto, A.; Conti, P. Development of Rhodesain Inhibitors with a 3-Bromoisoxazoline Warhead. *ChemMedChem* **2013**, *8* (12), 2070–2076. https://doi.org/10.1002/cmdc.201300390.

(41) Ettari, R.; Previti, S.; Cosconati, S.; Kesselring, J.; Schirmeister, T.; Grasso, S.; Zappalà, M. Synthesis and Biological Evaluation of Novel Peptidomimetics as Rhodesain Inhibitors. *J. Enzyme Inhib. Med. Chem.* **2016**, *31* (6), 1184–1191. https://doi.org/10.3109/14756366.2015.1108972.

(42) Ettari, R.; Pinto, A.; Previti, S.; Tamborini, L.; Angelo, I. C.; La Pietra, V.; Marinelli, L.; Novellino, E.; Schirmeister, T.; Zappalà, M.; Grasso, S.; De Micheli, C.; Conti, P. Development of Novel Dipeptide-like Rhodesain Inhibitors Containing the 3-Bromoisoxazoline Warhead in a Constrained Conformation. *Bioorg. Med. Chem.* **2015**, *23* (21), 7053–7060. https://doi.org/10.1016/j.bmc.2015.09.029.

(43) Braga, S. F. P.; Martins, L. C.; da Silva, E. B.; Sales Júnior, P. A.; Murta, S. M. F.; Romanha, A. J.; Soh, W. T.; Brandstetter, H.; Ferreira, R. S.; de Oliveira, R. B. Synthesis and Biological Evaluation of Potential Inhibitors of the Cysteine Proteases Cruzain and Rhodesain Designed by Molecular Simplification. *Bioorg. Med. Chem.* **2017**, *25* (6), 1889–1900. https://doi.org/10.1016/j.bmc.2017.02.009.

(44) de Souza, M. L.; de Oliveira Rezende Junior, C.; Ferreira, R. S.; Espinoza Chávez, R. M.; Ferreira, L. L. G.; Slafer, B. W.; Magalhães, L. G.; Krogh, R.; Oliva, G.; Cruz, F. C.; Dias, L. C.; Andricopulo, A. D. Discovery of Potent, Reversible, and Competitive Cruzain Inhibitors with Trypanocidal Activity: A Structure-Based Drug Design Approach. *J. Chem. Inf. Model.* **2020**, *60* (2), 1028–1041. https://doi.org/10.1021/acs.jcim.9b00802.

(45) Pauli, I.; Ferreira, L. G.; de Souza, M. L.; Oliva, G.; Ferreira, R. S.; Dessoy, M. A.; Slafer, B. W.; Dias, L. C.; Andricopulo, A. D. Molecular Modeling and Structure–Activity Relationships for a Series of Benzimidazole Derivatives as Cruzain Inhibitors. *Future Med. Chem.* **2017**, *9* (7), 641–657. https://doi.org/10.4155/fmc-2016-0236.

(46) Andrade, M. M. S.; Martins, L. C.; Marques, G. V. L.; Silva, C. A.; Faria, G.; Caldas, S.; dos Santos, J. S.; Leclercq, S. Y.; Maltarollo, V. G.; Ferreira, R. S.; Oliveira, R. B. Synthesis of Quinoline Derivatives as Potential Cysteine Protease Inhibitors. *Future Med. Chem.* **2020**, *12* (7), fmc-2019-0201. https://doi.org/10.4155/fmc-2019-0201.

(47) Pereira, G. A. N.; da Silva, E. B.; Braga, S. F. P.; Leite, P. G.; Martins, L. C.; Vieira, R. P.; Soh, W. T.; Villela, F. S.; Costa, F. M. R.; Ray, D.; de Andrade, S. F.; Brandstetter, H.; Oliveira, R. B.; Caffrey, C. R.; Machado, F. S.; Ferreira, R. S. Discovery and Characterization of Trypanocidal Cysteine Protease Inhibitors from the 'Malaria Box.' *Eur. J. Med. Chem.* **2019**, *179*, 765–778. https://doi.org/10.1016/j.ejmech.2019.06.062.

(48) Gui, L.; Zhang, X.; Li, K.; Frankowski, K. J.; Li, S.; Wong, D. E.; Moen, D. R.; Porubsky, P. R.; Lin, H. J.; Schoenen, F. J.; Chou, T.-F. Evaluating P97 Inhibitor

Analogues for Potency against P97-P37 and P97-Npl4-Ufd1 Complexes. *ChemMedChem* **2016**, *11* (9), 953–957. https://doi.org/10.1002/cmdc.201600036.

(49) Ismail, R. S. M.; Abou-Seri, S. M.; Eldehna, W. M.; Ismail, N. S. M.; Elgazwi, S. M.; Ghabbour, H. A.; Ahmed, M. S.; Halaweish, F. T.; Abou El Ella, D. A. Novel Series of 6-(2-Substitutedacetamido)-4-Anilinoquinazolines as EGFR-ERK Signal Transduction Inhibitors in MCF-7 Breast Cancer Cells. *Eur. J. Med. Chem.* **2018**, *155*, 782–796. https://doi.org/10.1016/j.ejmech.2018.06.024.

(50) Van Horn, K. S.; Zhu, X.; Pandharkar, T.; Yang, S.; Vesely, B.; Vanaerschot, M.; Dujardin, J.-C.; Rijal, S.; Kyle, D. E.; Wang, M. Z.; Werbovetz, K. A.; Manetsch, R. Antileishmanial Activity of a Series of N 2 , N 4 -Disubstituted Quinazoline-2,4-Diamines. *J. Med. Chem.* **2014**, *57* (12), 5141–5156. https://doi.org/10.1021/jm5000408.

(51) Guillon, J.; Cohen, A.; Boudot, C.; Valle, A.; Milano, V.; Das, R. N.; Guédin, A.; Moreau, S.; Ronga, L.; Savrimoutou, S.; Demourgues, M.; Reviriego, E.; Rubio, S.; Ferriez, S.; Agnamey, P.; Pauc, C.; Moukha, S.; Dozolme, P.; Nascimento, S. Da; Laumaillé, P.; Bouchut, A.; Azas, N.; Mergny, J.-L.; Mullié, C.; Sonnet, P.; Courtioux, B. Design, Synthesis, and Antiprotozoal Evaluation of New 2,4-Bis[(Substituted-Aminomethyl)Phenyl]Quinoline, 1,3-Bis[(Substituted-Aminomethyl)Phenyl]Isoquinoline and 2,4-Bis[(Substituted-Aminomethyl)Phenyl]Quinazoline Derivatives. *J. Enzyme Inhib. Med. Chem.* **2020**, *35* (1), 432–459. https://doi.org/10.1080/14756366.2019.1706502.

(52) Pobsuk, N.; Suphakun, P.; Hannongbua, S.; Nantasenamat, C.; Choowongkomon, K.; Gleeson, M. P. Synthesis, Plasmodium Falciparum Inhibitory Activity, Cytotoxicity and Solubility of N2 ,N4 -Disubstituted Quinazoline-2,4-Diamines. *Med. Chem. (Los. Angeles).* **2019**, *15* (6), 693–704. https://doi.org/10.2174/1573406415666181219100307.

(53) Fleeman, R.; Van Horn, K. S.; Barber, M. M.; Burda, W. N.; Flanigan, D. L.; Manetsch, R.; Shaw, L. N. Characterizing the Antimicrobial Activity of N 2 , N 4 -Disubstituted Quinazoline-2,4-Diamines toward Multidrug-Resistant Acinetobacter

Baumannii. *Antimicrob. Agents Chemother.* **2017**, *61* (6). https://doi.org/10.1128/AAC.00059-17.

(54) Reis, S. V. dos; Ribeiro, N. S.; Rocha, D. A.; Fortes, I. S.; Trentin, D. da S.; Andrade, S. F. de; Macedo, A. J. N 4 -benzyl-N 2 -phenylquinazoline-2,4-diamine Compound Presents Antibacterial and Antibiofilm Effect against Staphylococcus Aureus and Staphylococcus Epidermidis. *Chem. Biol. Drug Des.* **2020**, *96* (6), 1372–1379. https://doi.org/10.1111/cbdd.13745.

(55) Bianco, A.; Reghellin, V.; Donnici, L.; Fenu, S.; Alvarez, R.; Baruffa, C.; Peri, F.; Pagani, M.; Abrignani, S.; Neddermann, P.; De Francesco, R. Metabolism of Phosphatidylinositol 4-Kinase IIIα-Dependent PI4P Is Subverted by HCV and Is Targeted by a 4-Anilino Quinazoline with Antiviral Activity. *PLoS Pathog.* **2012**, *8* (3), e1002576. https://doi.org/10.1371/journal.ppat.1002576.

(56) Wang, M.; Zhang, G.; Wang, Y.; Wang, J.; Zhu, M.; Cen, S.; Wang, Y. Design, Synthesis and Anti-Influenza A Virus Activity of Novel 2,4-Disubstituted Quinazoline Derivatives. *Bioorg. Med. Chem. Lett.* **2020**, *30* (11), 127143. https://doi.org/10.1016/j.bmcl.2020.127143.

(57) Zhang, G.; Wang, X.; Li, C.; Yin, D. Palladium-Catalyzed Cross-Coupling of Electron-Deficient Heteroaromatic Amines with Heteroaryl Halides. *Synth. Commun.* **2013**, *43* (3), 456–463. https://doi.org/10.1080/00397911.2011.603068.

(58) Andrade, S.; Campos, E.; Teixeira, C.; Bandeira, C.; Lavorato, S.; Romeiro, N.; Bertollo, C.; Oliveira, M.; Souza-Fagundes, E.; Alves, R. Synthesis of Novel 2,3,4-Trisubstituted-Oxazolidine Derivatives and In Vitro Cytotoxic Evaluation. *Med. Chem. (Los. Angeles).* **2014**, *10* (6), 609–618. https://doi.org/10.2174/1573406411309666005 7.

(59) Li, F.; Frett, B.; Li, H. Selective Reduction of Halogenated Nitroarenes with Hydrazine Hydrate in the Presence of Pd/C. *Synlett* **2014**, *25* (10), 1403–1408. https://doi.org/10.1055/s-0033-1339025.

(60) Barbosa da Silva, E.; Rocha, D. A.; Fortes, I. S.; Yang, W.; Monti, L.; Siqueira-Neto, J. L.; Caffrey, C. R.; McKerrow, J.; Andrade, S. F.; Ferreira, R. S. Structure-Based Optimization of Quinazolines as Cruzain and TbrCATL Inhibitors. J. Med. Chem. 2021, 64 (17), 13054–13071. https://doi.org/10.1021/acs.jmedchem.1c01151.

(61) Wang, S.-B.; Cui, M.-T.; Wang, X.-F.; Ohkoshi, E.; Goto, M.; Yang, D.-X.; Li, L.; Yuan, S.; Morris-Natschke, S. L.; Lee, K.-H.; Xie, L. Synthesis, Biological Evaluation, and Physicochemical Property Assessment of 4-Substituted 2-Phenylaminoquinazolines as Mer Tyrosine Kinase Inhibitors. *Bioorg. Med. Chem.* **2016**, *24* (13), 3083–3092. https://doi.org/10.1016/j.bmc.2016.05.025.

(62) Gilson, P. R.; Tan, C.; Jarman, K. E.; Lowes, K. N.; Curtis, J. M.; Nguyen, W.; Di Rago, A. E.; Bullen, H. E.; Prinz, B.; Duffy, S.; Baell, J. B.; Hutton, C. A.; Jousset Subroux, H.; Crabb, B. S.; Avery, V. M.; Cowman, A. F.; Sleebs, B. E. Optimization of 2-Anilino 4-Amino Substituted Quinazolines into Potent Antimalarial Agents with Oral in Vivo Activity. *J. Med. Chem.* **2017**, *60* (3), 1171–1188. https://doi.org/10.1021/acs.jmedchem.6b01673.

(63) Chou, T.; Li, K.; Frankowski, K. J.; Schoenen, F. J.; Deshaies, R. J. Structure–Activity Relationship Study Reveals ML240 and ML241 as Potent and Selective Inhibitors of P97 ATPase. *ChemMedChem* **2013**, *8* (2), 297–312. https://doi.org/10.1002/cmdc.201200520.

(64) Sun, W.; Hu, S.; Fang, S.; Yan, H. Design, Synthesis and Biological Evaluation of Pyrimidine-Based Derivatives as VEGFR-2 Tyrosine Kinase Inhibitors. *Bioorg. Chem.* **2018**, *78*, 393–405. https://doi.org/10.1016/j.bioorg.2018.04.005.

(65) Liang, M.; Tarr, T. B.; Bravo-Altamirano, K.; Valdomir, G.; Rensch, G.; Swanson, L.; DeStefino, N. R.; Mazzarisi, C. M.; Olszewski, R. A.; Wilson, G. M.; Meriney, S. D.; Wipf, P. Synthesis and Biological Evaluation of a Selective N- and P/Q-Type Calcium Channel Agonist. *ACS Med. Chem. Lett.* **2012**, *3* (12), 985–990. https://doi.org/10.1021/ml3002083..

(66) Boudreau, P. D.; Miller, B. W.; McCall, L.-I.; Almaliti, J.; Reher, R.; Hirata, K.; Le, T.; Siqueira-Neto, J. L.; Hook, V.; Gerwick, W. H. Design of Gallinamide A Analogs as Potent Inhibitors of the Cysteine Proteases Human Cathepsin L and Trypanosoma Cruzi Cruzain. *J. Med. Chem*. **2019**, 62, 9026−9044.

(67) Hirumi, H.; Hirumi, K. Continuous Cultivation of Trypanosoma Brucei Blood Stream Forms in a Medium Containing a Low Concentration of Serum Protein without Feeder Cell Layers. J. Parasitol. 1989, 75 (6), 985. https://doi.org/10.2307/3282883.

(68) http://tryps.rockefeller.edu/trypsru2_culture_media_preparation.html. No Title.

4.7 Supplementary Material

Structure-based optimization of quinazolines as cruzain and *Tbr*CATL inhibitors

NMR and MS Spectra

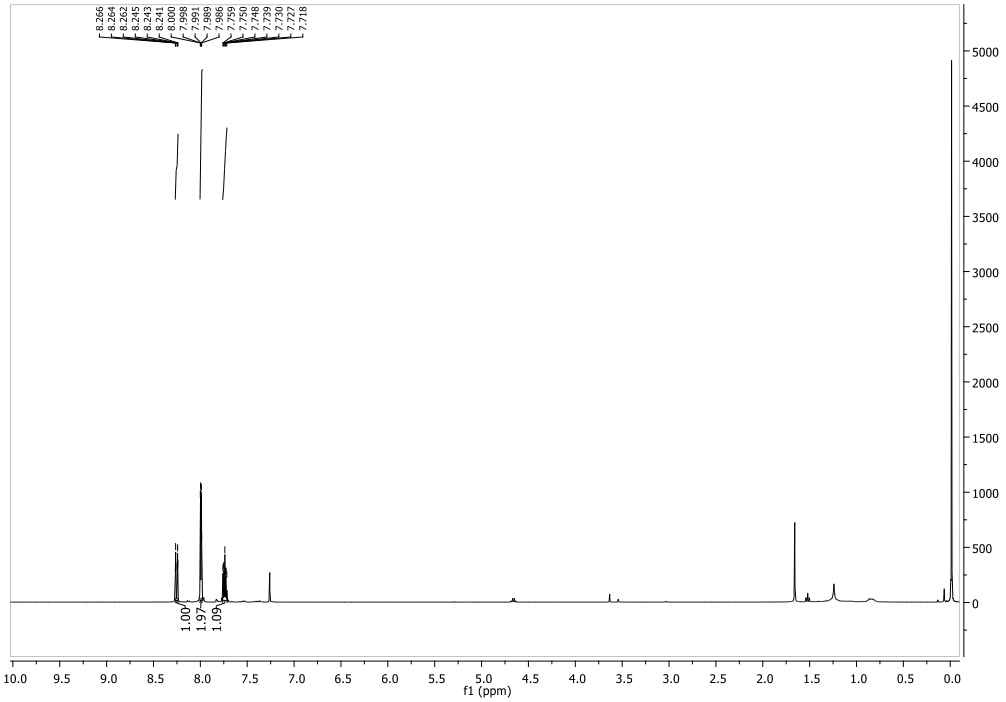

Figure 15 – ^{1}H NMR (400 MHz, $CDCl_3$) *2,4-dichloroquinazoline* **3**.

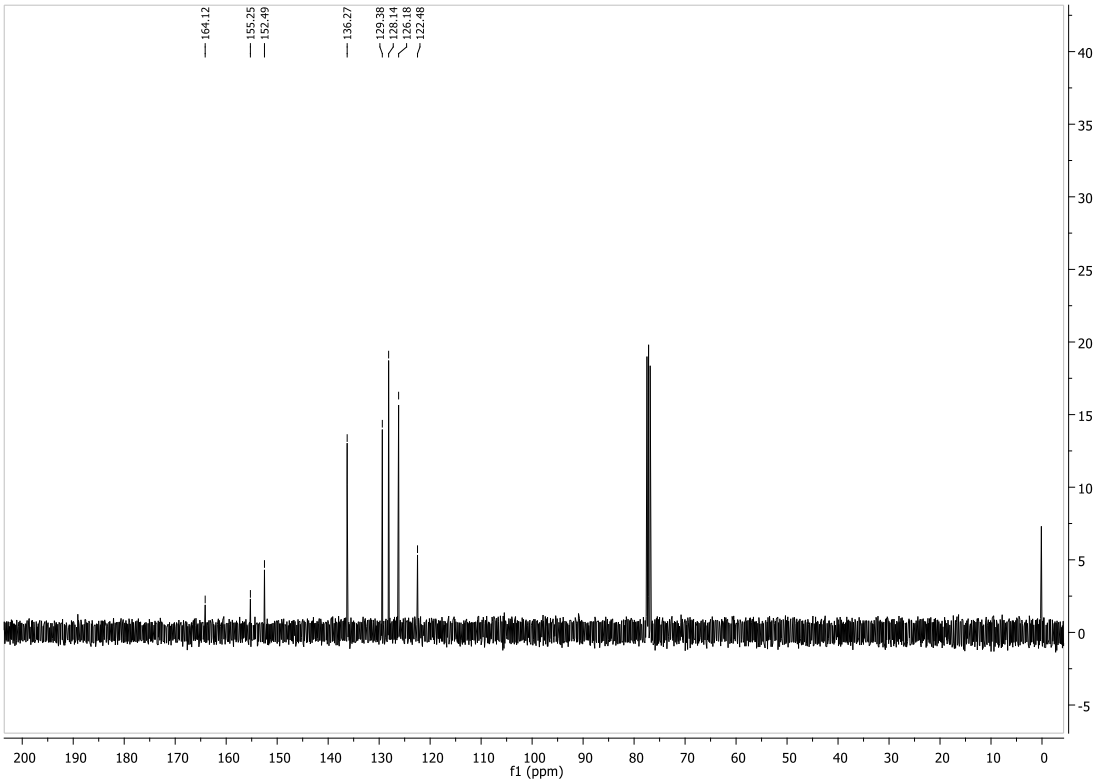

Figure 16 – ^{13}C NMR (100 MHz, $CDCl_3$) *2,4-dichloroquinazoline* **3**.

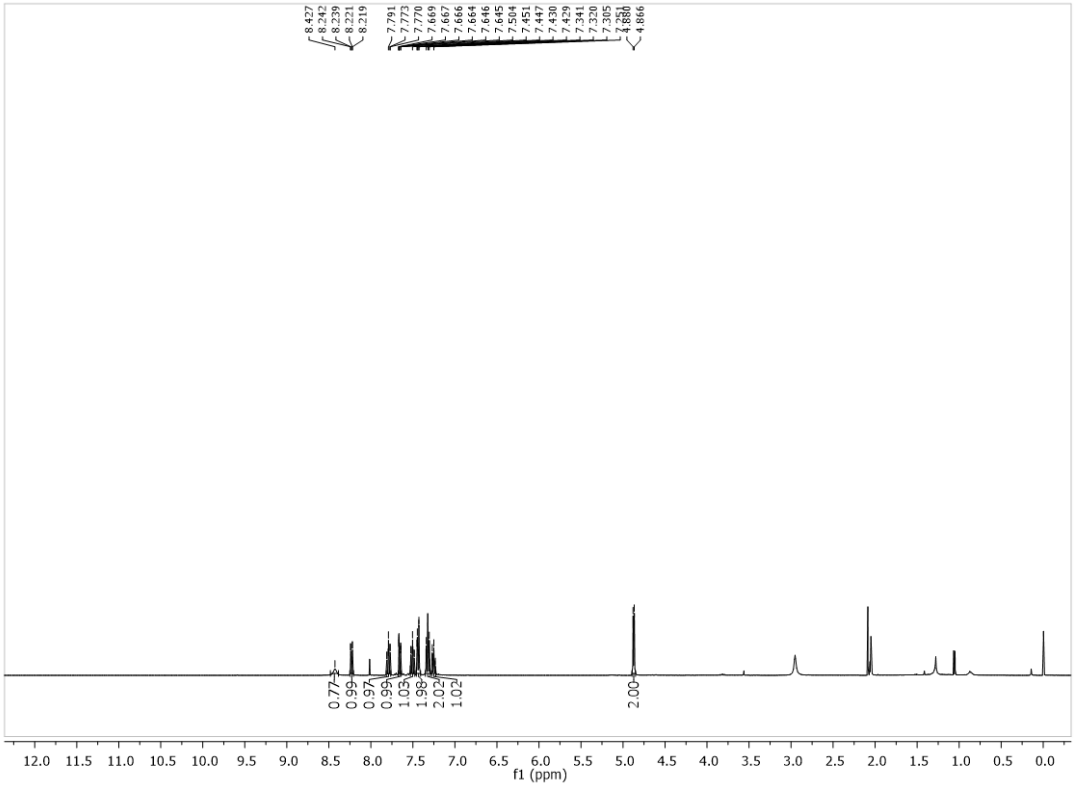

Figure 17 – ^{1}H NMR (400 MHz, $(CD_3)_2CO$ N-benzyl-2-chloroquinazolin-4-amine **4a**.

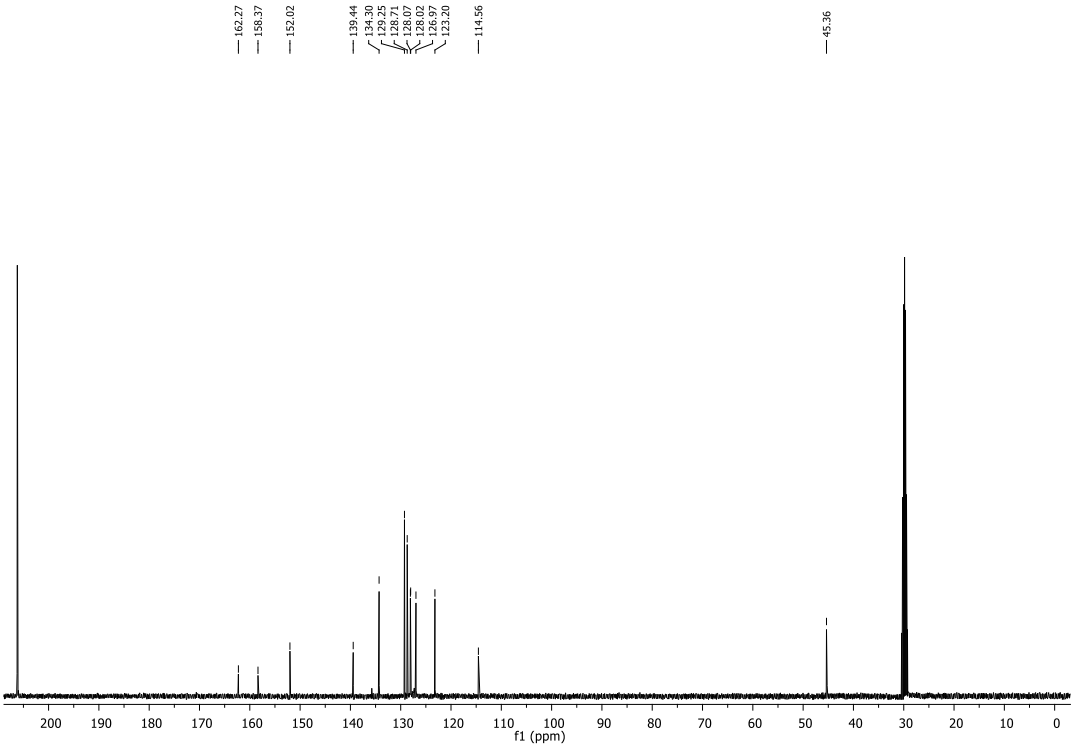

Figure 18 – ^{13}C NMR (100 MHz, $(CD_3)_2CO$ N-benzyl-2-chloroquinazolin-4-amine **4a**.

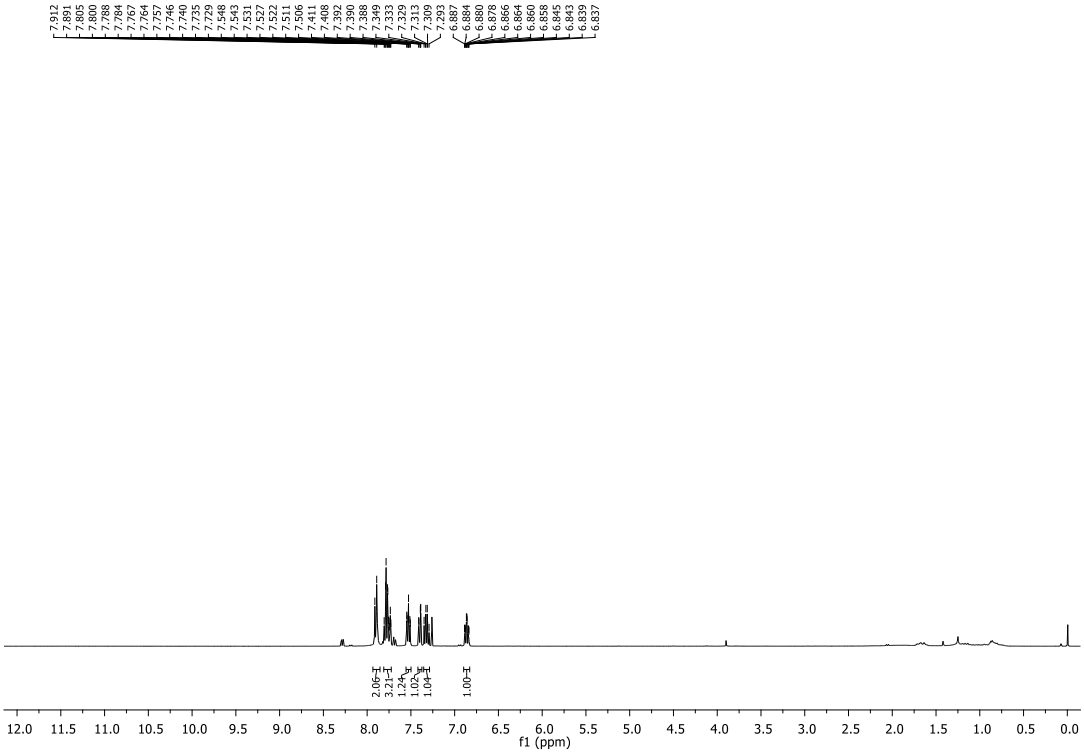

Figure 19 – ^{1}H NMR (400 MHz, $CDCl_3$) of 2-chloro-N-(3-fluorophenyl)quinazolin-4-amine **4b**.

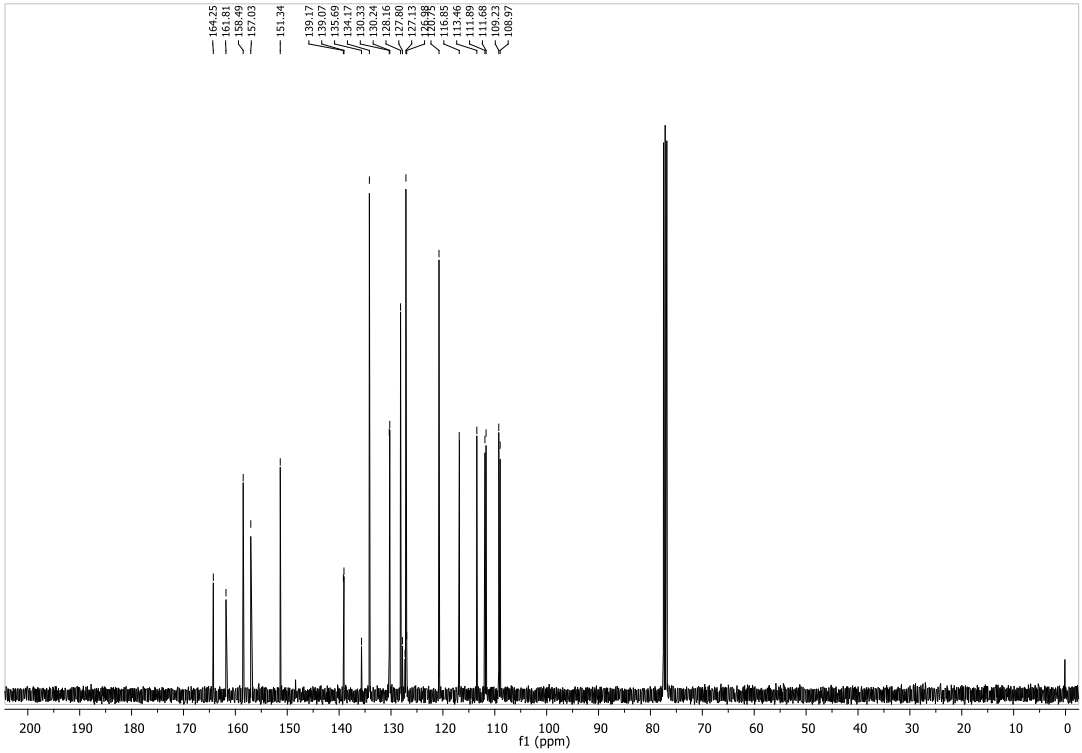

Figure 20 – ^{13}C NMR (100 MHz, $CDCl_3$) of 2-chloro-N-(3-fluorophenyl)quinazolin-4-amine **4b**.

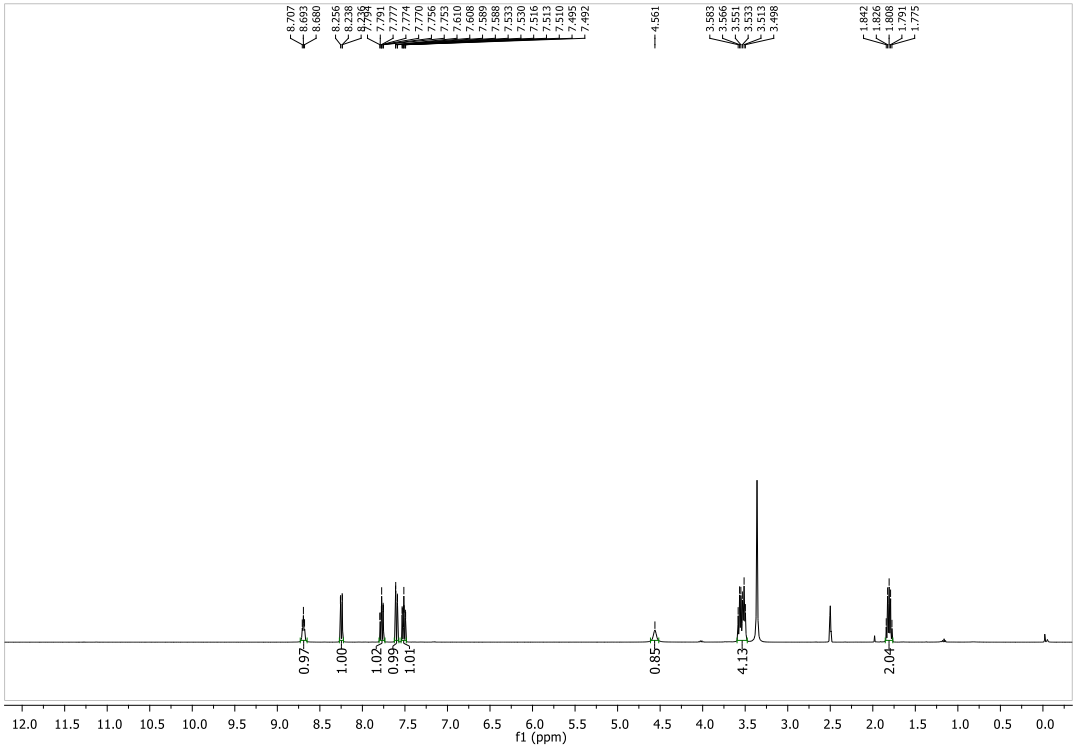

Figure 21 – ^{1}H NMR (400 MHz, DMSO-d_6) of 3-((2-(chloroamino)quinazolin-4-yl)amino) propan-1-ol **4c**.

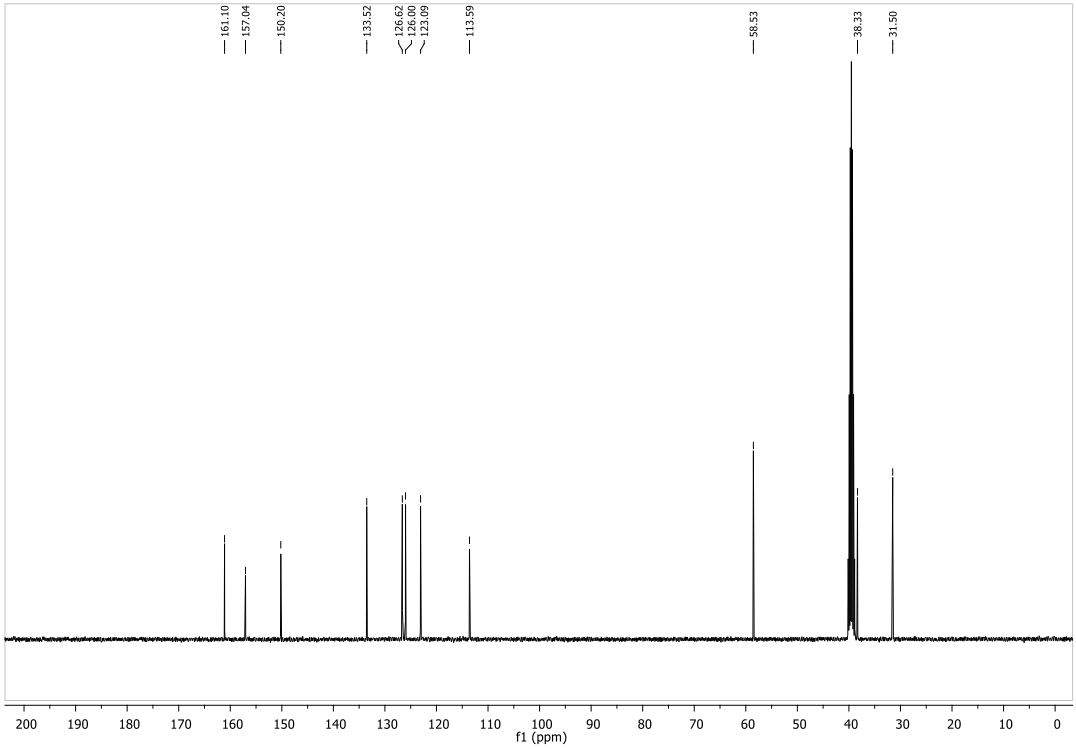

Figure 22 – ^{13}C NMR (100 MHz, DMSO-d_6) of 3-((2-(chloroamino)quinazolin-4-yl)amino)propan-1-ol **4c**.

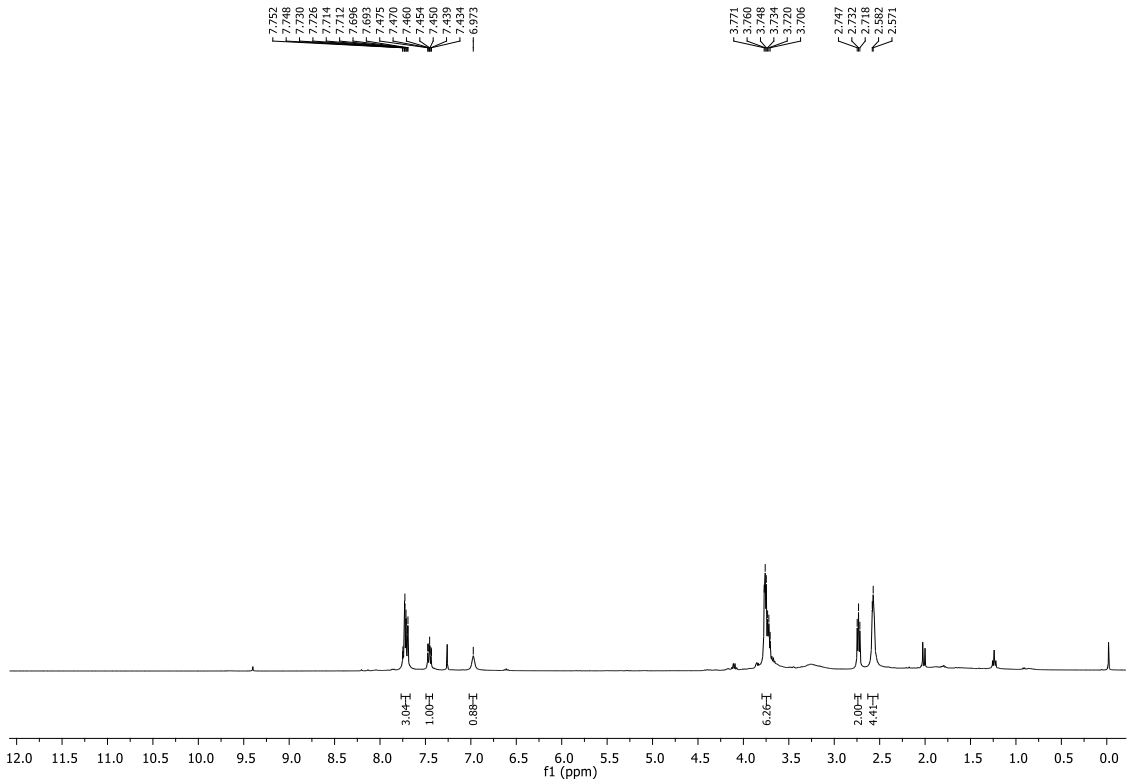

Figure 23 – ^{1}H NMR (400 MHz, $CDCl_3$) of 2-chloro-N-(2-morpholinoethyl)quinazolin-4-amine **5d.**

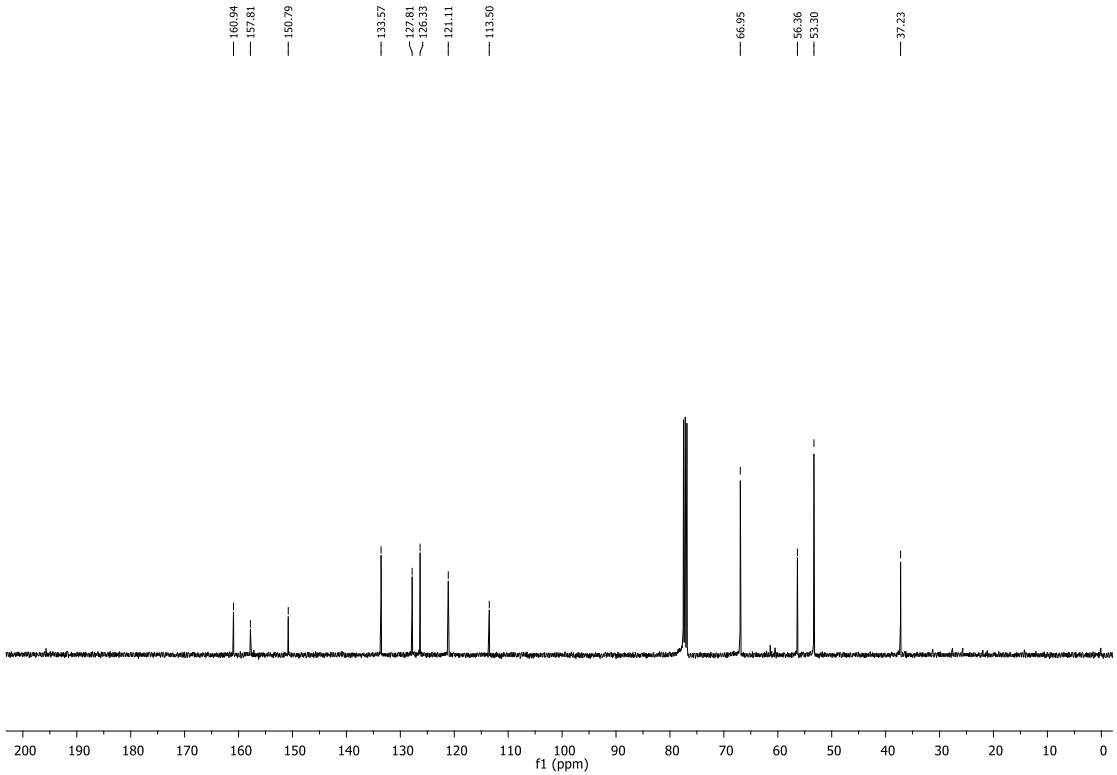

Figure 24 – ^{13}C NMR (100 MHz, $CDCl_3$) of 2-chloro-N-(2-morpholinoethyl)quinazolin-4-amine **5d.**

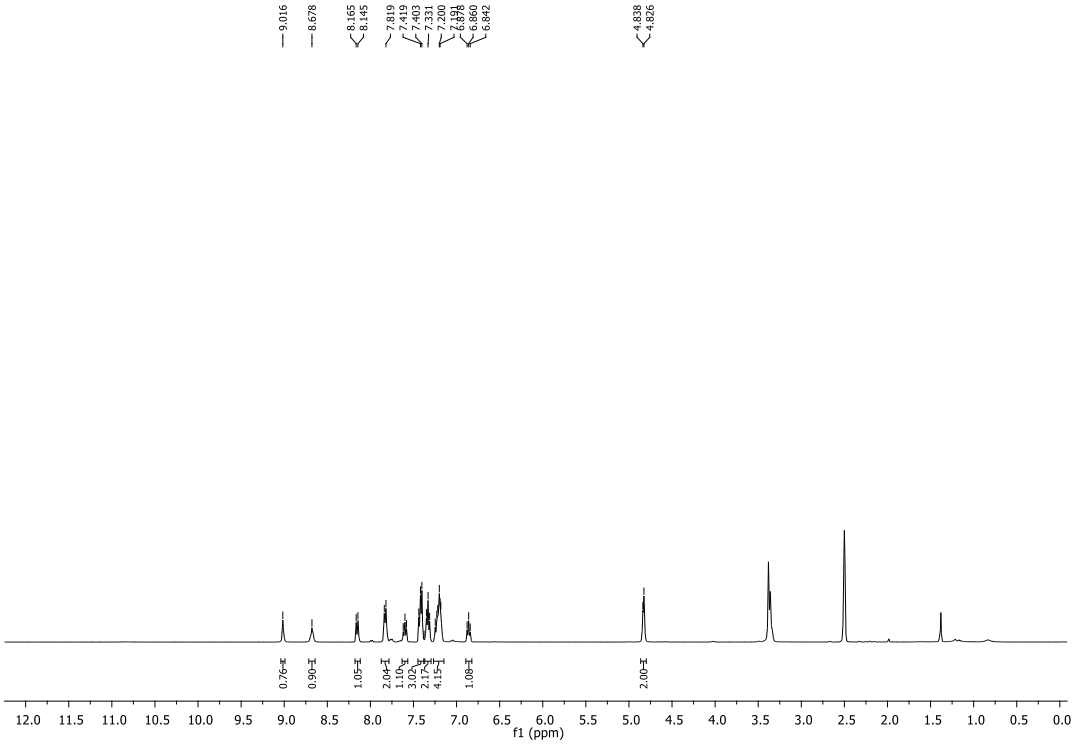

Figure 25 – ^{1}H NMR (400 MHz, DMSO-*d6*) of **PH100**.

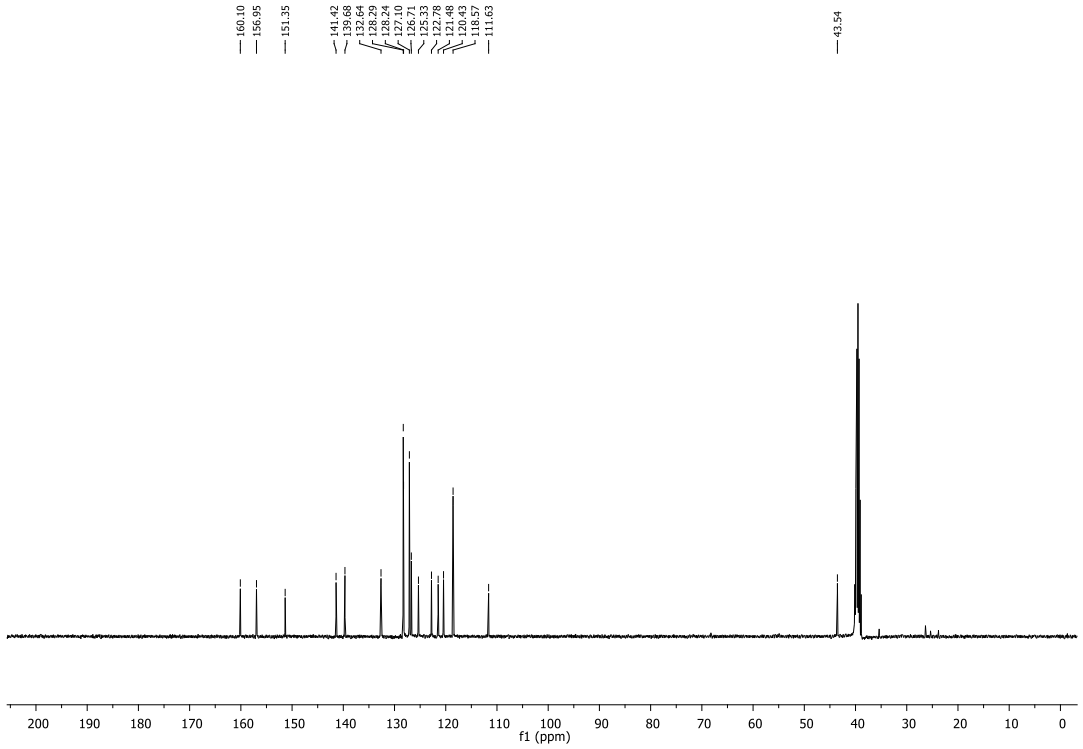

Figure 26 – ^{13}C NMR (100 MHz, DMSO-*d6*) of **PH100**.

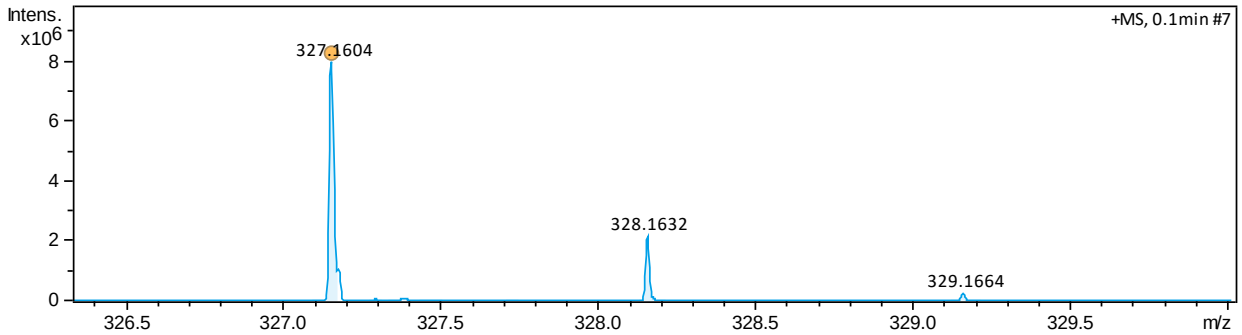

Figure 27 – Mass spectrum of **PH100.**

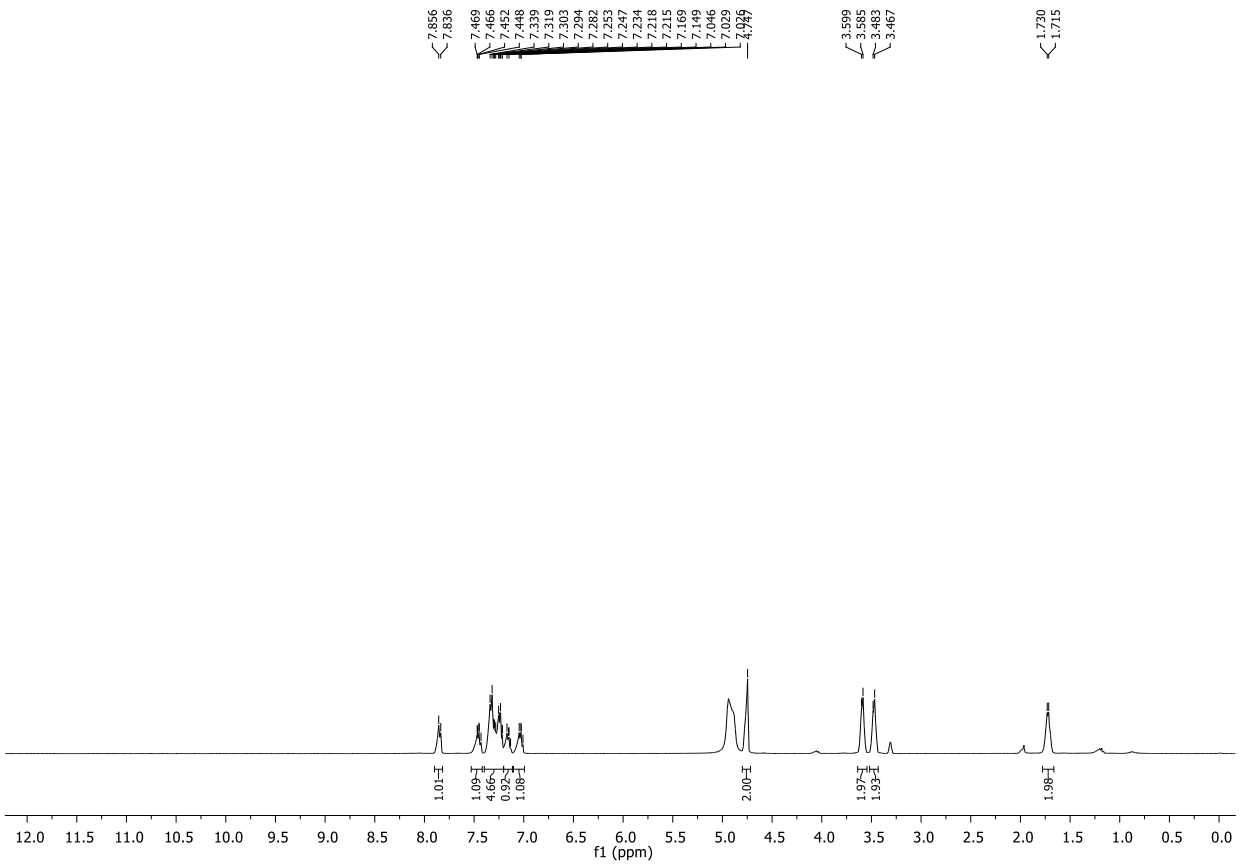

Figure 28 – ^{1}H NMR (400 MHz, DMSO-*d6*) of **PH101**.

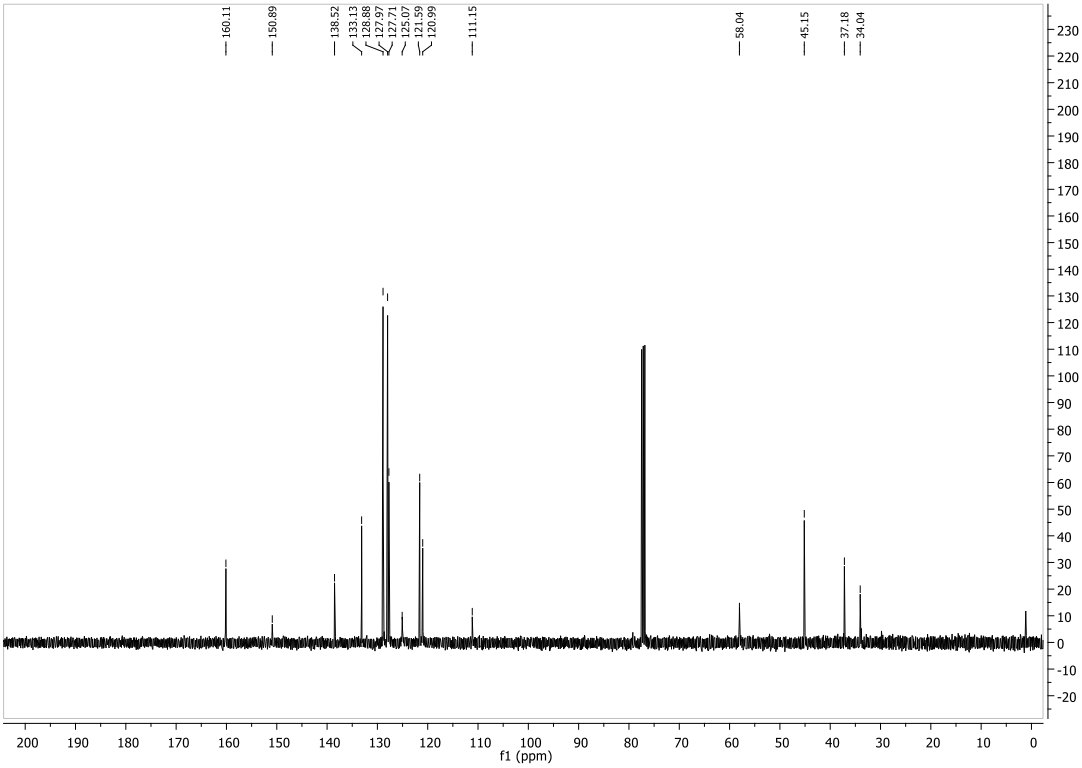

Figure 29 – ^{13}C NMR (100 MHz, $CDCl_3$) of **PH101**.

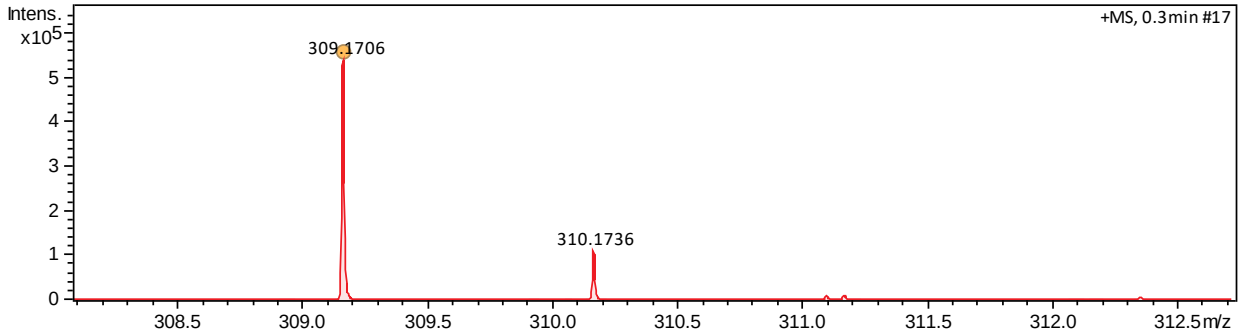

Figure 30 – Mass spectrum of **PH101.**

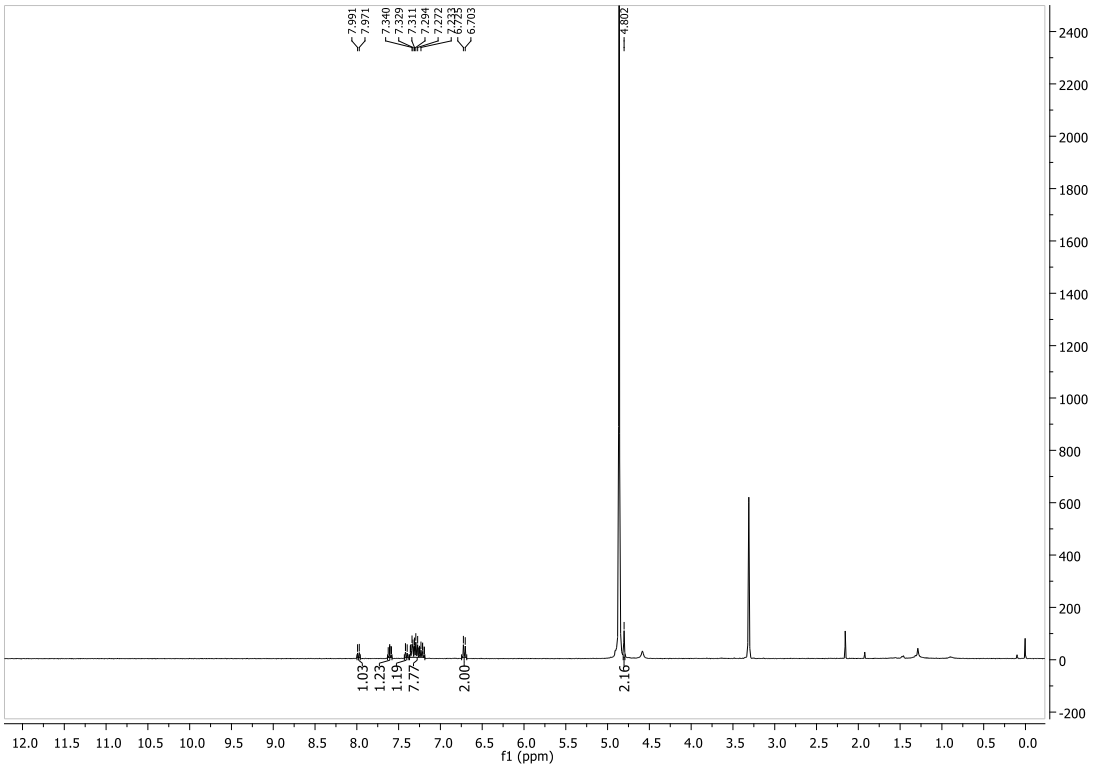

Figure 31 – ^{1}H NMR (400 MHz, CD_3OD) of **PH102**.

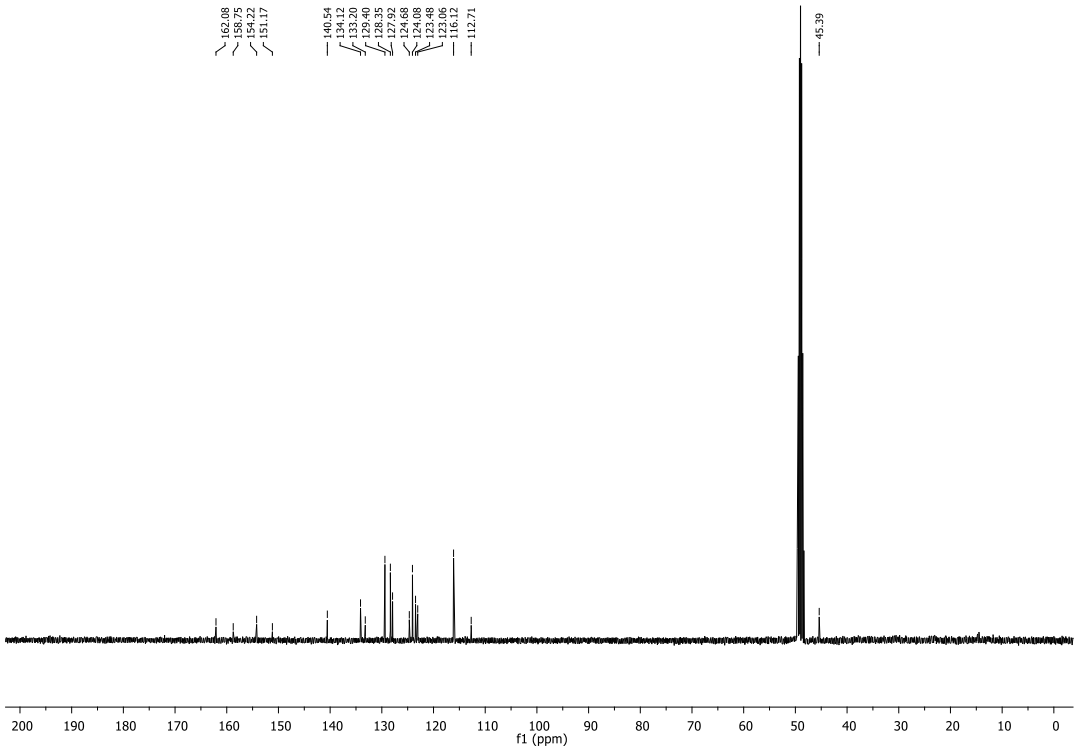

Figure 32 – ^{13}C NMR (100 MHz, CD_3OD) of **PH102**.

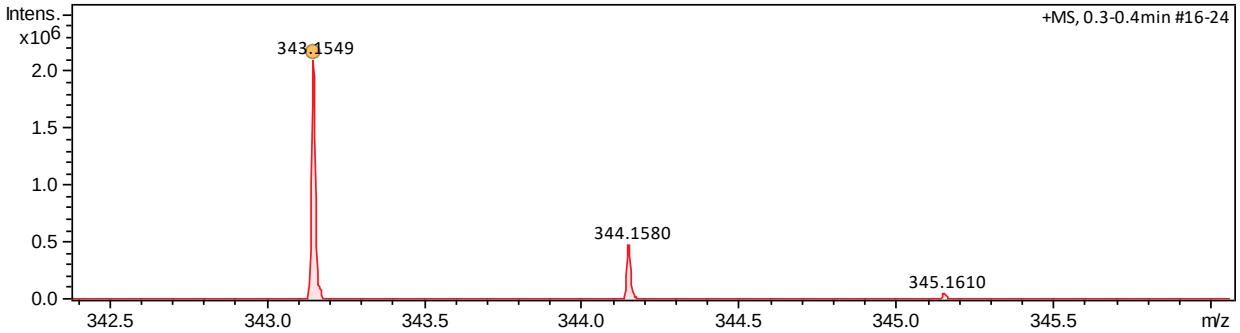

Figure 33 – Mass spectrum of **PH102**.

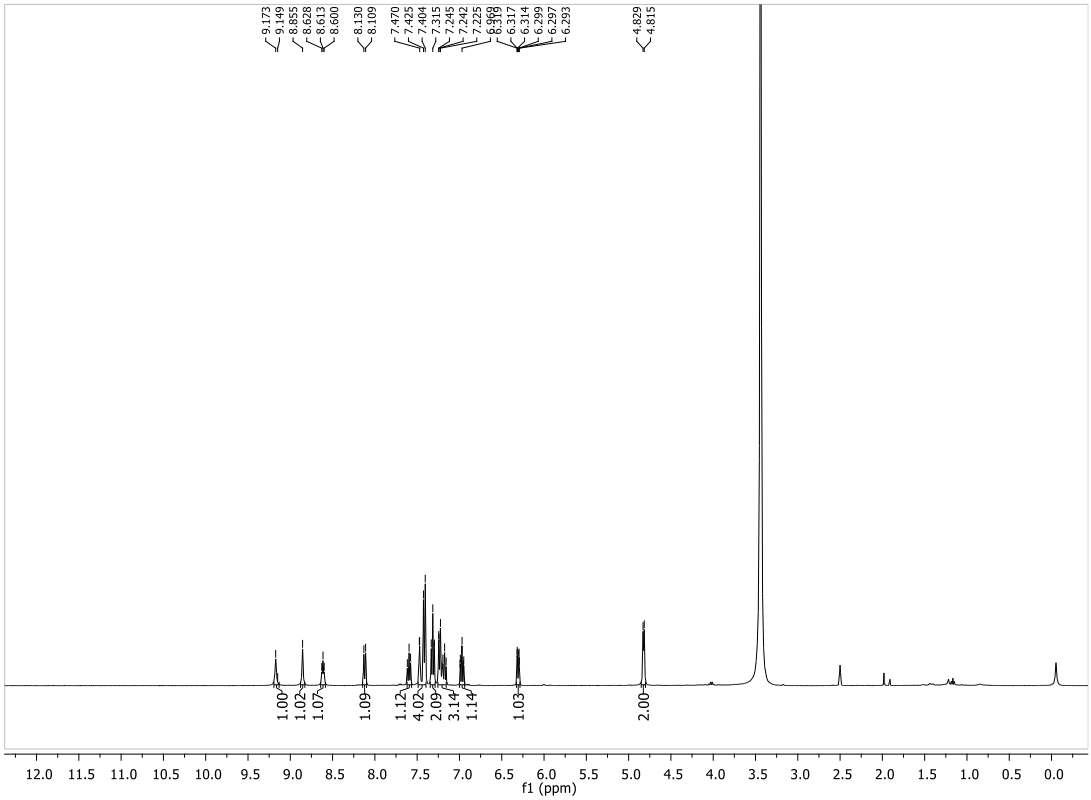

Figure 34 – ^{1}H NMR (400 MHz, DMSO-*d*6) of **PH103**.

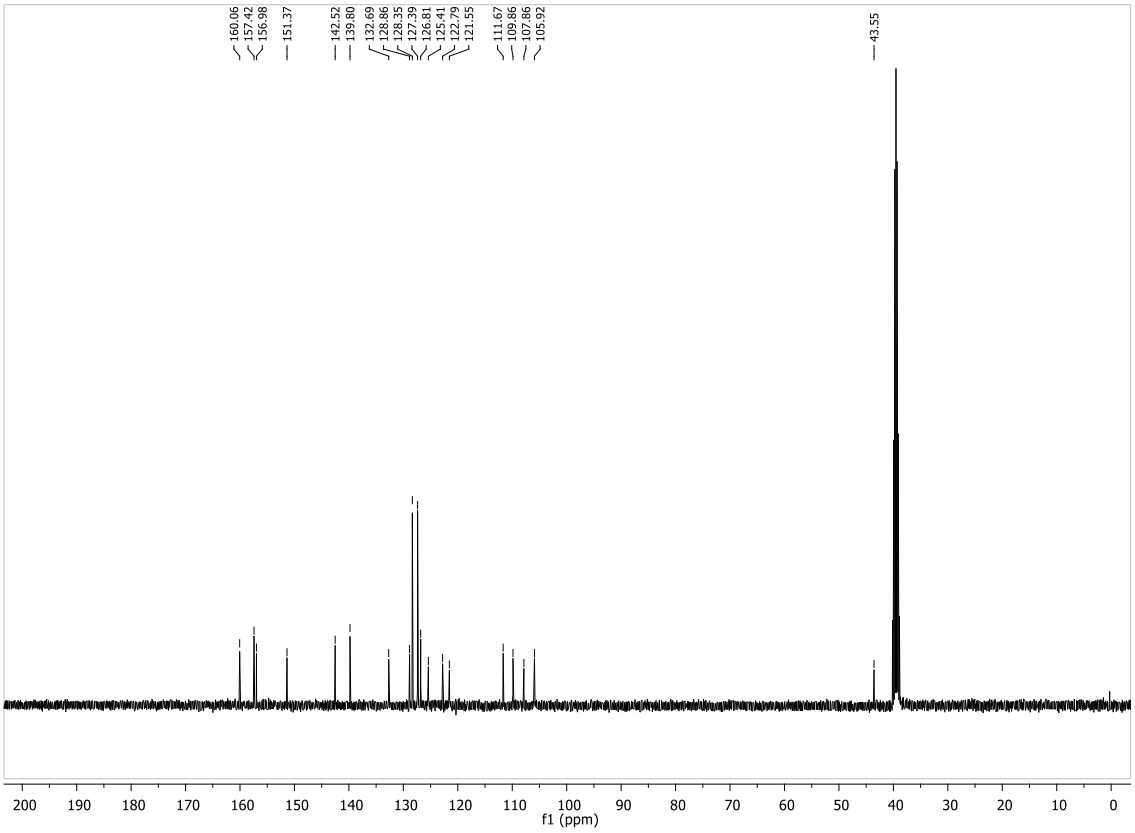

Figure 35 – ^{13}C NMR (100 MHz, DMSO-*d*6) of **PH103**.

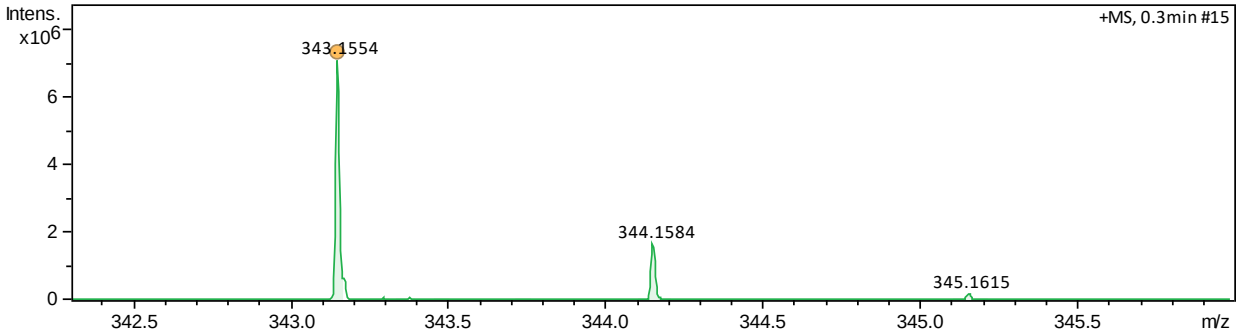

Figure 36 – Mass spectrum of **PH103**.

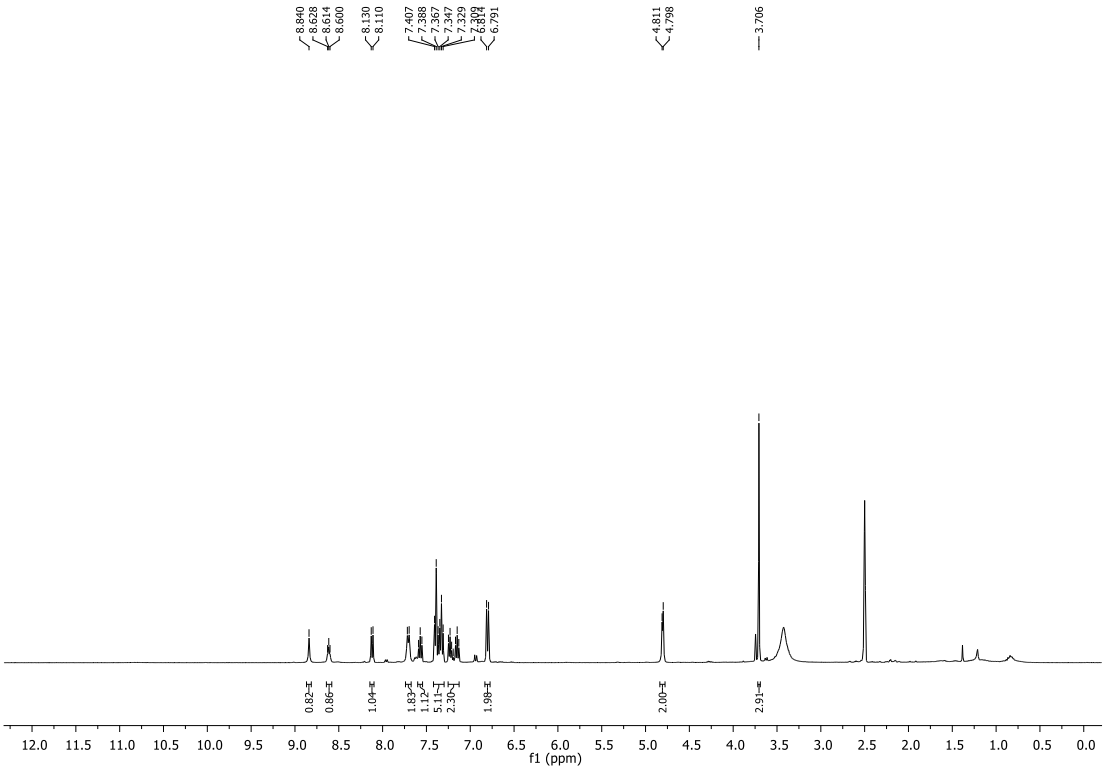

Figure 37 – ^{1}H NMR (400 MHz, DMSO-*d*6) of **PH106**.

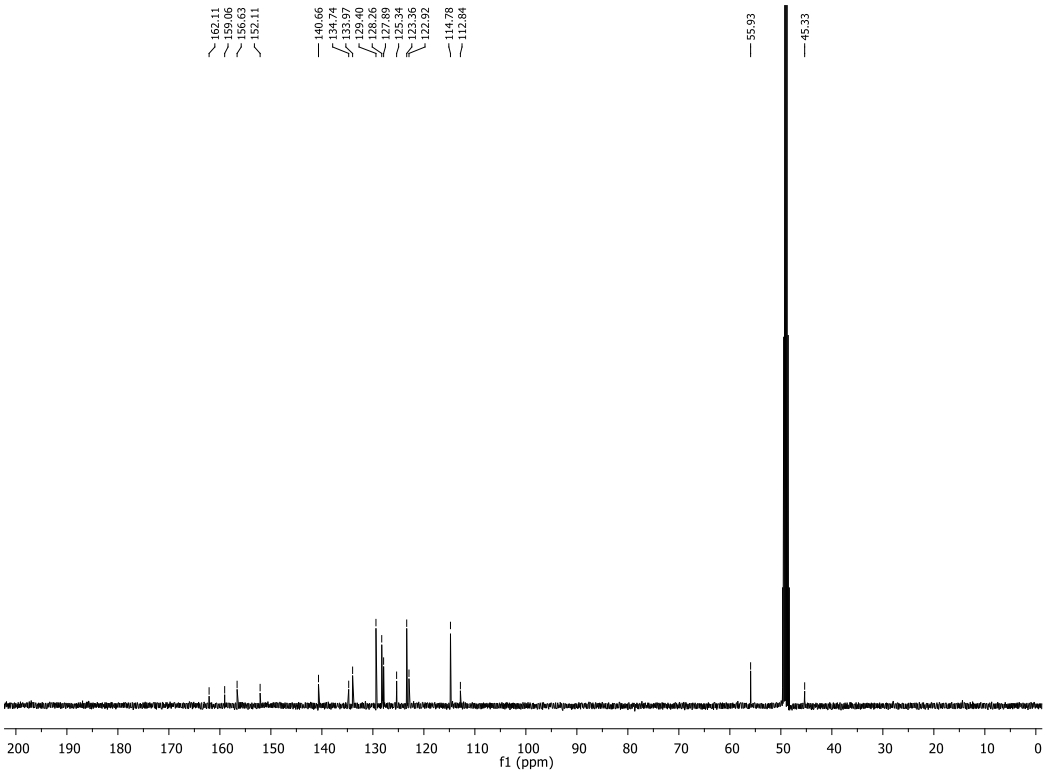

Figure 38 – ^{13}C NMR (100 MHz, CD_3OD) of **PH106**.

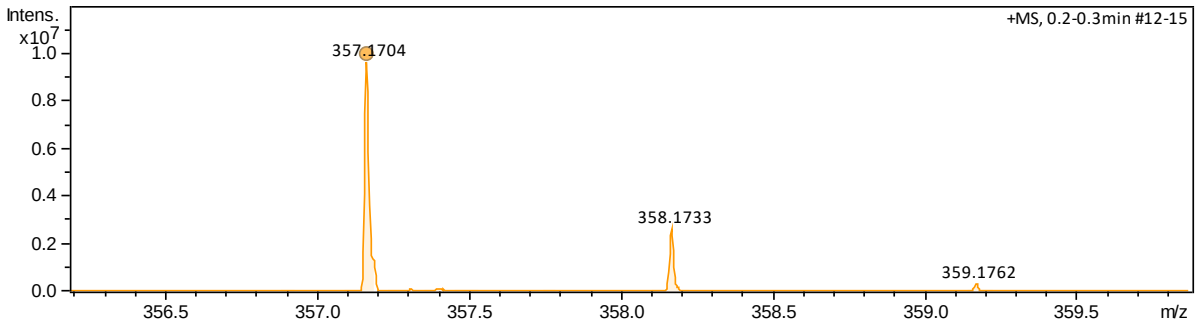

Figure 39 – Mass spectrum of **PH106**.

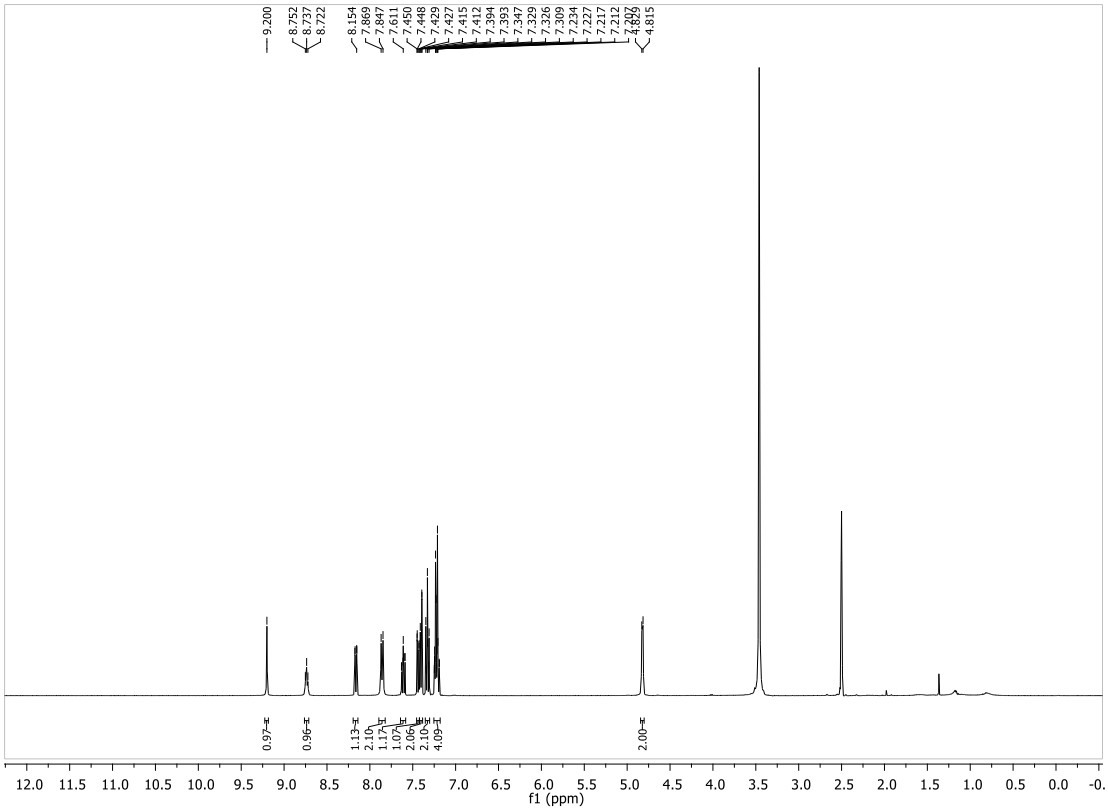

Figure 40 – ^{1}H NMR (400 MHz, DMSO-*d6*) of **PH107**.

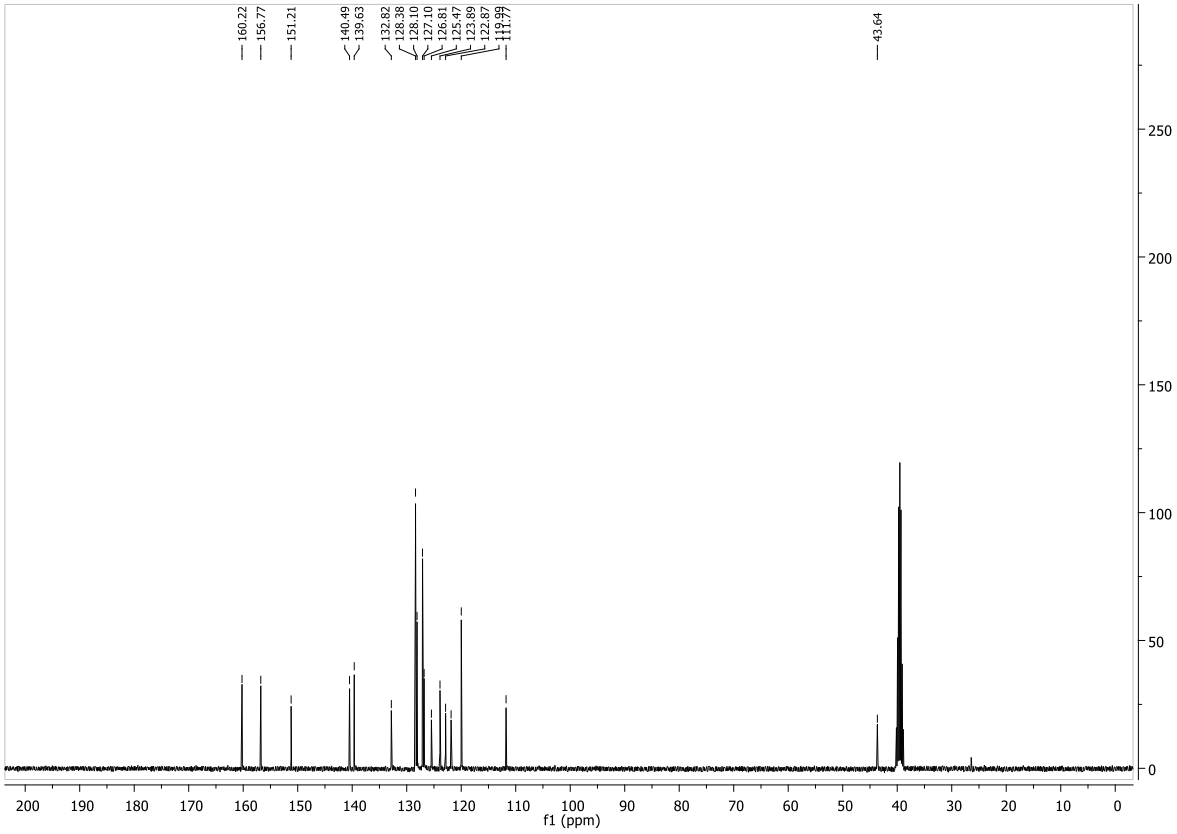

Figure 41 – ^{13}C NMR (100 MHz, DMSO-*d6*) of **PH107**.

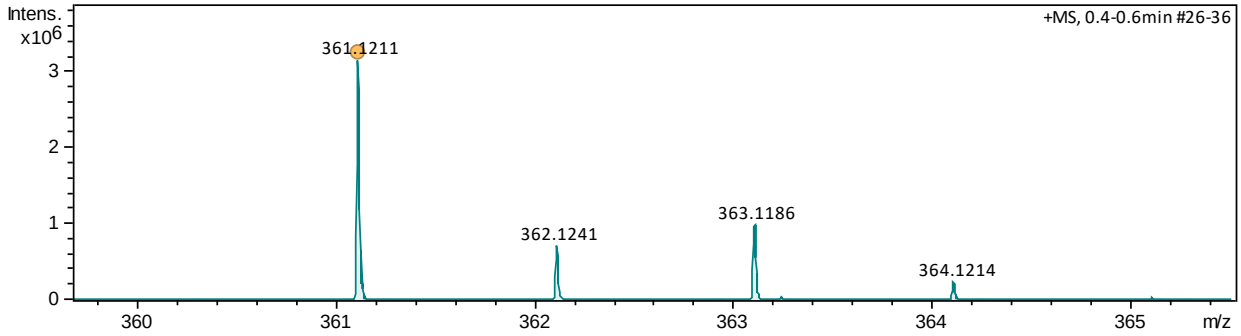

Figure 42 – Mass spectrum of **PH107**.

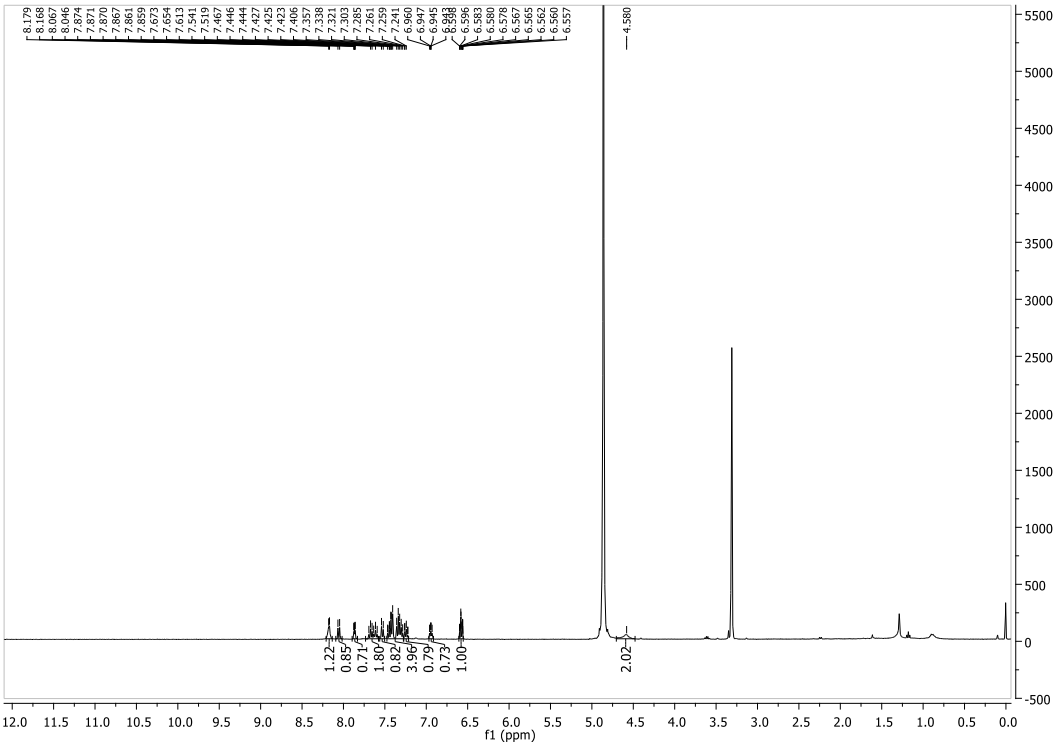

Figure 43 – ^{1}H NMR (400 MHz, CD_3OD) of **PH104**.

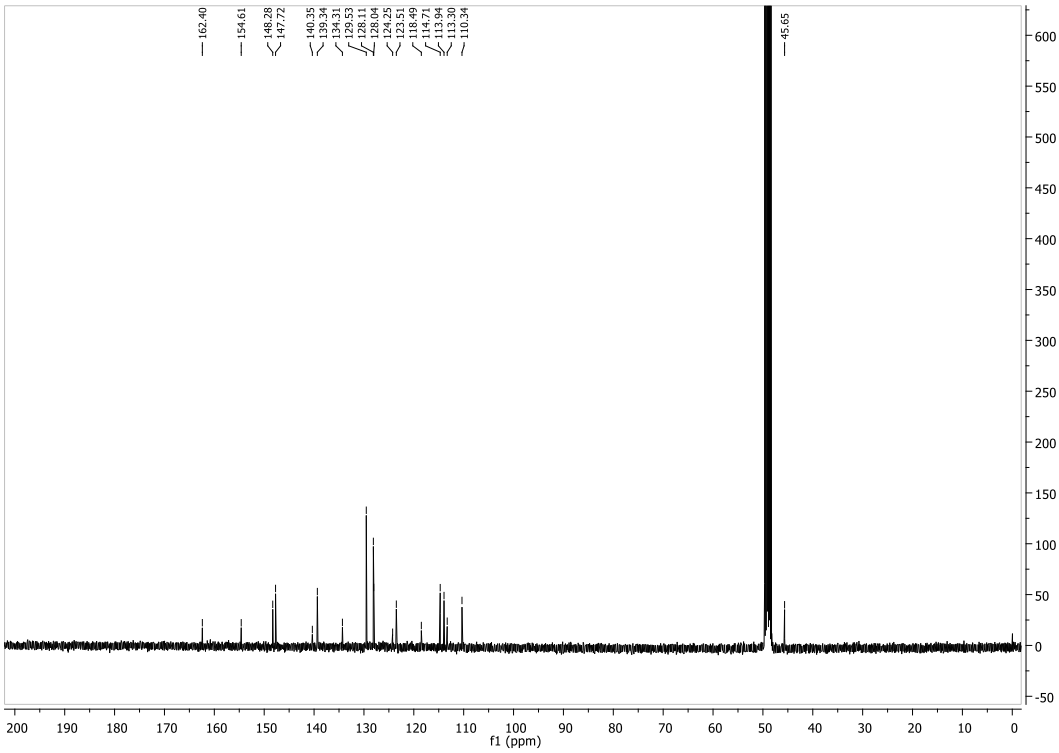

Figure 44 – ^{13}C NMR (100 MHz, CD_3OD) of **PH104**.

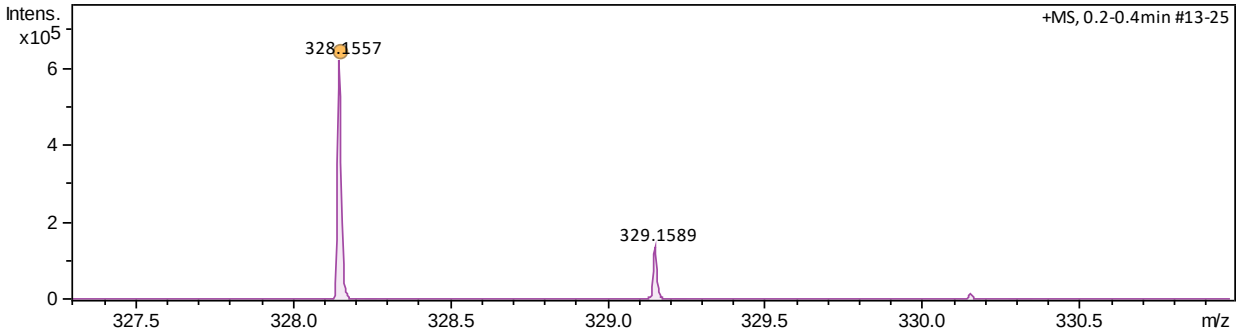

Figure 45 – Mass spectrum of **PH104**.

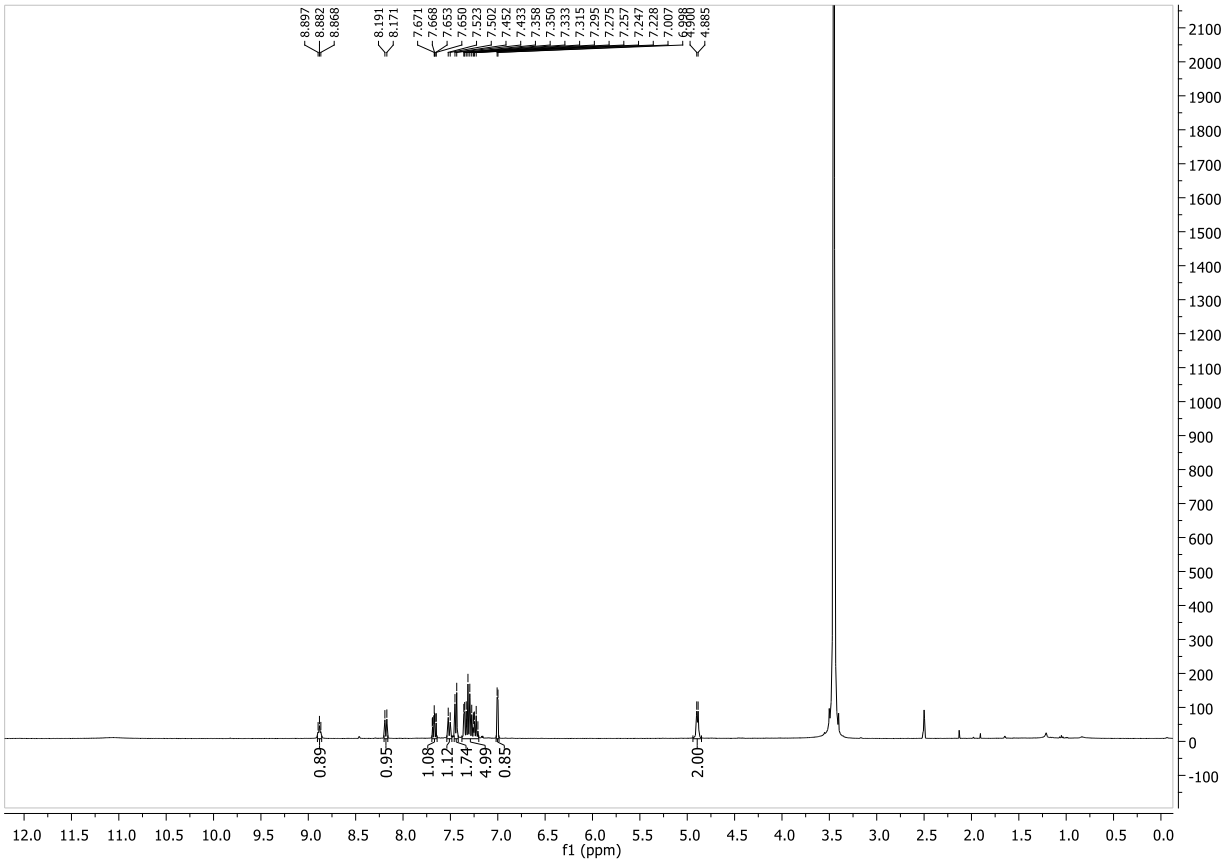

Figure 46 – ^{1}H NMR (400 MHz, DMSO-*d*6) of **PH105**.

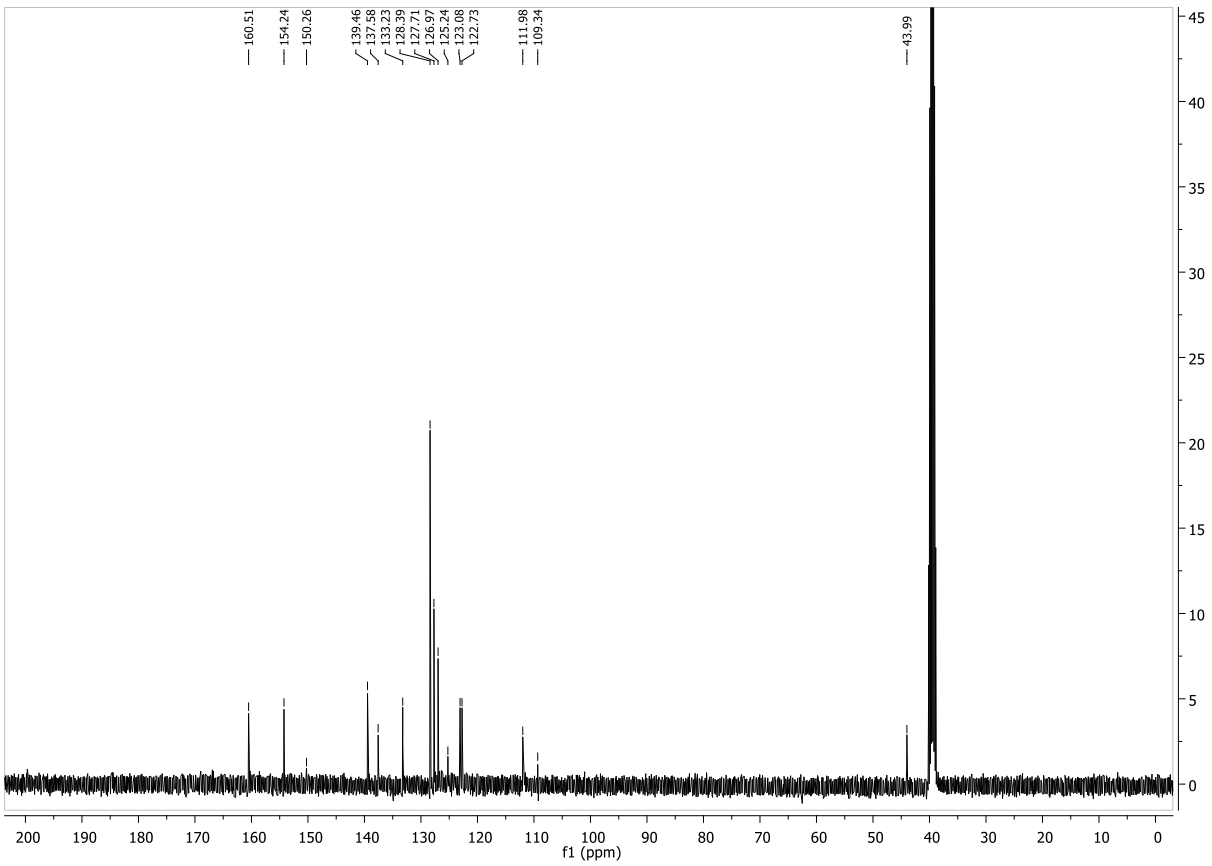

Figure 47 – ^{13}C NMR (100 MHz, CD_3OD) of **PH105**.

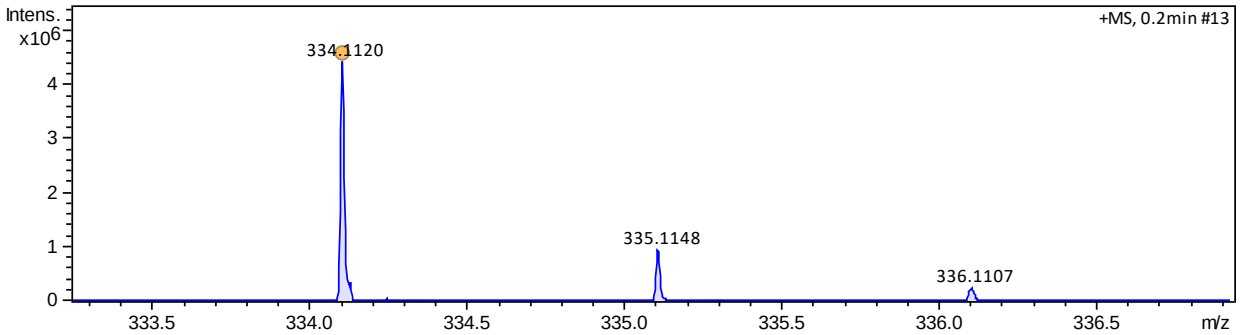

Figure 48 – Mass spectrum of **PH105**.

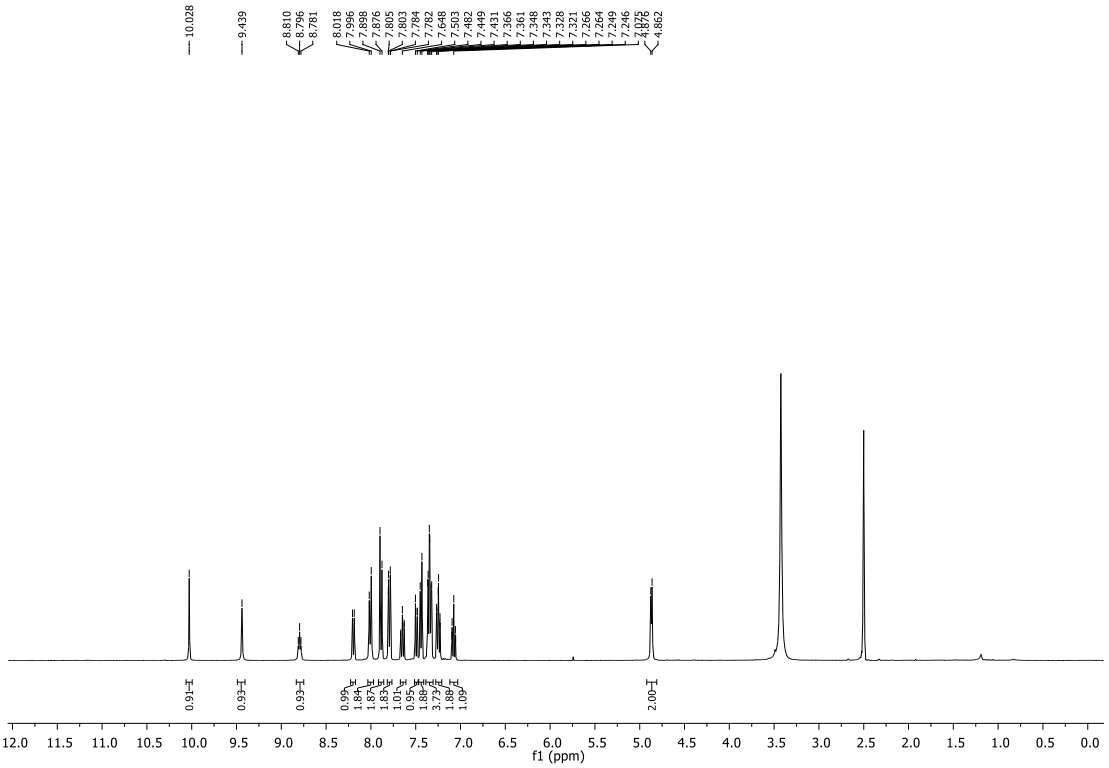

Figure 49 – ^{1}H NMR (400 MHz, DMSO-*d*6) of **PH108**.

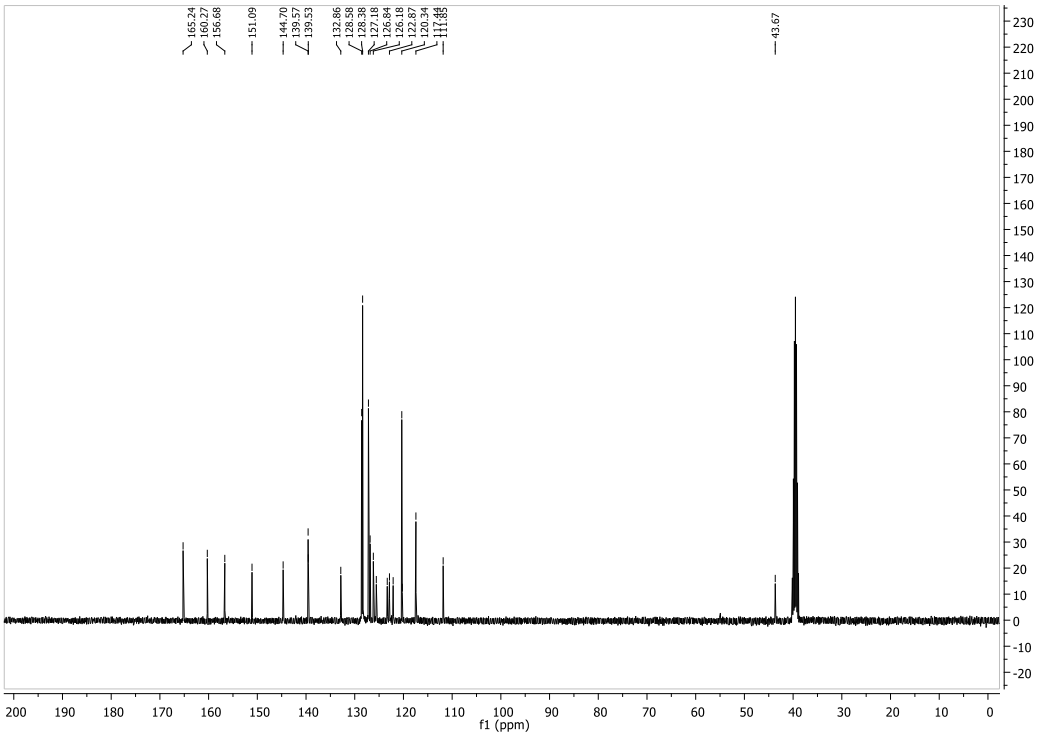

Figure 50 – ^{13}C NMR (100 MHz, DMSO-*d*6) of **PH108**.

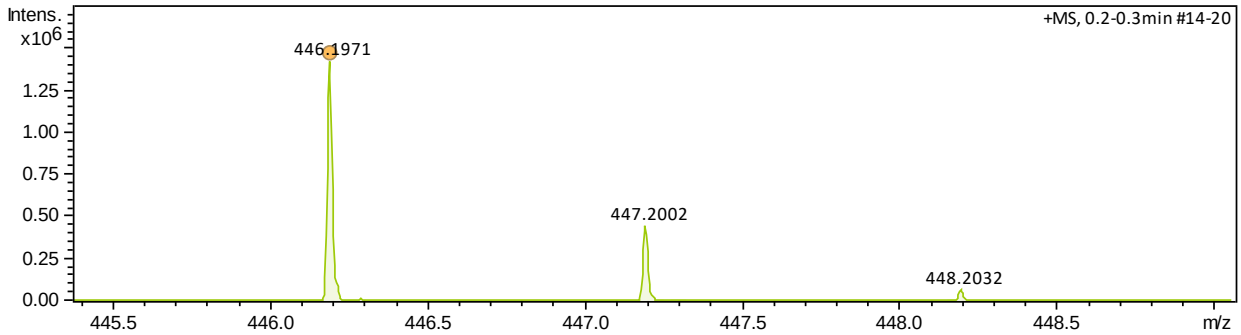

Figure 51 – Mass spectrum of **PH108**.

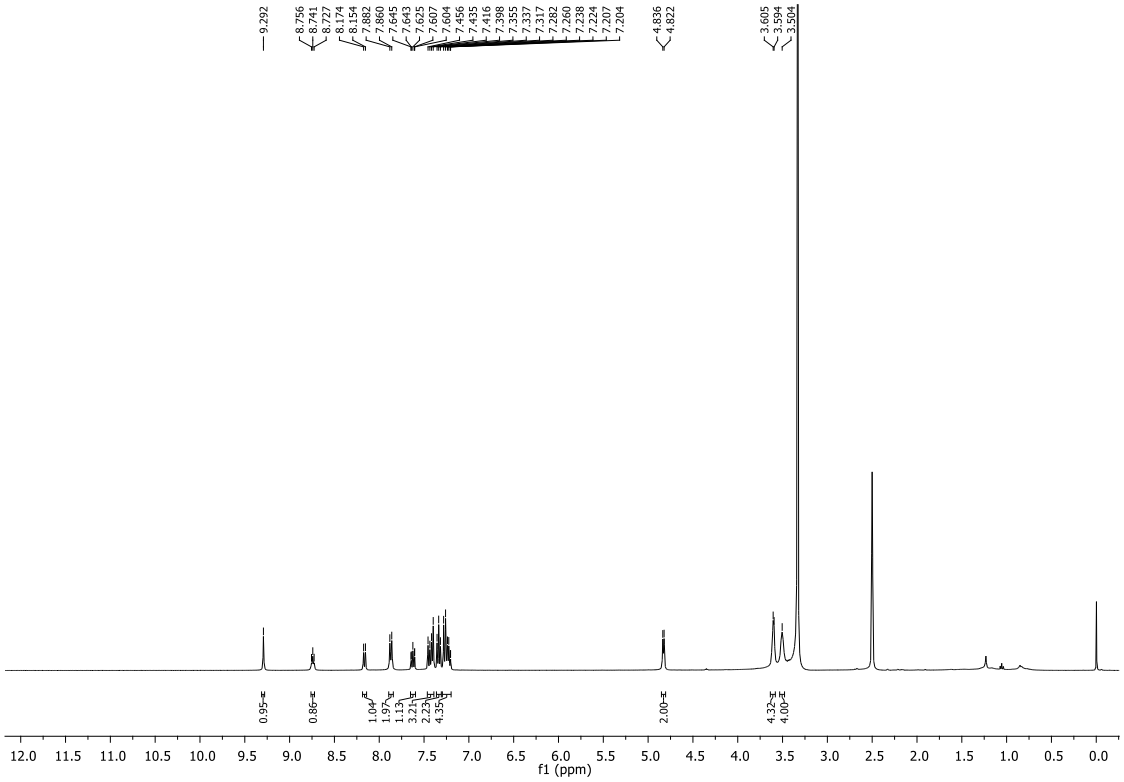

Figure 52 – ^{1}H NMR (400 MHz, DMSO-*d*6) of **PH109**.

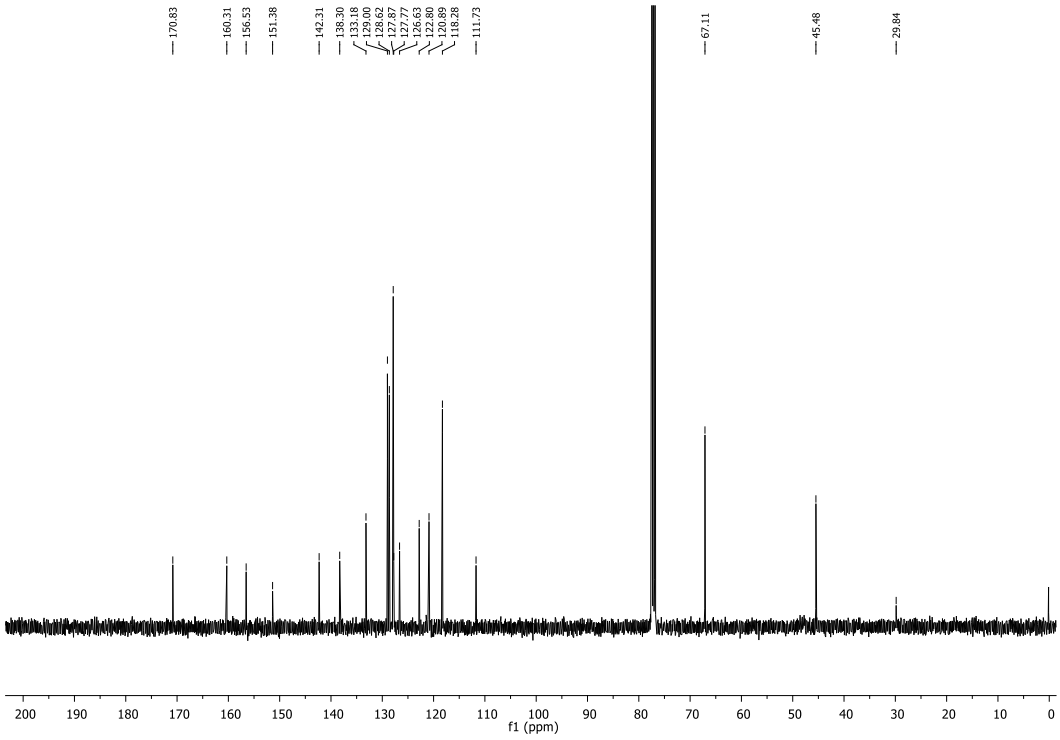

Figure 53 – ^{13}C NMR (100 MHz, $CDCl_3$) of **PH109**.

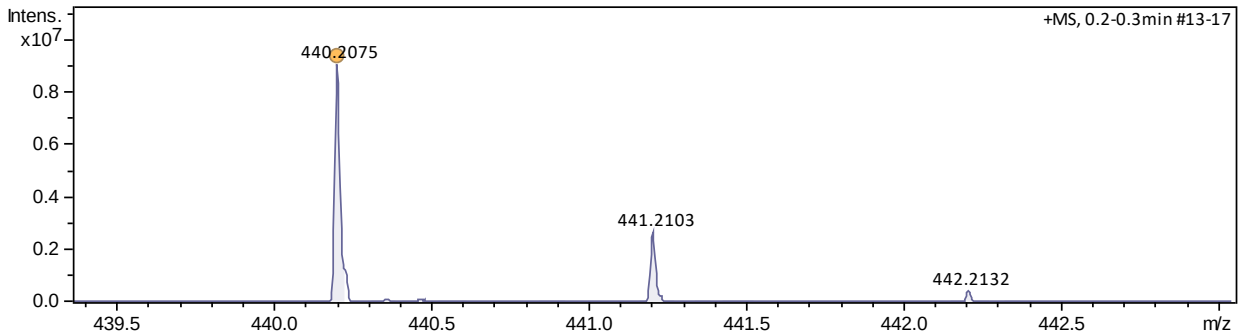

Figure 54 – Mass spectrum of **PH109**.

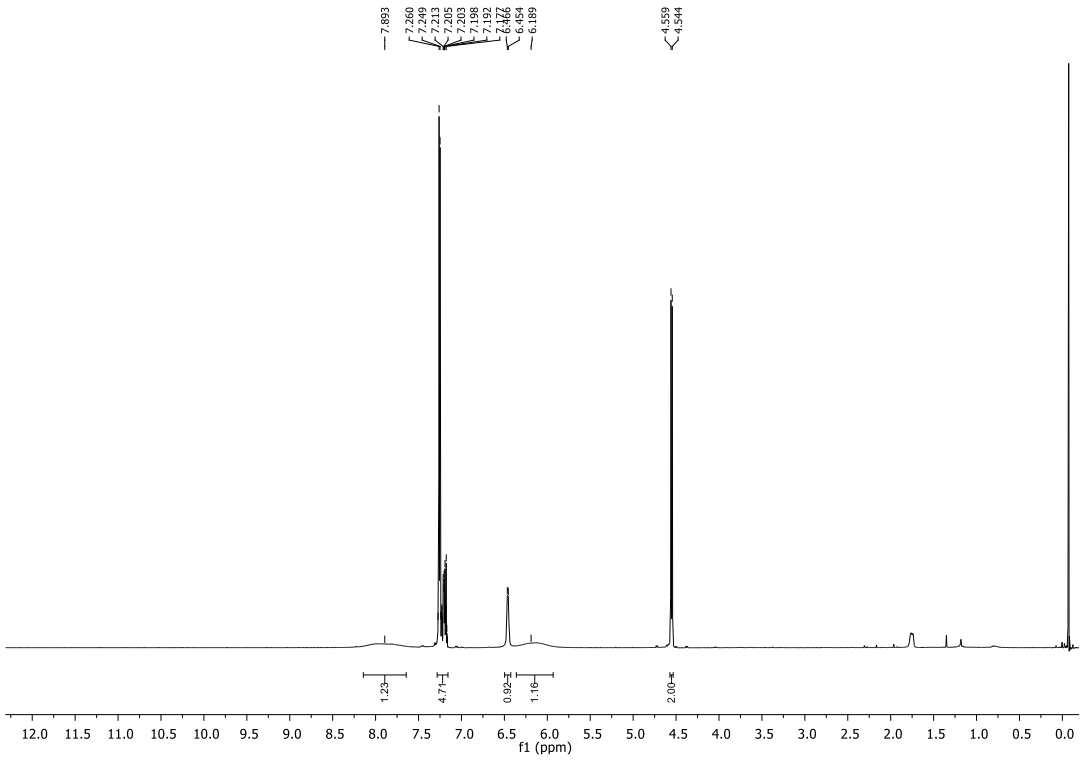

Figure 55 – ^{1}H NMR (400 MHz, $CDCl_3$) of **9**.

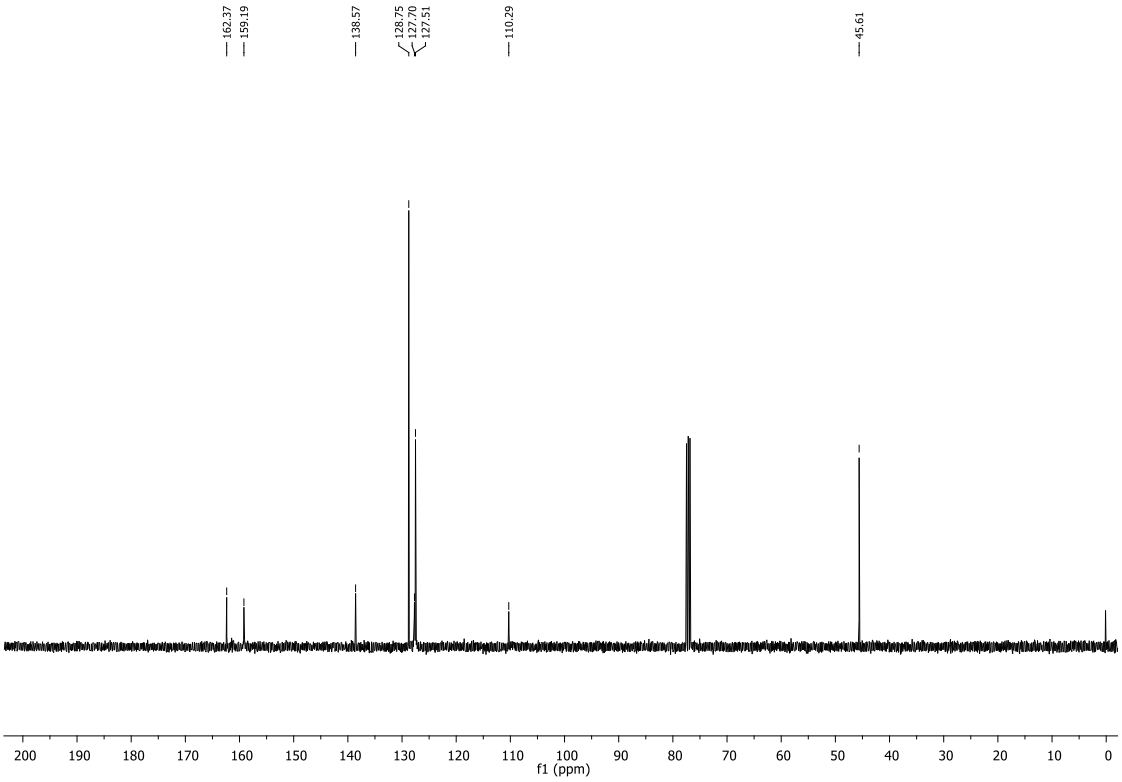

Figure 56 – ^{13}C NMR (100 MHz, $CDCl_3$) of **9**.

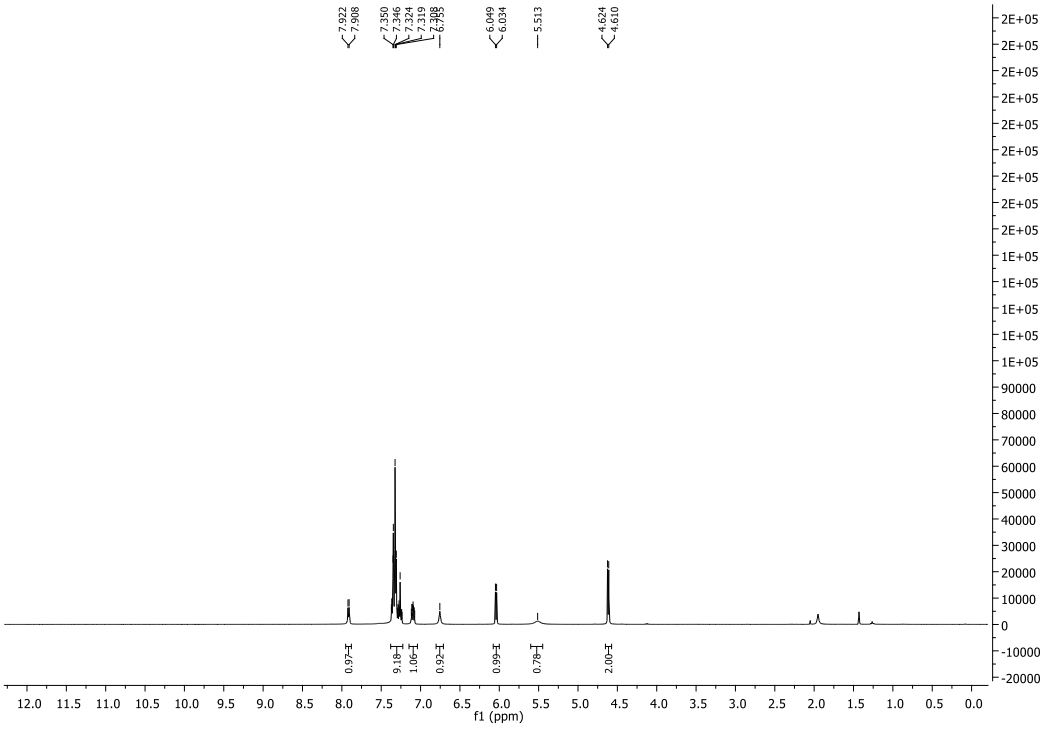

Figure 57 – ^{1}H NMR (400 MHz, $CDCl_3$) of **PH110**.

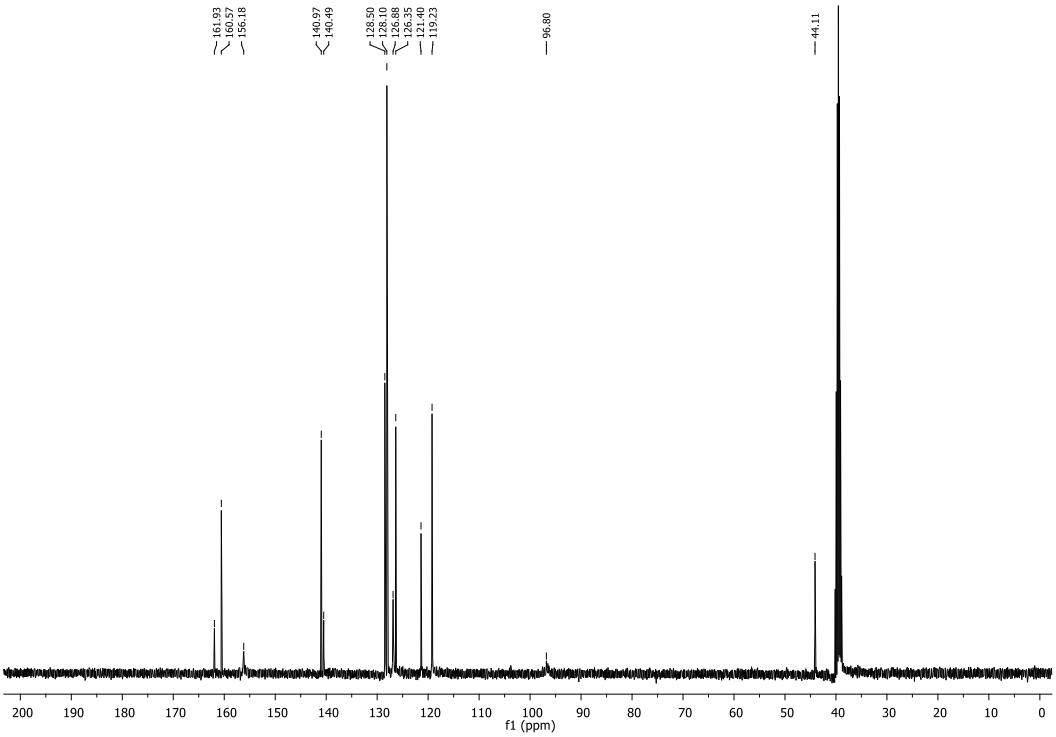

Figure 58 – ^{13}C NMR (100 MHz, DMSO-*d6*) of **PH110**.

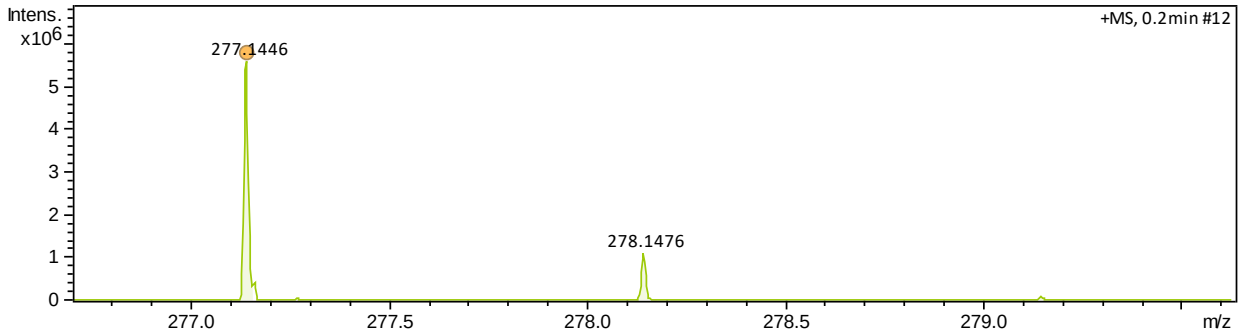

Figure 59 – Mass spectrum of **PH110**.

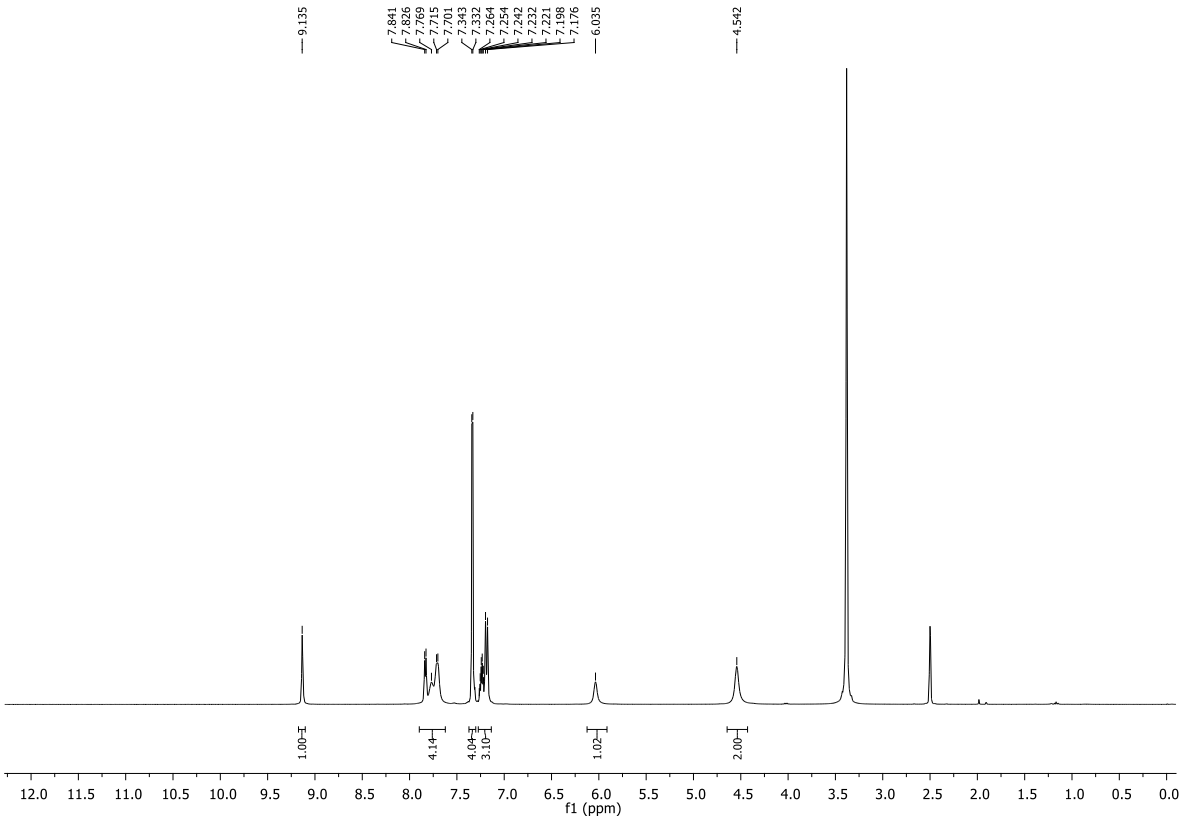

Figure 60 – ^{1}H NMR (400 MHz, DMSO-*d6*) of **PH112**.

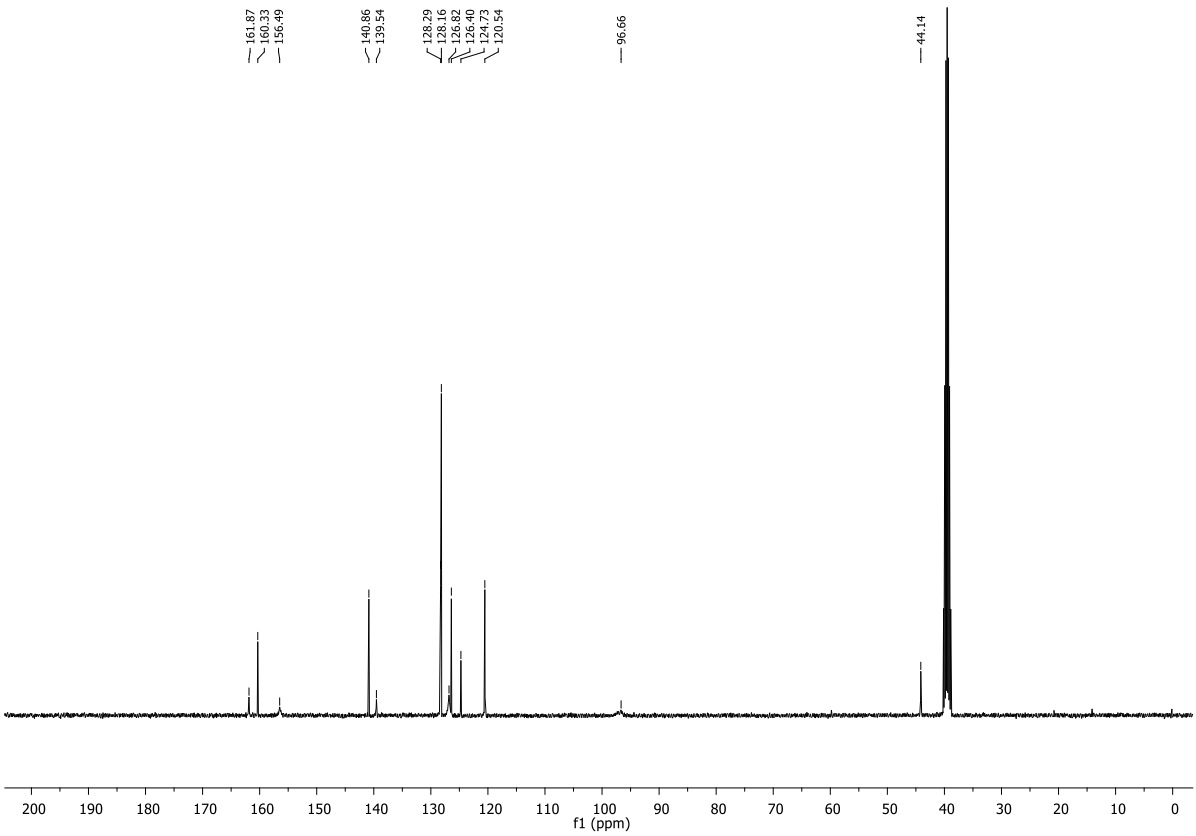

Figure 61 – ^{13}C NMR (100 MHz, DMSO-*d6*) of **PH112**.

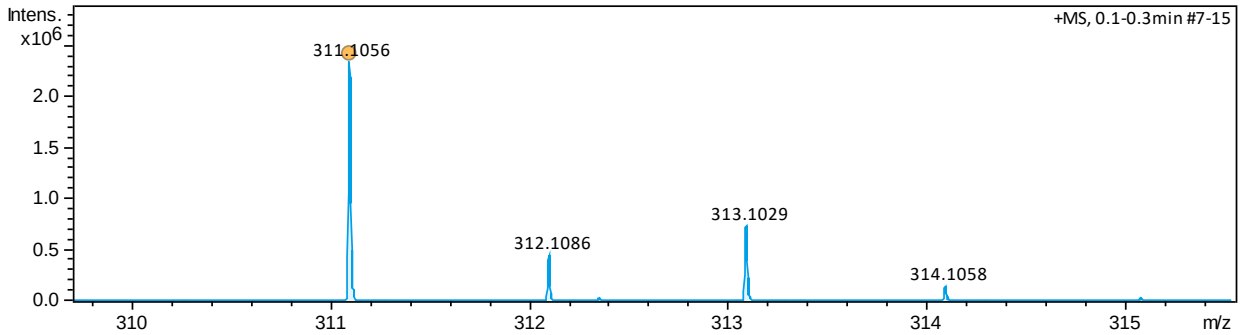

Figure 62 – Mass spectrum of **PH112**.

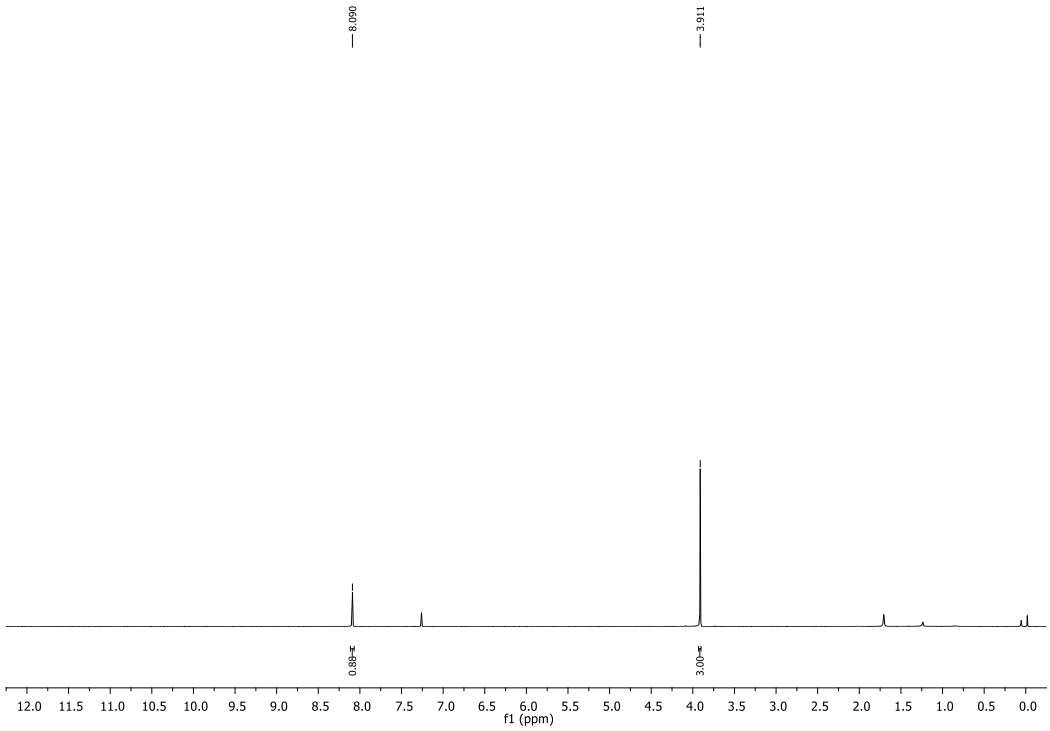

Figure 63 – ^{1}H NMR (400 MHz, $CDCl_3$) of 2,6-dichloro-9-methyl-9H-purine **11**.

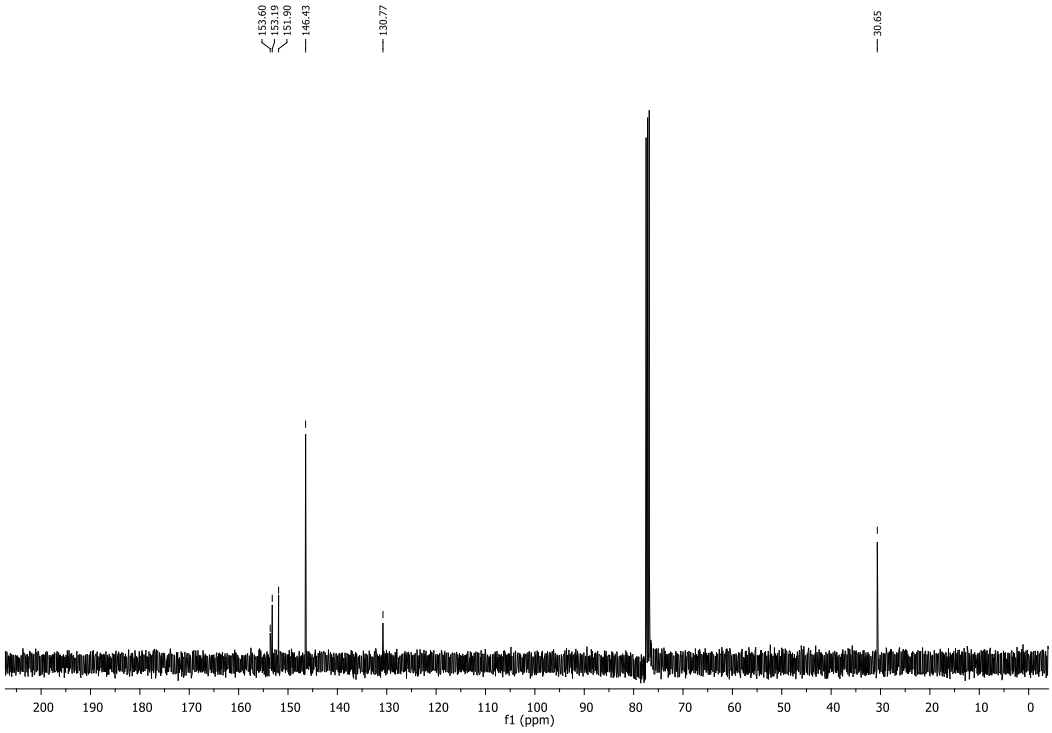

Figure 64 – ^{13}C NMR (100 MHz, $CDCl_3$) of 2,6-dichloro-9-methyl-9H-purine **11**.

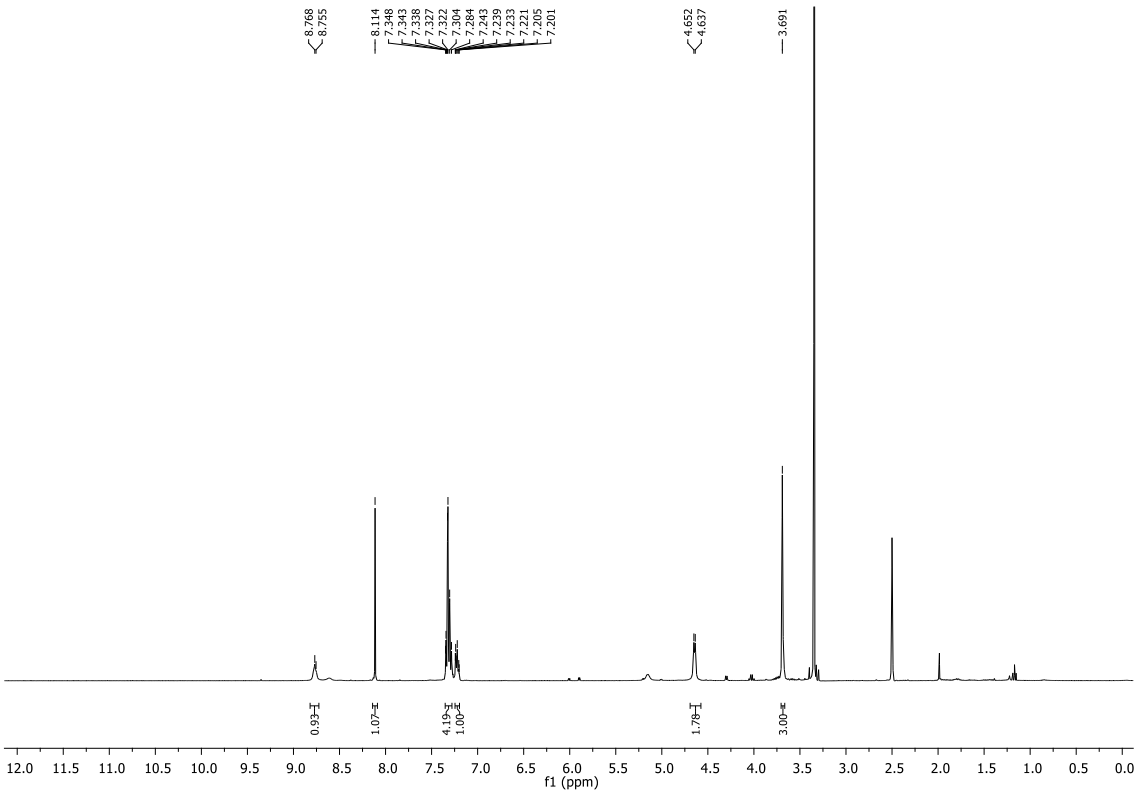

Figure 65 – ^{1}H NMR (400 MHz, DMSO-*d6*) of **12**.

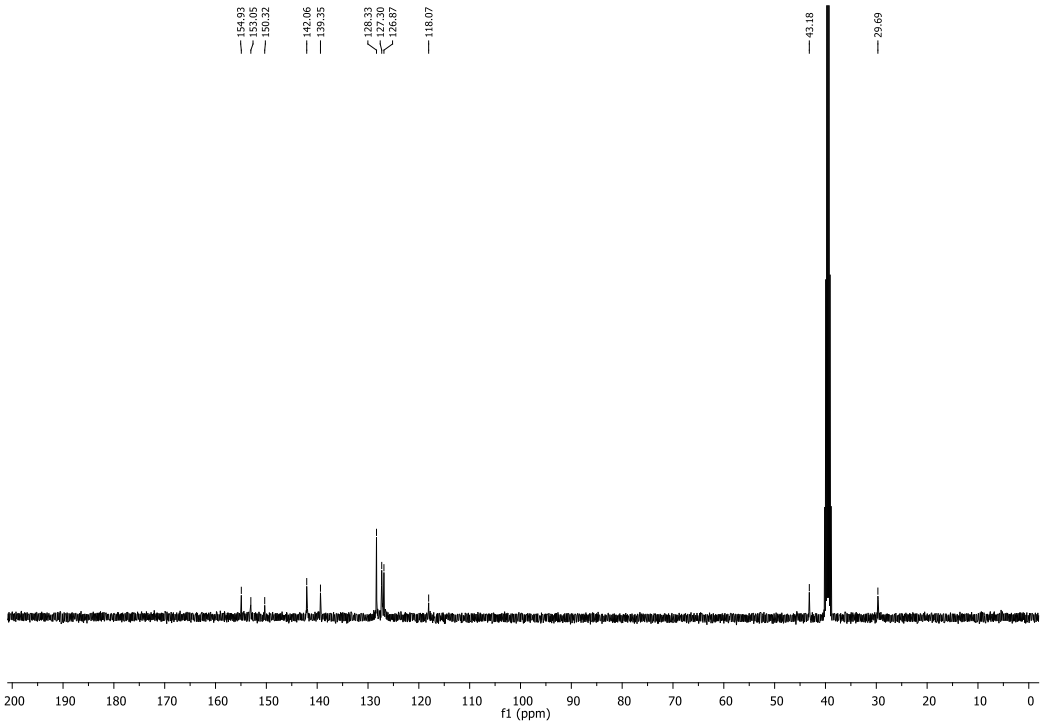

Figure 66 – ^{13}C NMR (100 MHz, DMSO-*d6*) of **12**.

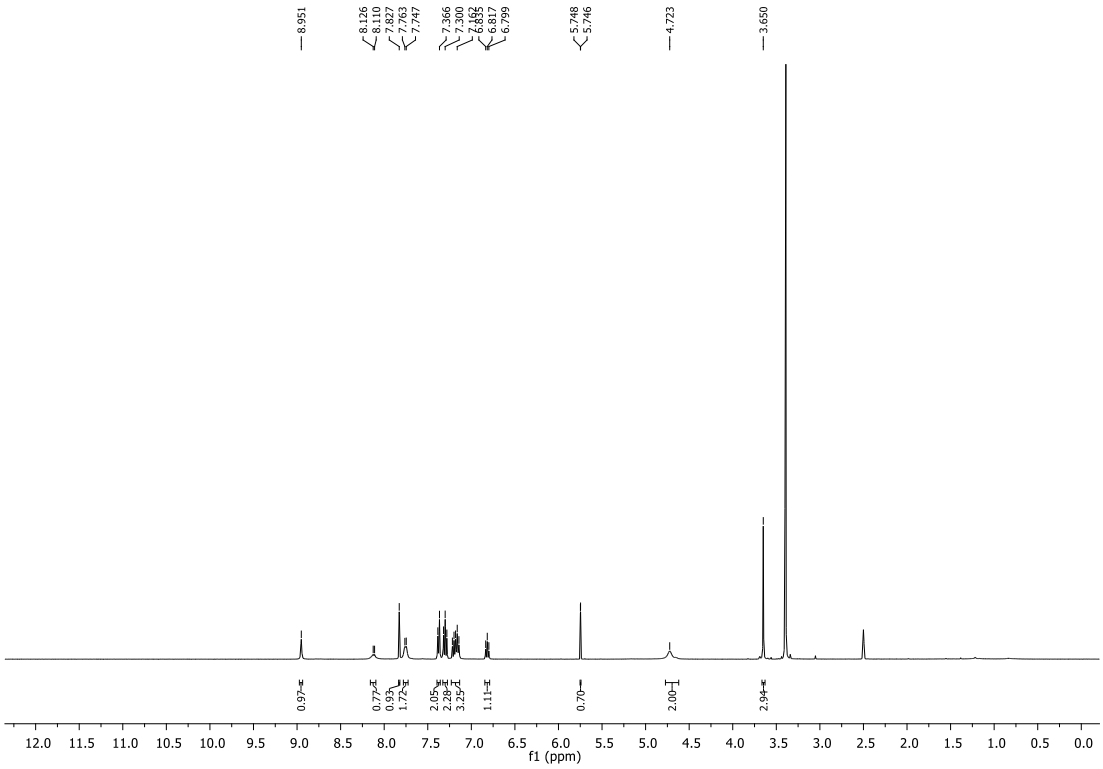

Figure 67 – ^{1}H NMR (400 MHz, DMSO-*d6*) of **PH111**.

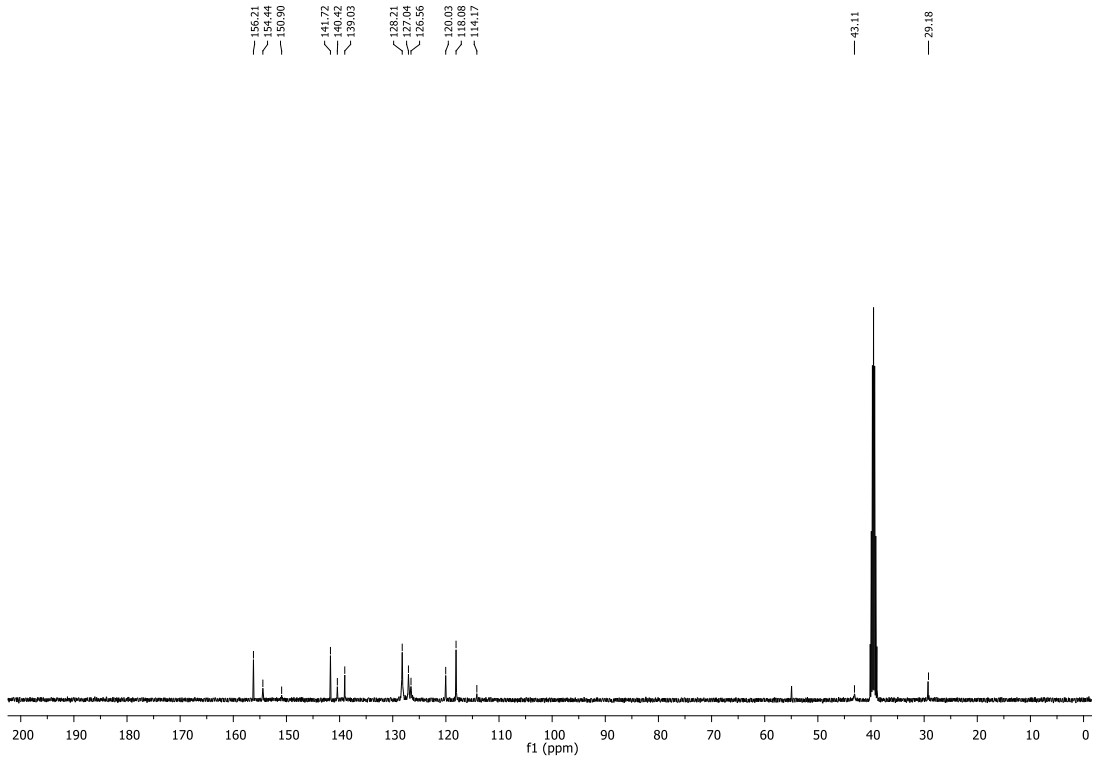

Figure 68 – ^{13}C NMR (100 MHz, DMSO-*d6*) of **PH111**.

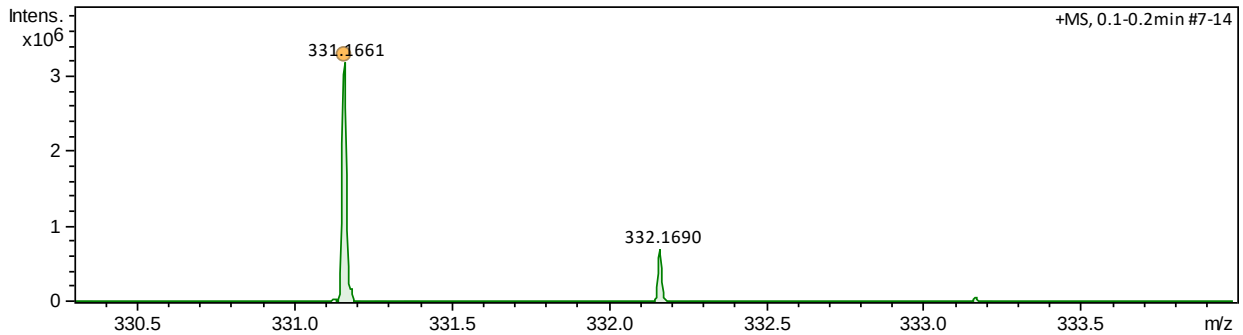

Figure 69 – Mass spectrum of **PH111**.

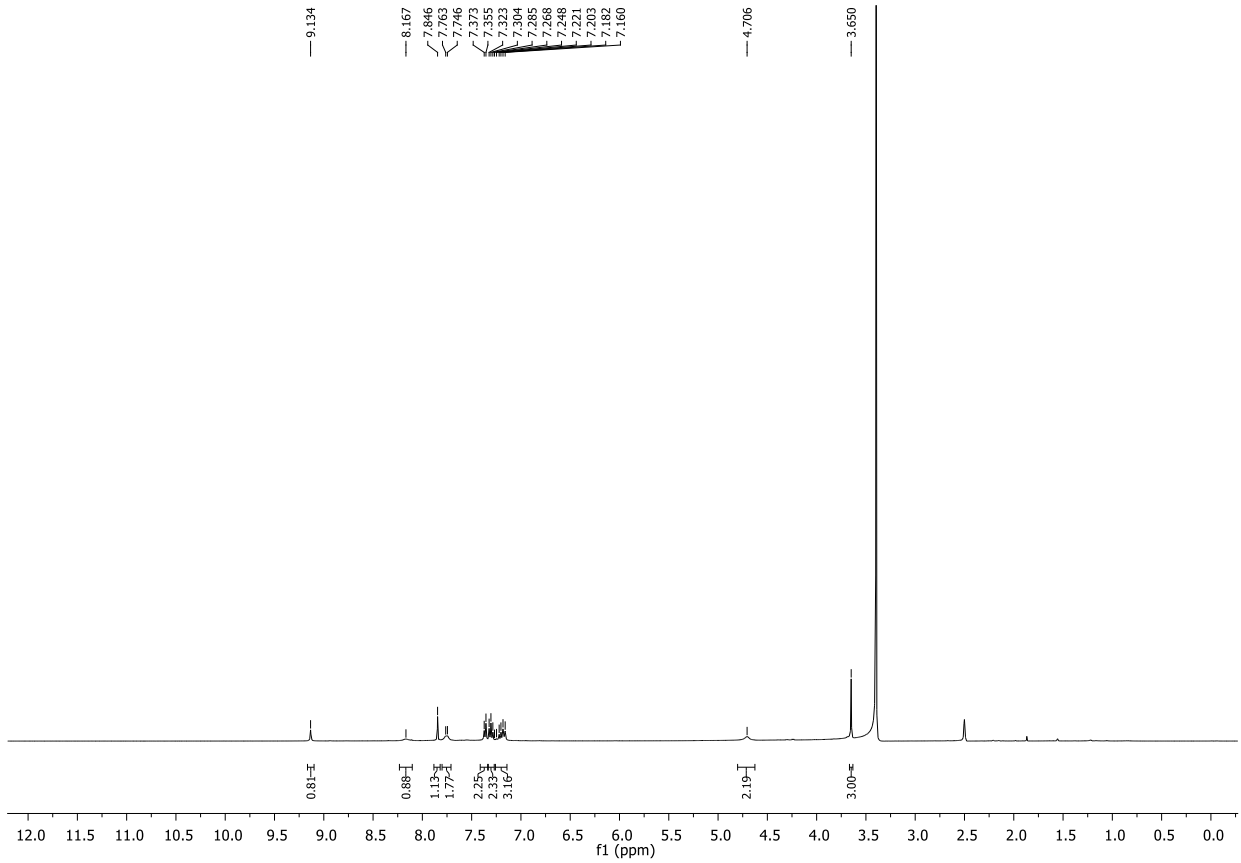

Figure 70 – ^{1}H NMR (400 MHz, DMSO-*d6*) of **PH113**.

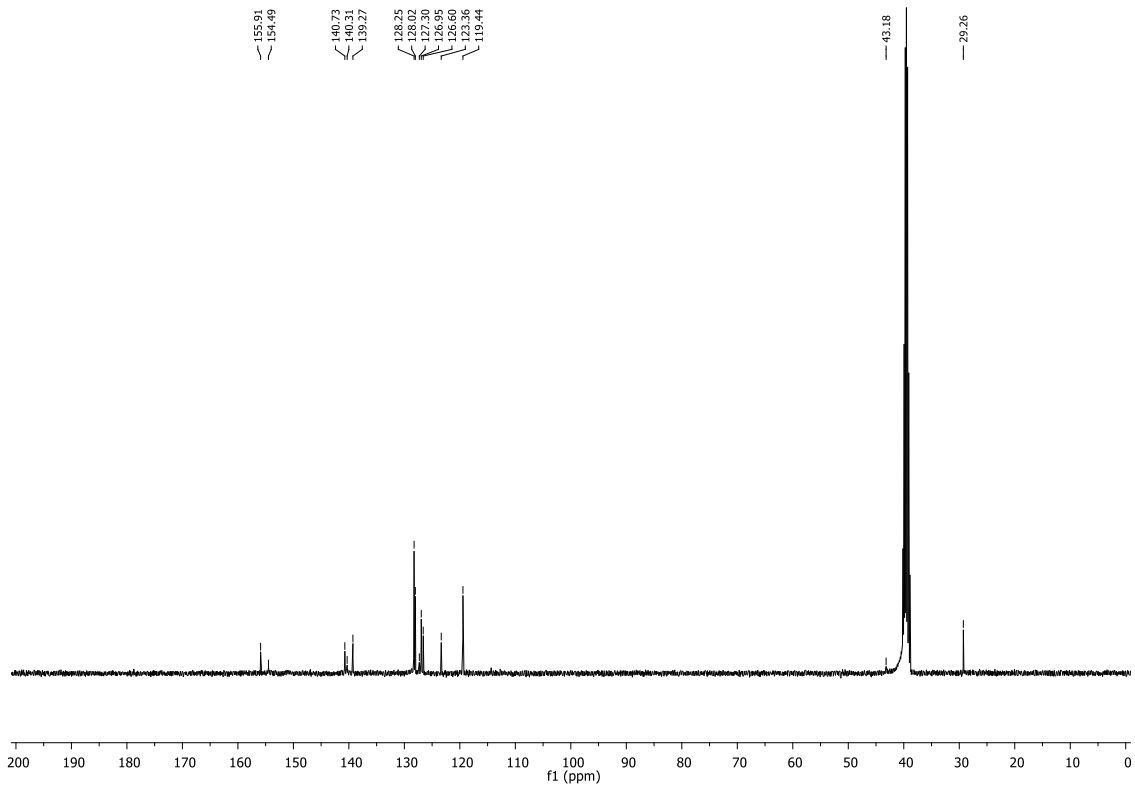

Figure 71 – ^{13}C NMR (100 MHz, DMSO-*d6*) of **PH113**.

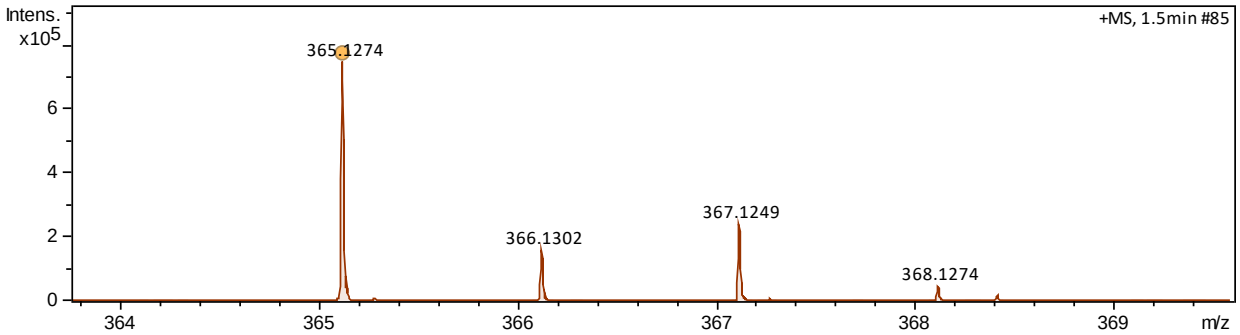

Figure 72 – Mass spectrum of **PH113**.

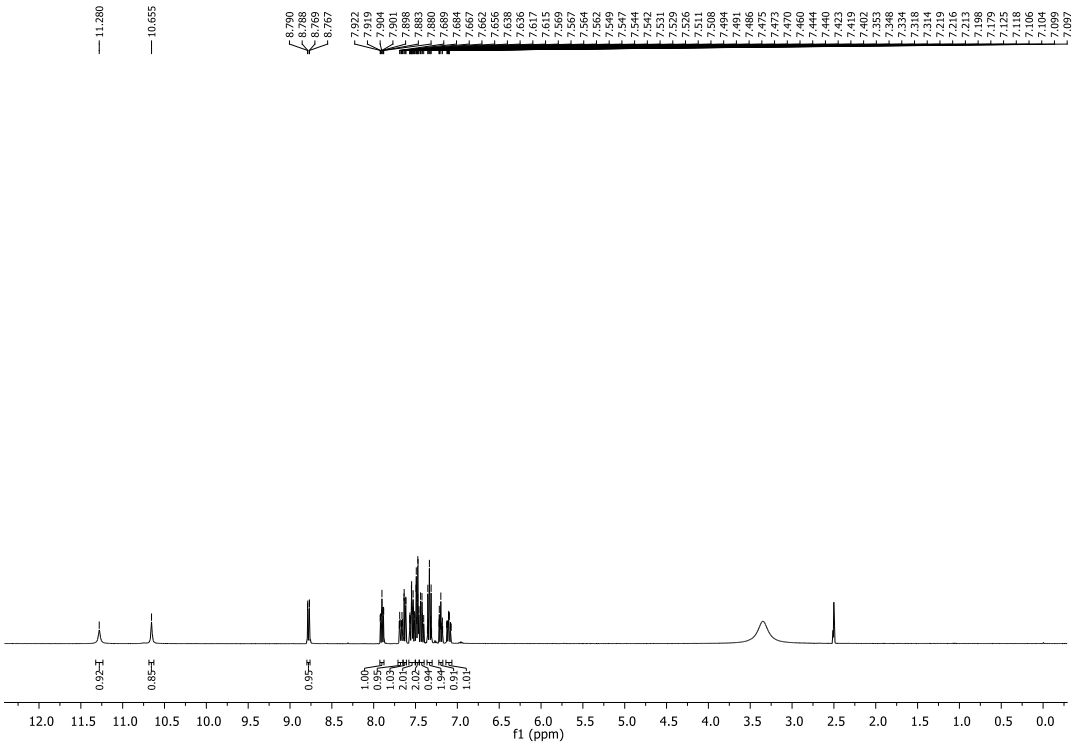

Figure 73 – ^{1}H NMR (400 MHz, DMSO-*d6*) of **PH114**.

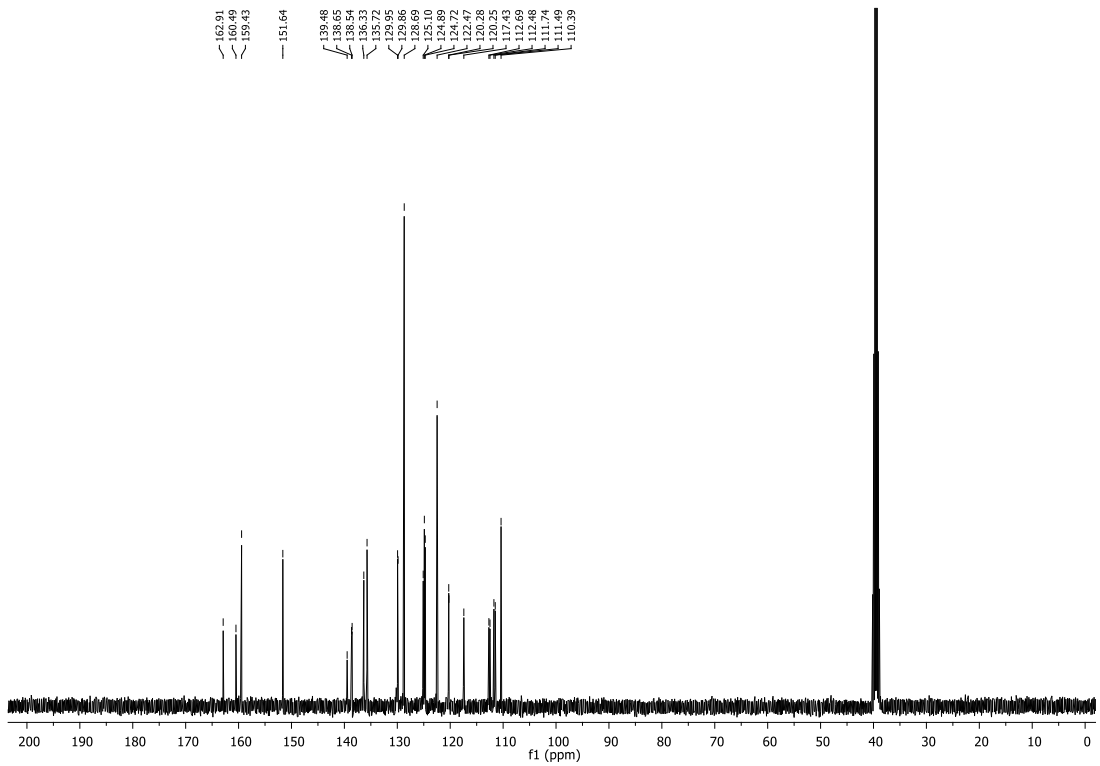

Figure 74 – ^{13}C NMR (100 MHz, DMSO-*d6*) of **PH114**.

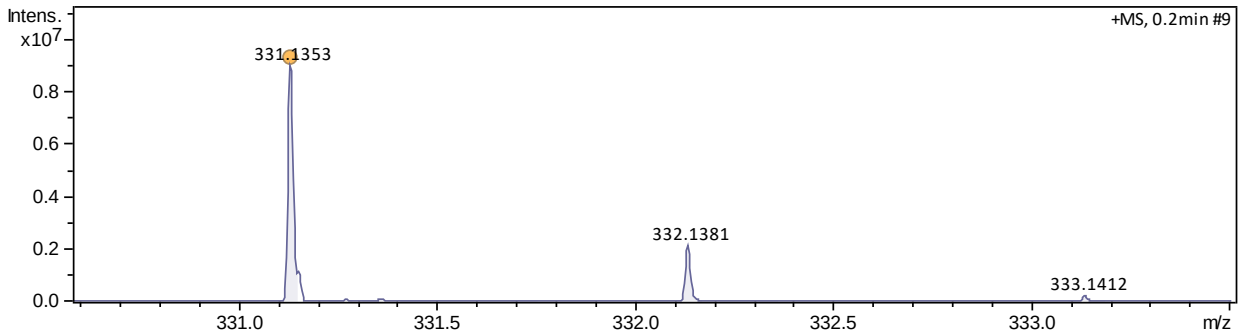

Figure 75 – Mass spectrum of **PH114**.

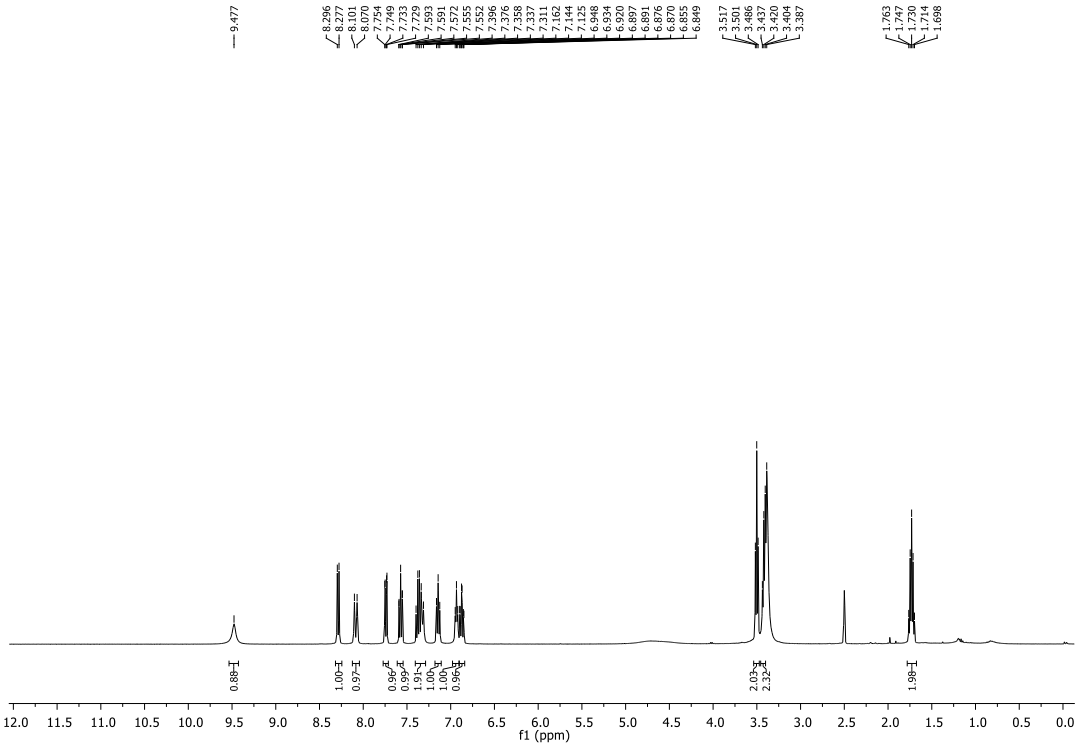

Figure 76 – ^{1}H NMR (400 MHz, DMSO-*d6*) of **PH115**.

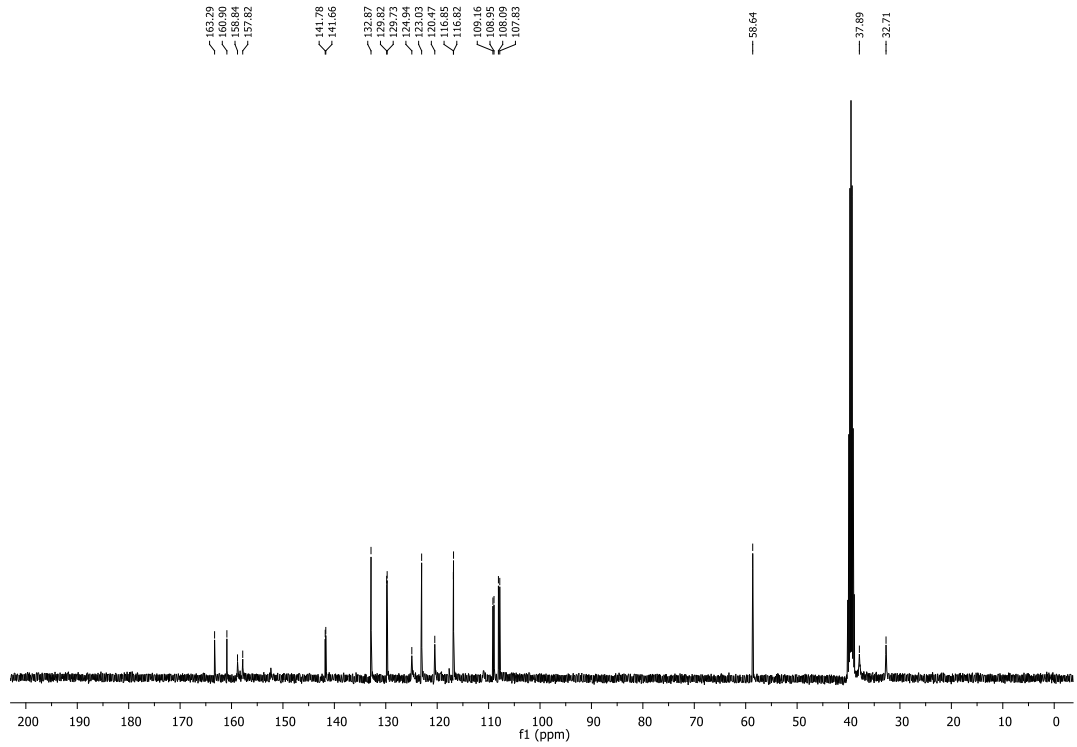

Figure 77 – ^{13}C NMR (100 MHz, DMSO-*d6*) of **PH115**.

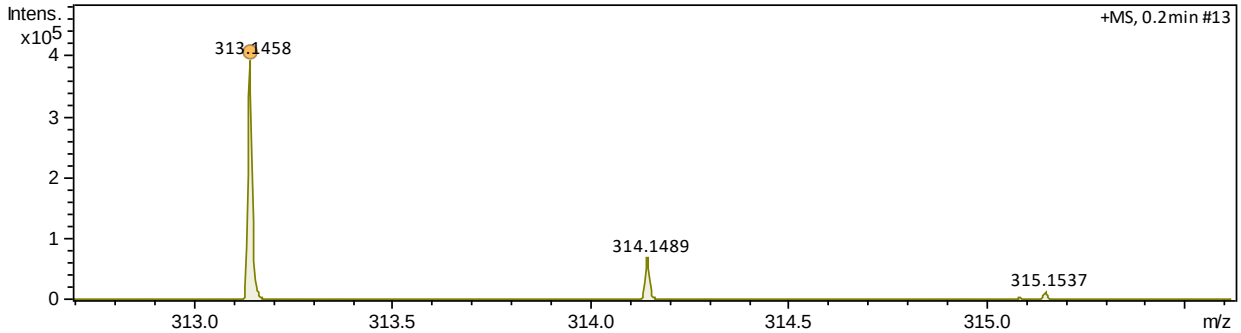

Figure 78 – Mass spectrum of **PH115**.

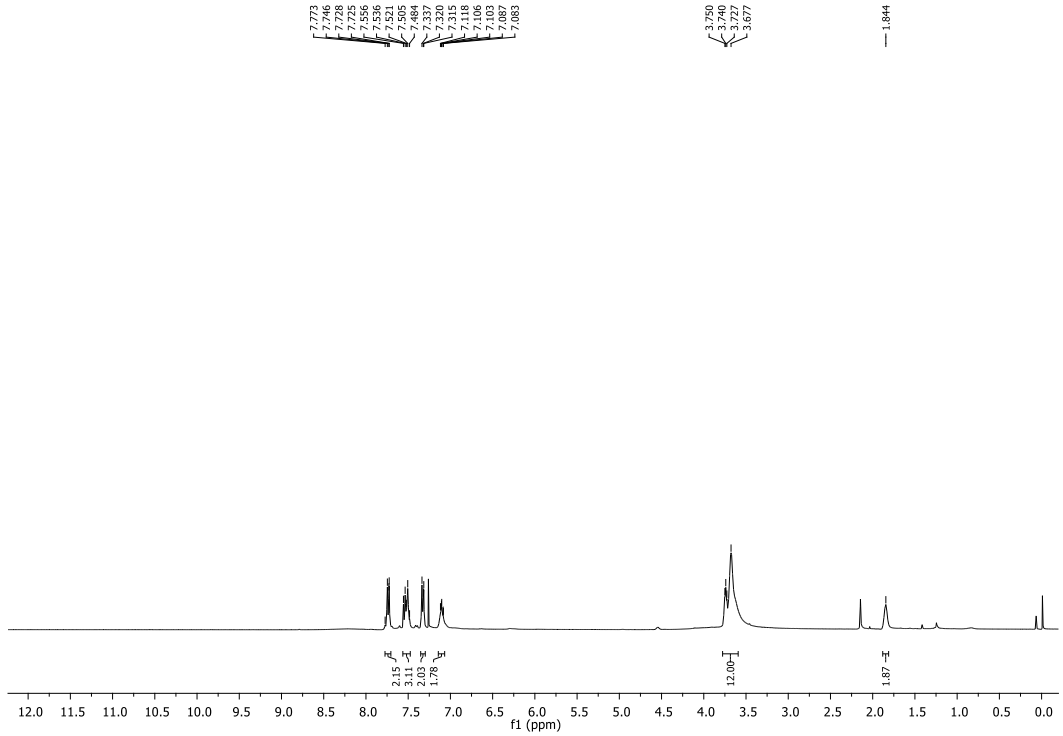

Figure 79 – ^{1}H NMR (400 MHz, $CDCl_3$) of **PH116**.

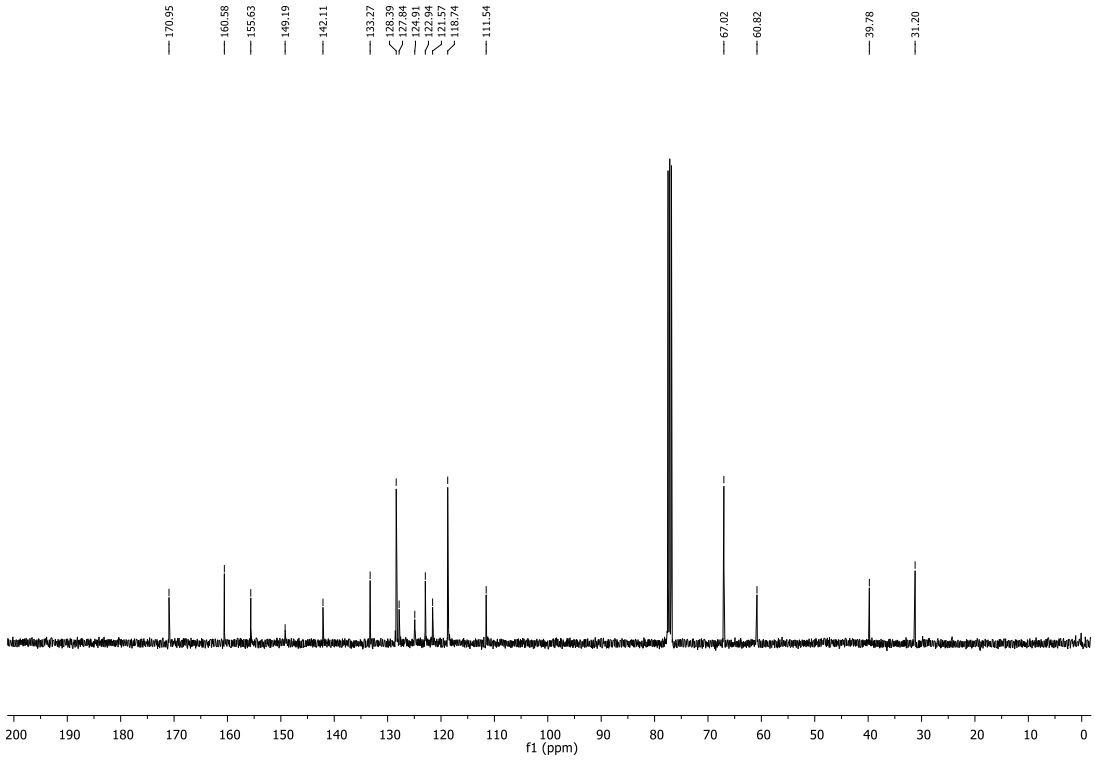

Figure 80 – ^{13}C NMR (100 MHz, $CDCl_3$) of **PH116**.

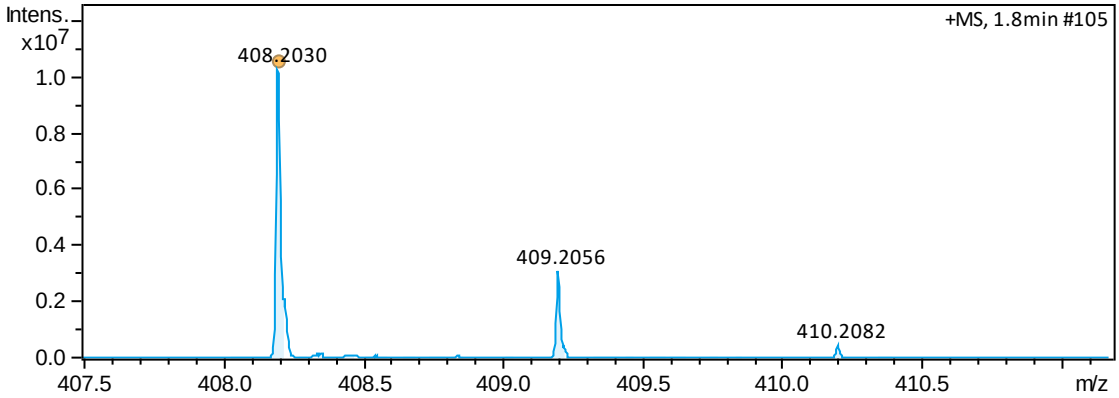

Figure 81 – Mass spectrum of **PH116**.

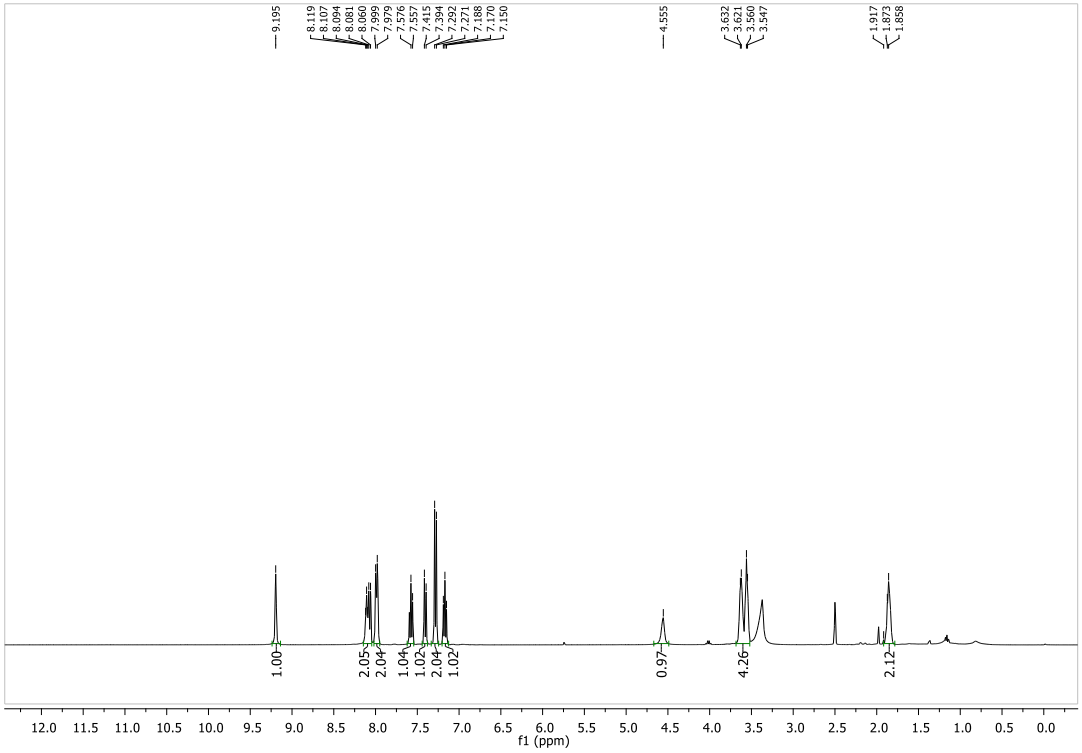

Figure 82 – ^{1}H NMR (400 MHz, DMSO-*d6*) of **PH118**.

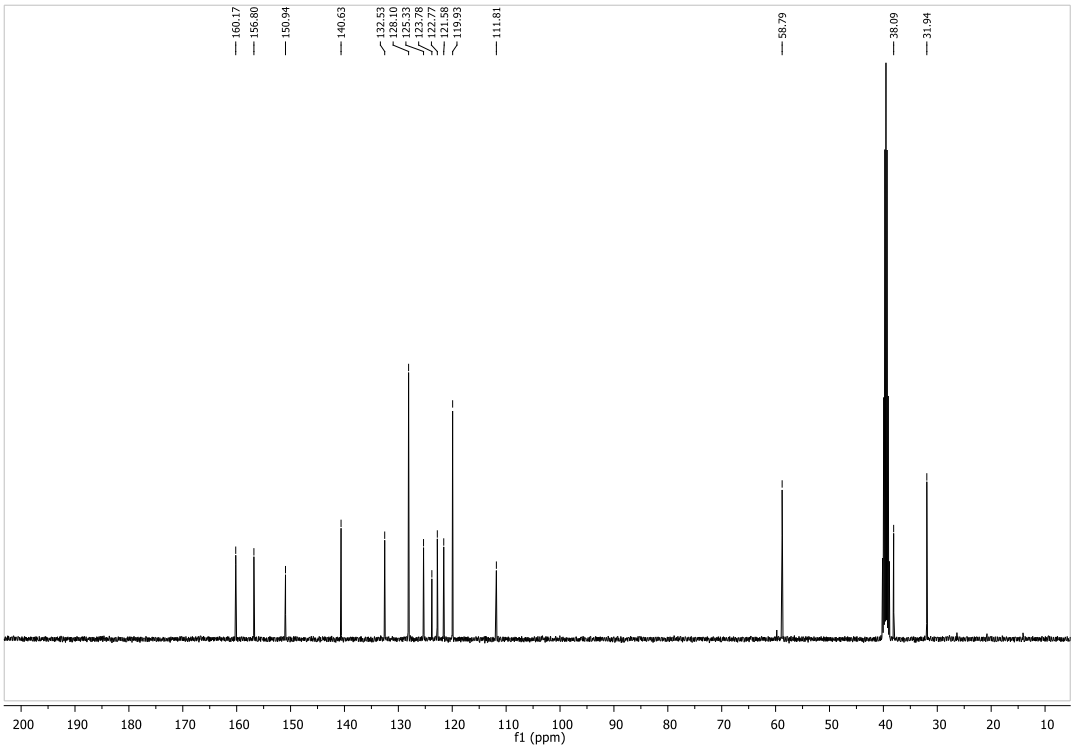

Figure 83 – ^{13}C NMR (100 MHz, DMSO-*d6*) of **PH118**.

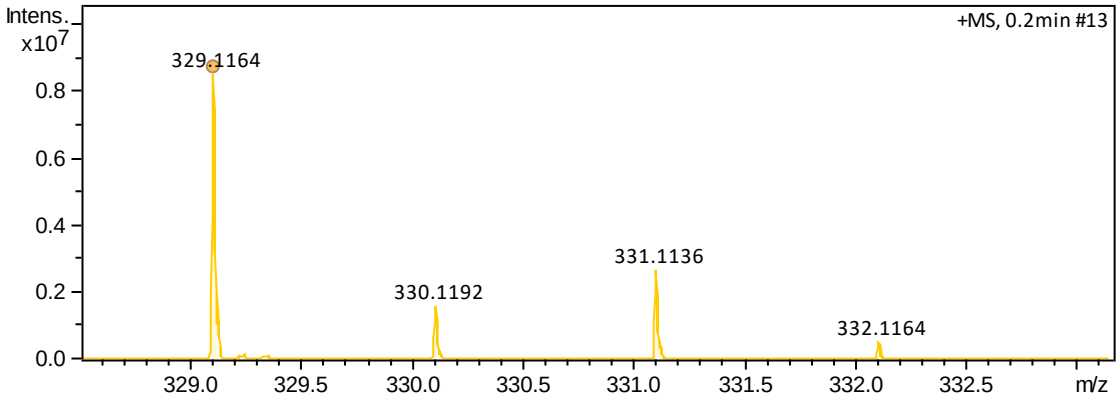

Figure 84 – Mass spectrum of **PH118**.

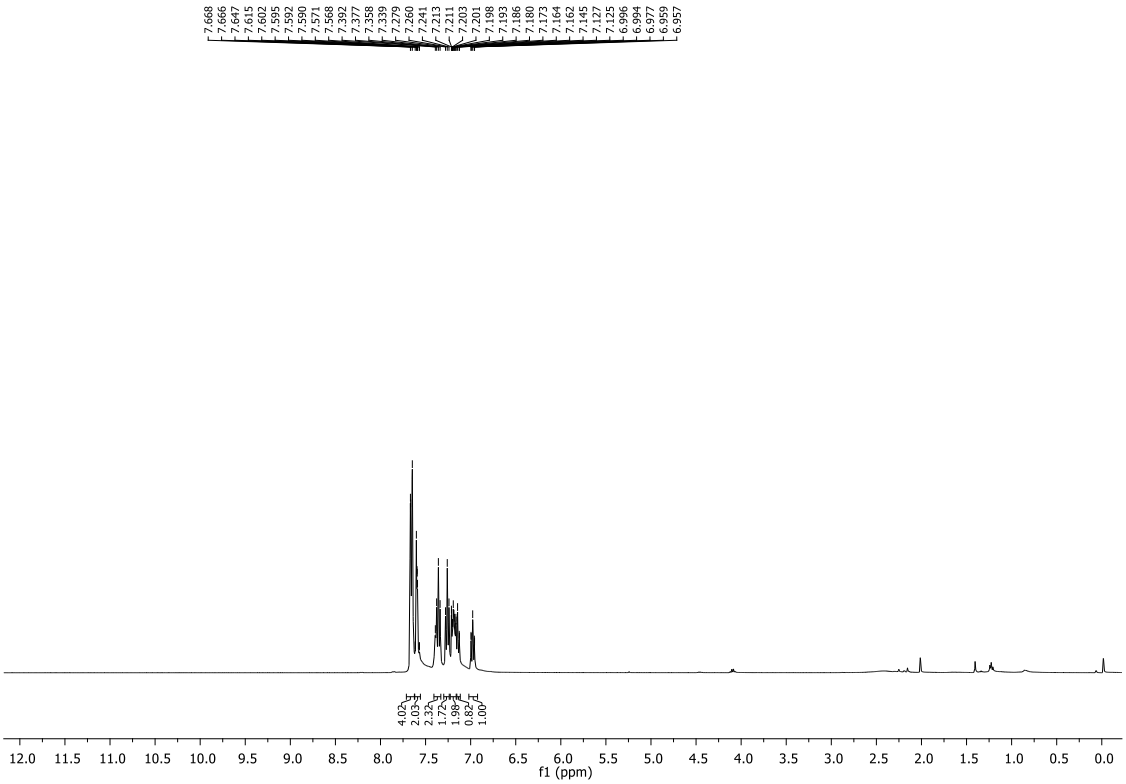

Figure 85 – ^{1}H NMR (400 MHz, $CDCl_3$) of **PH117**.

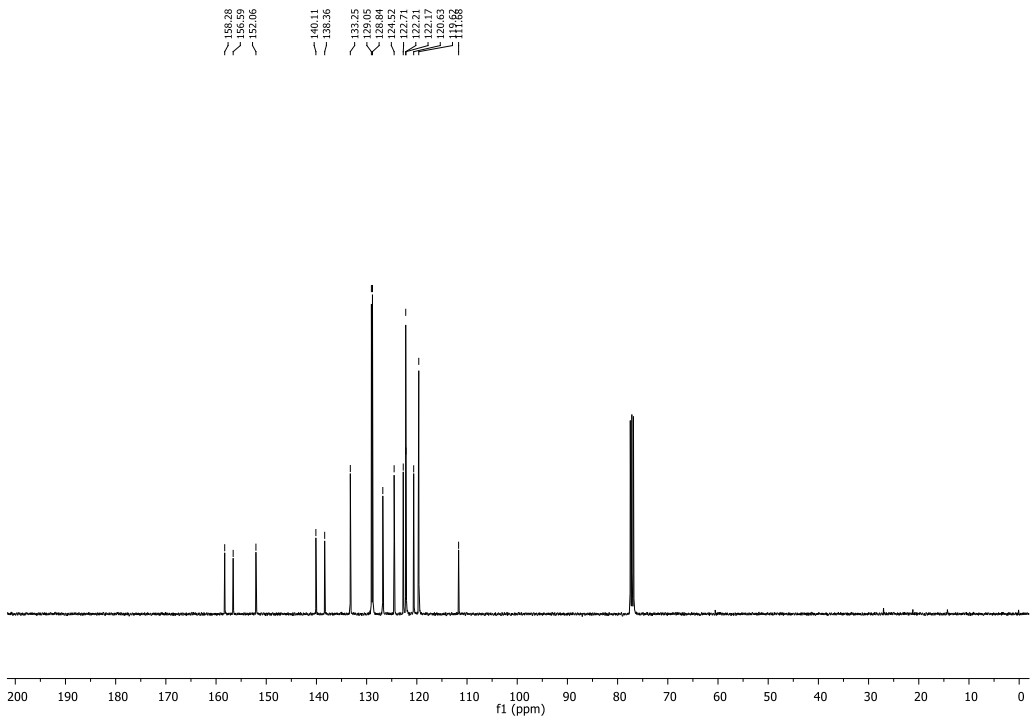

Figure 86 – ^{13}C NMR (100 MHz, $CDCl_3$) of **PH117**.

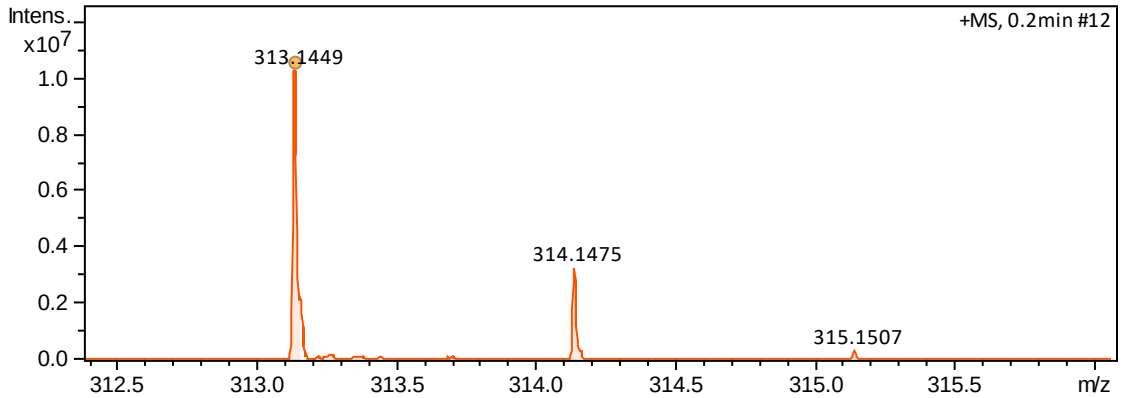

Figure 87 – Mass spectrum of **PH117**.

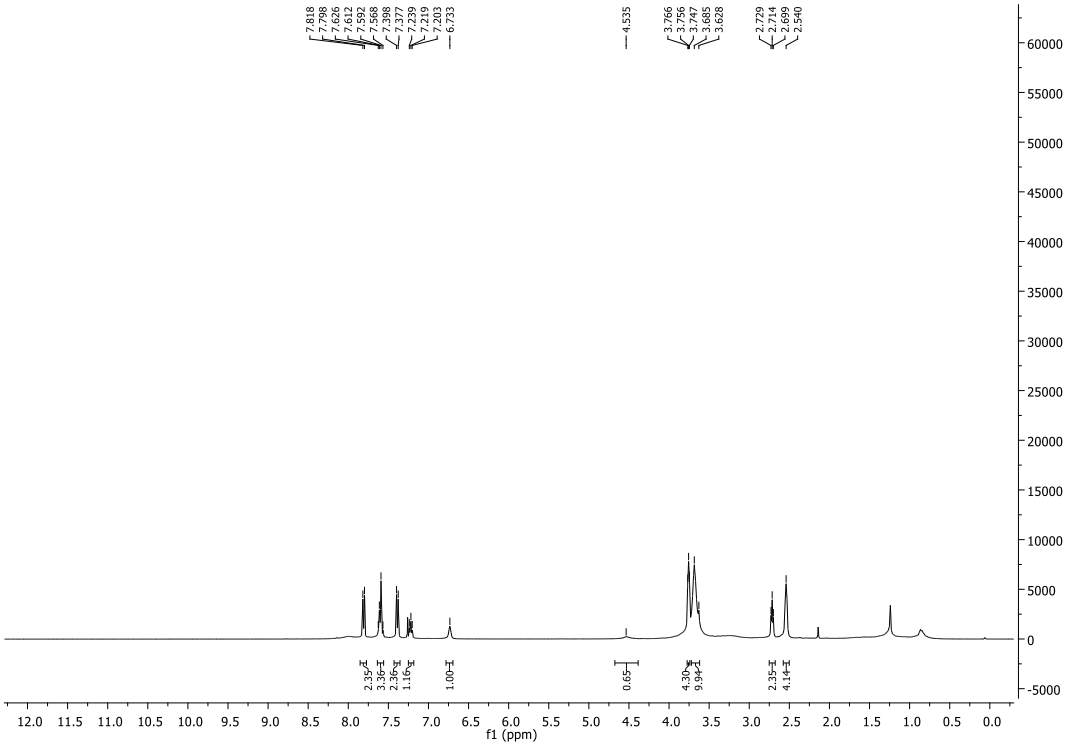

Figure 88 – ^{1}H NMR (400 MHz, $CDCl_3$) of **PH119**.

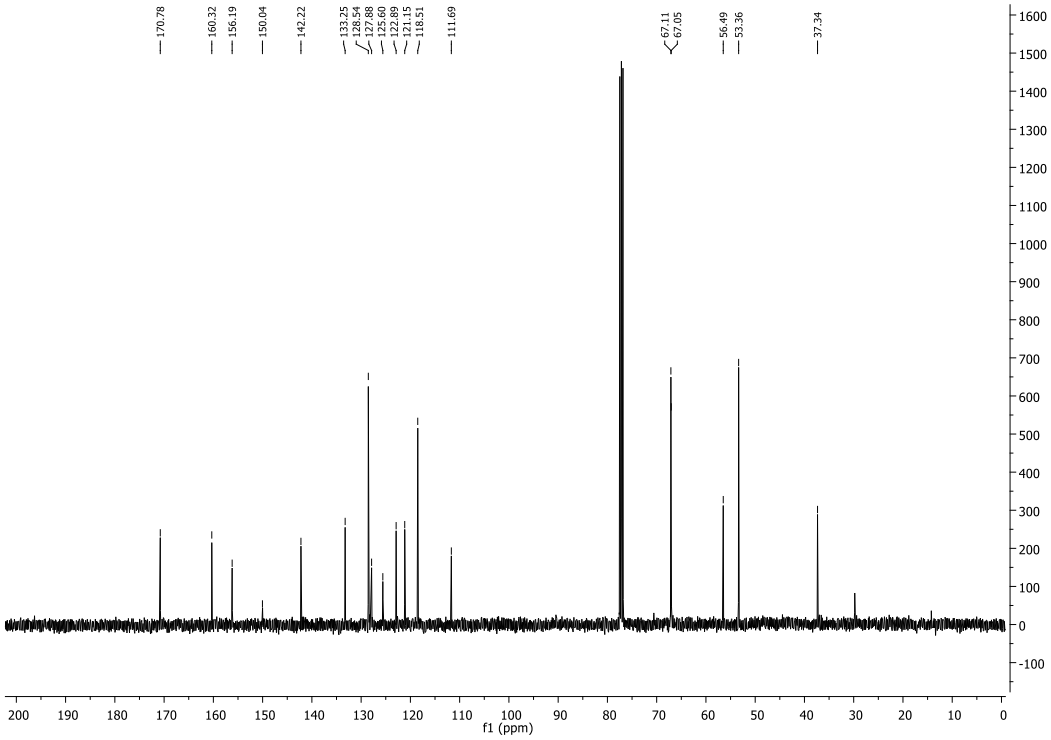

Figure 89 – ^{13}C NMR (100 MHz, $CDCl_3$) of **PH119**.

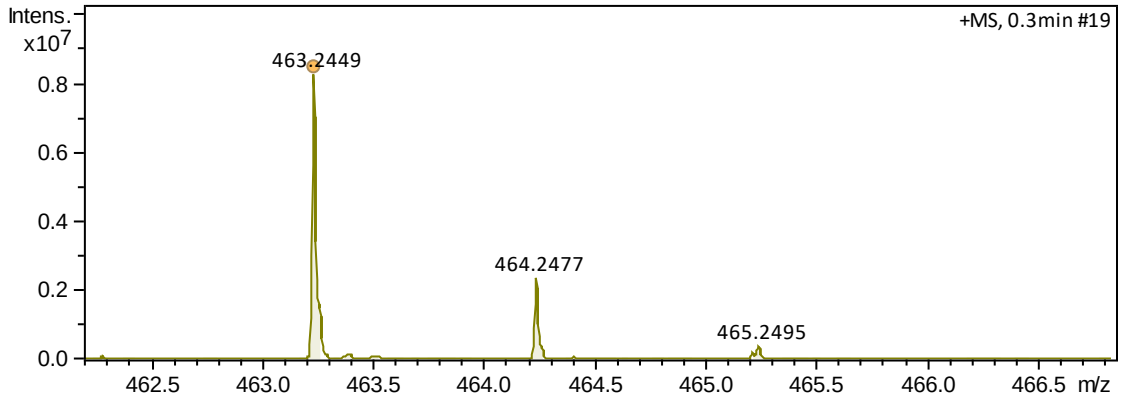

Figure 90 – Mass spectrum of **PH119**.

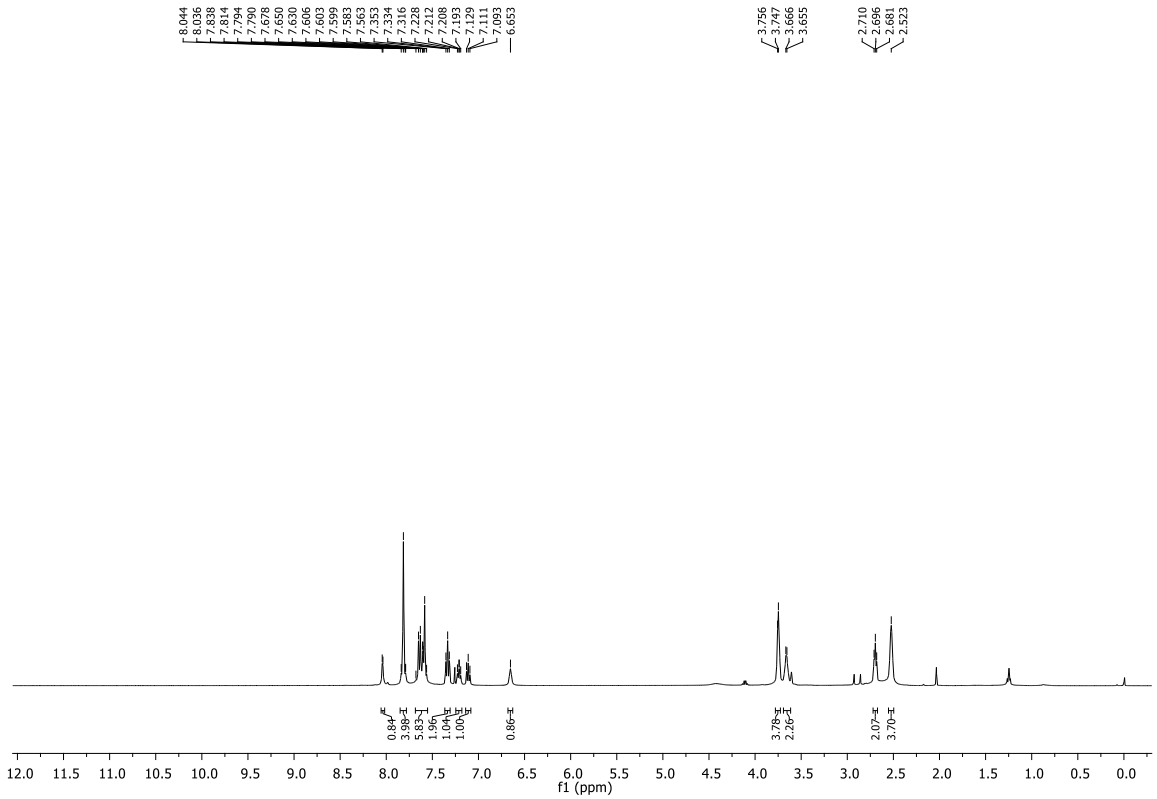

Figure 91 – ^{1}H NMR (400 MHz, $CDCl_3$) of **PH120**.

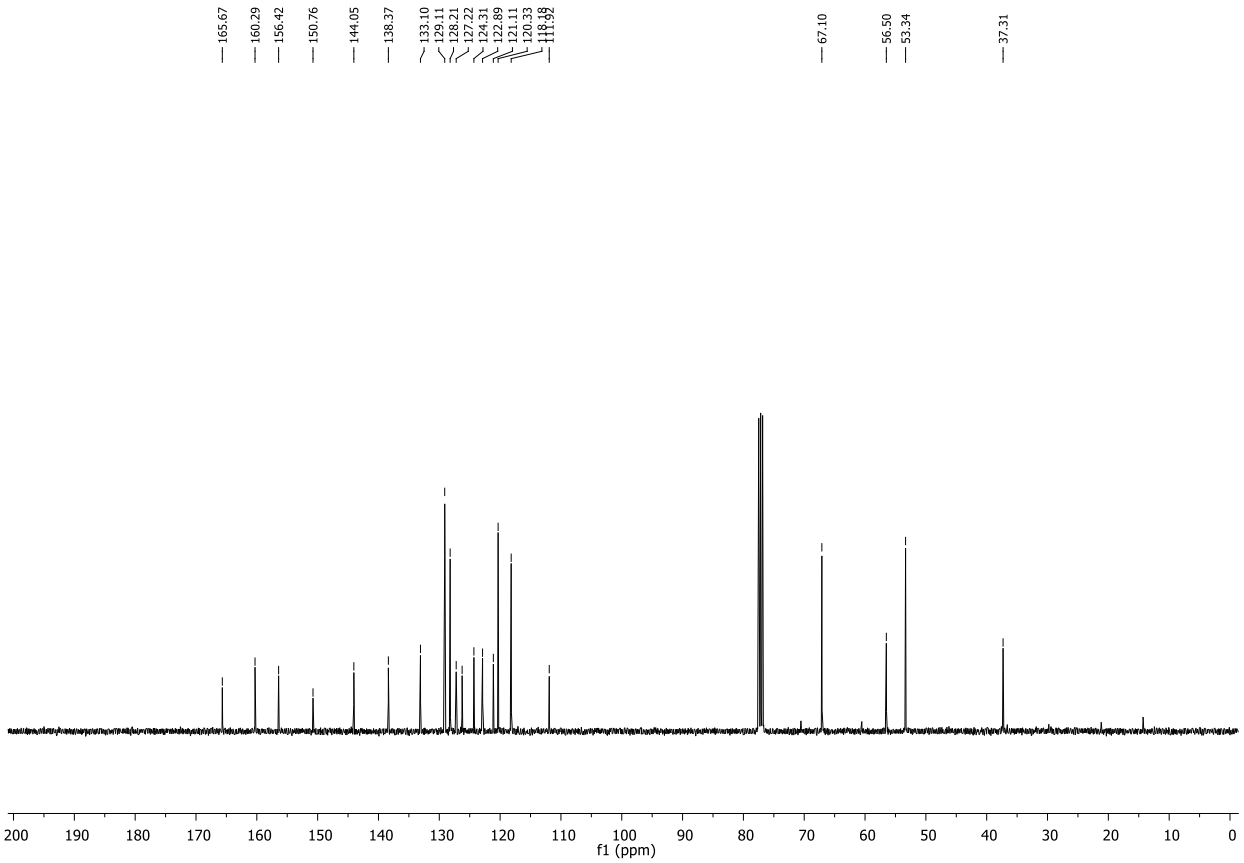

Figure 92 – ^{13}C NMR (100 MHz, $CDCl_3$) of **PH120**.

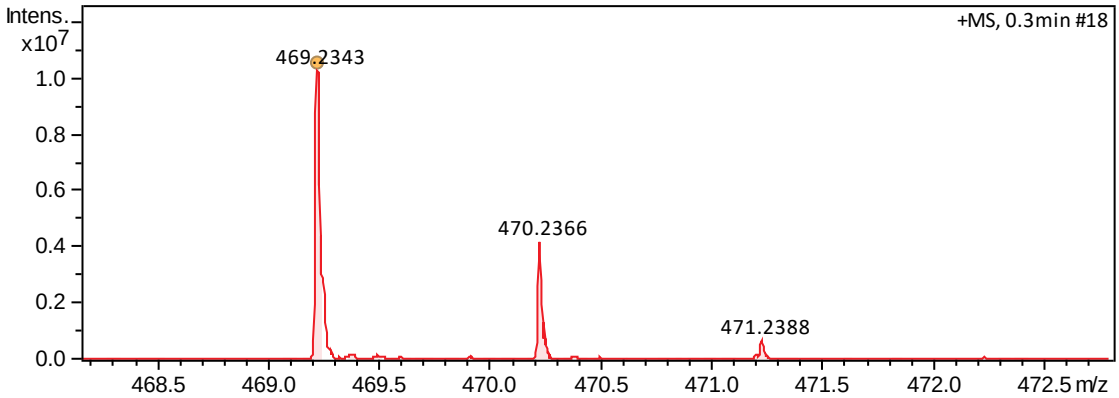

Figure 93 – Mass spectrum of **PH120**.

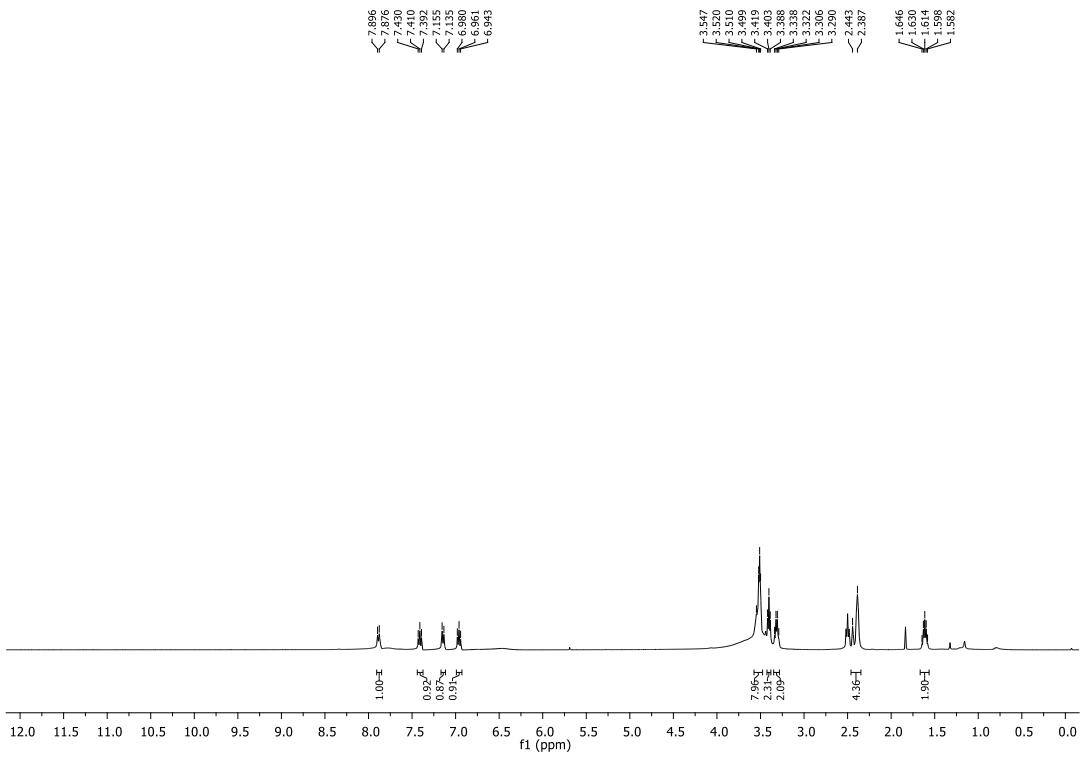

Figure 94 – ^{1}H NMR (400 MHz, DMSO-*d6*) of **PH121**.

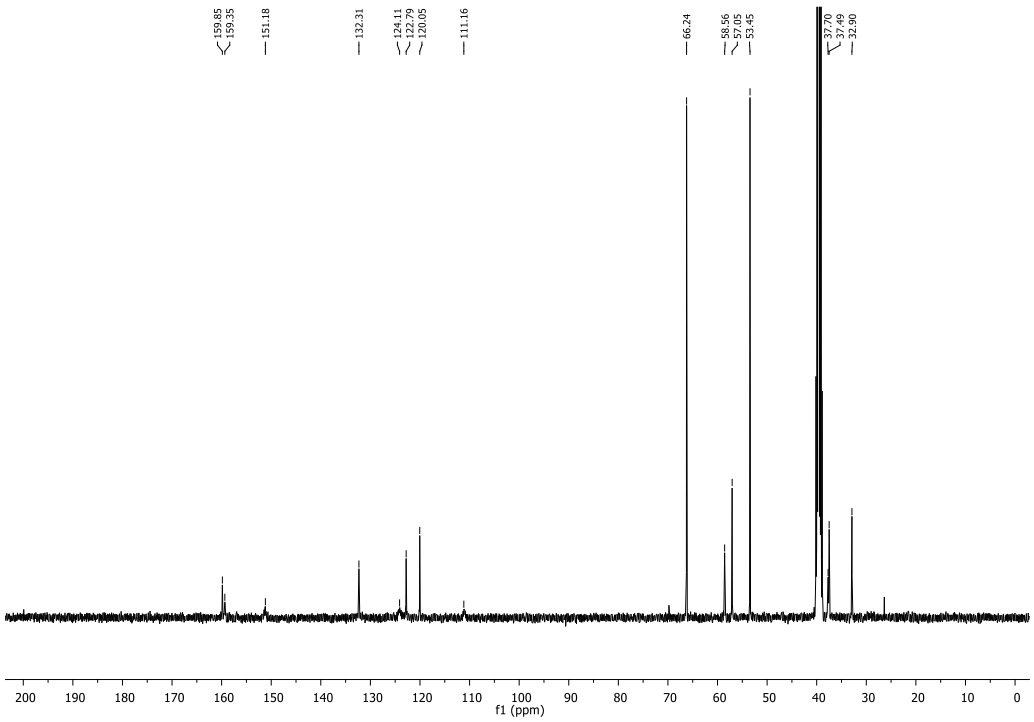

Figure 95 – ^{13}C NMR (100 MHz, DMSO-*d6*) of **PH121**.

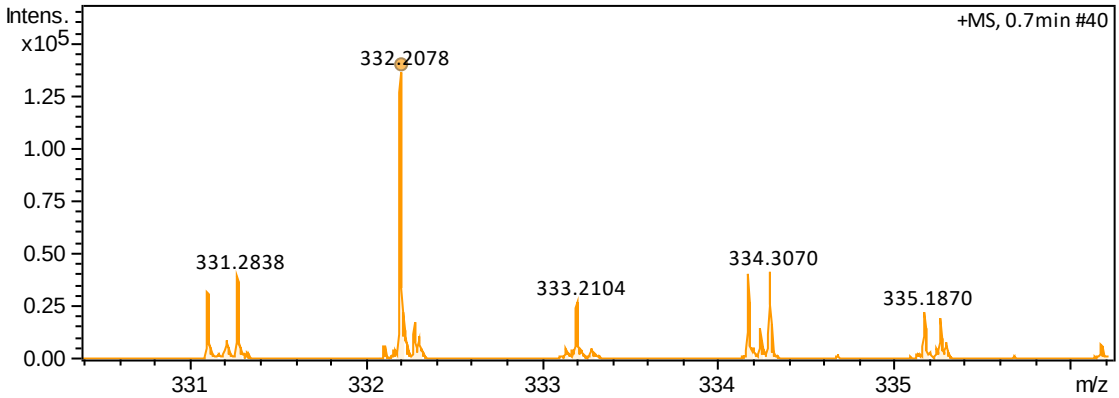

Figure 96 – Mass spectrum of **PH121**.

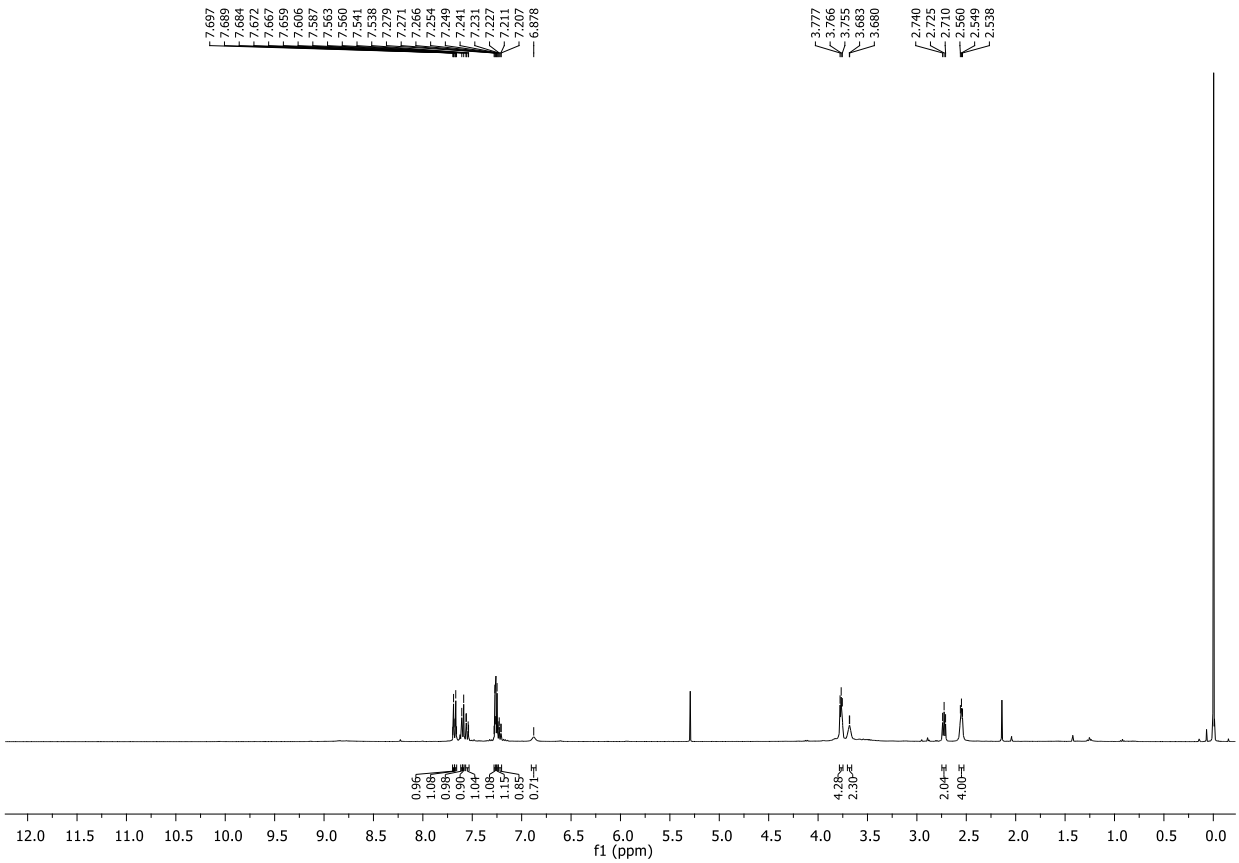

Figure 97 – ^{1}H NMR (400 MHz, $CDCl_3$) of **PH122**.

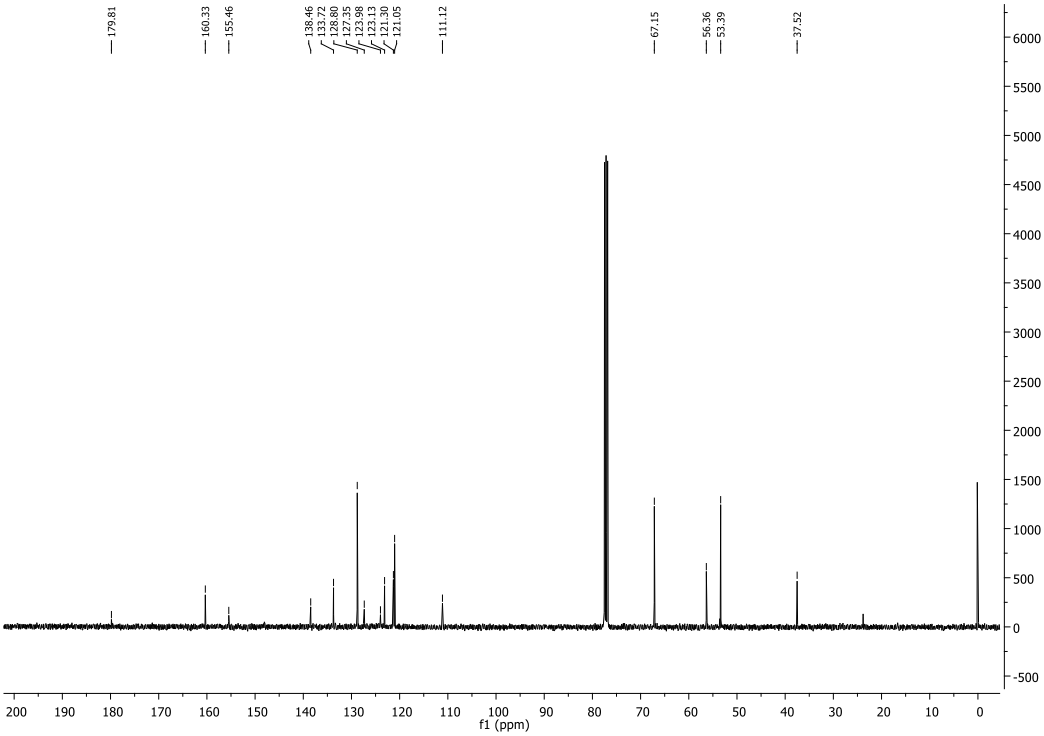

Figure 98 – ^{13}C NMR (100 MHz, $CDCl_3$) of **PH122**.

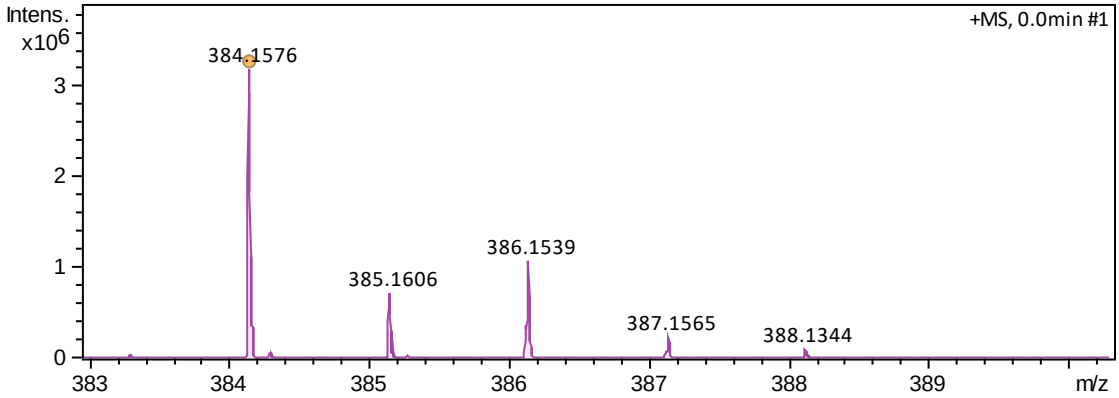

Figure 99 – Mass spectrum of **PH122**.

HPLC ANALISYS

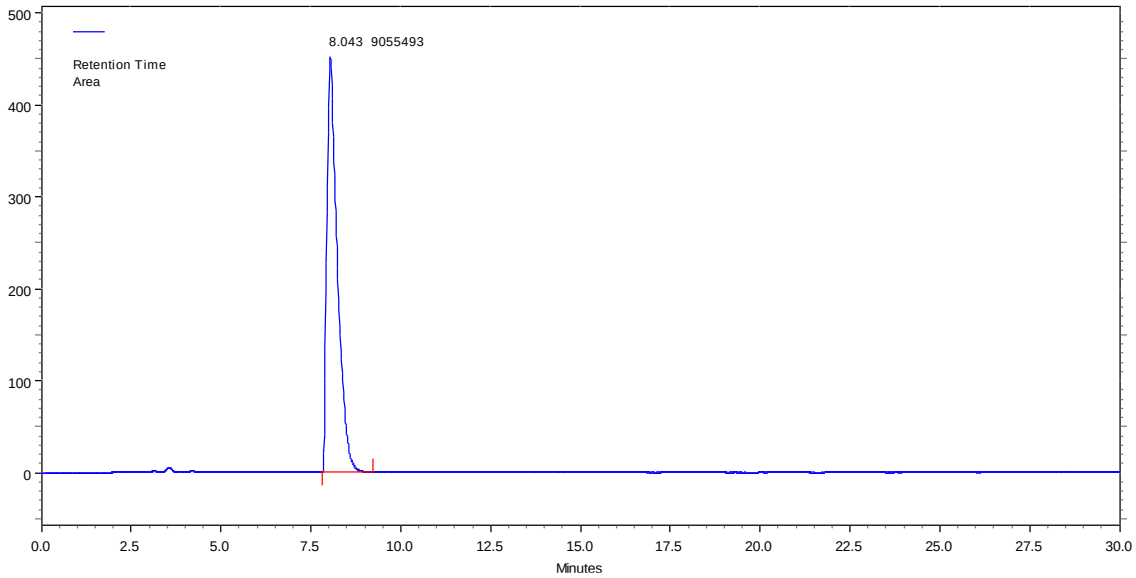

Figure 100 – HPLC chromatogram of **PH100**. Mobile phase: 0.1% aqueous TFA/ acetonitrile (50:50).

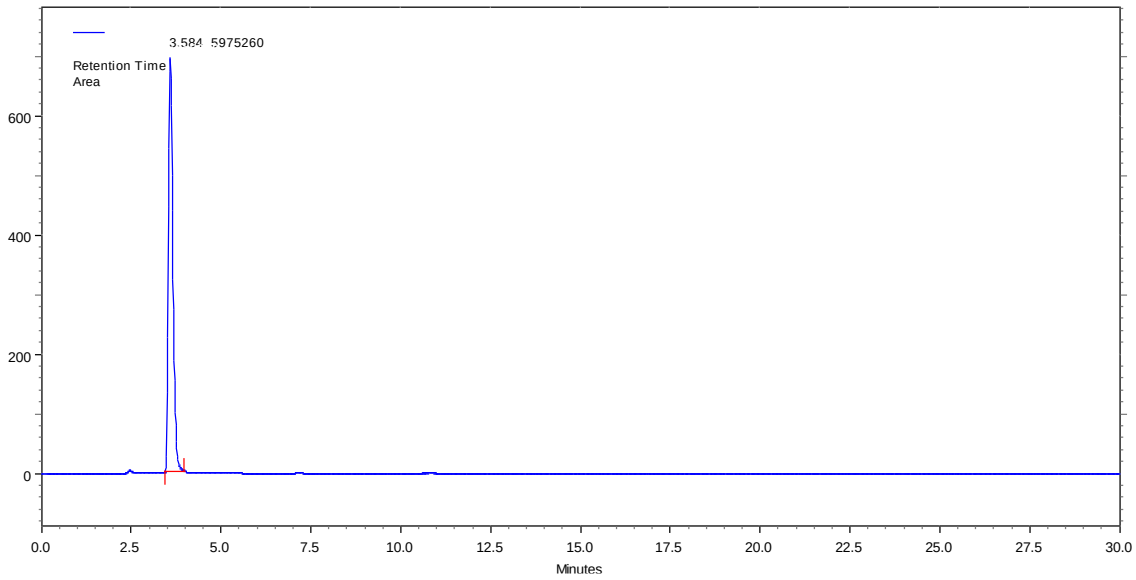

Figure 101 – HPLC chromatogram of **PH101**. Mobile phase: 0.1% aqueous TFA/ acetonitrile (50:50).

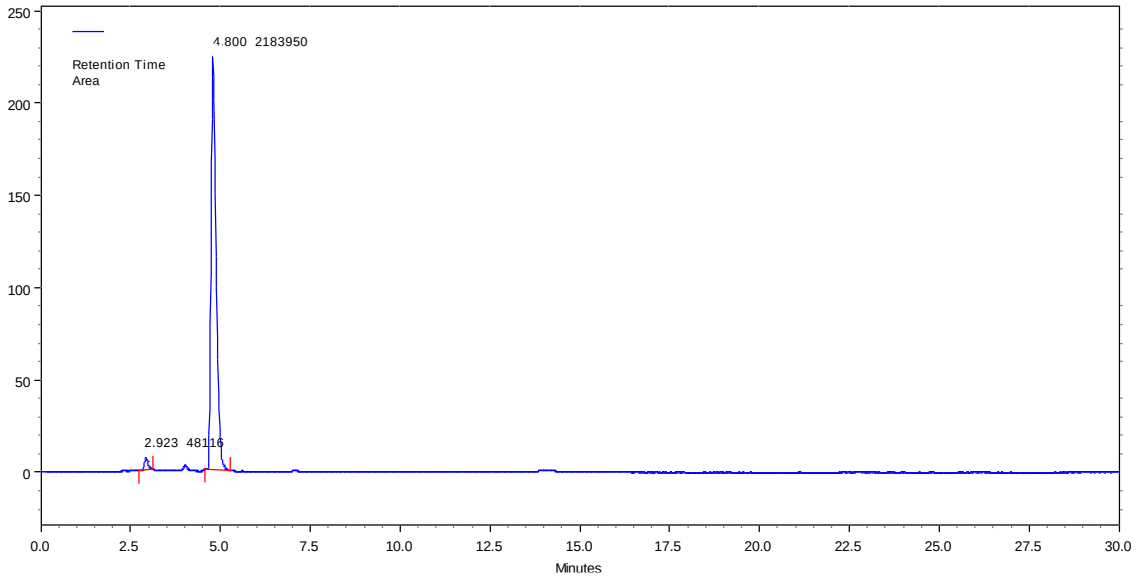

Figure 102 – HPLC chromatogram of **PH102**. Mobile phase: 0.1% aqueous TFA/ acetonitrile (50:50).

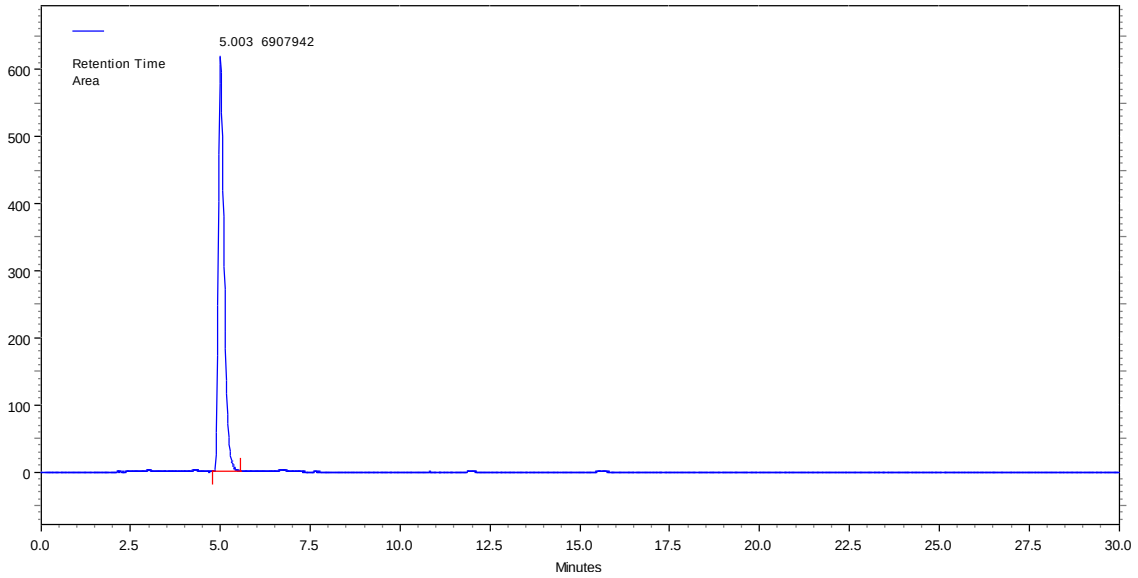

Figure 103 – HPLC chromatogram of **PH103**. Mobile phase: 0.1% aqueous TFA/ acetonitrile (50:50).

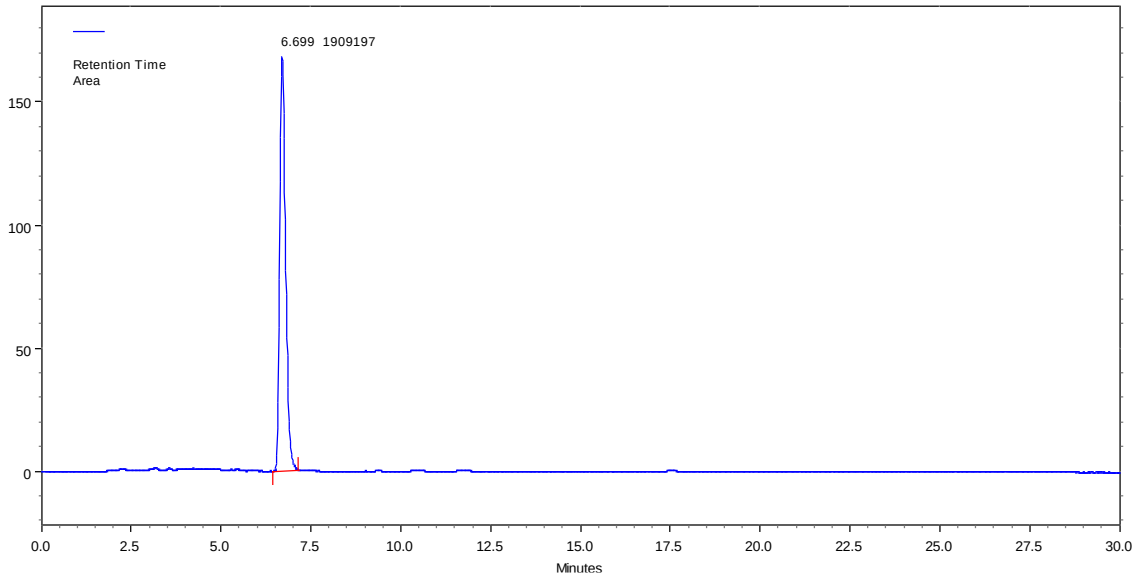

Figure 104 – HPLC chromatogram of **PH104**. Mobile phase: 0.1% aqueous TFA/ acetonitrile (50:50).

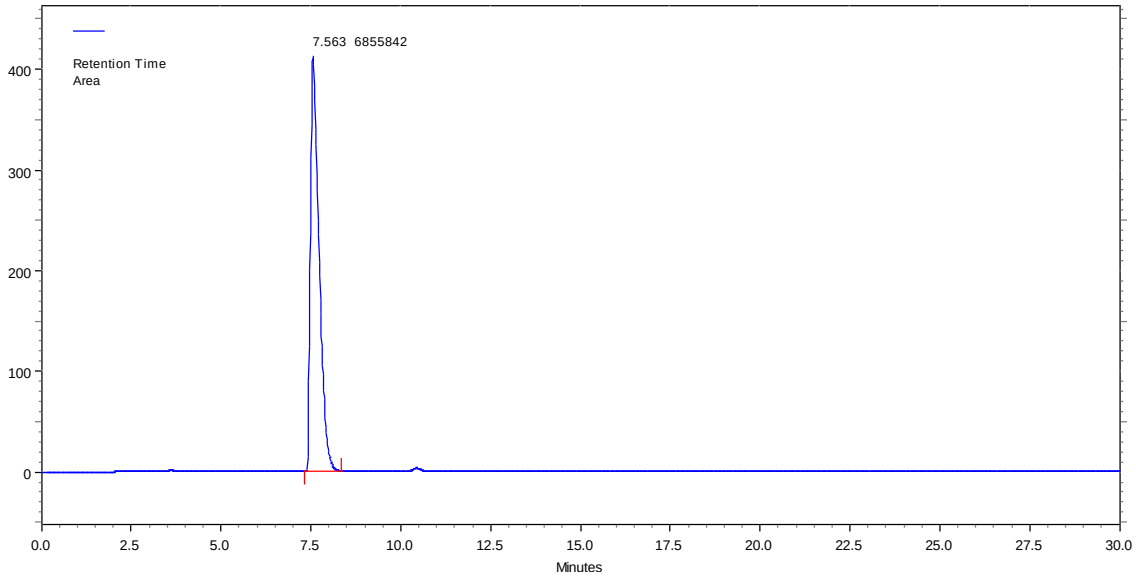

Figure 105 – HPLC chromatogram of **PH106**. Mobile phase: 0.1% aqueous TFA/ acetonitrile (50:50).

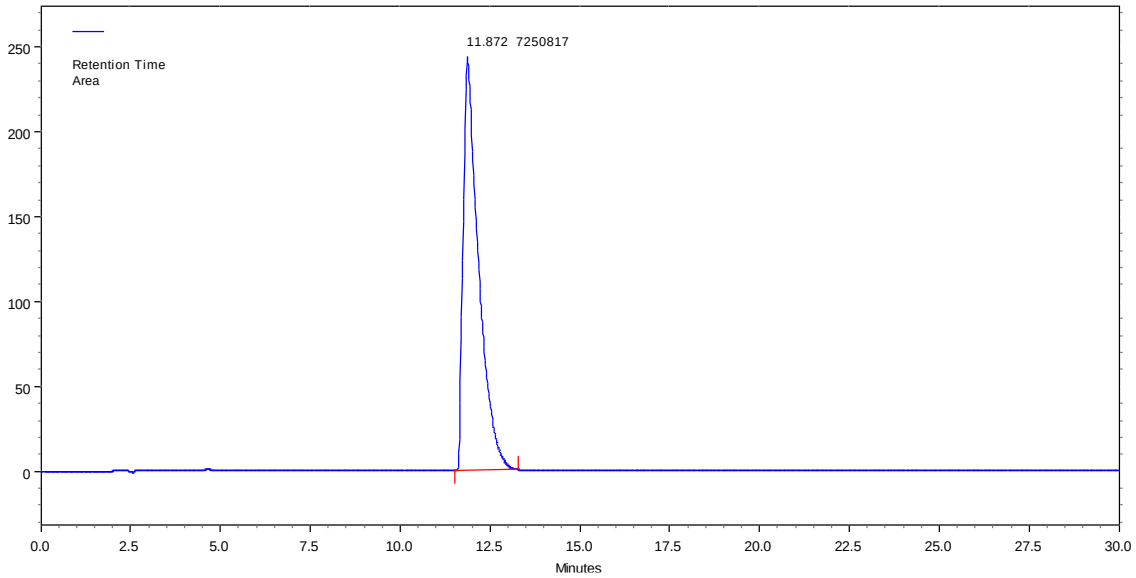

Figure 106 – HPLC chromatogram of **PH107**. Mobile phase: 0.1% aqueous TFA/ acetonitrile (50:50).

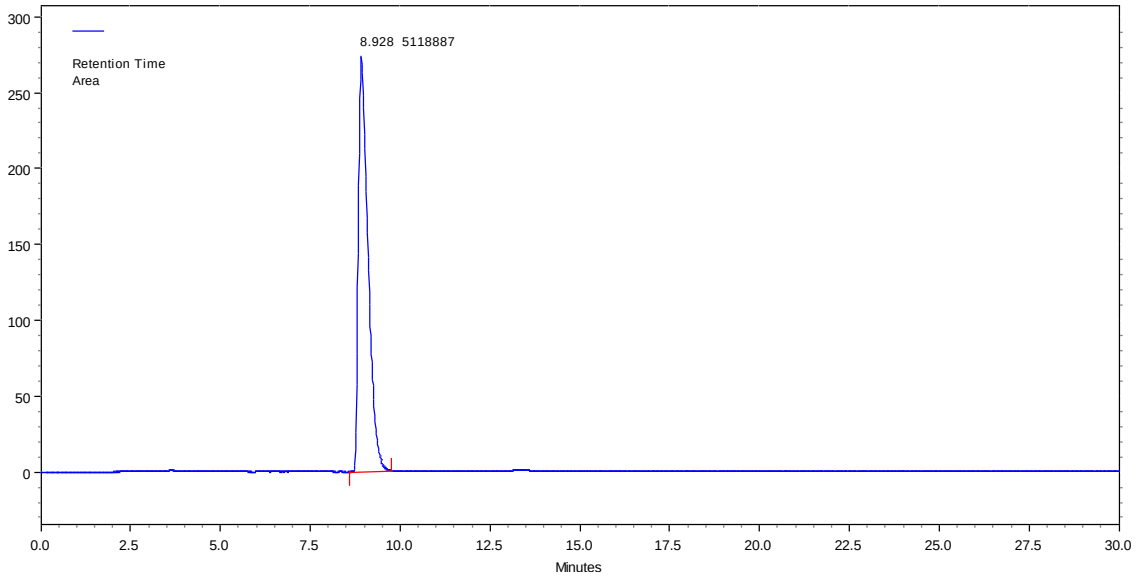

Figure 107 – HPLC chromatogram of **PH108**. Mobile phase: 0.1% aqueous TFA/ acetonitrile (50:50).

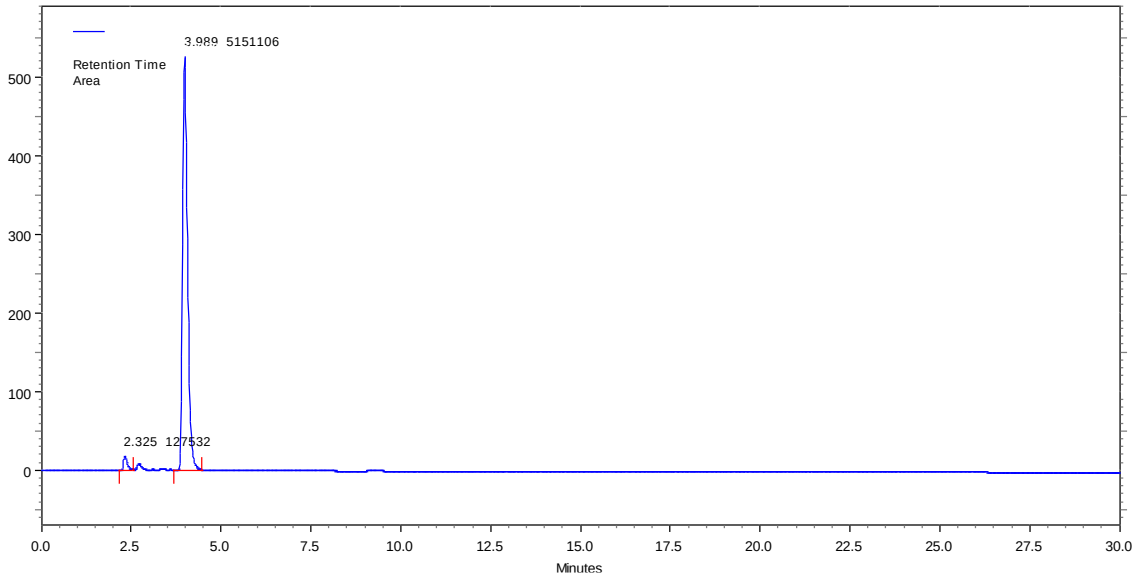

Figure 108 – HPLC chromatogram of **PH109**. Mobile phase: 0.1% aqueous TFA/ acetonitrile (50:50).

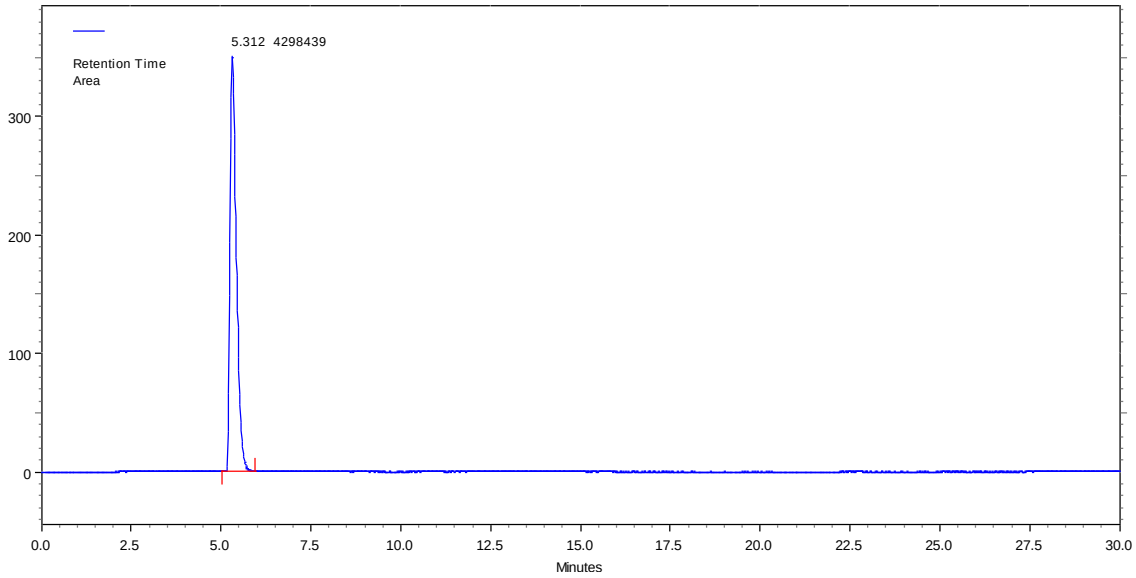

Figure 109 – HPLC chromatogram of **PH110**. Mobile phase: 0.1% aqueous TFA/ acetonitrile (50:50).

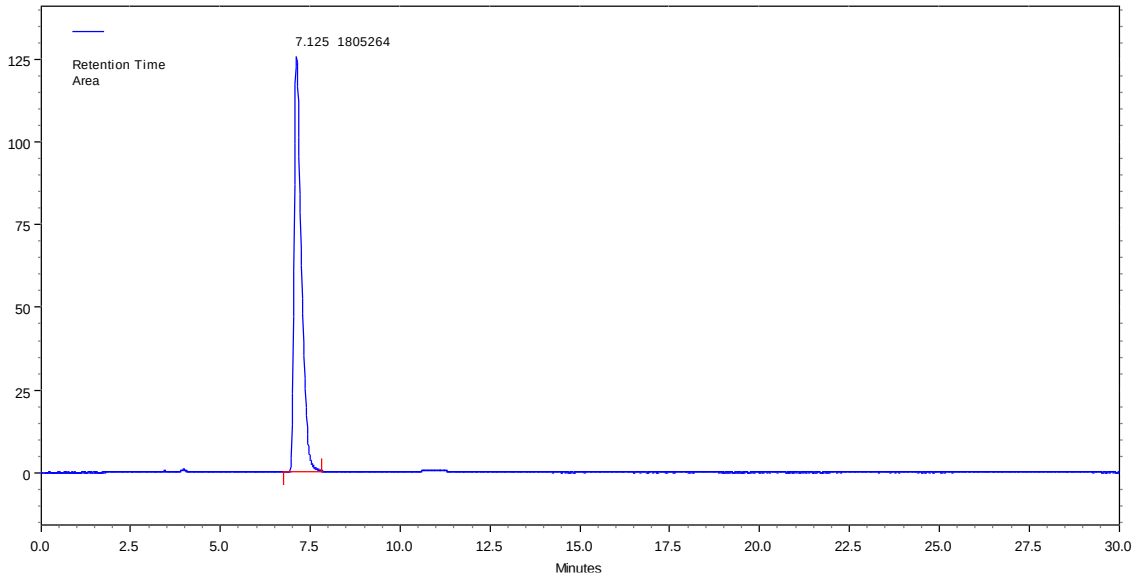

Figure 110 – HPLC chromatogram of **PH112**. Mobile phase: 0.1% aqueous TFA/ acetonitrile (50:50).

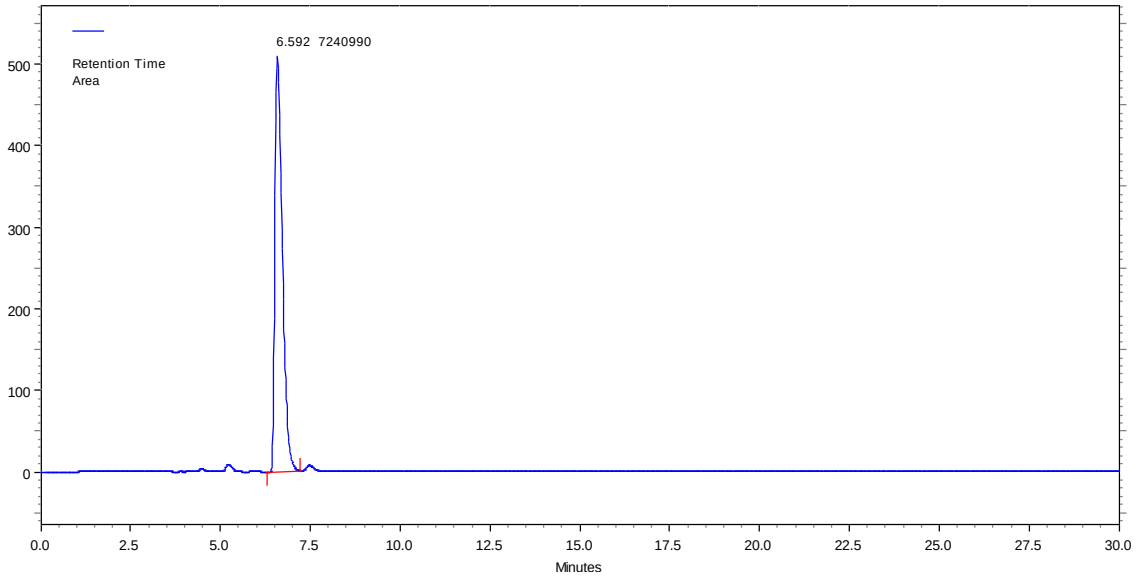

Figure 111 – HPLC chromatogram of **PH111**. Mobile phase: 0.1% aqueous TFA/ acetonitrile (50:50).

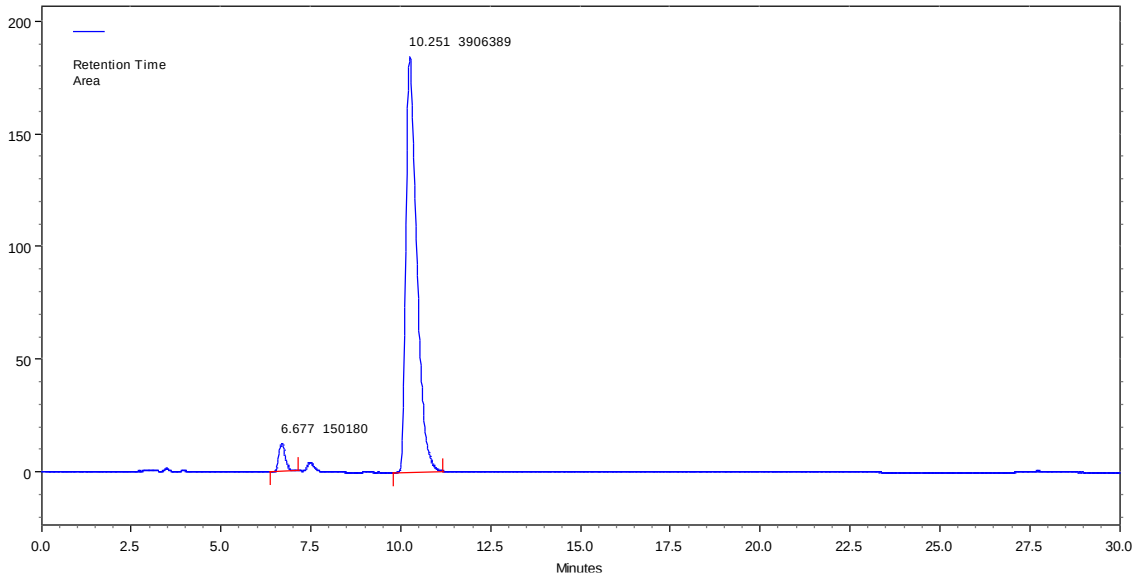

Figure 112 – HPLC chromatogram of **PH113**. Mobile phase: 0.1% aqueous TFA/ acetonitrile (50:50).

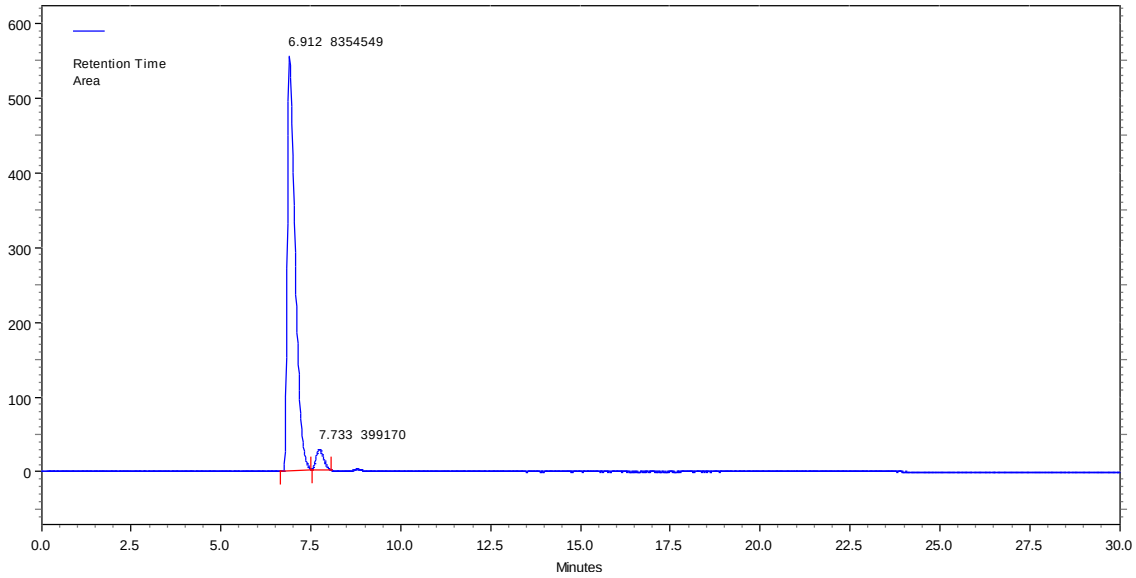

Figure 113 – HPLC chromatogram of **PH114**. Mobile phase: 0.1% aqueous TFA/ acetonitrile (50:50).

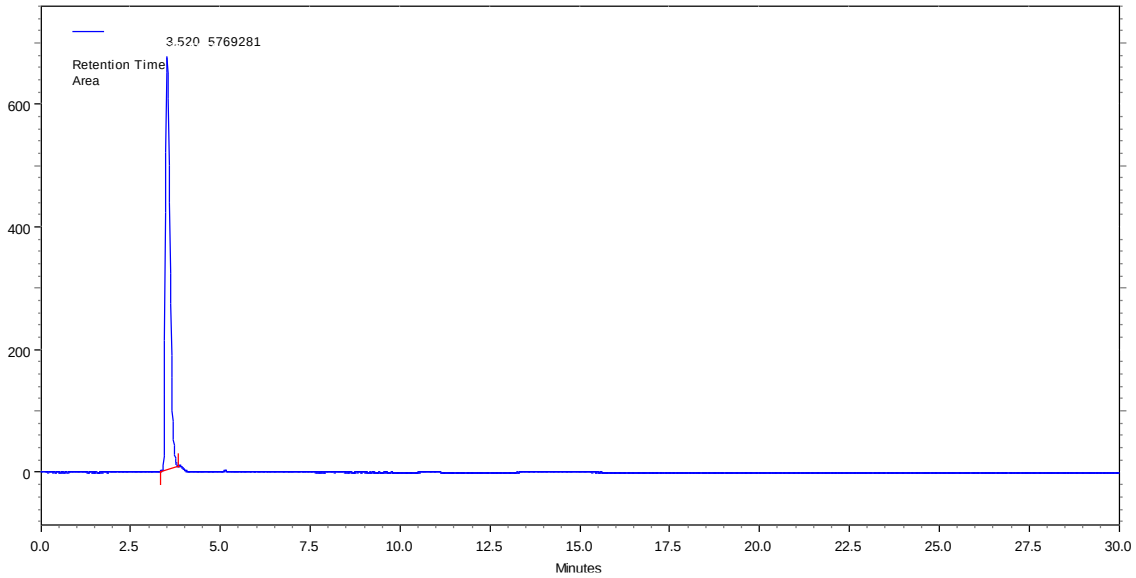

Figure 114 – HPLC chromatogram of **PH115**. Mobile phase: 0.1% aqueous TFA/ acetonitrile (50:50).

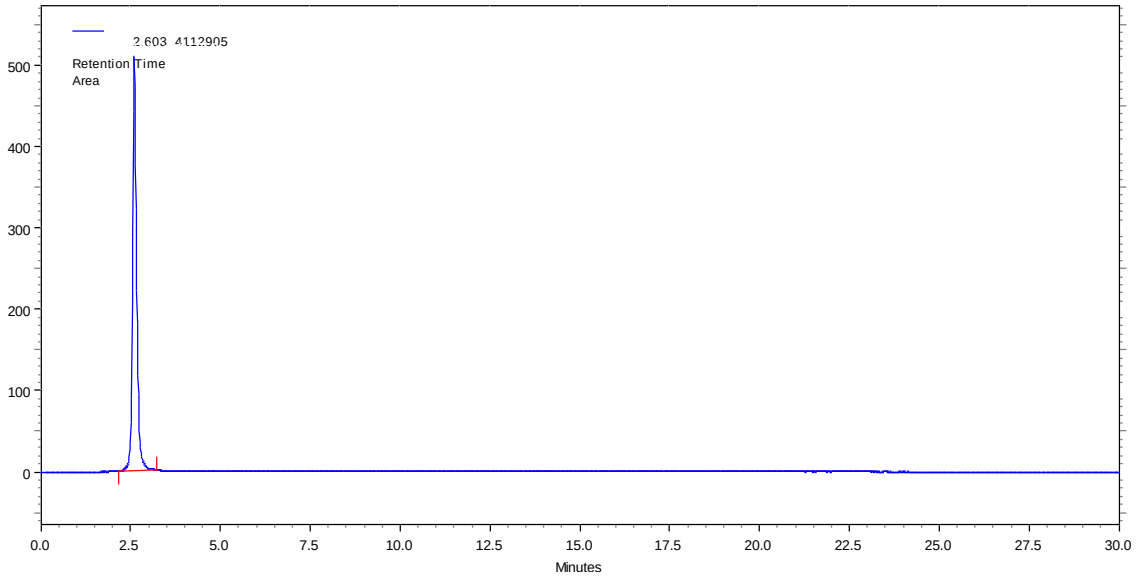

Figure 115 – HPLC chromatogram of **PH116**. Mobile phase: 0.1% aqueous TFA/ acetonitrile (50:50).

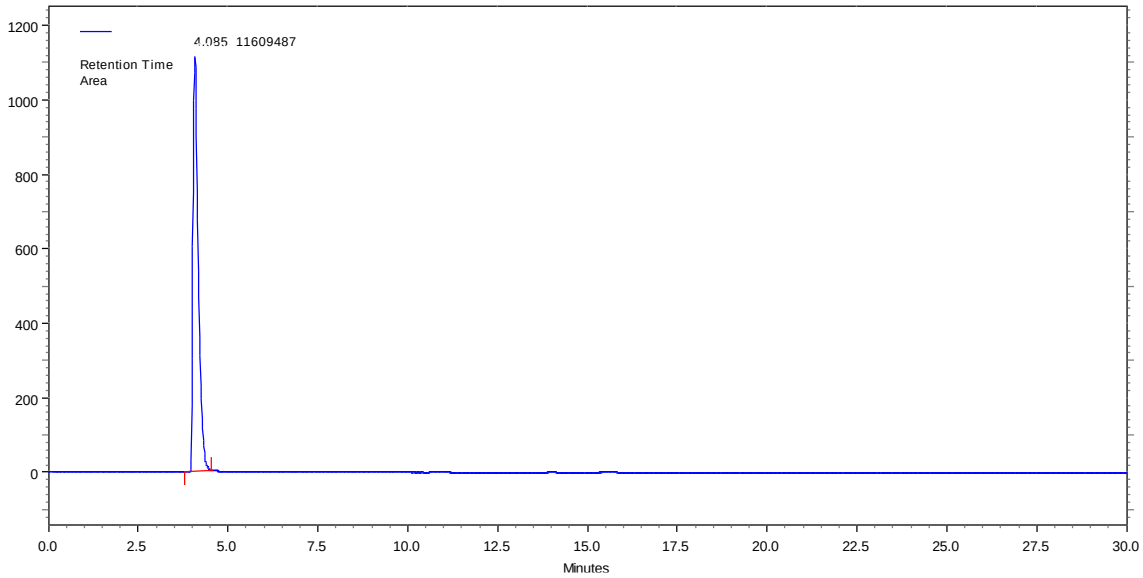

Figure 116 – HPLC chromatogram of **PH118**. Mobile phase: 0.1% aqueous TFA/ acetonitrile (50:50).

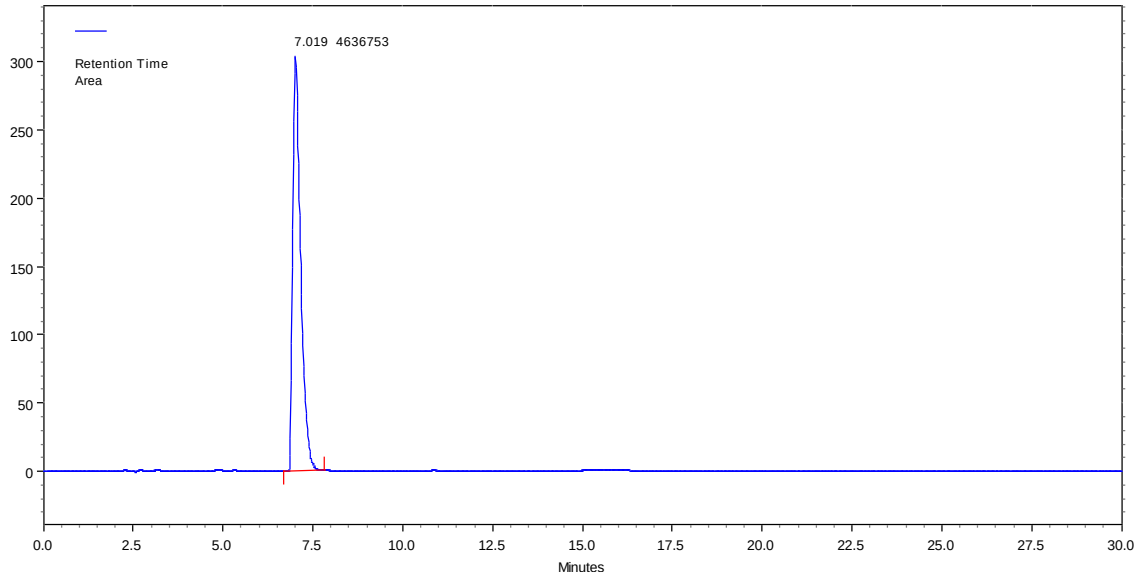

Figure 117 – HPLC chromatogram of **PH117**. Mobile phase: 0.1% aqueous TFA/ acetonitrile (50:50).

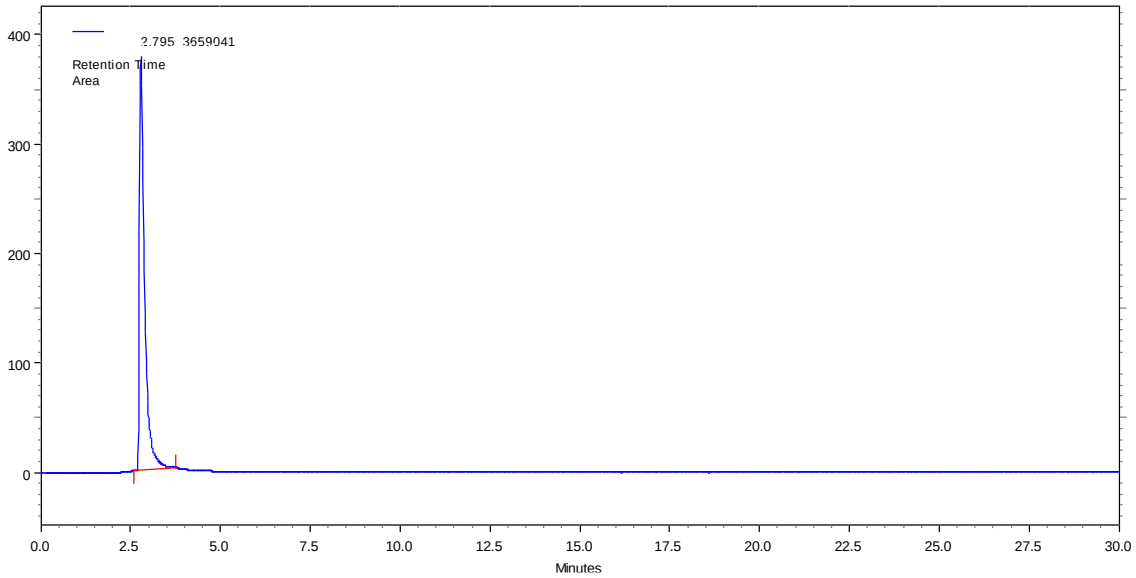

Figure 118 – HPLC chromatogram of **PH119**. Mobile phase: 0.1% aqueous TFA/ acetonitrile (65:35).

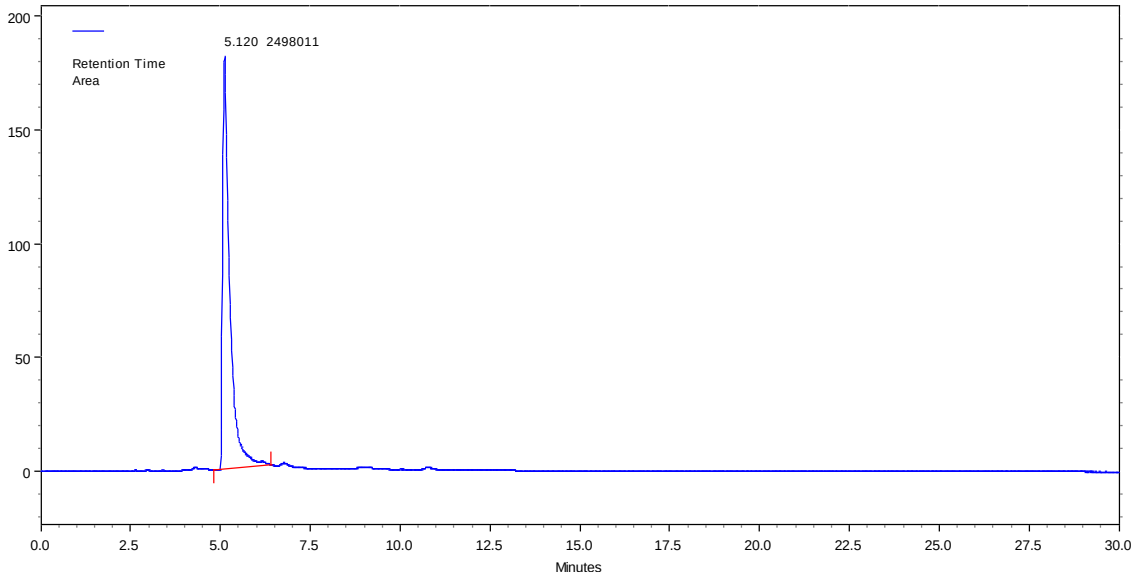

Figure 119 – HPLC chromatogram of **PH120**. Mobile phase: 0.1% aqueous TFA/ acetonitrile (65:35).

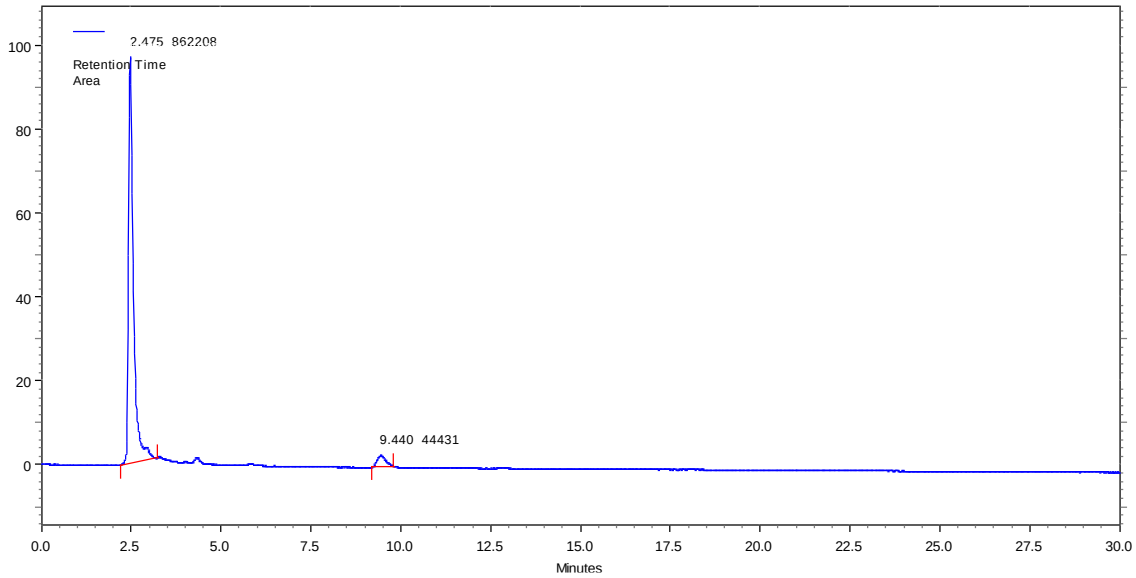

Figure 120 – HPLC chromatogram of **PH121**. Mobile phase: 0.1% aqueous TFA/ acetonitrile (65:35).

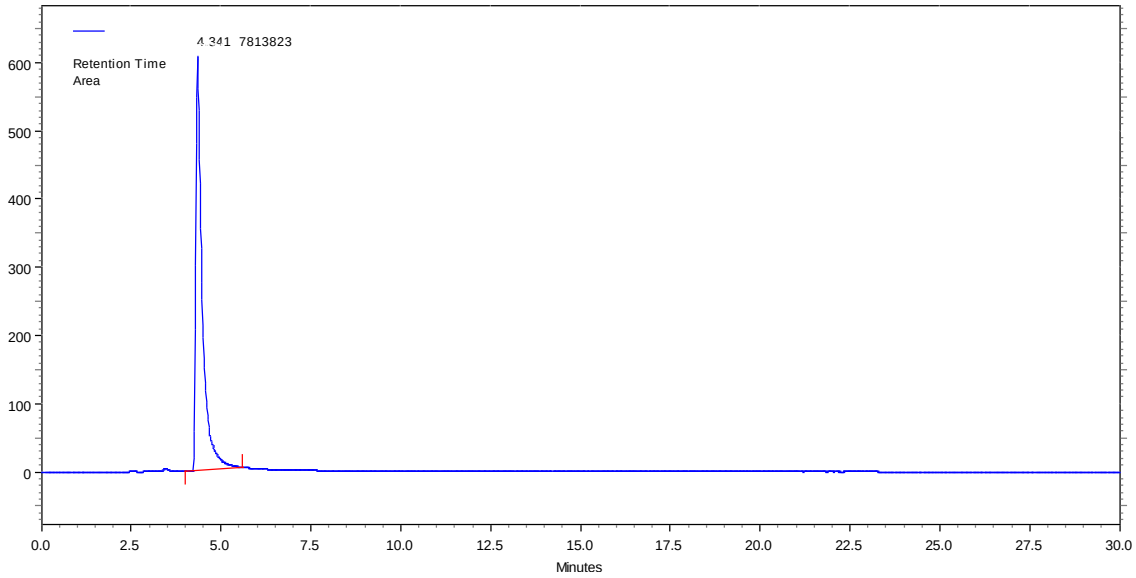

Figure 121 – HPLC chromatogram of **PH122**. Mobile phase: 0.1% aqueous TFA/ acetonitrile (65:35).

5 Discussão Geral

O texto completo desta seção, que na tese defendida ocupa o intervalo de páginas 177-200, foi suprimido por tratar-se de informações para publicação em periódico científico. Consta da discussão dos resultados obtidos neste trabalho e de breve relação estrutura atividade dos compostos relatados.

6 Conclusões

O texto completo desta seção, que na tese defendida ocupa a página 201, foi suprimido por tratar-se de informações para publicação em periódico científico. Consta da conclusão deste trabalho, destacando os resultados mais relevantes.

Referências

(1) https://www.cdc.gov/parasites/chagas/gen_info/detailed.html. *CDC*.

(2) https://www.who.int/. *WHO*. https://www.who.int/.

(3) https://dndi.org/. *https://dndi.org/*. https://dndi.org/.

(4) Dias, L. C.; Dessoy, M. A.; Silva, J. J. N.; Thiemann, O. H.; Oliva, G.; Andricopulo, A. D. Quimioterapia Da Doença de Chagas: Estado Da Arte e Perspectivas No Desenvolvimento de Novos Fármacos. *Química Nova* **2009**, *32* (9), 2444–2457. https://doi.org/10.1590/S0100-40422009000900038.

(5) Doyle, P. S.; Zhou, Y. M.; Hsieh, I.; Greenbaum, D. C.; McKerrow, J. H.; Engel, J. C. The Trypanosoma Cruzi Protease Cruzain Mediates Immune Evasion. *PLoS Pathogens* **2011**, *7* (9), e1002139. https://doi.org/10.1371/journal.ppat.1002139.

(6) de Bona, E.; Lidani, K. C. F.; Bavia, L.; Omidian, Z.; Gremski, L. H.; Sandri, T. L.; Messias Reason, I. J. de. Autoimmunity in Chronic Chagas Disease: A Road of Multiple Pathways to Cardiomyopathy? *Frontiers in Immunology* **2018**, *9* (AUG). https://doi.org/10.3389/fimmu.2018.01842.

(7) Georg, I.; Hasslocher-Moreno, A. M.; Xavier, S. S.; Holanda, M. T. de; Roma, E. H.; Bonecini-Almeida, M. da G. Evolution of Anti-Trypanosoma Cruzi Antibody Production in Patients with Chronic Chagas Disease: Correlation between Antibody Titers and Development of Cardiac Disease Severity. *PLOS Neglected Tropical Diseases* **2017**, *11* (7), e0005796. https://doi.org/10.1371/journal.pntd.0005796.

(8) Cox, F. E. G. History of Sleeping Sickness (African Trypanosomiasis). *Infectious Disease Clinics of North America* **2004**, *18* (2), 231–245. https://doi.org/10.1016/j.idc.2004.01.004.

(9) Ferreira, L. G.; Andricopulo, A. D. Targeting Cysteine Proteases in Trypanosomatid Disease Drug Discovery. *Pharmacology & Therapeutics* **2017**, *180*, 49–61. https://doi.org/10.1016/j.pharmthera.2017.06.004.

(10) Organization, W. H. *Control and Surveillance of Human African Trypanosomiasis: Report of a WHO Expert Committee*; 2013.

(11) Docampo, R.; Moreno, S. N. J. Free Radical Metabolites in the Mode of Action of Chemotherapeutic Agents and Phagocytic Cells on Trypanosoma Cruzi.

Clinical Infectious Diseases **1984**, *6* (2), 223–238. https://doi.org/10.1093/clinids/6.2.223.

(12) Sueth-Santiago, V.; Decote-Ricardo, D.; Morrot, A.; Freire-de-Lima, C. G.; Lima, M. E. F. Challenges in the Chemotherapy of Chagas Disease: Looking for Possibilities Related to the Differences and Similarities between the Parasite and Host. *World Journal of Biological Chemistry* **2017**, *8* (1), 57. https://doi.org/10.4331/wjbc.v8.i1.57.

(13) Hall, B. S.; Wilkinson, S. R. Activation of Benznidazole by Trypanosomal Type I Nitroreductases Results in Glyoxal Formation. *Antimicrobial Agents and Chemotherapy* **2012**, *56* (1), 115–123. https://doi.org/10.1128/AAC.05135-11.

(14) Patterson, S.; Wyllie, S. Nitro Drugs for the Treatment of Trypanosomatid Diseases: Past, Present, and Future Prospects. *Trends in Parasitology* **2014**, *30* (6), 289–298. https://doi.org/10.1016/j.pt.2014.04.003.

(15) Urbina, J. A.; Docampo, R. Specific Chemotherapy of Chagas Disease: Controversies and Advances. *Trends in Parasitology* **2003**, *19* (11), 495–501. https://doi.org/10.1016/j.pt.2003.09.001.

(16) Bermudez, J.; Davies, C.; Simonazzi, A.; Pablo Real, J.; Palma, S. Current Drug Therapy and Pharmaceutical Challenges for Chagas Disease. *Acta Tropica* **2016**, *156*, 1–16. https://doi.org/10.1016/j.actatropica.2015.12.017.

(17) da Silva, E. B.; Oliveira e Silva, D. A.; Oliveira, A. R.; da Silva Mendes, C. H.; dos Santos, T. A. R.; da Silva, A. C.; de Castro, M. C. A.; Ferreira, R. S.; Moreira, D. R. M.; Cardoso, M. V. de O.; de Simone, C. A.; Pereira, V. R. A.; Leite, A. C. L. Desing and Synthesis of Potent Anti - Trypanosoma Cruzi Agents New Thiazoles Derivatives Which Induce Apoptotic Parasite Death. *European Journal of Medicinal Chemistry* **2017**, *130*, 39–50. https://doi.org/10.1016/j.ejmech.2017.02.026.

(18) Sajid, M.; Robertson, S. A.; Brinen, L. S.; McKerrow, J. H. Cruzain; 2011; pp 100–115. https://doi.org/10.1007/978-1-4419-8414-2_7.

(19) Coura, J. R.; Borges-Pereira, J. Chagas Disease: What Is Known and What Should Be Improved: A Systemic Review. *Rev Soc Bras Med Trop* **2012**, *45* (3), 286–296. https://doi.org/10.1590/S0037-86822012000300002.

(20) Mott, B. T.; Ferreira, R. S.; Simeonov, A.; Jadhav, A.; Ang, K. K.-H.; Leister, W.; Shen, M.; Silveira, J. T.; Doyle, P. S.; Arkin, M. R.; McKerrow, J. H.; Inglese, J.; Austin, C. P.; Thomas, C. J.; Shoichet, B. K.; Maloney, D. J. Identification and

Optimization of Inhibitors of Trypanosomal Cysteine Proteases: Cruzain, Rhodesain, and TbCatB. *Journal of Medicinal Chemistry* **2010**, *53* (1), 52–60. https://doi.org/10.1021/jm901069a.

(21) Hawking, F. Concentration of Bayer 205 (Germanin) in Human Blood and Cerebrospinal Fluid after Treatment. *Trans R Soc Trop Med Hyg* **1940**, *34* (1), 37–52. https://doi.org/10.1016/S0035-9203(40)90088-8.

(22) Delespaux, V.; de Koning, H. P. Drugs and Drug Resistance in African Trypanosomiasis. *Drug Resistance Updates* **2007**, *10* (1–2), 30–50. https://doi.org/10.1016/j.drup.2007.02.004.

(23) Capela; Moreira; Lopes. An Overview of Drug Resistance in Protozoal Diseases. *International Journal of Molecular Sciences* **2019**, *20* (22), 5748. https://doi.org/10.3390/ijms20225748.

(24) P. De Koning, H. The Drugs of Sleeping Sickness: Their Mechanisms of Action and Resistance, and a Brief History. *Tropical Medicine and Infectious Disease* **2020**, *5* (1), 14. https://doi.org/10.3390/tropicalmed5010014.

(25) Wilkinson, S. R.; Kelly, J. M. Trypanocidal Drugs: Mechanisms, Resistance and New Targets. *Expert Reviews in Molecular Medicine* **2009**, *11*, e31. https://doi.org/10.1017/S1462399409001252.

(26) Ettari, R.; Previti, S.; Tamborini, L.; Cullia, G.; Grasso, S.; Zappalà, M. The Inhibition of Cysteine Proteases Rhodesain and TbCatB: A Valuable Approach to Treat Human African Trypanosomiasis. *Mini-Reviews in Medicinal Chemistry* **2016**, *16* (17), 1374–1391. https://doi.org/10.2174/1389557515666160509125243.

(27) Blum, J.; Nkunku, S.; Burri, C. Clinical Description of Encephalopathic Syndromes and Risk Factors for Their Occurrence and Outcome during Melarsoprol Treatment of Human African Trypanosomiasis. *Tropical Medicine and International Health* **2001**, *6* (5), 390–400. https://doi.org/10.1046/j.1365-3156.2001.00710.x.

(28) Clayton, J. Chagas Disease: Pushing through the Pipeline. *Nature* **2010**, *465* (S7301), S12–S15. https://doi.org/10.1038/nature09224.

(29) Deeks, E. D. Fexinidazole: First Global Approval. *Drugs* **2019**, *79* (2), 215–220. https://doi.org/10.1007/s40265-019-1051-6.

(30) Lindner, A. K.; Lejon, V.; Chappuis, F.; Seixas, J.; Kazumba, L.; Barrett, M. P.; Mwamba, E.; Erphas, O.; Akl, E. A.; Villanueva, G.; Bergman, H.; Simarro, P.;

Kadima Ebeja, A.; Priotto, G.; Franco, J. R. New WHO Guidelines for Treatment of Gambiense Human African Trypanosomiasis Including Fexinidazole: Substantial Changes for Clinical Practice. *The Lancet Infectious Diseases* **2020**, *20* (2), e38–e46. https://doi.org/10.1016/S1473-3099(19)30612-7.

(31) Torreele, E.; Bourdin Trunz, B.; Tweats, D.; Kaiser, M.; Brun, R.; Mazué, G.; Bray, M. A.; Pécoul, B. Fexinidazole – A New Oral Nitroimidazole Drug Candidate Entering Clinical Development for the Treatment of Sleeping Sickness. *PLoS Neglected Tropical Diseases* **2010**, *4* (12), e923. https://doi.org/10.1371/journal.pntd.0000923.

(32) McGrath, M. E.; Eakin, A. E.; Engel, J. C.; McKerrow, J. H.; Craik, C. S.; Fletterick, R. J. The Crystal Structure of Cruzain: A Therapeutic Target for Chagas' Disease. *Journal of Molecular Biology* **1995**, *247* (2), 251–259. https://doi.org/10.1006/jmbi.1994.0137.

(33) Martinez-Mayorga, K.; Byler, K. G.; Ramirez-Hernandez, A. I.; Terrazas-Alvares, D. E. Cruzain Inhibitors: Efforts Made, Current Leads and a Structural Outlook of New Hits. *Drug Discovery Today* **2015**, *20* (7), 890–898. https://doi.org/10.1016/j.drudis.2015.02.004.

(34) Cazzulo, J.; Stoka, V.; Turk, V. The Major Cysteine Proteinase of Trypanosoma Cruzi: A Valid Target for Chemotherapy of Chagas Disease. *Current Pharmaceutical Design* **2001**, *7* (12), 1143–1156. https://doi.org/10.2174/1381612013397528.

(35) Siqueira-Neto, J. L.; Debnath, A.; McCall, L.-I.; Bernatchez, J. A.; Ndao, M.; Reed, S. L.; Rosenthal, P. J. Cysteine Proteases in Protozoan Parasites. *PLOS Neglected Tropical Diseases* **2018**, *12* (8), e0006512. https://doi.org/10.1371/journal.pntd.0006512.

(36) Steverding, D.; Caffrey, C. R. Should the Enzyme Name 'Rhodesain' Be Discontinued? *Molecular and Biochemical Parasitology* **2021**, *245*, 111395. https://doi.org/10.1016/j.molbiopara.2021.111395.

(37) Santos, C. C.; Coombs, G. H.; Lima, A. P. C. A.; Mottram, J. C. Role of the Trypanosoma Brucei Natural Cysteine Peptidase Inhibitor ICP in Differentiation and Virulence. *Molecular Microbiology* **2007**, *66* (4), 991–1002. https://doi.org/10.1111/j.1365-2958.2007.05970.x.

(38) da Silva, E. B.; do Nascimento Pereira, G. A.; Ferreira, R. S. Trypanosomal Cysteine Peptidases: Target Validation and Drug Design Strategies. In

Comprehensive Analysis of Parasite Biology: From Metabolism to Drug Discovery; Wiley-VCH Verlag GmbH & Co. KGaA: Weinheim, Germany, 2016; pp 121–145. https://doi.org/10.1002/9783527694082.ch5.

(39) Kerr, I. D.; Lee, J. H.; Farady, C. J.; Marion, R.; Rickert, M.; Sajid, M.; Pandey, K. C.; Caffrey, C. R.; Legac, J.; Hansell, E.; McKerrow, J. H.; Craik, C. S.; Rosenthal, P. J.; Brinen, L. S. Vinyl Sulfones as Antiparasitic Agents and a Structural Basis for Drug Design. *Journal of Biological Chemistry* **2009**, *284* (38), 25697–25703. https://doi.org/10.1074/jbc.M109.014340.

(40) Palmer, J. T.; Rasnick, D.; Klaus, J. L.; Bromme, D. Vinyl Sulfones as Mechanism-Based Cysteine Protease Inhibitors. *Journal of Medicinal Chemistry* **1995**, *38* (17), 3193–3196. https://doi.org/10.1021/jm00017a002.

(41) Santos, M.; Moreira, R. Michael Acceptors as Cysteine Protease Inhibitors. *Mini-Reviews in Medicinal Chemistry* **2007**, *7* (10), 1040–1050. https://doi.org/10.2174/138955707782110105.

(42) Engel, J. C.; Doyle, P. S.; Palmer, J. T.; Hsieh, I.; Bainton, D. F.; McKerrow, J. H. Cysteine Protease Inhibitors Alter Golgi Complex Ultrastructure and Function in Trypanosoma Cruzi. *Journal of Cell Science* **1998**, *111*, 597–606.

(43) Engel, J. C.; Doyle, P. S.; Hsieh, I.; McKerrow, J. H. Cysteine Protease Inhibitors Cure an Experimental Trypanosoma Cruzi Infection. *Journal of Experimental Medicine* **1998**, *188* (4), 725–734. https://doi.org/10.1084/jem.188.4.725.

(44) Kerr, I. D.; Wu, P.; Marion-Tsukamaki, R.; Mackey, Z. B.; Brinen, L. S. Crystal Structures of TbCatB and Rhodesain, Potential Chemotherapeutic Targets and Major Cysteine Proteases of Trypanosoma Brucei. *PLoS Neglected Tropical Diseases* **2010**, *4* (6), e701. https://doi.org/10.1371/journal.pntd.0000701.

(45) Roush, W. R.; Cheng, J.; Knapp-Reed, B.; Alvarez-Hernandez, A.; McKerrow, J. H.; Hansell, E.; Engel, J. C. Potent Second Generation Vinyl Sulfonamide Inhibitors of the Trypanosomal Cysteine Protease Cruzain. *Bioorganic & Medicinal Chemistry Letters* **2001**, *11* (20), 2759–2762. https://doi.org/10.1016/S0960-894X(01)00566-2.

(46) Jacobsen, W.; Christians, U.; Benet, L. Z. In Vitro Evaluation of the Disposition of A Novel Cysteine Protease Inhibitor. *Drug Metabolism and Disposition* **2000**, *28* (11), 1343 LP – 1351.

(47) Doyle, P. S.; Zhou, Y. M.; Engel, J. C.; McKerrow, J. H. A Cysteine Protease Inhibitor Cures Chagas' Disease in an Immunodeficient-Mouse Model of

Infection. *Antimicrobial Agents and Chemotherapy* **2007**, *51* (11), 3932–3939. https://doi.org/10.1128/AAC.00436-07.

(48) Barr, S. C.; Warner, K. L.; Kornreic, B. G.; Piscitelli, J.; Wolfe, A.; Benet, L.; McKerrow, J. H. A Cysteine Protease Inhibitor Protects Dogs from Cardiac Damage during Infection by Trypanosoma Cruzi. *Antimicrobial Agents and Chemotherapy* **2005**, *49* (12), 5160–5161. https://doi.org/10.1128/AAC.49.12.5160-5161.2005.

(49) Jaishankar, P.; Hansell, E.; Zhao, D.-M.; Doyle, P. S.; McKerrow, J. H.; Renslo, A. R. Potency and Selectivity of P2/P3-Modified Inhibitors of Cysteine Proteases from Trypanosomes. *Bioorganic & Medicinal Chemistry Letters* **2008**, *18* (2), 624–628. https://doi.org/10.1016/j.bmcl.2007.11.070.

(50) Bryant, C.; Kerr, I. D.; Debnath, M.; Ang, K. K. H.; Ratnam, J.; Ferreira, R. S.; Jaishankar, P.; Zhao, D.; Arkin, M. R.; McKerrow, J. H.; Brinen, L. S.; Renslo, A. R. Novel Non-Peptidic Vinylsulfones Targeting the S2 and S3 Subsites of Parasite Cysteine Proteases. *Bioorganic & Medicinal Chemistry Letters* **2009**, *19* (21), 6218–6221. https://doi.org/10.1016/j.bmcl.2009.08.098.

(51) Chen, Y. T.; Brinen, L. S.; Kerr, I. D.; Hansell, E.; Doyle, P. S.; McKerrow, J. H.; Roush, W. R. In Vitro and In Vivo Studies of the Trypanocidal Properties of WRR-483 against Trypanosoma Cruzi. *PLoS Neglected Tropical Diseases* **2010**, *4* (9), e825. https://doi.org/10.1371/journal.pntd.0000825.

(52) Dunny, E.; Doherty, W.; Evans, P.; Malthouse, J. P. G.; Nolan, D.; Knox, A. J. S. Vinyl Sulfone-Based Peptidomimetics as Anti-Trypanosomal Agents: Design, Synthesis, Biological and Computational Evaluation. *Journal of Medicinal Chemistry* **2013**, *56* (17), 6638–6650. https://doi.org/10.1021/jm400294w.

(53) Doherty, W.; James, J.; Evans, P.; Martin, L.; Adler, N.; Nolan, D.; Knox, A. Preparation, Anti-Trypanosomal Activity and Localisation of a Series of Dipeptide-Based Vinyl Sulfones. *Org. Biomol. Chem.* **2014**, *12* (38), 7561–7571. https://doi.org/10.1039/C4OB01412J.

(54) Royo, S.; Rodríguez, S.; Schirmeister, T.; Kesselring, J.; Kaiser, M.; González, F. V. Dipeptidyl Enoates As Potent Rhodesain Inhibitors That Display a Dual Mode of Action. *ChemMedChem* **2015**, *10* (9), 1484–1487. https://doi.org/10.1002/cmdc.201500204.

(55) Jones, B. D.; Tochowicz, A.; Tang, Y.; Cameron, M. D.; McCall, L.-I.; Hirata, K.; Siqueira-Neto, J. L.; Reed, S. L.; McKerrow, J. H.; Roush, W. R. Synthesis and

Evaluation of Oxyguanidine Analogues of the Cysteine Protease Inhibitor WRR-483 against Cruzain. *ACS Medicinal Chemistry Letters* **2016**, *7* (1), 77–82. https://doi.org/10.1021/acsmedchemlett.5b00336.

(56) Latorre, A.; Schirmeister, T.; Kesselring, J.; Jung, S.; Johé, P.; Hellmich, U. A.; Heilos, A.; Engels, B.; Krauth-Siegel, R. L.; Dirdjaja, N.; Bou-Iserte, L.; Rodríguez, S.; González, F. V. Dipeptidyl Nitroalkenes as Potent Reversible Inhibitors of Cysteine Proteases Rhodesain and Cruzain. *ACS Medicinal Chemistry Letters* **2016**, *7* (12), 1073–1076. https://doi.org/10.1021/acsmedchemlett.6b00276.

(57) Chenna, B. C.; Li, L.; Mellott, D. M.; Zhai, X.; Siqueira-Neto, J. L.; Calvet Alvarez, C.; Bernatchez, J. A.; Desormeaux, E.; Alvarez Hernandez, E.; Gomez, J.; McKerrow, J. H.; Cruz-Reyes, J.; Meek, T. D. Peptidomimetic Vinyl Heterocyclic Inhibitors of Cruzain Effect Antitrypanosomal Activity. *Journal of Medicinal Chemistry* **2020**, *63* (6), 3298–3316. https://doi.org/10.1021/acs.jmedchem.9b02078.

(58) Fonseca, N. C.; da Cruz, L. F.; da Silva Villela, F.; do Nascimento Pereira, G. A.; de Siqueira-Neto, J. L.; Kellar, D.; Suzuki, B. M.; Ray, D.; de Souza, T. B.; Alves, R. J.; Júnior, P. A. S.; Romanha, A. J.; Murta, S. M. F.; McKerrow, J. H.; Caffrey, C. R.; de Oliveira, R. B.; Ferreira, R. S. Synthesis of a Sugar-Based Thiosemicarbazone Series and Structure-Activity Relationship versus the Parasite Cysteine Proteases Rhodesain, Cruzain, and Schistosoma Mansoni Cathepsin B1. *Antimicrobial Agents and Chemotherapy* **2015**, *59* (5), 2666–2677. https://doi.org/10.1128/AAC.04601-14.

(59) Espíndola, J. W. P.; Cardoso, M. V. de O.; Filho, G. B. de O.; Oliveira e Silva, D. A.; Moreira, D. R. M.; Bastos, T. M.; Simone, C. A. de; Soares, M. B. P.; Villela, F. S.; Ferreira, R. S.; Castro, M. C. A. B. de; Pereira, V. R. A.; Murta, S. M. F.; Sales Junior, P. A.; Romanha, A. J.; Leite, A. C. L. Synthesis and Structure–Activity Relationship Study of a New Series of Antiparasitic Aryloxyl Thiosemicarbazones Inhibiting Trypanosoma Cruzi Cruzain. *European Journal of Medicinal Chemistry* **2015**, *101*, 818–835. https://doi.org/10.1016/j.ejmech.2015.06.048.

(60) Caputto, M. E.; Fabian, L. E.; Benítez, D.; Merlino, A.; Ríos, N.; Cerecetto, H.; Moltrasio, G. Y.; Moglioni, A. G.; González, M.; Finkielsztein, L. M. Thiosemicarbazones Derived from 1-Indanones as New Anti-Trypanosoma

Cruzi Agents. *Bioorganic & Medicinal Chemistry* **2011**, *19* (22), 6818–6826. https://doi.org/10.1016/j.bmc.2011.09.037.

(61) Rocha, D. A.; Silva, E. B.; Fortes, I. S.; Lopes, M. S.; Ferreira, R. S.; Andrade, S. F. Synthesis and Structure-Activity Relationship Studies of Cruzain and Rhodesain Inhibitors. *European Journal of Medicinal Chemistry* **2018**, *157*, 1426–1459. https://doi.org/10.1016/j.ejmech.2018.08.079.

(62) de Moraes Gomes, P. A. T.; de Oliveira Barbosa, M.; Farias Santiago, E.; de Oliveira Cardoso, M. V.; Capistrano Costa, N. T.; Hernandes, M. Z.; Moreira, D. R. M.; da Silva, A. C.; dos Santos, T. A. R.; Pereira, V. R. A.; Brayner dos Santosd, F. A.; do Nascimento Pereira, G. A.; Ferreira, R. S.; Leite, A. C. L. New 1,3-Thiazole Derivatives and Their Biological and Ultrastructural Effects on Trypanosoma Cruzi. *European Journal of Medicinal Chemistry* **2016**, *121*, 387–398. https://doi.org/10.1016/j.ejmech.2016.05.050.

(63) de Oliveira Filho, G. B.; Cardoso, M. V. de O.; Espíndola, J. W. P.; Oliveira e Silva, D. A.; Ferreira, R. S.; Coelho, P. L.; Anjos, P. S. dos; Santos, E. de S.; Meira, C. S.; Moreira, D. R. M.; Soares, M. B. P.; Leite, A. C. L. Structural Design, Synthesis and Pharmacological Evaluation of Thiazoles against Trypanosoma Cruzi. *European Journal of Medicinal Chemistry* **2017**, *141*, 346–361. https://doi.org/10.1016/j.ejmech.2017.09.047.

(64) Silva-Júnior, E. F.; Silva, E. P. S.; França, P. H. B.; Silva, J. P. N.; Barreto, E. O.; Silva, E. B.; Ferreira, R. S.; Gatto, C. C.; Moreira, D. R. M.; Siqueira-Neto, J. L.; Mendonça-Júnior, F. J. B.; Lima, M. C. A.; Bortoluzzi, J. H.; Scotti, M. T.; Scotti, L.; Meneghetti, M. R.; Aquino, T. M.; Araújo-Júnior, J. X. Design, Synthesis, Molecular Docking and Biological Evaluation of Thiophen-2-Iminothiazolidine Derivatives for Use against Trypanosoma Cruzi. *Bioorganic & Medicinal Chemistry* **2016**, *24* (18), 4228–4240. https://doi.org/10.1016/j.bmc.2016.07.013.

(65) Avelar, L. A. A.; Camilo, C. D.; de Albuquerque, S.; Fernandes, W. B.; Gonçalez, C.; Kenny, P. W.; Leitão, A.; McKerrow, J. H.; Montanari, C. A.; Orozco, E. V. M.; Ribeiro, J. F. R.; Rocha, J. R.; Rosini, F.; Saidel, M. E. Molecular Design, Synthesis and Trypanocidal Activity of Dipeptidyl Nitriles as Cruzain Inhibitors. *PLOS Neglected Tropical Diseases* **2015**, *9* (7), e0003916. https://doi.org/10.1371/journal.pntd.0003916.

(66) Löser, R.; Schilling, K.; Dimmig, E.; Gütschow, M. Interaction of Papain-like Cysteine Proteases with Dipeptide-Derived Nitriles †. *Journal of Medicinal Chemistry* **2005**, *48* (24), 7688–7707. https://doi.org/10.1021/jm050686b.

(67) Giroud, M.; Kuhn, B.; Saint-Auret, S.; Kuratli, C.; Martin, R. E.; Schuler, F.; Diederich, F.; Kaiser, M.; Brun, R.; Schirmeister, T.; Haap, W. 2 H -1,2,3-Triazole-Based Dipeptidyl Nitriles: Potent, Selective, and Trypanocidal Rhodesain Inhibitors by Structure-Based Design. *Journal of Medicinal Chemistry* **2018**, *61* (8), 3370–3388. https://doi.org/10.1021/acs.jmedchem.7b01870.

(68) Silva, J. R. A.; Cianni, L.; Araujo, D.; Batista, P. H. J.; de Vita, D.; Rosini, F.; Leitão, A.; Lameira, J.; Montanari, C. A. Assessment of the Cruzain Cysteine Protease Reversible and Irreversible Covalent Inhibition Mechanism. *Journal of Chemical Information and Modeling* **2020**, *60* (3), 1666–1677. https://doi.org/10.1021/acs.jcim.9b01138.

(69) Burtoloso, A. C. B.; de Albuquerque, S.; Furber, M.; Gomes, J. C.; Gonçalez, C.; Kenny, P. W.; Leitão, A.; Montanari, C. A.; Quilles, J. C.; Ribeiro, J. F. R.; Rocha, J. R. Anti-Trypanosomal Activity of Non-Peptidic Nitrile-Based Cysteine Protease Inhibitors. *PLOS Neglected Tropical Diseases* **2017**, *11* (2), e0005343. https://doi.org/10.1371/journal.pntd.0005343.

(70) Ettari, R.; Tamborini, L.; Angelo, I. C.; Grasso, S.; Schirmeister, T.; Lo Presti, L.; De Micheli, C.; Pinto, A.; Conti, P. Development of Rhodesain Inhibitors with a 3-Bromoisoxazoline Warhead. *ChemMedChem* **2013**, *8* (12), 2070–2076. https://doi.org/10.1002/cmdc.201300390.

(71) Ettari, R.; Previti, S.; Cosconati, S.; Kesselring, J.; Schirmeister, T.; Grasso, S.; Zappalà, M. Synthesis and Biological Evaluation of Novel Peptidomimetics as Rhodesain Inhibitors. *Journal of Enzyme Inhibition and Medicinal Chemistry* **2016**, *31* (6), 1184–1191. https://doi.org/10.3109/14756366.2015.1108972.

(72) Ettari, R.; Pinto, A.; Previti, S.; Tamborini, L.; Angelo, I. C.; La Pietra, V.; Marinelli, L.; Novellino, E.; Schirmeister, T.; Zappalà, M.; Grasso, S.; De Micheli, C.; Conti, P. Development of Novel Dipeptide-like Rhodesain Inhibitors Containing the 3-Bromoisoxazoline Warhead in a Constrained Conformation. *Bioorganic & Medicinal Chemistry* **2015**, *23* (21), 7053–7060. https://doi.org/10.1016/j.bmc.2015.09.029.

(73) Pauli, I.; Ferreira, L. G.; de Souza, M. L.; Oliva, G.; Ferreira, R. S.; Dessoy, M. A.; Slafer, B. W.; Dias, L. C.; Andricopulo, A. D. Molecular Modeling and

Structure–Activity Relationships for a Series of Benzimidazole Derivatives as Cruzain Inhibitors. *Future Medicinal Chemistry* **2017**, *9* (7), 641–657. https://doi.org/10.4155/fmc-2016-0236.

(74) Braga, S. F. P.; Martins, L. C.; da Silva, E. B.; Sales Júnior, P. A.; Murta, S. M. F.; Romanha, A. J.; Soh, W. T.; Brandstetter, H.; Ferreira, R. S.; de Oliveira, R. B. Synthesis and Biological Evaluation of Potential Inhibitors of the Cysteine Proteases Cruzain and Rhodesain Designed by Molecular Simplification. *Bioorganic & Medicinal Chemistry* **2017**, *25* (6), 1889–1900. https://doi.org/10.1016/j.bmc.2017.02.009.

(75) de Souza, M. L.; de Oliveira Rezende Junior, C.; Ferreira, R. S.; Espinoza Chávez, R. M.; Ferreira, L. L. G.; Slafer, B. W.; Magalhães, L. G.; Krogh, R.; Oliva, G.; Cruz, F. C.; Dias, L. C.; Andricopulo, A. D. Discovery of Potent, Reversible, and Competitive Cruzain Inhibitors with Trypanocidal Activity: A Structure-Based Drug Design Approach. *Journal of Chemical Information and Modeling* **2020**, *60* (2), 1028–1041. https://doi.org/10.1021/acs.jcim.9b00802.

(76) Andrade, M. M. S.; Martins, L. C.; Marques, G. V. L.; Silva, C. A.; Faria, G.; Caldas, S.; dos Santos, J. S.; Leclercq, S. Y.; Maltarollo, V. G.; Ferreira, R. S.; Oliveira, R. B. Synthesis of Quinoline Derivatives as Potential Cysteine Protease Inhibitors. *Future Medicinal Chemistry* **2020**, *12* (7), fmc-2019-0201. https://doi.org/10.4155/fmc-2019-0201.

(77) Ferreira, R. S.; Simeonov, A.; Jadhav, A.; Eidam, O.; Mott, B. T.; Keiser, M. J.; McKerrow, J. H.; Maloney, D. J.; Irwin, J. J.; Shoichet, B. K. Complementarity Between a Docking and a High-Throughput Screen in Discovering New Cruzain Inhibitors. *Journal of Medicinal Chemistry* **2010**, *53* (13), 4891–4905. https://doi.org/10.1021/jm100488w.

(78) Pereira, G. A. N.; da Silva, E. B.; Braga, S. F. P.; Leite, P. G.; Martins, L. C.; Vieira, R. P.; Soh, W. T.; Villela, F. S.; Costa, F. M. R.; Ray, D.; de Andrade, S. F.; Brandstetter, H.; Oliveira, R. B.; Caffrey, C. R.; Machado, F. S.; Ferreira, R. S. Discovery and Characterization of Trypanocidal Cysteine Protease Inhibitors from the 'Malaria Box.' *European Journal of Medicinal Chemistry* **2019**, *179*, 765–778. https://doi.org/10.1016/j.ejmech.2019.06.062.

(79) Ismail, R. S. M.; Abou-Seri, S. M.; Eldehna, W. M.; Ismail, N. S. M.; Elgazwi, S. M.; Ghabbour, H. A.; Ahmed, M. S.; Halaweish, F. T.; Abou El Ella, D. A. Novel Series of 6-(2-Substitutedacetamido)-4-Anilinoquinazolines as EGFR-ERK

Signal Transduction Inhibitors in MCF-7 Breast Cancer Cells. *European Journal of Medicinal Chemistry* **2018**, *155*, 782–796. https://doi.org/10.1016/j.ejmech.2018.06.024.

(80) Gui, L.; Zhang, X.; Li, K.; Frankowski, K. J.; Li, S.; Wong, D. E.; Moen, D. R.; Porubsky, P. R.; Lin, H. J.; Schoenen, F. J.; Chou, T.-F. Evaluating P97 Inhibitor Analogues for Potency against P97-P37 and P97-Npl4-Ufd1 Complexes. *ChemMedChem* **2016**, *11* (9), 953–957. https://doi.org/10.1002/cmdc.201600036.

(81) Van Horn, K. S.; Zhu, X.; Pandharkar, T.; Yang, S.; Vesely, B.; Vanaerschot, M.; Dujardin, J.-C.; Rijal, S.; Kyle, D. E.; Wang, M. Z.; Werbovetz, K. A.; Manetsch, R. Antileishmanial Activity of a Series of N 2 , N 4 -Disubstituted Quinazoline-2,4-Diamines. *Journal of Medicinal Chemistry* **2014**, *57* (12), 5141–5156. https://doi.org/10.1021/jm5000408.

(82) Pobsuk, N.; Suphakun, P.; Hannongbua, S.; Nantasenamat, C.; Choowongkomon, K.; Gleeson, M. P. Synthesis, Plasmodium Falciparum Inhibitory Activity, Cytotoxicity and Solubility of N2 ,N4 -Disubstituted Quinazoline-2,4-Diamines. *Medicinal Chemistry* **2019**, *15* (6), 693–704. https://doi.org/10.2174/1573406415666181219100307.

(83) Guillon, J.; Cohen, A.; Boudot, C.; Valle, A.; Milano, V.; Das, R. N.; Guédin, A.; Moreau, S.; Ronga, L.; Savrimoutou, S.; Demourgues, M.; Reviriego, E.; Rubio, S.; Ferriez, S.; Agnamey, P.; Pauc, C.; Moukha, S.; Dozolme, P.; Nascimento, S. Da; Laumaillé, P.; Bouchut, A.; Azas, N.; Mergny, J.-L.; Mullié, C.; Sonnet, P.; Courtioux, B. Design, Synthesis, and Antiprotozoal Evaluation of New 2,4-Bis[(Substituted-Aminomethyl)Phenyl]Quinoline, 1,3-Bis[(Substituted-Aminomethyl)Phenyl]Isoquinoline and 2,4-Bis[(Substituted-Aminomethyl)Phenyl]Quinazoline Derivatives. *Journal of Enzyme Inhibition and Medicinal Chemistry* **2020**, *35* (1), 432–459. https://doi.org/10.1080/14756366.2019.1706502.

(84) Weber, J. I.; Rigo, G. V.; Rocha, D. A.; Fortes, I. S.; Seixas, A.; de Andrade, S. F.; Tasca, T. Modulation of Peptidases by 2,4-Diamine-Quinazoline Derivative Induces Cell Death in the Amitochondriate Parasite Trichomonas Vaginalis. *Biomedicine & Pharmacotherapy* **2021**, *139*, 111611. https://doi.org/10.1016/j.biopha.2021.111611.

(85) Reis, S. V. dos; Ribeiro, N. S.; Rocha, D. A.; Fortes, I. S.; Trentin, D. da S.; Andrade, S. F. de; Macedo, A. J. N 4 -benzyl-N 2 -phenylquinazoline-2,4-diamine Compound Presents Antibacterial and Antibiofilm Effect against Staphylococcus Aureus and Staphylococcus Epidermidis. *Chemical Biology & Drug Design* **2020**, *96* (6), 1372–1379. https://doi.org/10.1111/cbdd.13745.

(86) Fleeman, R.; Van Horn, K. S.; Barber, M. M.; Burda, W. N.; Flanigan, D. L.; Manetsch, R.; Shaw, L. N. Characterizing the Antimicrobial Activity of N 2 , N 4 -Disubstituted Quinazoline-2,4-Diamines toward Multidrug-Resistant Acinetobacter Baumannii. *Antimicrobial Agents and Chemotherapy* **2017**, *61* (6). https://doi.org/10.1128/AAC.00059-17.

(87) Wang, M.; Zhang, G.; Wang, Y.; Wang, J.; Zhu, M.; Cen, S.; Wang, Y. Design, Synthesis and Anti-Influenza A Virus Activity of Novel 2,4-Disubstituted Quinazoline Derivatives. *Bioorganic & Medicinal Chemistry Letters* **2020**, *30* (11), 127143. https://doi.org/10.1016/j.bmcl.2020.127143.

(88) Bianco, A.; Reghellin, V.; Donnici, L.; Fenu, S.; Alvarez, R.; Baruffa, C.; Peri, F.; Pagani, M.; Abrignani, S.; Neddermann, P.; De Francesco, R. Metabolism of Phosphatidylinositol 4-Kinase IIIα-Dependent PI4P Is Subverted by HCV and Is Targeted by a 4-Anilino Quinazoline with Antiviral Activity. *PLoS Pathogens* **2012**, *8* (3), e1002576. https://doi.org/10.1371/journal.ppat.1002576.

(89) Barbosa da Silva, E.; Rocha, D. A.; Fortes, I. S.; Yang, W.; Monti, L.; Siqueira-Neto, J. L.; Caffrey, C. R.; McKerrow, J.; Andrade, S. F.; Ferreira, R. S. Structure-Based Optimization of Quinazolines as Cruzain and TbrCATL Inhibitors. *Journal of Medicinal Chemistry* **2021**, *64* (17), 13054–13071. https://doi.org/10.1021/acs.jmedchem.1c01151.

(90) Sharpless, K. B.; Amberg, W.; Bennani, Y. L.; Crispino, G. A.; Hartung, J.; Jeong, K. S.; Kwong, H. L.; Morikawa, K.; Wang, Z. M. The Osmium-Catalyzed Asymmetric Dihydroxylation: A New Ligand Class and a Process Improvement. *The Journal of Organic Chemistry* **1992**, *57* (10), 2768–2771. https://doi.org/10.1021/jo00036a003.

(91) Clayden, J. P.; Greeves, N.; Warren, S. *Organic Chemistry*; 2012.

(92) Liao, L.-X.; Wang, Z.-M.; Zhang, H.-X.; Zhou, W.-S. A New Concise Stereoselective Method for the Preparation of a β-Hydroxyfurfurylamine Derivative and Synthesis of 1-Deoxyazasugar Isomers. *Tetrahedron:*

Asymmetry **1999**, *10* (18), 3649–3657. https://doi.org/10.1016/S0957-4166(99)00382-1.

(93) Kaiser, C. R. RMN 2D: Detecção Inversa e Gradiente de Campo Na Determinação Estrutural de Compostos Orgânicos. *Química Nova* **2000**, *23* (2), 231–236. https://doi.org/10.1590/S0100-40422000000200014.

(94) Zhang, G.; Wang, X.; Li, C.; Yin, D. Palladium-Catalyzed Cross-Coupling of Electron-Deficient Heteroaromatic Amines with Heteroaryl Halides. *Synthetic Communications* **2013**, *43* (3), 456–463. https://doi.org/10.1080/00397911.2011.603068.

(95) Monti, L.; Wang, S. C.; Oukoloff, K.; Smith, A. B.; Brunden, K. R.; Caffrey, C. R.; Ballatore, C. Brain-Penetrant Triazolopyrimidine and Phenylpyrimidine Microtubule Stabilizers as Potential Leads to Treat Human African Trypanosomiasis. *ChemMedChem* **2018**, *13* (17), 1751–1754. https://doi.org/10.1002/cmdc.201800404.

(96) Hirumi, H.; Hirumi, K. Continuous Cultivation of Trypanosoma Brucei Blood Stream Forms in a Medium Containing a Low Concentration of Serum Protein without Feeder Cell Layers. *The Journal of Parasitology* **1989**, *75* (6), 985. https://doi.org/10.2307/3282883.

(97) Faria, J.; Moraes, C. B.; Song, R.; Pascoalino, B. S.; Lee, N.; Siqueira-Neto, J. L.; Cruz, D. J. M.; Parkinson, T.; Ioset, J.-R.; Cordeiro-da-Silva, A.; Freitas-Junior, L. H. Drug Discovery for Human African Trypanosomiasis. *Journal of Biomolecular Screening* **2015**, *20* (1), 70–81. https://doi.org/10.1177/1087057114556236.

Anexos

O texto completo desta seção, que na tese defendida ocupa o intervalo de páginas 217-220, foi suprimido por tratar-se de informações para publicação em periódico científico. Consta da disposição de todos os espectros de Infravermelho, RMN de Hidrogênio e de Carbono referentes a alguns compostos apresentados na tese defendida.